



**FIRE RESEARCH AND DEVELOPMENT TECHNICAL REPORT**

# UL 9540A Installation Level Tests with Outdoor Lithium-ion Energy Storage System Mockups

*April 12, 2021*

Adam Barowy  
Alex Klieger  
Jack Regan  
Mark McKinnon, Ph.D., P.E.



**Empowering Trust<sup>®</sup>**

## Executive Summary

The UL 9540A test standard develops data on the fire and deflagration hazards from thermal runaway and its propagation through energy storage systems. The standard provides a systematic evaluation of thermal runaway and propagation in energy storage system at cell, module, unit, and installation levels. The data from the testing may be used to design fire protection methods to mitigate against the hazards generated. The data generated from each level of testing is summarized in Table E1.

**Table E1 – Test Levels in UL 9540A (4<sup>th</sup> Edition).**

Test level	Data developed
Cell	<ul style="list-style-type: none"> <li>a. Methodology required to initiate thermal runaway for testing.</li> <li>b. Cell surface temperature at onset of gas venting and thermal runaway.</li> <li>c. Gas composition, volume, and explosibility parameters.</li> </ul>
Module	<ul style="list-style-type: none"> <li>a. Number of initiating cells required for propagation of thermal runaway.</li> <li>b. Heat, smoke, and flammable gas release rates and total release quantity.</li> <li>c. Observations of external flame extension.</li> <li>d. Observations of deflagration and debris hazards.</li> </ul>
Unit	<ul style="list-style-type: none"> <li>a. Extent of thermal runaway propagation.</li> <li>b. Heat, smoke, and flammable gas release rates and total release quantity.</li> <li>c. Observations of external flame extension, deflagration, and debris hazards, and re-ignition hazards.</li> <li>d. Thermal exposure (temperature on adjacent walls, and target units; heat flux to adjacent walls, target units, and egress pathways)</li> </ul>
Installation	<ul style="list-style-type: none"> <li>a. Evaluation of fire protection method.</li> <li>b. Fire growth control.</li> <li>c. Extent of thermal runaway propagation.</li> <li>d. Design features related to containment of thermal runaway gases and heat that create an explosion hazard.</li> <li>e. Deflagration protection system.</li> <li>f. Egress protection.</li> <li>g. Thermal exposure to adjacent surfaces.</li> <li>h. Observations of flaming outside the installation</li> <li>i. Observations of reignition.</li> <li>j. Deflagration and debris.</li> </ul>

This report presents the results of three installation level tests conducted between June 19 and July 9, 2020, in the UL Large Scale Fire Test Facility in Northbrook, Ill. The installation level test included a mock-up Initiating Energy Storage System (ESS) Unit and two Target Units installed within an International Organization for Standardization (ISO) container outfitted with deflagration protection vents. All tests were conducted with an identical lithium-ion (li-ion) battery configuration. The Initiating ESS Unit included nine modules with a total capacity of 28.9 kWh. Each mock-up module included nine mock-up cells. Each mock-up cell was composed of thirty 18650 li-ion cells for an equivalent capacity of 99 Ah in each mock-up cell. The Target Units were loaded to one-third capacity of the Initiating Unit.



## UL 9540A INSTALLATION LEVEL TESTS WITH OUTDOOR LITHIUM-ION ENERGY STORAGE SYSTEM MOCKUPS

Test 1 was a baseline performance test and did not utilize any active fire suppression systems. Test 2 included a Novec 1230 system discharged upon activation of two smoke detectors installed inside the container. The clean agent system in this test was designed for an 8.0 v% concentration of Novec 1230. Test 3 incorporated a dry pipe water suppression system to provide a uniform 0.5 gpm/ft<sup>2</sup> delivered spray density at the top of the ESS unit enclosures. The waterflow was triggered by the activation of a standard response sprinkler link after a 30-second delay to simulate filling the sprinkler delivery pipe with water.

Test 1 developed data on hazards developed in the absence of active ventilation or fire suppression system intervention. A partial volume deflagration occurred when the gases generated from the first cell thermal runaway were ignited 30 seconds after thermal runaway. During the test, propagation of thermal runaway extended through all modules of the Initiating Unit and Left Target Unit within three hours. The modules of the Front Target Unit did not experience thermal runaway but exceeded the cell vent temperature, which was the target unit temperature performance criteria. Wall temperatures exceeded the performance criteria for combustible construction materials. Flammable gases accumulated in the container as each module experienced thermal runaway. Gas concentrations inside the container eventually accumulated to 40–60 v% in the container, which was above the upper flammability limit (UFL) of the cell level battery gases.

Test 2 included Novec 1230, which was deployed one minute after thermal runaway, upon activation of both installed smoke detectors. Gradual stratification was observed between an opaque lower layer of gases and vapors and a transparent upper layer. Within 28 minutes of the initial Novec 1230 discharge, gases accumulated in the upper gas layer ignited and resulted in an unusually slow deflagration with respect to the characterized burning properties of the battery gas. A deflagration occurred inside the container 44 minutes after the first thermal runaway and 43 minutes after Novec 1230 discharge. One module had experienced thermal runaway at the time of the deflagration. Following the deflagration, Test 2 developed similarly to Test 1. Thermal runaway was observed in all modules of the Initiating Unit and Left Target Unit. The modules of the Front Target Unit did not experience thermal runaway but did exceed the target unit temperature performance criteria. Flammable gases accumulated in the container with each thermal runaway event and exceeded the upper flammability limit of the cell vent gases.

Test 3 utilized a water suppression system above the ESS units. Prior to the activation of the water suppression system, performance criteria for combustible materials were exceeded on the instrumented walls. Water application protected adjacent exposures, as evidenced by reduced temperatures on the instrumented walls and target units. A deflagration occurred in Test 3, 42 minutes after the first thermal runaway event, while the suppression system was active. Four modules had experienced thermal runaway at this time. Thermal runaway propagated through the Initiating Unit during waterflow as well as while waterflow was discontinued. Unlike Test 1 and Test 2, thermal runaway was observed only in one module of the Left Target Unit, during the period after waterflow was discontinued. Furthermore, temperatures measured on the Front Target Unit complied with the target unit temperature performance criteria for the duration of the test. Thermal runaway gases accumulated inside the container as additional modules experienced thermal runaway. Gas concentrations inside the container ultimately exceeded the upper flammability limit for the cell gas mixture.



# Acknowledgements

UL thanks the members of the project technical panel, listed below, for providing technical input to planning of this project and contributing valuable feedback during the execution of the tests.

Bob Zalosh	Firexplo
FDNY Sustainability Unit and HazMat Operations	Fire Department of the City of New York (FDNY)
Tom Abbott	Surprise (Ariz.) Fire Department





# Table of Contents

<b>Executive Summary</b>	<b>i</b>
<b>Acknowledgements</b>	<b>iii</b>
<b>Table of Contents</b>	<b>iv</b>
<b>Table of Tables</b>	<b>vii</b>
<b>Table of Figures</b>	<b>viii</b>
<b>1 Introduction</b>	<b>1</b>
1.1 Objectives	3
1.2 Scope	3
1.3 Technical Plan	3
1.4 Glossary	4
<b>2 Setup</b>	<b>5</b>
2.1 Energy Storage System Mockup Construction	5
2.1.1 ISO Container	5
2.1.2 Energy Storage System Units	12
<b>2.2 Instrumentation</b>	<b>19</b>
2.2.1 Container	21
2.2.2 ESS Units	24
2.2.3 Fire Service Size-up Equipment	25
<b>3 Procedure</b>	<b>36</b>
<b>4 Results</b>	<b>37</b>
4.1 Test 1 – Li-Ion ESS Installation without Fire Suppression System	37
4.1.1 Timeline	37
4.1.2 Comparison of Test 1 Results to UL 9540A Performance Metrics	40
4.1.3 Thermal Runaway Propagation	49
4.1.4 Test Conditions Inside ISO Container	52
4.1.5 Smoke and Gas Detector Activation	55



# UL 9540A INSTALLATION LEVEL TESTS WITH OUTDOOR LITHIUM-ION ENERGY STORAGE SYSTEM MOCKUPS

4.1.6 Fire Suppression System Operation	60
4.1.7 Fire Service Size-up Equipment	60
<b>4.2 Test 2 – Li-Ion ESS Installation with Novec 1230 Clean Agent System</b>	<b>74</b>
4.2.1 Timeline	74
4.2.2 Comparison of Test 2 Results to UL 9540A Performance Metrics	77
4.2.3 Thermal Runaway Propagation	89
4.2.4 Test Conditions Inside ISO Container	92
4.2.5 Smoke and Gas Detector Activation	99
4.2.6 Fire Suppression System Operation	104
4.2.7 Fire Service Size-up Equipment	107
<b>4.3 Test 3 - Li-Ion ESS Installation with 0.5 gpm/ft<sup>2</sup> Actual Delivered Density Water Spray</b>	<b>125</b>
4.3.1 Timeline	125
4.3.2 Comparison of Test 3 Results to 9540A Performance Metrics	128
4.3.3 Thermal Runaway Propagation	138
4.3.4 Test Conditions Inside ISO Container	141
4.3.5 Smoke and Gas Detector Activation	147
4.3.6 Fire Suppression System Operation	153
4.3.7 Fire Service Size-up Equipment	154
<b>5 Discussion of Results</b>	<b>170</b>
<b>5.1 Detection</b>	<b>170</b>
<b>5.2 Thermal Runaway Propagation</b>	<b>171</b>
<b>5.3 Thermal Exposure</b>	<b>173</b>
<b>5.4 Gas and Deflagration Hazards</b>	<b>175</b>
<b>5.5 Fire Service Size-Up Indicators of a Thermal Runaway Event</b>	<b>176</b>
<b>5.6 Test Termination</b>	<b>178</b>
<b>6 Summary of Findings</b>	<b>180</b>
<b>7 Fire Service Tactical Considerations</b>	<b>185</b>
<b>8 References</b>	<b>191</b>
<b>Appendix A: Detailed Visual Timeline of Test 1 Events</b>	<b>196</b>



UL 9540A INSTALLATION LEVEL TESTS WITH OUTDOOR LITHIUM-ION ENERGY  
STORAGE SYSTEM MOCKUPS

**Appendix B: Detailed Visual Timeline of Test 2 Events** **209**

**Appendix C: Detailed Visual Timeline of Test 3 Events** **223**



## Table of Tables

Table 1 – Test levels in UL 9540A. ....	2
Table 2 – Cell level thermal runaway properties. ....	13
Table 3 – Initiating cell, module, and unit characteristics. ....	14
Table 4 – Initiating unit spacing relative to target units and adjacent walls. ....	18
Table 5 – Analytical and wall-mounted gas measurement equipment. ....	23
Table 6 – Gas sensor technologies. ....	27
Table 7 – Typical cross-sensitivities for the electrochemical sensors in these tests. ....	28
Table 8 – Correction factors for a typical catalytic bead LEL sensor calibrated for Methane. ....	29
Table 9 – Camera numbering and locations. ....	34
Table 10 – Test 1 performance . ....	40
Table 11 – Thermal runaway propagation times for Test 1. ....	50
Table 12 – Combustible gas detector response summary for Test 1. ....	56
Table 13 – Test 2 Performance. ....	77
Table 14 – Thermal runaway propagation times for Test 2. ....	91
Table 15 – Combustible gas detector response summary for Test 2. ....	101
Table 16 – Test 3 Performance. ....	128
Table 17 – Thermal runaway propagation times for Test 3. ....	140
Table 18 – Combustible gas detector response summary for Test 3. ....	150
Table 19 – Summary of water flow volumes for Test 3. ....	153
Table 20 – Timeline of major events for Test 1. ....	196
Table 21 – Timeline of major events for Test 2. ....	209
Table 22 - Timeline of major events for Test 3. ....	223

## Table of Figures

Figure 1 – ISO Container photo (left) and overall plan view dimensions (right).....	5
Figure 2 – Wall construction details, cross-section view. ....	5
Figure 3 – Wall construction layout, plan view. ....	6
Figure 4 – Side A wall construction layout, elevation view. ....	6
Figure 5 – Side B wall construction layout, elevation view. ....	6
Figure 6 – Side C wall construction layout, elevation view. ....	7
Figure 7 – Side D wall construction layout, elevation view. ....	7
Figure 8 – Deflagration vent locations, plan view. ....	8
Figure 9 – External (left) and internal view (right) of deflagration vents. ....	9
Figure 10 – Clean agent piping system to a central discharge nozzle, plan view.....	9
Figure 11 – Clean agent piping system to a central discharge nozzle, elevation view. .	10
Figure 12 – Clean agent discharge nozzle. ....	10
Figure 13 – Positive pressure relief vent (left) and negative pressure relief vent (right).	10
Figure 14 – Water suppression nozzle arrangement and spray pattern, elevation view. .....	11
Figure 15 – Nozzle arrangement above ESS unit enclosures, plan view. ....	11
Figure 16 – Location of four water suppression nozzles above ESS unit enclosures. ..	12
Figure 17 – Initiating Cell (left) and Initiating Module (right) constructed from 18650 cells. .....	15
Figure 18 – Initiating Unit construction. ....	15
Figure 19 – Left Target Unit layout. ....	16
Figure 20 – Front Target Unit layout.....	17
Figure 21 – Single dummy unit (left) and double dummy unit (right). ....	17
Figure 22 – Initiating unit and target unit spacing. ....	18
Figure 23 – Initiating Unit, Left Target Unit, and double dummy unit (left); Front Target Unit, single dummy unit, and double dummy unit (right).....	19
Figure 24 – Instrumentation key. ....	20
Figure 25 – Container instrumentation plan view. ....	20
Figure 26 – Container instrumentation elevation view (long axis). ....	21
Figure 27 – Container instrumentation elevation view (short axis). ....	21
Figure 28 – Schmidt-Boelter heat flux gauge. ....	22
Figure 29 – Heat flux gauges installed for Left Target Unit (left) and Front Target Unit (right),.....	25
Figure 30 – Fire service portable gas meter locations.....	26
Figure 31 – Exterior camera locations.....	33
Figure 32 – Interior camera locations.....	34
Figure 33 – Sequence of events in Test 1 leading up to 34 minutes of test time. ....	38
Figure 34 – Sequence of events in test 1 from 34 to 194 minutes of test time.....	39
Figure 35 – Sequence of events in test 1 from 194 to 209 minutes of test time. ....	39
Figure 36 – Rear wall temperatures measured during Test 1. ....	41
Figure 37 – Side wall temperatures measured in Test 1. ....	42
Figure 38 – Incident heat fluxes to rear and side walls measured in Test 1.....	43

**UL 9540A INSTALLATION LEVEL TESTS WITH OUTDOOR LITHIUM-ION ENERGY STORAGE SYSTEM MOCKUPS**

Figure 39 – Thermal damage to walls photographed during test termination and overhaul after Test 1. .... 43

Figure 40 – Temperatures measured in Left Target Unit during Test 1..... 44

Figure 41 – Temperatures measured in Front Target Unit during Test 1 ..... 45

Figure 42 – Incident heat flux measured in Front and Left Target Units during Test 1.. 46

Figure 43 – Flaming outside the test container through cable conduit in Test 1..... 46

Figure 44 – Heat flux measured in the egress path for Test 1..... 47

Figure 45 – Sequence of reignition during overhaul of Test 1 (test time 03:29:21 to 03:57:00). .... 47

Figure 46 – Re-ignited fire observed during overhaul of Test 1 (four hours after test start). .... 48

Figure 47 – Thermal runaway propagation within the Initiating Module in Test 1..... 49

Figure 48 – Temperatures measured throughout the Initiating Unit during Test 1. .... 50

Figure 49 – Condition of Initiating Unit after Test 1. .... 51

Figure 50 – Container gas temperatures measured during Test 1. .... 52

Figure 51 – Gases measured in the container from thermal runaway through propagation of thermal runaway to other modules in Test 1. .... 53

Figure 52 – Gas conditions measured in the container for the duration of Test 1. .... 54

Figure 53 – Condition of container after Test 1 overhaul..... 55

Figure 54 – Smoke layer condition upon activation of both smoke detectors in Test 1. 55

Figure 55 – Extinction coefficient measurements made by smoke obscuration meter for Test 1 from the beginning of the test through the propagation of thermal runaway to additional modules. .... 56

Figure 56 – Total hydrocarbon concentration compared with commercial combustible gas detector response immediately after thermal runaway in Test 1 (test time 00:25:00 to 00:30:00). .... 57

Figure 57 – Total hydrocarbon concentration compared with commercial combustible gas detector response in Test 1 (test time 00:25:00 to 00:50:00). .... 58

Figure 58 – Commercial hydrogen detector measurement compared with carbon monoxide and hydrogen concentrations measured in Test 1. .... 59

Figure 59 – Wall surface temperatures during Test 1. Vertical lines denote events corresponding to the images in the figure below. .... 60

Figure 60 – Changes in thermal imaging view over the course of Test 1. Left column shows B-side of the container (insulated wall construction) and right column shows D-side of container (bare metal construction). .... 61

Figure 61 – Temperature difference between inside and outside surface of container during Test 1. .... 62

Figure 62 – View of left side (B-side) of container 23 minutes after the initial thermal runaway (50 minutes after test start). .... 63

Figure 63 – Vapor cloud formation and development in standard (left) and thermal imaging (right) camera views during Test 1..... 64

Figure 64 – LEL measurements from portable gas meters in Test 1..... 65

Figure 65 – Hydrogen gas concentration measured by Interior Meter 1 and Exterior Meter 1 in Test 1. .... 66

Figure 66 – Carbon monoxide (CO) concentration measured by fire service portable gas meters in Test 1. .... 68



**UL 9540A INSTALLATION LEVEL TESTS WITH OUTDOOR LITHIUM-ION ENERGY STORAGE SYSTEM MOCKUPS**

Figure 67 – Hydrogen cyanide (HCN) concentration measured by fire service portable gas meters in Test 1..... 70

Figure 68 – Hydrogen sulfide (H<sub>2</sub>S) concentration measured by fire service portable gas meters in Test 1. .... 71

Figure 69 – Oxygen (O<sub>2</sub>) concentration measured by fire service portable gas meters in Test 1. .... 72

Figure 70 – Volatile organic compound (VOC) concentration measured by fire service portable gas meters in Test 1..... 73

Figure 71 – Sequence of events in Test 2 leading up to 57 minutes of test time. .... 75

Figure 72 – Sequence of events in Test 2 from 72 to 185 minutes of test time..... 76

Figure 73 – Rear wall temperatures measured during Test 2. .... 78

Figure 74 – Side wall temperatures measured during Test 2, ..... 79

Figure 75 – Incident heat flux measured to rear and side walls during Test 2..... 80

Figure 76 – Temperatures measured in Left Target Unit during Test 2..... 81

Figure 77 – Condition of Left Target Unit after Test 2. .... 82

Figure 78 – Temperatures measured in Front Target Unit from thermal runaway to carbon dioxide system discharge during Test 2. .... 83

Figure 79 – Temperatures measured in Front Target Unit during Test 2. .... 83

Figure 80 – Incident heat flux measured in Front Target Unit during Test 2..... 84

Figure 81 – Condition of a module in Front Target Unit after Test 2. .... 85

Figure 82 – Flaming observed intermittently through instrumentation opening in container wall in Test 2. .... 85

Figure 83 – Short duration flaming observed from deflagration vents. .... 85

Figure 84 – Flaming of container contents after door opening in Test 2. .... 86

Figure 85 – Deflagration images from Test 2. .... 87

Figure 86 – Heat flux measured in the egress path during Test 2..... 88

Figure 87 – Temperatures measured throughout the Initiating Module indicate propagation of thermal runaway in Test 2. .... 89

Figure 88 – Temperatures measured throughout the Initiating Unit during Test 2. .... 90

Figure 89 – Condition of Initiating Unit after Test 2. .... 91

Figure 90 – Container gas temperatures measured during Test 2..... 92

Figure 91 – Container gas temperatures measured before and after opening of the container door during Test 2. .... 93

Figure 92 – Sequence of reignition in Test 2 (test time 02:37:36 to 02:38:01). .... 94

Figure 93 – Gases measured in the container from thermal runaway to ignition in Test 2. .... 96

Figure 94 – Gas conditions measured in the container for the duration of Test 2. .... 97

Figure 95 – Condition of container after Test 2 overhaul..... 98

Figure 96 – Condition of deflagration vent after Test 2..... 98

Figure 97 – Smoke layer condition upon activation of near (left) and far (right) smoke detectors in Test 2..... 99

Figure 98 – Extinction coefficient measurements made by smoke obscuration meter for Test 2 from the beginning of the test through ignition..... 100

Figure 99 – Commercial carbon monoxide detector response compared with carbon monoxide concentrations measured in Test 2..... 101



# UL 9540A INSTALLATION LEVEL TESTS WITH OUTDOOR LITHIUM-ION ENERGY STORAGE SYSTEM MOCKUPS

Figure 100 – Total hydrocarbon concentration compared with commercial combustible gas detector response in Test 2 (test time 00:28:00 to 00:40:00). ..... 102

Figure 101 – Total hydrocarbon concentration compared with commercial combustible gas detector response in Test 2 (test time 00:25:00 to 00:80:00). ..... 103

Figure 102 – Commercial hydrogen detector measurement compared with carbon monoxide and hydrogen concentrations measured in Test 2. .... 104

Figure 103 – Container pressure measured during Novec 1230 discharge in Test 2.. 104

Figure 104 – THC measurements at floor and ceiling after Novec 1230 deployment show progressive stratification in Test 2. .... 105

Figure 105 – Visual stratification aligned with steady decrease in THC concentrations at ceiling in Test 2 (test time 43:00, 48:00, and 53:00). .... 106

Figure 106 – Images of combustion in upper layer at 56:44 (left) and 56:48 (right) in Test 2. .... 106

Figure 107 – Wall surface temperatures during the period from the first thermal runaway event until propagation of thermal runaway to additional modules. Vertical lines denote events corresponding to the images in Figure 108, Figure 109, and Figure 110 below. .... 107

Figure 108 – Changes in IR view from thermal runaway in Initiating Module to Novec 1230 discharge in Test 2. Left column shows A-B corner of the container (insulated wall construction) and right column shows D-side of container (bare metal construction).. 108

Figure 109 – Changes in thermal imaging view before and after initial flaming in the container in Test 2. Left column shows A-B corner of the container (insulated wall construction) and right column shows D-side of container (bare metal construction).. 109

Figure 110 – Changes in thermal imaging view before and after deflagration in Test 2. Left column shows A-B corner of the container (insulated wall construction) and right column shows D-side of container (bare metal construction). .... 110

Figure 111 – Wall surface temperatures during the period before and after the container doors were opened in Test 2. Vertical lines denote events corresponding to the images in Figure 112 below. .... 111

Figure 112 – Changes in thermal imaging view immediately before and 60 seconds after the container doors were opened, which occurred 2:37:36 after test start in Test 2. Left column shows A-B corner of the container (insulated wall construction) and right column shows D-side of container (bare metal construction). .... 112

Figure 113 – Temperature difference between inside and outside surface of container during Test 2. .... 113

Figure 114 – Vapor cloud formation and development in standard (left) and thermal imaging (right) camera views during Test 2. .... 114

Figure 115 – Interior view of gas ignition 56:40 after test start. Note the lack of thermal signature in the thermal imaging camera compared to the visible burning in the standard camera view. .... 115

Figure 116 – Flammable gas concentration measurements from portable gas meters in Test 2. .... 117

Figure 117 – Hydrogen gas concentration measured by MultiRAE Lite Diffusion meters inside and outside of container in Test 2. .... 118

Figure 118 – Carbon monoxide (CO) concentration measured by fire service portable gas meters in Test 2. .... 119





**UL 9540A INSTALLATION LEVEL TESTS WITH OUTDOOR LITHIUM-ION ENERGY STORAGE SYSTEM MOCKUPS**

Figure 119 – Hydrogen cyanide (HCN) concentration measured by fire service portable gas meters in Test 2..... 121

Figure 120 – Hydrogen sulfide (H<sub>2</sub>S) concentration measured by fire service portable gas meters in Test 2. .... 122

Figure 121 – Oxygen (O<sub>2</sub>) concentration measured by fire service portable gas meters in Test 2. .... 123

Figure 122 – Volatile organic compound (VOC) concentration measured by fire service portable gas meters in Test 2..... 124

Figure 123 – Sequence of events in Test 3 leading up to 40 minutes of test time. .... 125

Figure 124 – Sequence of events in test 1 from 72 to 149 minutes of test time. .... 127

Figure 125 – Final thermal runaway at 02:39:22 (TR + 01:59:30). .... 127

Figure 126 – Temperatures measured on the rear wall during Test 3 from the Initiating Cell thermal runaway through the deflagration..... 129

Figure 127 – Temperatures measured on the side wall during Test 3 from the Initiating Cell thermal runaway through the deflagration..... 129

Figure 128 – Temperatures measured on the rear wall during Test 3..... 130

Figure 129 – Temperatures measured on the side wall during Test 3. .... 131

Figure 130 – Incident heat flux to rear and side walls measured during Test 3..... 132

Figure 131 – Temperatures measured in Left Target Unit during Test 3..... 133

Figure 132 – Temperatures measured in Front Target Unit during Test 3. .... 134

Figure 133 – Incident heat flux to Left and Front Target Units measured during Test 3. .... 134

Figure 134 – Condition of Left Target Unit (left), Initiating Unit (left), and Front Target Unit (right) after Test 3..... 135

Figure 135 – Deflagration and side vent operation in Test 3 (test time 01:11:55). .... 136

Figure 136 – Heat flux measured in the egress path during Test 3..... 137

Figure 137 – Temperatures of cells in the Initiating Module from the first thermal runaway through propagation of thermal runaway to other modules in Test 3..... 138

Figure 138 – Temperatures measured inside Initiating Unit modules. .... 139

Figure 139 – Condition of InitUnitMod2 with waterline visible after Test 3. .... 140

Figure 140 – Container gas temperatures measured from the initiating cell thermal runaway through the propagation of thermal runaway to other modules in Test 3..... 141

Figure 141 – Container gas temperatures measured during Test 3..... 142

Figure 142 – Gases measured in the container from Initiating Cell venting through thermal runaway propagation to additional modules in Test 3. .... 143

Figure 143 – Gas conditions measured in the container for the duration of Test 3. .... 144

Figure 144 – Snapshot of thermal imaging camera facing the Initiating Unit suggesting additional off-gassing or flaming (test time 00:54:06). .... 144

Figure 145 – Condition of side wall next to the Initiating Unit after Test 3..... 146

Figure 146 – Photograph of Target Units and container after Test 3. .... 146

Figure 147 – View from floor up toward smoke layer when the near (left) and far (right) smoke detectors alarmed in Test 3. .... 147

Figure 148 – Extinction coefficient measurements made by smoke obscuration meter for Test 3 from the beginning of the test through thermal runaway propagation into additional modules..... 148



**UL 9540A INSTALLATION LEVEL TESTS WITH OUTDOOR LITHIUM-ION ENERGY STORAGE SYSTEM MOCKUPS**

Figure 149 – Commercial carbon monoxide detector response compared with carbon monoxide concentrations measured in Test 3..... 149

Figure 150 – Total hydrocarbon concentration compared with commercial combustible gas detector response in Test 3 (test time 00:29:00 to 00:34:00). ..... 151

Figure 151 – Total hydrocarbon concentration compared with commercial combustible gas detector response in Test 3 (test time 00:25:00 to 00:55:00). ..... 152

Figure 152 – Total hydrocarbon concentration compared with commercial combustible gas detector response in Test 3 (test time 00:25:00 to 00:75:00). ..... 152

Figure 153 – Wall surface temperatures during Test 3. Vertical lines denote events corresponding to the images in Figure 154, Figure 155, and Figure 156. .... 154

Figure 154 – Changes in thermal imaging view immediately before and 10 seconds after the initial flaming in Test 3. Left column shows A-B corner of the container (insulated wall construction) and right column shows D-side of container (bare metal construction).. 155

Figure 155 – Changes in thermal imaging view immediately before and five seconds after the deflagration and second temperature peak of Test 3. Left column shows A-B corner of the container (insulated wall construction) and right column shows D-side of container (bare metal construction)..... 156

Figure 156 – Changes in thermal imaging view immediately before, three minutes after, and six minutes after the sprinklers were shut off in the container in Test 3. Left column shows A-B corner of the container (insulated wall construction) and right column shows D-side of container (bare metal construction)..... 157

Figure 157 – Temperature differential between inside and outside surface of container during Test 3. .... 158

Figure 158 – Vapor cloud formation and development in standard (left) and thermal imaging (right) camera views during Test 3..... 159

Figure 159 – Percentage of LEL measured by portable gas meters in Test 3..... 161

Figure 160 – Hydrogen gas (H<sub>2</sub>) concentrations measured by portable gas meters in Test 3. .... 163

Figure 161 – Carbon monoxide (CO) concentration measured by portable gas meters in Test 3. .... 164

Figure 162 – Hydrogen cyanide (HCN) concentration measured by portable gas meters in Test 3. .... 166

Figure 163 – Hydrogen sulfide (H<sub>2</sub>S) concentrations measured by portable gas meters in Test 3. .... 167

Figure 164 – Oxygen (O<sub>2</sub>) concentrations measured by portable gas meters in Test 3. .... 168

Figure 165 – Volatile organic compound (VOC) concentrations measured by portable gas meter on A-side of container in Test 3..... 169



# 1 Introduction

UL published the first edition of UL 9540A in November 2017 [1]. Subsequent battery energy storage industry demand drove the rapid development of refinements to the standard, culminating in the publication of ANSI/CAN/UL 9540A, 4<sup>th</sup> edition in November 2019. UL 9540A is the referenced standard for meeting ESS thermal runaway fire safety testing requirements specified within NFPA 855, Standard for the Installation of Stationary Energy Storage Systems [2], the International Fire Code (IFC) [3], the International Residential Code (IRC) [4], and the New York City Fire Code 3 RCNY 608-01, Outdoor Stationary Storage Battery Systems [5]. UL 9540A stakeholders include but are not limited to: the battery energy storage industry, end users of ESS, authorities having jurisdiction (AHJs), insurers, the fire service, fire protection engineers, and the code and standards development community.

UL 9540A develops data on the fire and deflagration hazards from thermal runaway and its propagation through ESSs. The standard provides a systematic evaluation of thermal runaway and propagation in energy storage systems at cell, module, unit, and installation levels. The data from the testing enables the design fire and explosion protection methods to mitigate against the hazards generated. The data generated from each level of testing is summarized in Table 1.

**UL 9540A INSTALLATION LEVEL TESTS WITH OUTDOOR LITHIUM-ION ENERGY STORAGE SYSTEM MOCKUPS**

**Table 1 – Test levels in UL 9540A.**

<b>Test level</b>	<b>Data developed</b>
Cell	<ul style="list-style-type: none"> <li>a. Methodology required to initiate thermal runaway for testing.</li> <li>b. Cell surface temperature at onset of gas venting and thermal runaway.</li> <li>c. Gas composition, volume and explosibility parameters.</li> </ul>
Module	<ul style="list-style-type: none"> <li>a. Number of initiating cells required for propagation of thermal runaway.</li> <li>b. Heat release rate and total heat released.</li> <li>c. Smoke release rate and total smoke released.</li> <li>d. Flammable gas generation rates and composition.</li> <li>e. Observations of external flame extension.</li> <li>f. Observations of deflagration and debris hazards.</li> </ul>
Unit	<ul style="list-style-type: none"> <li>a. Extent of thermal runaway propagation</li> <li>b. Heat release rate and total heat released.</li> <li>c. Smoke release rate and total smoke released.</li> <li>d. Flammable gas generation rates and composition.</li> <li>e. Observations of external flame extension.</li> <li>f. Observations of deflagration and debris hazards.</li> <li>g. Thermal exposure (temperature on adjacent walls, and target units; heat flux to adjacent walls, target units, and egress pathways)</li> <li>h. Deflagration and debris.</li> <li>i. Observations of reignition.</li> </ul>
Installation	<ul style="list-style-type: none"> <li>a. Evaluation of fire protection method.</li> <li>b. Fire growth control.</li> <li>c. Extent of thermal runaway propagation.</li> <li>d. Design features related to containment of thermal runaway gases and heat that could create an explosion hazard.</li> <li>e. Deflagration protection system.</li> <li>f. Egress protection.</li> <li>g. Thermal exposure (temperature on adjacent walls, ceiling, and target units; heat flux to adjacent walls, target units, and egress pathways)</li> <li>h. Observations of flaming outside the installation.</li> <li>i. Observations of reignition.</li> <li>j. Deflagration and debris.</li> </ul>



# UL 9540A INSTALLATION LEVEL TESTS WITH OUTDOOR LITHIUM-ION ENERGY STORAGE SYSTEM MOCKUPS

## 1.1 Objectives

The test series was conducted with the following objectives:

1. Develop non-proprietary UL 9540A data at installation level with representative li-ion chemistry battery products undergoing thermal runaway with and without active fire protection systems.
2. Develop fire service size-up considerations using typical fire service hazard evaluation equipment under anticipated li-ion ESS thermal runaway use conditions. Collaboration with the UL Firefighter Safety Research Institute enabled inclusion of fire service considerations into the design of the test setup and the development of incident size-up considerations for ESS installation fire incidents.

## 1.2 Scope

The scope of this investigation was limited to a UL-designed mockup of an outdoor modular walk-in ESS using one lithium nickel cobalt aluminum oxide (NCA) lithium-ion cathode chemistry installed in a 20 ft ISO intermodal container.

## 1.3 Technical Plan

Three tests were planned to pursue the objectives:

- Test 1 – Li-ion ESS installation without an active fire suppression system
- Test 2 – Li-Ion ESS installation with a Novec 1230 clean agent system
- Test 3 – Li-Ion ESS installation With 0.5 gpm/ft<sup>2</sup> actual delivered density water spray



# UL 9540A INSTALLATION LEVEL TESTS WITH OUTDOOR LITHIUM-ION ENERGY STORAGE SYSTEM MOCKUPS

## 1.4 Glossary

**BATTERY ENERGY STORAGE SYSTEM (BESS)** – Stationary equipment that receives electrical energy and then utilizes batteries to store that energy to supply electrical energy at some future time. The BESS at a minimum consists of one or more modules, including a power conditioning system (PCS), a battery management system (BMS), and a balance of plant components [1].

**CELL** – The basic functional electrochemical unit containing an assembly of electrodes, electrolyte, separators, container, and terminals. It is a source of electrical energy by direct conversion of chemical energy [1].

**DEFLAGRATION** – Propagation of a combustion zone at a velocity less than the speed of sound in the unreacted medium [6].

**IMMEDIATELY DANGEROUS TO LIFE OR HEALTH (IDLH)** – An atmospheric concentration of any toxic, corrosive, or asphyxiant substance that poses an immediate threat to life or would interfere with an individual's ability to escape from a dangerous atmosphere [7].

**MODULE** – A subassembly that is a component of a BESS that consists of a group of cells or electrochemical capacitors connected together in a series and/or parallel configuration (sometimes referred to as a block) with or without protective devices and monitoring circuitry [1].

**RE-IGNITION** – Additional cell thermal runaway(s) in damaged energy storage equipment that occur a significant amount of time after an initial thermal runaway incident and that may lead to renewed propagation of thermal runaways and/or ignition of combustible materials.

**THERMAL RUNAWAY** – When an electrochemical cell increases its temperature through self-heating in an uncontrollable fashion. The thermal runaway progresses when the cell's generation of heat occurs at a higher rate than the heat it can dissipate. This may lead to fire, explosion, and gas evolution [1].

**UNIT** – A frame, rack, or enclosure that consists of a functional BESS that includes components and subassemblies, such as cells, modules, battery management systems, ventilation devices, and other ancillary equipment [1].

**VENTING** – Cell venting occurs when sufficient internal pressure is generated, typically from the vaporization of liquid electrolyte, to operate a safety vent or otherwise rupture a cell casing/container.



## 2 Setup

### 2.1 Energy Storage System Mockup Construction

#### 2.1.1 ISO Container

A standard size 20-ft ISO container was utilized to represent an outdoor, ground mounted ESS installation. The container measured nominally 8 ft wide, 8 ft high, and 20 ft long. Modifications were made to the ISO container for deflagration vents as well as clean agent pressure relief vents, as pictured in Figure 1 and described in the following sections.

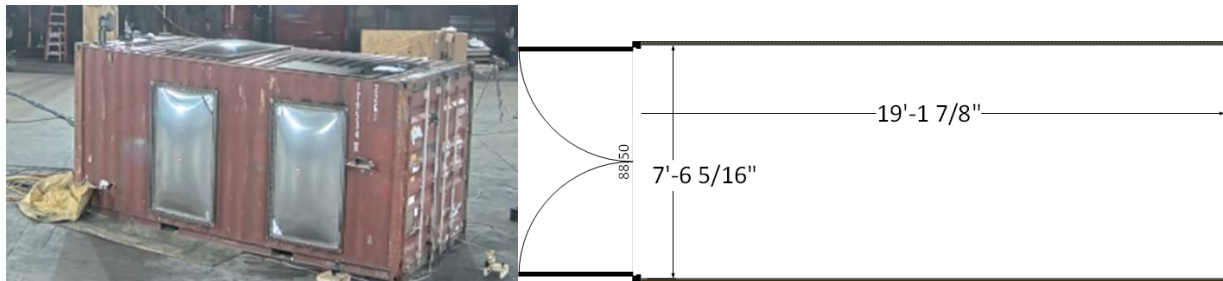


Figure 1 – ISO Container photo (left) and overall plan view dimensions (right).

#### Wall Construction

Three different types of wall construction were built up over the container walls, as detailed in Figure 2. The different wall constructions were designed to enable comparison of internal and external temperature measurements with thermal imaging, and associated impact on incident size-up considerations. The three different wall constructions represent different interior finish configurations observed through UL’s experience testing commercial ESSs. Figure 3 through Figure 7 illustrate the locations of each wall construction type within the container.

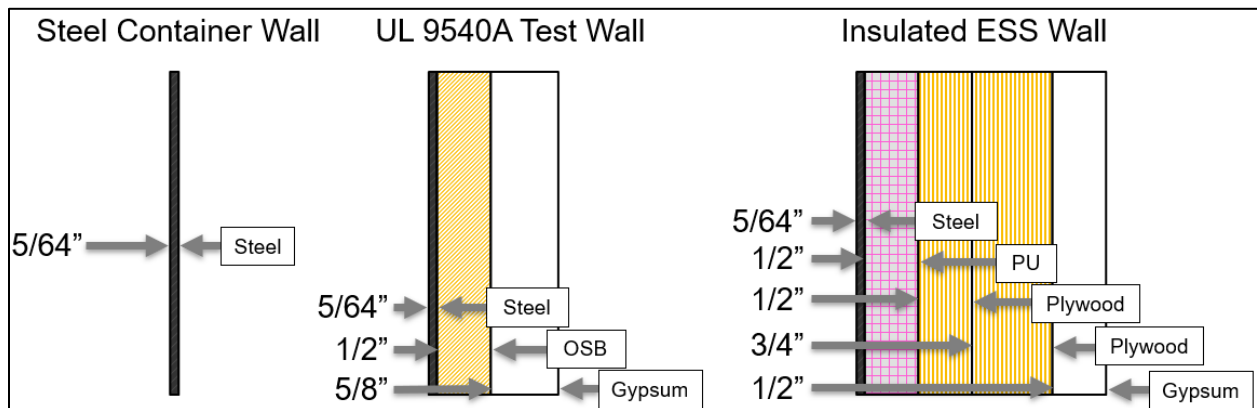
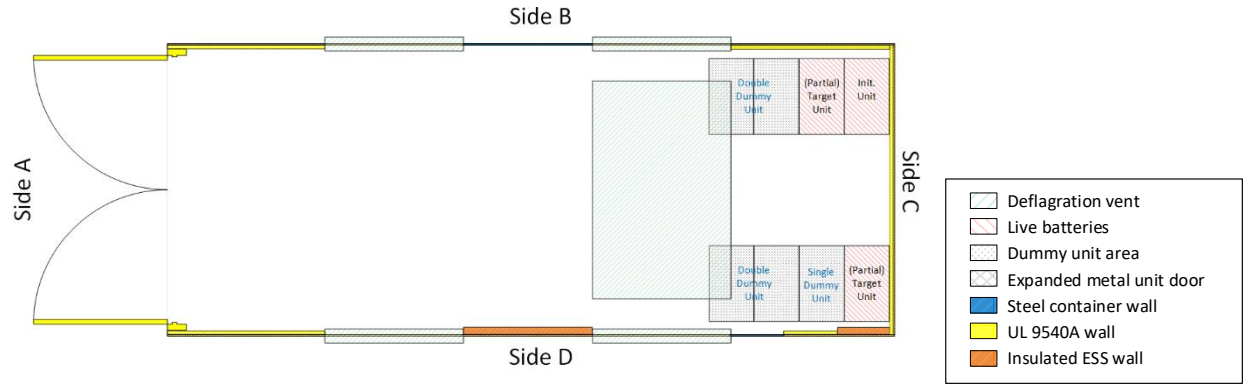


Figure 2 – Wall construction details, cross-section view.



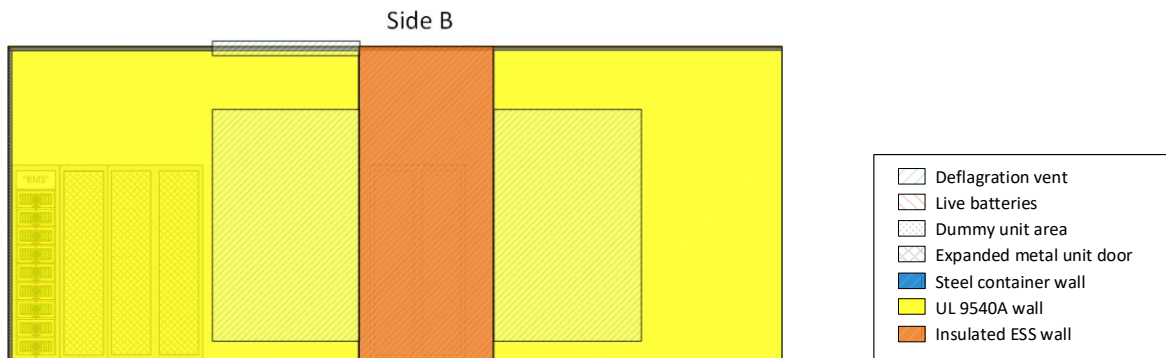
# UL 9540A INSTALLATION LEVEL TESTS WITH OUTDOOR LITHIUM-ION ENERGY STORAGE SYSTEM MOCKUPS



**Figure 3 – Wall construction layout, plan view.**



**Figure 4 – Side A wall construction layout, elevation view.**



**Figure 5 – Side B wall construction layout, elevation view.**



UL 9540A INSTALLATION LEVEL TESTS WITH OUTDOOR LITHIUM-ION ENERGY STORAGE SYSTEM MOCKUPS

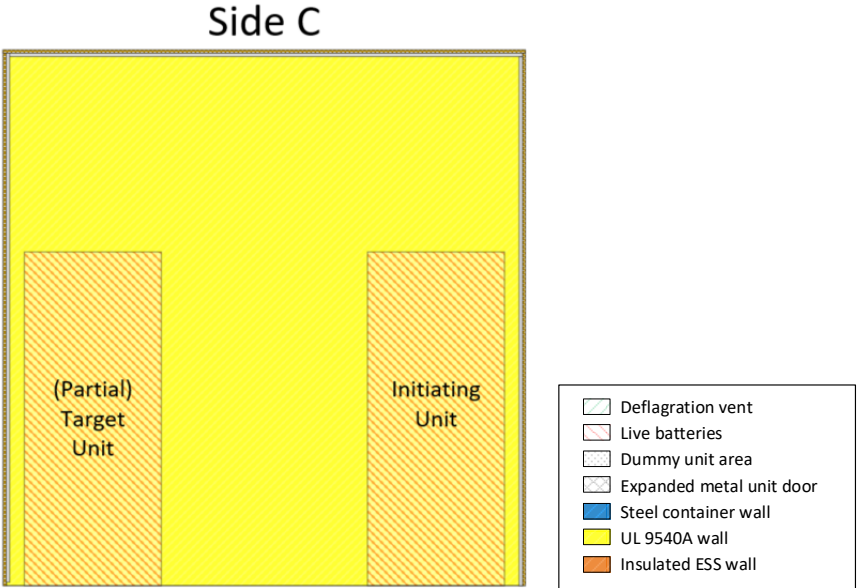


Figure 6 – Side C wall construction layout, elevation view.

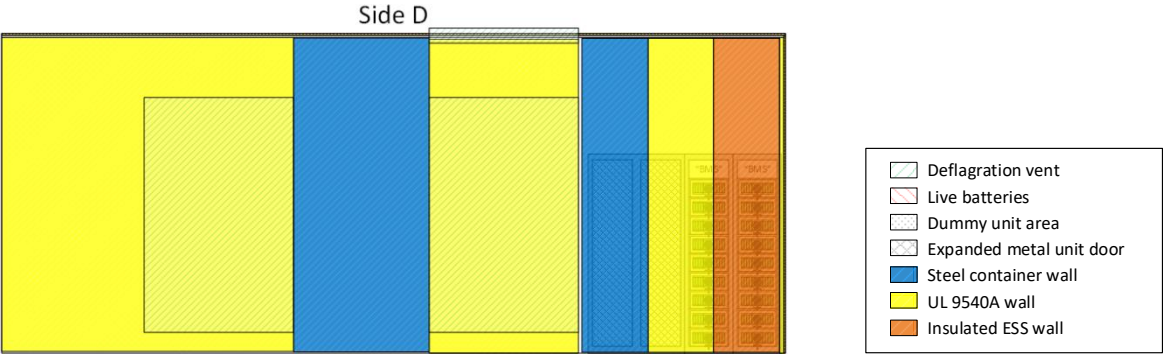


Figure 7 – Side D wall construction layout, elevation view.

# UL 9540A INSTALLATION LEVEL TESTS WITH OUTDOOR LITHIUM-ION ENERGY STORAGE SYSTEM MOCKUPS

## Deflagration Vents

Five vents were installed on the container for relief of pressure developed by deflagration. The size, position, and quantity of vents were determined using NFPA 68, Standard on Explosion Protection by Deflagration Venting [6]. The properties of the battery gas used in the calculations were determined from UL 9540A cell level testing and are shown in Table 2. Four vents were installed symmetrically along the long axis of the container. A fifth vent was installed in the ceiling of the container, as illustrated in Figure 8 and Figure 9.<sup>1</sup> Each vent was 44 in by 69 in with a static activation pressure of 0.5 psig  $\pm$  0.25 psig.

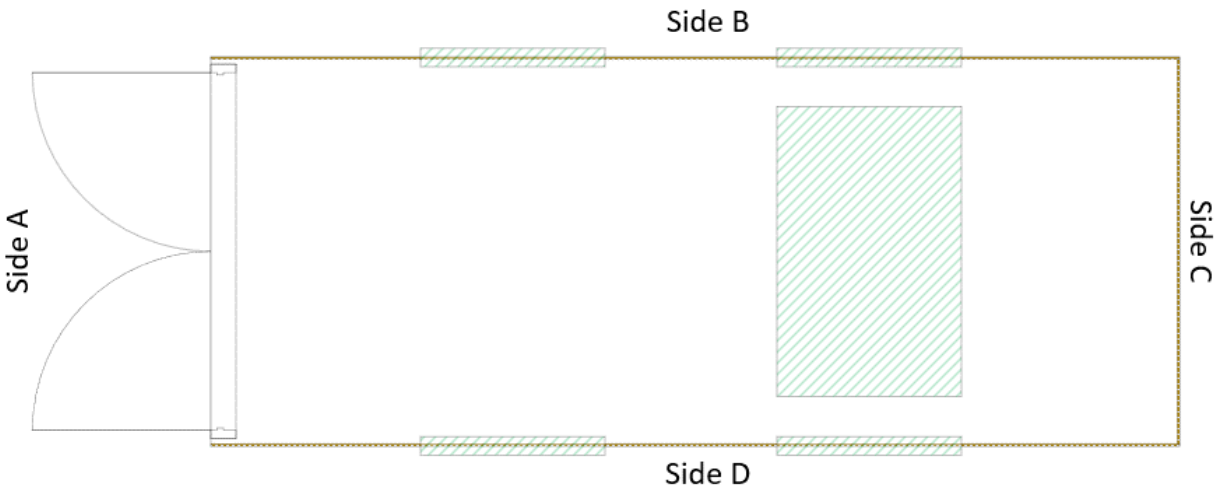


Figure 8 – Deflagration vent locations, plan view.



<sup>1</sup> Smaller panels shown in the right side of Figure 9 were for clean agent system pressure relief.

## UL 9540A INSTALLATION LEVEL TESTS WITH OUTDOOR LITHIUM-ION ENERGY STORAGE SYSTEM MOCKUPS

Figure 9 – External (left) and internal view (right) of deflagration vents.

### Clean Agent Suppression System

The clean agent suppression system was conservatively designed for a Novec 1230 concentration of 8.0 v%, based on minimum agent design concentrations of 6.2 v% to 6.7 v% determined from cup burner tests of battery electrolytes [8]. The clean agent distributor developed a piping system design to achieve the design concentration of 8.0% for a 1,216 ft<sup>3</sup> protected design volume over a discharge time of 7.5 seconds, per NFPA 2001 requirements [9]. The final measured container volume was 1,169 ft<sup>3</sup>, resulting in a delivered concentration of approximately 8.3%. The discharge nozzle (Figure 12), Fike model #80-124-125-X, was located in the center of the container. The nozzle was designed with a 360° discharge pattern and was connected with the 1¼ in schedule 40 steel piping in a layout documented in Figure 10 and Figure 11. One 1 ft<sup>2</sup> positive pressure relief vent and one 1 ft<sup>2</sup> negative pressure relief vent were installed as pictured in Figure 13. The vents were installed to relieve positive and negative pressures imposed by discharging the clean agent system to prevent damage to the relatively low static activation pressure deflagration vent panels. The vents were engineered using the Guide to Estimating Enclosure Pressure and Pressure Relief Vent Area for Applications Using Clean Agent Fire Extinguishing Systems, 3rd edition [10]. The positive pressure vent was held closed under approximately 1lb weight loaded in the center of the panel. The negative pressure vent was pulled closed using a 5lb weight and a cable pulley system, attached to the center of the panel. The actuation pressures were 0.01 psig and 0.03 psig, respectively.

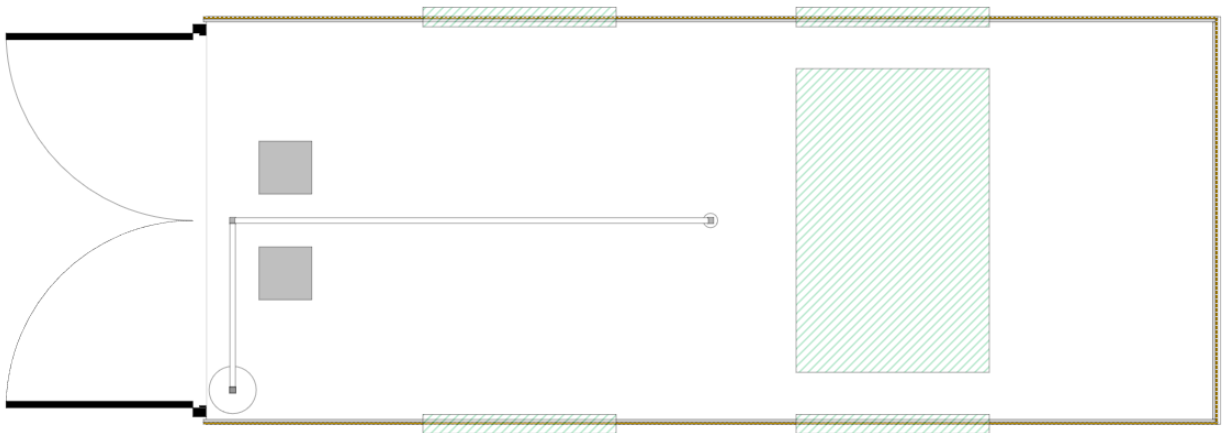


Figure 10 – Clean agent piping system to a central discharge nozzle, plan view.

UL 9540A INSTALLATION LEVEL TESTS WITH OUTDOOR LITHIUM-ION ENERGY STORAGE SYSTEM MOCKUPS

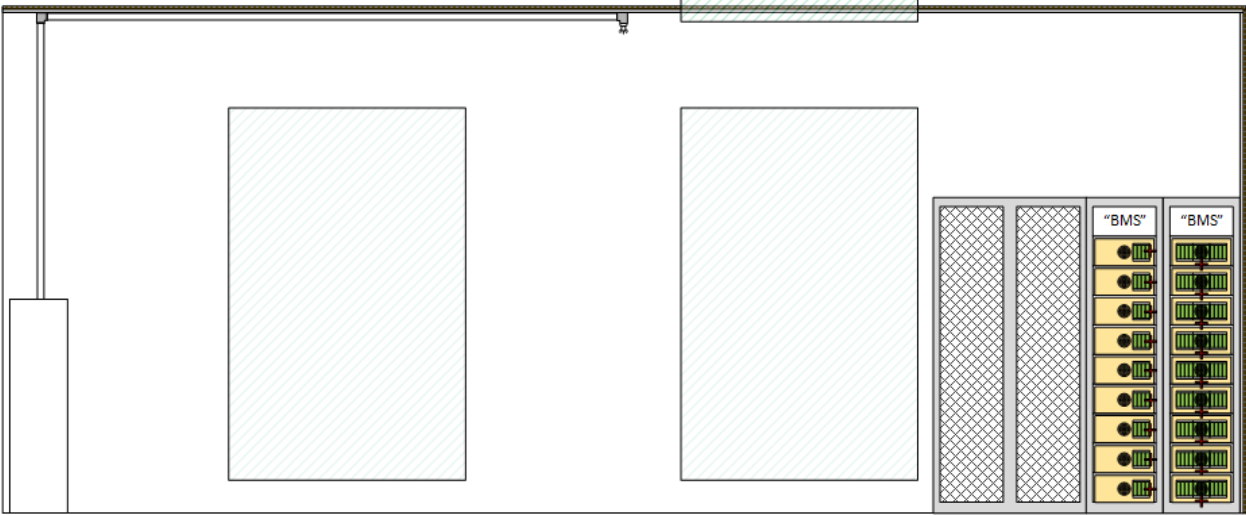


Figure 11 – Clean agent piping system to a central discharge nozzle, elevation view.



Figure 12 – Clean agent discharge nozzle.



Figure 13 – Positive pressure relief vent (left) and negative pressure relief vent (right).

# UL 9540A INSTALLATION LEVEL TESTS WITH OUTDOOR LITHIUM-ION ENERGY STORAGE SYSTEM MOCKUPS

## Water Suppression System

The water suppression system was engineered to represent a dry pipe system that provides a uniform 0.5 gpm/ft<sup>2</sup> delivered spray density at the elevation of the top of the ESS unit enclosures, as illustrated in Figure 14. The design density was selected to be consistent with FDNY ESS permitting requirements. Four open nozzles were utilized directly above the occupied ESS unit enclosures, as illustrated in Figure 15 and Figure 16. Each nozzle was a Spraying Systems Fulljet 35WSQ nozzle with a wide square spray pattern ( $k=1$ , at 50 psig).

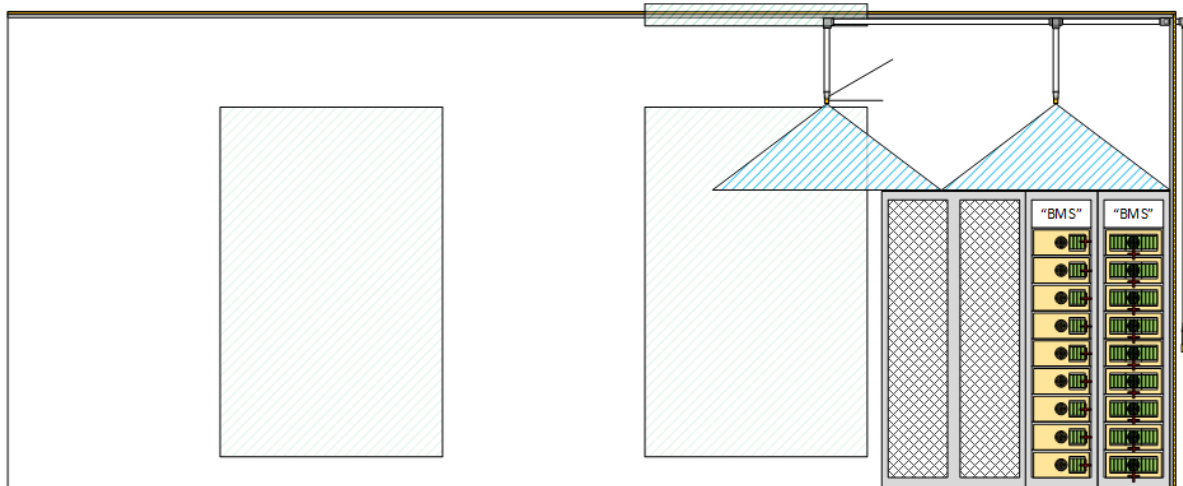


Figure 14 – Water suppression nozzle arrangement and spray pattern, elevation view.

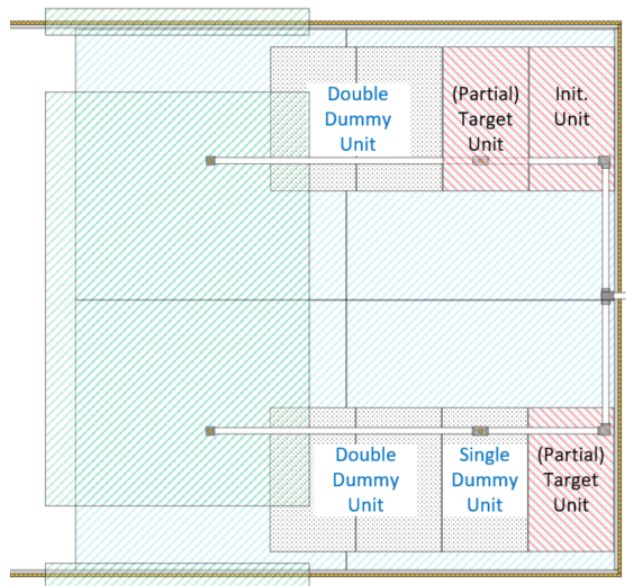


Figure 15 – Nozzle arrangement above ESS unit enclosures, plan view.



## UL 9540A INSTALLATION LEVEL TESTS WITH OUTDOOR LITHIUM-ION ENERGY STORAGE SYSTEM MOCKUPS



**Figure 16 – Location of four water suppression nozzles above ESS unit enclosures.**

Waterflow was initiated from the laboratory fire pump after the activation of a 165 °F standard response sprinkler link and a 30 second delay to simulate pipe filling from a siamese water connection. Actual water delivery included additional time to fill 65 ft of 1.5 in fire hose and the piping installed in the container. The sprinkler link was positioned in the center of the room and 6 in below the ceiling. The height was selected to be within the 1 in to 12 in range specified for smooth, unobstructed ceilings in NFPA 13 [11] and NFPA 15 [12].

### **2.1.2 Energy Storage System Units**

Inside the ISO container, the mock-up ESS was comprised of three different configurations: an Initiating Unit, two Target Units, and three dummy units. The Initiating Unit was filled with cells to its designed capacity and was used to create a condition of cell-to-cell propagating thermal runaway. Target Units, partially filled with cells, were placed adjacent to the Initiating Unit to enable the potential for unit-to-unit propagation of thermal runaway. Dummy units were used as ESS system mock-up visual aids.

#### **Initiating Unit**

The Initiating Unit included nine modules, each filled with nine mockup cells consisting of 30 component 18650 cells (Table 3). For these tests, unlike UL 9540A standard tests, the cells and modules were not electrically connected. Based on the previous cell, module, and unit test series, this configuration demonstrated the hazards of ESS installations effectively without requiring additional electrical connections. All cells in the ESS were charged to 100% state of charge.

## UL 9540A INSTALLATION LEVEL TESTS WITH OUTDOOR LITHIUM-ION ENERGY STORAGE SYSTEM MOCKUPS

The enclosures for cells and modules were made of ABS plastic. The module enclosures had vent holes in the center of the front and back faces to simulate similar vents in energy storage modules. The structure of the Initiating Unit was constructed from solid sheet steel panels with perforated steel shelves to support each module. The front of the Initiating Unit was open to the container. The back and right side of the Initiating Unit was covered by uninterrupted steel sheets. The left side was covered with expanded steel sheets. The openings in the expanded steel enabled the communication of hot gases from the Initiating Unit to the Left Target Unit during testing.

The Initiating Module (Figure 17) was installed in the position third from the bottom in the Initiating Unit (Figure 18). The numbering convention for the modules was numbered 1 to 9 from bottom to top. The Initiating (Mockup) Cell was located in the center of the Initiating Module. Within the Initiating (Mockup) Cell, flexible film heaters were wrapped around two component 18650 cells. One 18650 li-ion cell was heated to initiate the first thermal runaway event, and the second cell was available for the unlikely occurrence of a malfunction. The instrumented 18650 cells were heated at a rate of 6 °C/min.

The cell design was characterized by cell level UL 9540A testing. The properties presented in Table 2 were utilized for installation level performance criteria and associated hazard analyses.


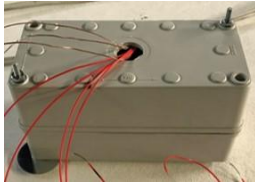


**Table 2 – Cell level thermal runaway properties.**

Property	Measurement
Cell vent temperature	130 °C
Thermal runaway temperature	204 °C
Gas volume	213 L
Gas composition	36.2 v% carbon monoxide; 22.1 v% carbon dioxide; 31.7 v% hydrogen; 10.0 v% hydrocarbons  <u>Hydrocarbon breakdown</u> 7.4 v% methane; 0.92 v% ethylene; 0.61 v% ethane; 0.22 v% propylene; 0.04 v% propane; 0.07 v% C4-hydrocarbons; 0.24 v% benzene; 0.03 v% toluene; 0.38 v% dimethyl carbonate
Gas LFL	8.9 v%
Gas UFL	40 v%
Gas Pmax	93 psig
Gas burning velocity	35 cm/s



**UL 9540A INSTALLATION LEVEL TESTS WITH OUTDOOR LITHIUM-ION ENERGY STORAGE SYSTEM MOCKUPS**

**Table 3 – Initiating cell, module, and unit characteristics.**

<b>Feature</b>	<b>18650 Component</b>	<b>Cell</b>	<b>Module</b>	<b>Unit</b>
Picture				
Capacity	3.2 Ah (12 Wh)	99 Ah (356 Wh)	891 Ah (3.2 kWh)	8019 Ah (28.9 kWh)
Nominal Voltage	3.6 V	3.6 V	3.6 V	3.6 V
Weight	45 g	1.7 kg	27.2 kg	225 kg
Quantity of 18650 li-ion cells	1	30	270	2,430
Dimensions	18 mm x 65 mm	172 mm x 92 mm x 92 mm	508 mm x 406 mm x 171 mm	1400 mm x 368 mm x 610 mm



# UL 9540A INSTALLATION LEVEL TESTS WITH OUTDOOR LITHIUM-ION ENERGY STORAGE SYSTEM MOCKUPS

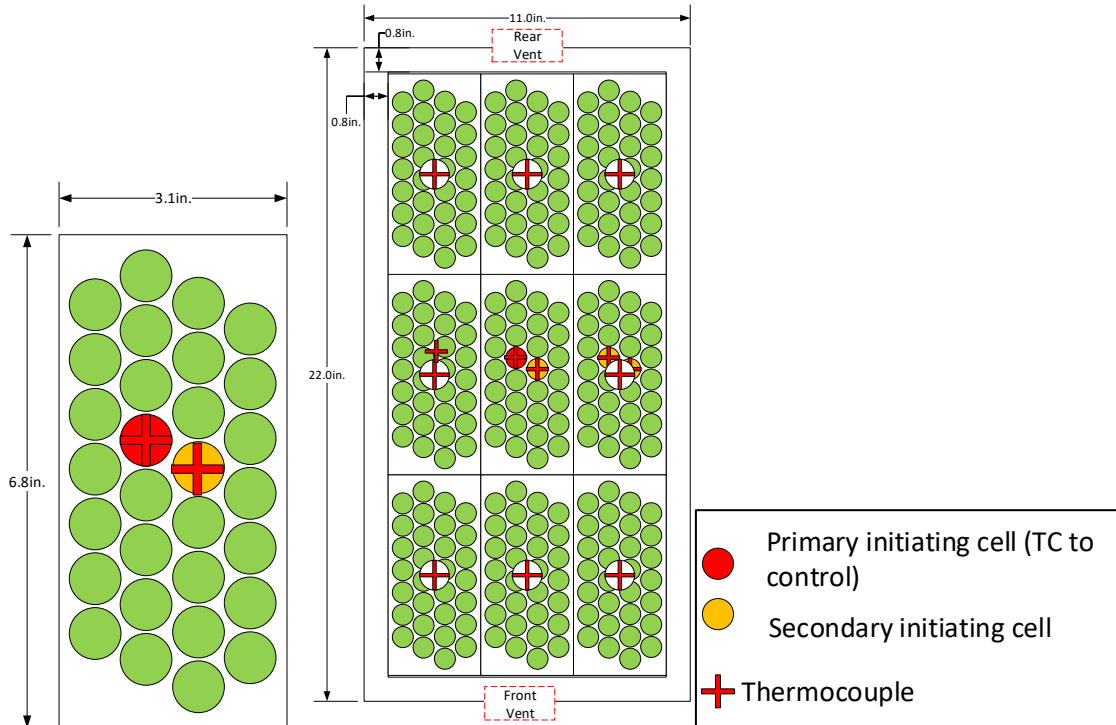


Figure 17 – Initiating Cell (left) and Initiating Module (right) constructed from 18650 cells.

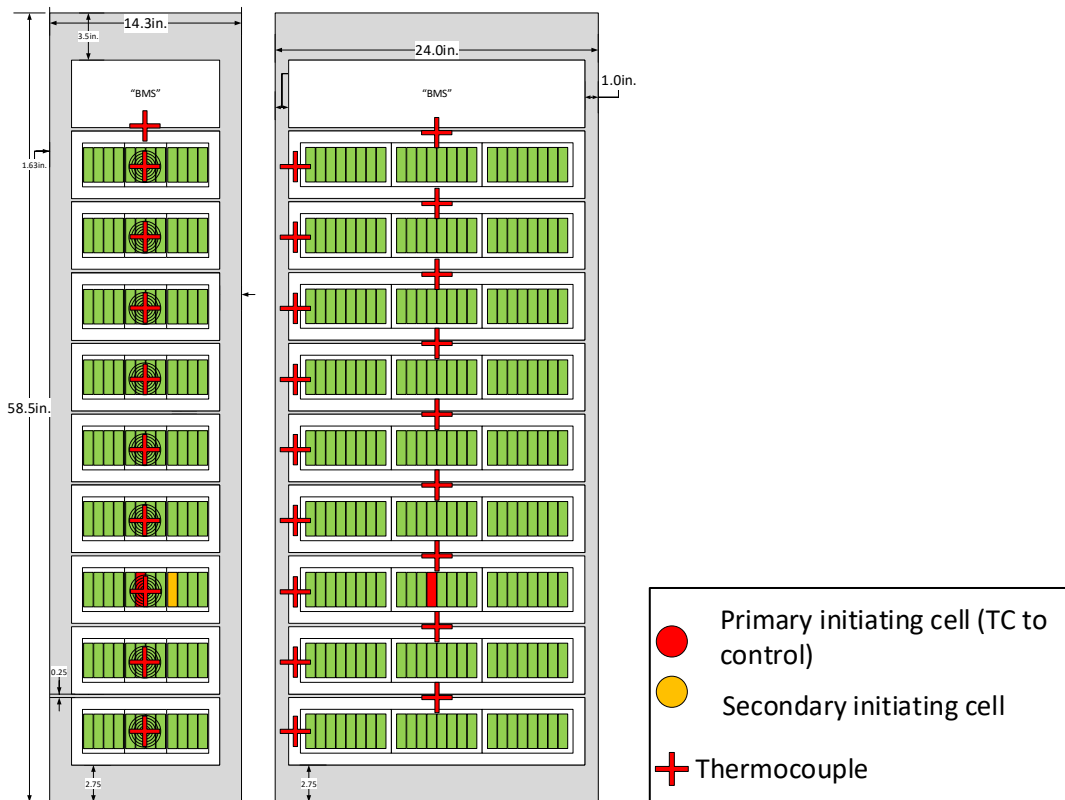


Figure 18 – Initiating Unit construction.

# UL 9540A INSTALLATION LEVEL TESTS WITH OUTDOOR LITHIUM-ION ENERGY STORAGE SYSTEM MOCKUPS

## Target Units

Two Target Units were positioned adjacent to the side and front of the Initiating Unit. The construction of these units was consistent with the Initiating Unit, except each target unit was loaded with one third of the cells of the Initiating Unit, equal to 780 total 18650 cells. For clarity, these units have been marked on drawings as “(Partial) Target Units” to indicate that they contained li-ion cells. The cells were positioned within the Target Unit closest to the Initiating Unit. All cells in the Target Units were charged to 100% state of charge. Although UL 9540A does not require live cells in the target units to evaluate performance criteria, the cells were included in these tests to exemplify the phenomena of thermal runaway propagation between neighboring units.

The layouts for the Left Target Unit and Front Target Unit are included in Figure 19 and Figure 20, respectively.

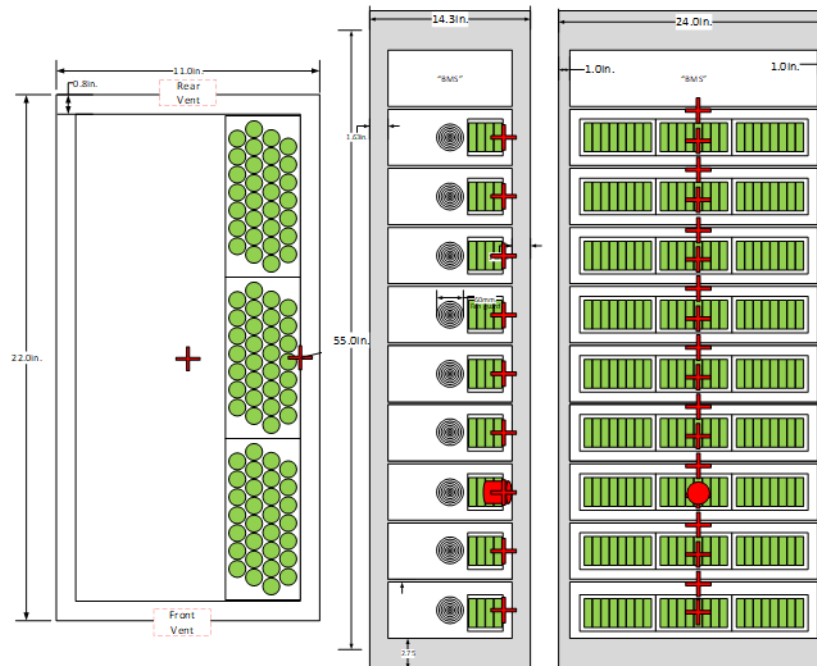


Figure 19 – Left Target Unit layout.

# UL 9540A INSTALLATION LEVEL TESTS WITH OUTDOOR LITHIUM-ION ENERGY STORAGE SYSTEM MOCKUPS

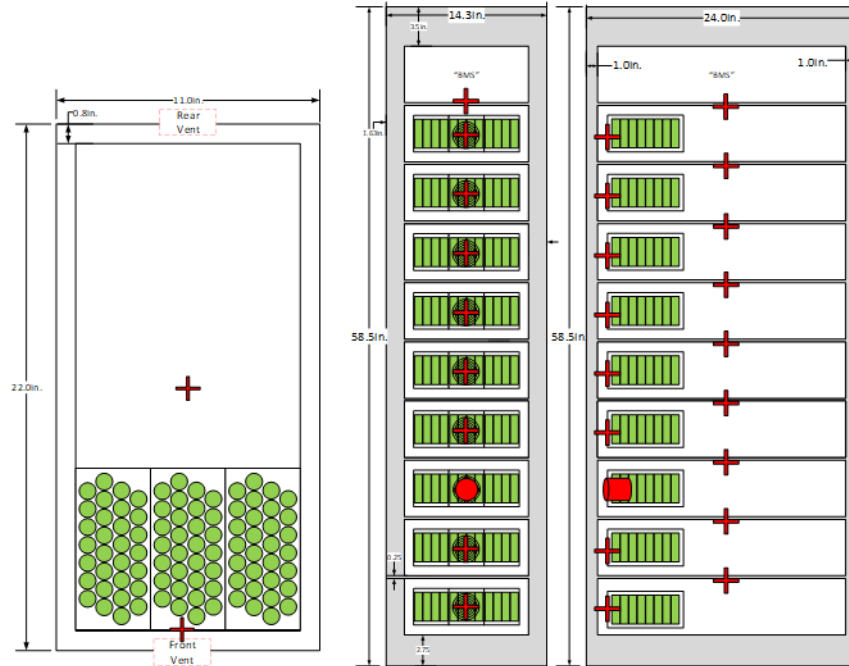


Figure 20 – Front Target Unit layout.

## Dummy Units

Dummy units (Figure 21) were included adjacent to the Target Units to create realistic obstructions in the ESS installation as visual aids.

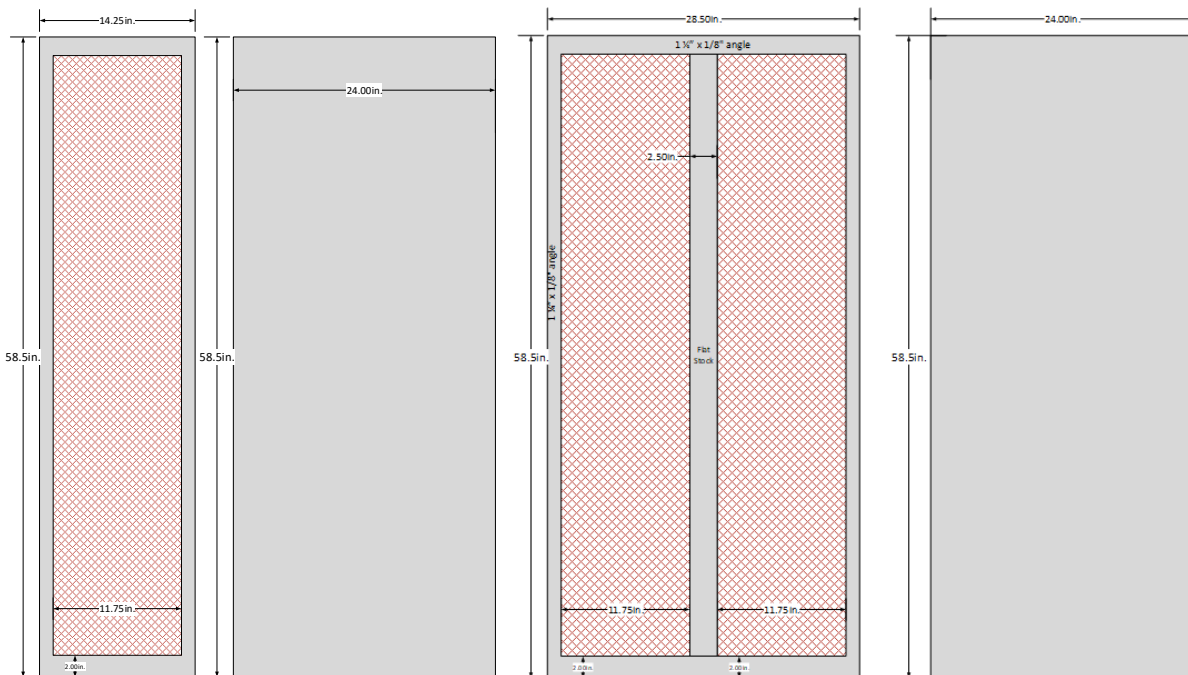
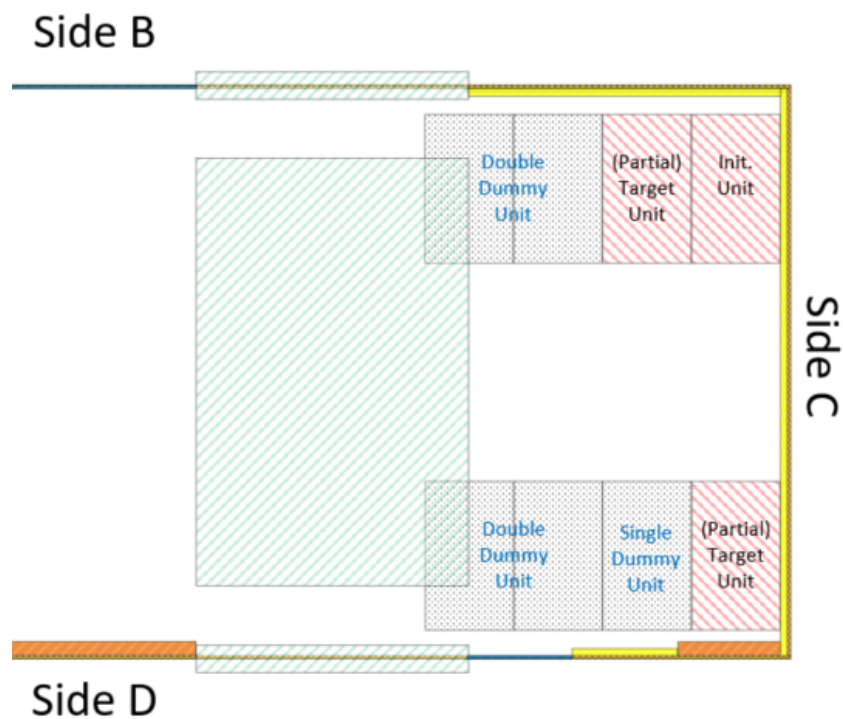


Figure 21 – Single dummy unit (left) and double dummy unit (right).

## UL 9540A INSTALLATION LEVEL TESTS WITH OUTDOOR LITHIUM-ION ENERGY STORAGE SYSTEM MOCKUPS

Per the guidelines of UL 9540A 4<sup>th</sup> edition, one complete unit charged to 100% was positioned as the Initiating Unit. The Initiating Unit was placed in a corner next to two instrumented walls and two instrumented Target Units. Next to the Target Units, dummy units were placed to represent realistic obstructions and installation conditions. There was 0 in of spacing between the Initiating Unit and the Left Target Unit, as well as the side instrumented wall. The Initiating Unit was placed with 3 in of clearance between the unit and the back instrumented wall. The Front Target Unit was placed across from the Initiating Unit, separated by a 35 in aisle, as summarized in Table 4. The installation is described in Figure 22 and pictured in Figure 23.

Details of the Initiating Unit, Targets, and instrumented walls are presented in the following sections.



**Figure 22 – Initiating unit and target unit spacing.**

**Table 4 – Initiating unit spacing relative to target units and adjacent walls.**

Dimension	Spacing
Aisle	35"
Unit side to wall	0"
Unit rear to wall	3"
Unit to unit	0"

## UL 9540A INSTALLATION LEVEL TESTS WITH OUTDOOR LITHIUM-ION ENERGY STORAGE SYSTEM MOCKUPS



**Figure 23 – Initiating Unit, Left Target Unit, and double dummy unit (left); Front Target Unit, single dummy unit, and double dummy unit (right).**

### **2.2 Instrumentation**

The instrumentation layout is illustrated in Figure 25 through Figure 27 with an instrumentation key included in Figure 24. Instrumentation was positioned to evaluate UL 9540A performance criteria, to characterize conditions inside the container, to consider gas detection approaches, to monitor the extent of thermal runaway propagation, and to provide data to develop firefighter size-up considerations.

# UL 9540A INSTALLATION LEVEL TESTS WITH OUTDOOR LITHIUM-ION ENERGY STORAGE SYSTEM MOCKUPS

	Pressure Transducers
	IR View Reference Thermocouples
	Gas Temperature Thermocouple Array
	Battery Temperature Thermocouples
	Wall Temp. Thermocouple Array (plan view)
	Smoke Detector
	Smoke Obscuration Meter
	Gas Measurement Probe
	Hydrogen Gas Detector
	LEL Gas Detector
	Carbon Monoxide Detector
	Heat Flux Gauge
	Deflagration Vent
	Live Batteries
	Dummy Unit Area
	Expanded Metal Unit Door

Figure 24 – Instrumentation key.

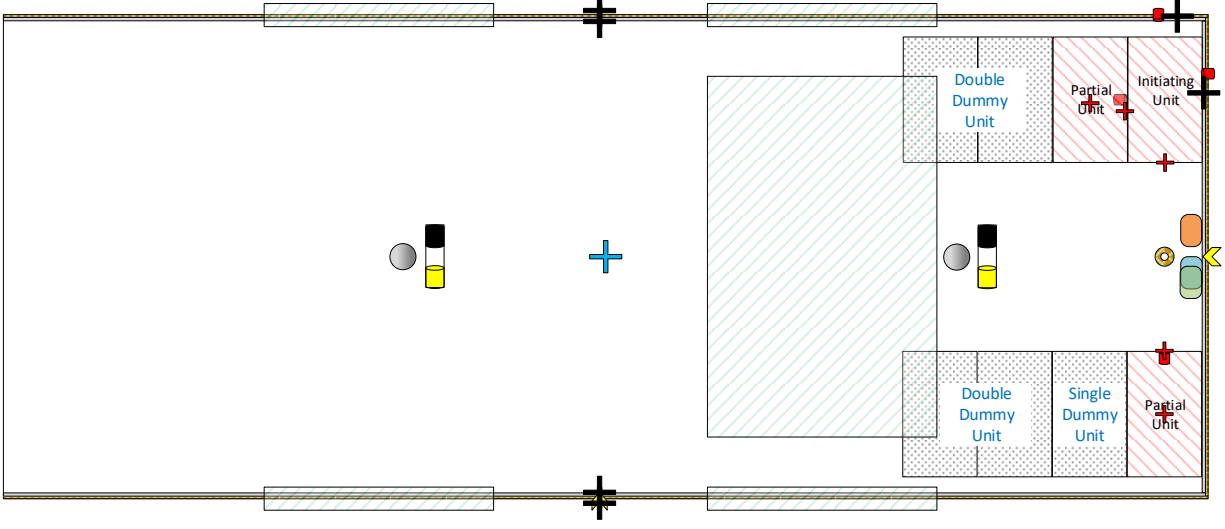


Figure 25 – Container instrumentation plan view.

# UL 9540A INSTALLATION LEVEL TESTS WITH OUTDOOR LITHIUM-ION ENERGY STORAGE SYSTEM MOCKUPS

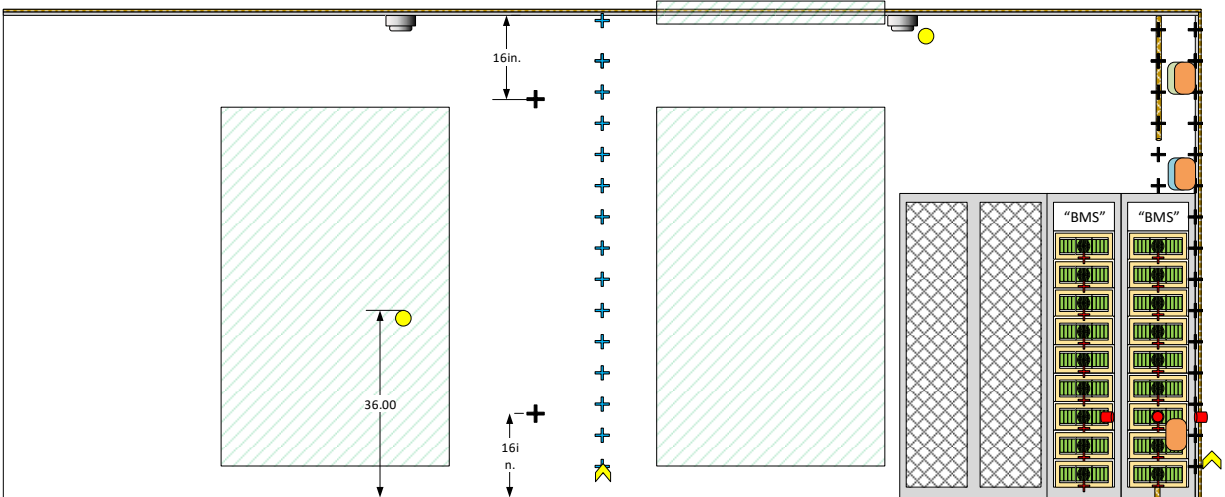


Figure 26 – Container instrumentation elevation view (long axis).

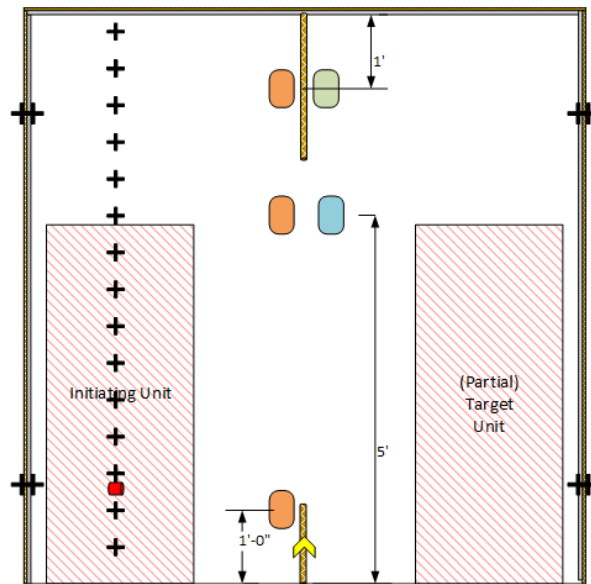


Figure 27 – Container instrumentation elevation view (short axis).

## 2.2.1 Container

Instrumentation was installed in the container to assess the conditions inside in terms of temperature, thermal exposure, pressure, and gas composition.

### Thermocouples

Container gas and wall surface temperatures were monitored using three thermocouple arrays and additional single point thermocouple measurements. Array thermocouples were 24 American Wire Gauge (AWG) Type K and single thermocouples were 30 AWG Type K. Wall surface temperatures are reported with 60-second averaging to assist with interpretation of results.



## UL 9540A INSTALLATION LEVEL TESTS WITH OUTDOOR LITHIUM-ION ENERGY STORAGE SYSTEM MOCKUPS

One thermocouple array was attached to each instrumented wall, to the side and rear of the Initiating Unit. The arrays were centered on the Initiating Unit with a thermocouple located every vertical 6 in from floor to ceiling. The walls instrumented with the thermocouple arrays were painted flat black to enhance and control emissivity. UL 9540A utilizes these temperature measurements to evaluate the performance criteria of UL 9540A Section 10.5.1:

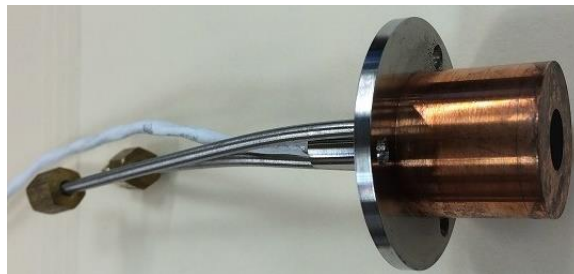
“For BESS units intended for installation in locations with combustible construction, surface temperature measurements along instrumented wall surfaces shall not exceed a temperature rise of 97 °C (175 °F) above ambient. Surface temperature rise is not applicable if the intended installation is composed completely of noncombustible materials in which wall assemblies, cables, wiring, and any other combustible materials are not to be present in the BESS installation. In this case, the report shall note that the installation shall contain no combustible materials.”

The third thermocouple array was installed in the center of container to measure gas temperatures. Thermocouples were installed every 6 in vertically from floor to ceiling.

Additional pairs of thermocouples were installed coaxially through the thickness of the wall in four locations on corresponding internal and external surfaces of the container. These thermocouples were used to compare the difference in thermal conditions from the interior or exterior of the container, and to serve as reference points for thermal imaging cameras.

### Heat Flux

One Schmidt-Boelter heat flux gauge was installed flush with the surface of each instrumented wall at the height of the Initiating Module to measure the thermal stress applied from the ESS to the adjacent wall. Wall surface heat flux measurements are reported with 60-second averaging.



**Figure 28 – Schmidt-Boelter heat flux gauge.**



# UL 9540A INSTALLATION LEVEL TESTS WITH OUTDOOR LITHIUM-ION ENERGY STORAGE SYSTEM MOCKUPS

## Pressure

Container pressure was measured with two pressure transducers. The pressure differential between the container and its exterior was measured with a differential pressure transducer with a range of -100 to 100 Torr (-1.9 to 1.9 psig). The absolute pressure inside the container was measured by an absolute pressure transducer with a range of 0 to 15 psia (vacuum to 15.5 Torr-g).

## Gas Analysis

A combination of analytical instruments and common industrial gas detectors were used to characterize the gas composition inside the container, as summarized in Table 5. Gas samples near the ceiling and floor were extracted from the container and transported by heated lines to analytical instruments. The sample taken near the ceiling was analyzed for oxygen, carbon monoxide, carbon dioxide, hydrogen, and total hydrocarbon concentrations. The sample taken near the floor was analyzed for total hydrocarbon concentrations to measure the stratification of lighter and heavier than air hydrocarbons.

Common industrial gas detectors included hydrogen detectors, carbon monoxide detectors, and combustible gas detectors. The industrial gas detectors were selected to be representative of the types that may be installed in ESS installations; the data from these meters is intended to represent what may be available for hazard assessment if the signals are remotely monitored. All three detector types were mounted on the wall between the Initiating Unit and Front Target Unit. Three combustible gas detectors were utilized to compare with total hydrocarbon measurements of stratification in the gas layer.

**Table 5 – Analytical and wall-mounted gas measurement equipment.**

Gas	Measurement Location	Measurement Principle
Oxygen	Ceiling probe	Paramagnetic
Carbon dioxide	Ceiling probe	Nondispersive Infrared (NDIR)
Carbon monoxide	Ceiling probe	NDIR
Carbon monoxide	Wall-mounted detector at 1.6 m	Electrochemical
Hydrogen	Ceiling probe	Palladium-nickel
Hydrogen	Wall-mounted detector at 2.1 m (ceiling)	Electrochemical
Total hydrocarbons	Ceiling probe; floor probe	Flame ionization detection (FID)
Combustible gas (%LEL, methane)	Wall-mounted detectors at: 0.3 m (floor) 1.6 m (middle) 2.1 m (ceiling)	Catalytic bead



# UL 9540A INSTALLATION LEVEL TESTS WITH OUTDOOR LITHIUM-ION ENERGY STORAGE SYSTEM MOCKUPS

## Smoke Measurement

Smoke was measured two ways: smoke obscuration and smoke detection.

### Smoke Obscuration

Smoke obscuration was measured at the ceiling adjacent to the smoke detector near the ESS unit enclosures and 3 ft above the floor below the second smoke detector. Obscuration was measured with a white light source and photocell receiver with a 3 ft path between them. Obscuration is calculated as extinction coefficient by:

$$k = -\frac{1}{L} \ln \left( \frac{I}{I_0} \right)$$

where  $k$  is the extinction coefficient ( $m^{-1}$ );  $I_0$  is the initial clear beam signal received by the photocell (V);  $I$  is the beam signal received by the photocell through the smoke layer (V); and  $L$  is the path length between light source and receiver (m).

### Smoke Detection

Two commercially available smoke detectors were installed along the centerline of the container and evenly spaced at one-third of the lengths of the container. The smoke detector closer to the Initiating Unit was labelled “Near” and the second was labelled “Far.” Both detectors were combination photoelectric/ionization. Smoke detectors were incorporated because of their common application as initiating devices for fire alarm and fire suppression systems.

## 2.2.2 ESS Units

### Initiator

Two 24 ga. Type K thermocouples were installed in each module of the initiating unit; one was installed on the underside of the lid in the center of the module, and one was installed inside the front vent opening of the module (Figure 18). Both thermocouples were used to determine whether thermal runaway had occurred within the module.

### Targets

Two 24 ga. Type thermocouples were installed in each module of the target units; one was installed on the underside of the lid in the center of the module, and one was installed on the inner side of the module closest to the Initiating Unit (Figure 19, Figure 20). These thermocouples were used to determine whether thermal runaway had occurred within the target modules. The thermocouple on the side closest to the Initiating Unit was used to evaluate the performance criteria within UL 9540A, 4<sup>th</sup> edition, Section 10.5.2:



## UL 9540A INSTALLATION LEVEL TESTS WITH OUTDOOR LITHIUM-ION ENERGY STORAGE SYSTEM MOCKUPS

“The surface temperature of modules within the BESS units adjacent to the initiating BESS unit shall not exceed the temperature at which thermally initiated cell venting occurs.”

Heat flux gauges were installed in each Target Unit at the same elevation (third from the bottom) as the Initiating Module within the Initiating Unit. Heat flux gauges were positioned facing towards the Initiating Module. Target heat flux measurements are reported with 60-second averaging.



Figure 29 – Heat flux gauges installed for Left Target Unit (left) and Front Target Unit (right),

### 2.2.3 Fire Service Size-up Equipment

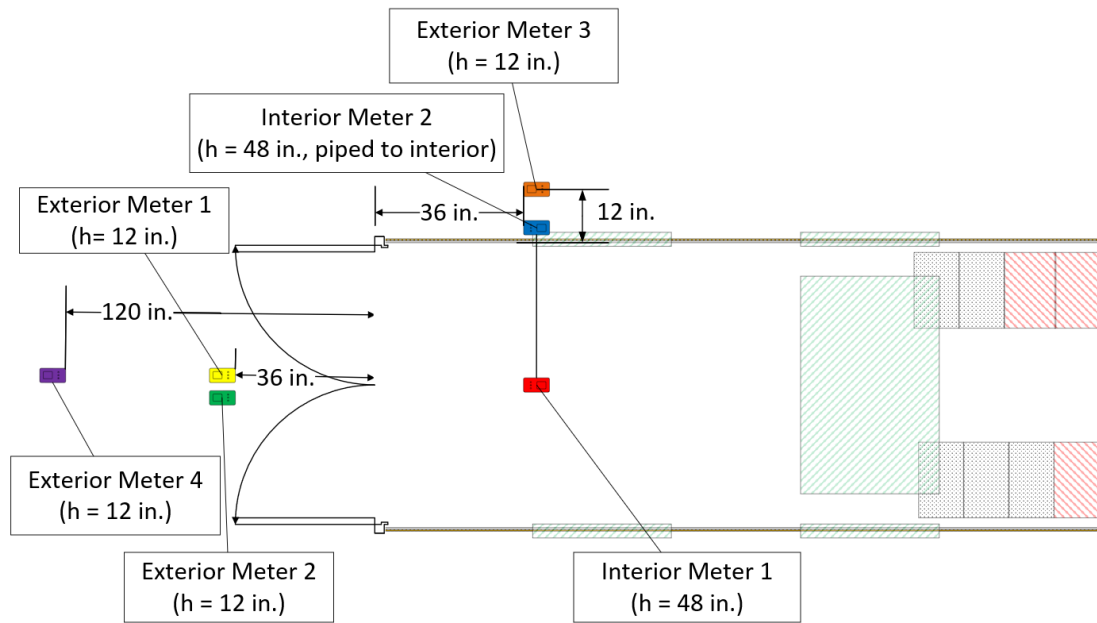
#### Portable Gas Meters

#### Meter Locations

Fire service portable gas monitors were placed at locations both inside and outside the container to assess their ability to detect products of thermal runaway and inform fire service size-up decisions. Four models of meter were used. Table 6 lists these meters, the labels that will refer to them in this document, and the quantities they measured. Figure 30 shows the location of the meters in and around the container. Two meters, labeled Interior Meter 1 and Interior Meter 2, had a sample point located inside of the container. The sample point was located 48 in above the ground and 36 in inside the container door, approximately at the standing height of a fire department entry team. Although the diffusion meter was located inside of the container itself, the pumped meter was connected to the sample location with a length of 3/8" stainless steel tubing.



## UL 9540A INSTALLATION LEVEL TESTS WITH OUTDOOR LITHIUM-ION ENERGY STORAGE SYSTEM MOCKUPS



**Figure 30 – Fire service portable gas meter locations.**

The exterior meters were elevated 12 in. above the ground in an effort to simulate firefighters sampling the vapor clouds traveling along the ground. Exterior Meter 3 was located on the B-side of the structure, 36 in. from the front wall offset 12 in. from the B-side of the container, as indicated in Figure 30. Two meters, one diffusion model and one pumped model (Exterior Meter 1 and Exterior Meter 2), were placed 36 in. offset from the centerline of the container doors, as shown in Figure 30. The final two meters were placed 120 in. back from the centerline of the container doors.

### Gas Sensor Technologies

A range of gas sensor technologies commonly utilized by fire service and hazardous materials personnel were used to monitor the experiments. The technologies used to instrument the experiments were chosen to represent a wide range of sensor technologies and manufacturers. The meters containing many of the sensors were typical multi-gas meters of both pumped and diffusion style. Gas meters are categorized as either pumped- or diffusion-style meters. The pumped meters included a sampling pump that can extract a sample from a remote location for analysis. Diffusion style meters require direct contact with the gas atmosphere to sample. Only the diffusion style meters were designed to measure hydrogen. The technologies utilized by each meter in this set of experiments are listed in Table 6.

The breadth of specific gases and measurement ranges for the sensors was chosen to correlate the conditions inside the ESS to the measurements yielded by fire service personnel conducting 360-degree size-ups. Additionally, measurements were utilized to investigate potential cross-sensitivities in the measurements due to the presence of gases

## UL 9540A INSTALLATION LEVEL TESTS WITH OUTDOOR LITHIUM-ION ENERGY STORAGE SYSTEM MOCKUPS

and vapors released during an ESS thermal runaway event and subsequent mitigation activities. The following sections provide some technical background on the sensor technologies and provide some general justification for their inclusion in these experiments.

**Table 6 – Gas sensor technologies.**

Meter Label	Interior Meter 1	Interior Meter 2	Exterior Meter 1	Exterior Meter 2	Exterior Meter 3	P4	D3
Style	Diffusion	Pumped	Diffusion	Pumped	Pumped	Pumped	Diffusion
<b>Measurements</b>							
O <sub>2</sub>	X		X	X	X	X	
CO	X	X	X	X	X	X	
HCN	X	X		X		X	
H <sub>2</sub> S		X	X		X	X	
H <sub>2</sub>	X		X				
Volatile Organic Compounds (Photoionization)				X			
LEL (NDIR)*		X					
LEL (Catalytic Bead)	X <sup>+</sup>	X <sup>+</sup>	X <sup>+</sup>	X <sup>+</sup>	X <sup>+</sup>	X <sup>+</sup>	

\* calibrated to LEL of methane gas

+ calibrated to LEL of pentane gas

### Electrochemical

Electrochemical sensors generally consist of at least three distinct components. These components include a sensing electrode, a counter electrode, and an ion conductor between the two electrodes. The operating principle of electrochemical gas sensors involves the reduction or oxidation of a target gas at the sensing electrode, which generates an electric potential or the flow of current through the ion conductor to the counter electrode. Electrochemical sensors may be the amperometric type, in which the measurand is the current between the electrodes, or the potentiometric type, in which the measurand is the electric potential between the two electrodes [13].

To relate the current or electric potential between the electrodes to a specific target gas concentration, the rate of gas flow to the sensing electrode must be controlled. This is often achieved using a diffusion film or a pinhole. The flow control mechanism may also incorporate filters to selectively allow gas species to come in contact with the sensing electrode. The flow control mechanism is a possible point of failure or source of uncertainty for electrochemical sensors that have been exposed to atmospheres that compromise the integrity of the mechanism. Silicon vapors, sulfuric acid gas, and excessive condensation of water vapor may foul the permeable diffusion film. Additionally, salt-water spray, basic gases, dust or oil mist, and frozen water may permanently affect the ability of the sensor to accurately measure gas concentrations.



## UL 9540A INSTALLATION LEVEL TESTS WITH OUTDOOR LITHIUM-ION ENERGY STORAGE SYSTEM MOCKUPS

Due to the relative simplicity of electrochemical gas sensors and the inability to completely filter out unwanted gas species, electrochemical sensors often suffer from cross-sensitivities in which the presence of a non-target gas interferes with the measurement and indicates an erroneously higher or lower target gas measurement. Table 7 shows typical cross sensitivities for the gases of interest in this work [14, 15, 16].

**Table 7 – Typical cross-sensitivities for the electrochemical sensors in these tests.**

<b>RAE Systems</b>				
Cross-Sensitivity %	Gas			
Sensor	CO	H <sub>2</sub> S	HCN	H <sub>2</sub>
<b>CO</b>	100%	0%	N/A	40%
<b>CO-H<sub>2</sub> Compensated</b>	100%	N/A	N/A	1%
<b>H<sub>2</sub>S</b>	1%	100%	N/A	N/A
<b>HCN</b>	5%	600%	100%	N/A
<b>H<sub>2</sub></b>	20%	20%	30%	100%
<b>MSA</b>				
Cross-Sensitivity %	Gas			
Sensor	CO	H <sub>2</sub> S	HCN	H <sub>2</sub>
<b>CO</b>	100%	0%	-5%	48%
<b>H<sub>2</sub>S</b>	1%	100%	-3%	0%
<b>HCN</b>	0%	400%	100%	0%
<b>Ventis</b>				
Cross-Sensitivity %	Gas			
Sensor	CO	H <sub>2</sub> S	HCN	H <sub>2</sub>
<b>CO</b>	100%	5%	15%	22%
<b>H<sub>2</sub>S</b>	1%	100%	-1%	0%
<b>HCN</b>	0%	10%	100%	0%

Electrochemical sensors are a low-cost and low-power option for measuring oxygen concentration as well as low-level concentrations of toxic gases (on the order of parts per million (ppm)). These advantages make electrochemical sensors ideal for portable multi-gas meters used by first responders and HAZMAT personnel. These advantages must be weighed against the limitations and cross-sensitivities of specific electrochemical sensors when determining which meters and sensors to use during an emergency response.

## UL 9540A INSTALLATION LEVEL TESTS WITH OUTDOOR LITHIUM-ION ENERGY STORAGE SYSTEM MOCKUPS

### Catalytic Bead

A catalytic bead sensor is comprised of a small catalytic bead supported by an electrically conductive wire. The catalyst facilitates combustion of a mixture of gases and vapors at temperatures significantly lower than would typically be required for combustion. Local combustion of the gas mixture on the surface of the catalytic bead increases the temperature of the wire in proportion to the concentration of a specific flammable gas in the mixture, which affects the electrical conductivity of the wire in a predictable way [17]. Catalytic bead sensors are typically only suitable for measuring the concentration of flammable gases up to the lower explosive limit (LEL).

Catalytic bead sensors can only provide an accurate assessment of the concentration of a gas when a single, known flammable gas is present in a mixture. This technology does not allow for identification and quantification of an unknown gas species or mixture. Most catalytic bead sensors are calibrated to a specific flammable gas (typically methane, propane, or pentane) and correction factors are used to convert a measurement from the calibration basis to the measured gas species basis. Table 8 shows a chart with typical correction factors for a catalytic bead sensor calibrated with methane [14]. Additionally, most catalytic bead sensors are affected by elevated gas temperature, and are not typically used in high temperature environments.

**Table 8 – Correction factors for a typical catalytic bead LEL sensor calibrated for Methane.**



## UL 9540A INSTALLATION LEVEL TESTS WITH OUTDOOR LITHIUM-ION ENERGY STORAGE SYSTEM MOCKUPS

Compound	LEL Relative Sensitivity <sup>1</sup>	LEL CF
Acetone	45	2.2
Ammonia	125	0.8
Benzene	40	2.5
Carbon monoxide	83	1.2
Cyclohexane	40	2.5
Ethanol	59	1.7
Ethyl acetate	45	2.2
Hydrogen	83	1.2
Isobutylene	67	1.5
Isopropanol	38	2.6
Leaded gasoline	42	2.4
Methane	100	1
Methanol	67	1.5
Methyl ethyl ketone	38	2.6
n-Butane	63	1.6
n-Heptane	37	2.7
n-Hexane	40	2.5
n-Octane	34	2.9
n-Pentane	50	2
Phosphine	385	0.26
Propane	63	1.6
Propene	59	1.7
Toluene	33	3
Turpentine	34	2.9

Because the operation of catalytic bead sensors depends on combustion of the sample gas mixture at the bead surface, this technology is only suitable in oxygen-containing atmospheres. Additionally, vitiated oxygen conditions and samples with a gas mixture concentration above the LEL may result in erroneously low measurements. The catalyst may lose sensitivity due to catalyst poisoning from specific trace gases. Common catalyst poisons include silicone, halocarbons, and metallo-organic compounds.

Catalytic bead sensors are particularly susceptible to poisoning and inhibitors. Sensor poisons are chemicals or substances that react directly with the heated catalyst to permanently damage the sensor. Inhibitors are chemicals that can temporarily affect the sensitivity of the sensor, and if a mixture of gases is combustible and contains an inhibitor, the sensor may not be able to detect the combustible gases. Some of the most common potential inhibitors are halogenated compounds, which include many clean agents that are available for suppression [18].

### Photoionization Detector (PID)

PIDs involve shining an ultraviolet (UV) light through a sample gas. If the photon energy of the UV light used in the PID is greater than the ionization energy of the target gas molecules, the molecules are ionized (electrons are ejected from the molecules). The ejected electrons are collected on charged grids and produce an electric current, which





## UL 9540A INSTALLATION LEVEL TESTS WITH OUTDOOR LITHIUM-ION ENERGY STORAGE SYSTEM MOCKUPS

is proportional to the amount of gas in the sample [19]. Gases with ionization energies higher than the lamp photon energy are typically not detected.

PIDs are useful because they are sensitive to volatile organic compounds (VOCs) that may be flammable or toxic but are not typically measured using a targeted electrochemical sensor and may detect these compounds at sub-ppm concentrations. Different UV lamp photon energies allow for either a wider range of gases detected (higher energy) or a more sensitive detector with a more selective list of possible gases detected (lower energy). This technology is unable to identify components of an unknown gas mixture but can indicate the presence and total concentration of VOCs within the range of ionization energies suitable for the UV lamp. Common compounds expected to be detected by a 10.6 eV lamp have been tabulated by the manufacturers [20].

### **Non-Dispersive Infrared (NDIR)**

NDIR sensors consist of a polychromatic light source, a detector, and a filter to selectively allow light with a specific band of wavelengths through to the detector. As infrared light interacts with gas molecules, a portion of the light is absorbed by the molecules, resulting in vibrations that increase the temperature of the gas. The amount of infrared light absorbed by the gas sample is directly proportional to the concentration of the target gas in the sample [21].

Specific chemical bonds absorb a unique wavelength of light in the infrared spectrum. The carbon dioxide covalent bonds absorb infrared light at 4.26 microns, and the carbon-hydrogen covalent bond common in hydrocarbons has a strong absorption peak from 3.3-3.5 microns. Detectors designed to measure concentrations of each of these gases incorporate a filter to allow light in these wavelength ranges to the detector.

NDIR detectors designed to measure hydrocarbon concentrations are not selective and are incapable of identifying specific gas species. Two advantages of NDIR sensors for LEL monitoring over catalytic bead sensors are that the sample gas atmosphere is not required to contain oxygen, and the sensor may be able to measure flammable gas concentrations above the LEL.

### **Solid-State (Metal-oxide Semiconductor)**

Solid-state sensors, also known as metal-oxide semiconductor sensors, are comprised of a thin layer of metal oxide on the surface of a non-conductor. The semiconductor layer connects two electrodes. In normal ambient air, electrons in the metal oxide are attracted toward oxygen, which is adsorbed at the surface of the semiconductor. This effectively results in no current flow through the semiconductor.

When a target gas from the atmosphere is present at the sensing surface, some of the adsorbed oxygen is reduced by the target gas molecules, which frees up electrons in the semiconductor. These free electrons effectively decrease the electrical resistance and allow current flow. The electrical resistance of the semiconductor varies logarithmically with the gas concentration [22].



## UL 9540A INSTALLATION LEVEL TESTS WITH OUTDOOR LITHIUM-ION ENERGY STORAGE SYSTEM MOCKUPS

This technology is sensitive but inherently non-specific, and cannot be used to identify the components in an unknown gas mixture. The sensitivity of the semiconductor sensor may be affected by humidity and temperature. This technology can only be used in an atmosphere with oxygen, and vitiated conditions may result in erroneous readings.



# UL 9540A INSTALLATION LEVEL TESTS WITH OUTDOOR LITHIUM-ION ENERGY STORAGE SYSTEM MOCKUPS

## Video Cameras

Thermal imaging and high-definition (HD) cameras were located both inside and outside the container to monitor test conditions and capture visual cues for fire service size-up considerations. Figure 31 and Figure 32 show the camera locations on the interior and exterior of the container, respectively. The cameras are numbered according to the convention in Table 9.

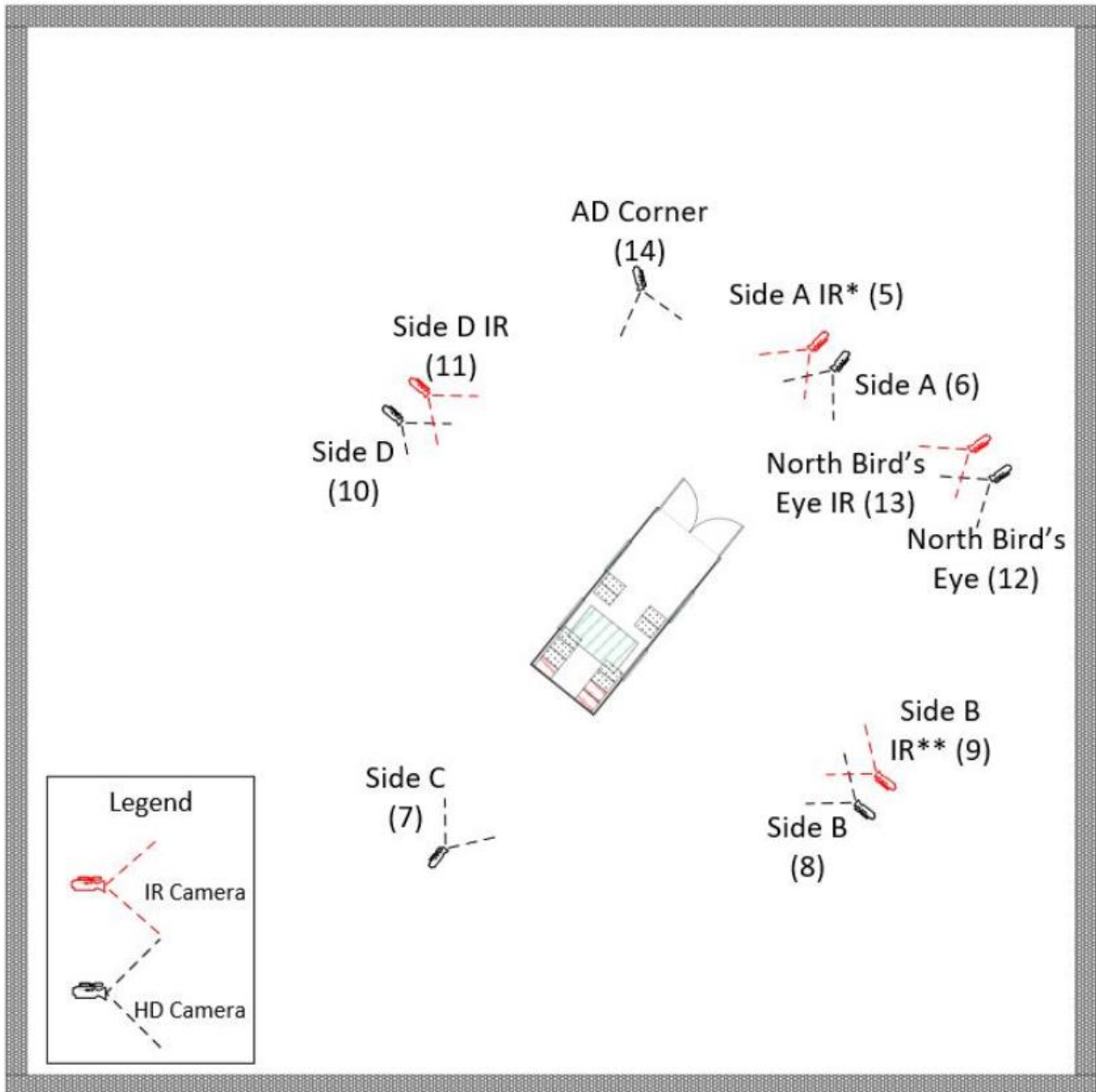
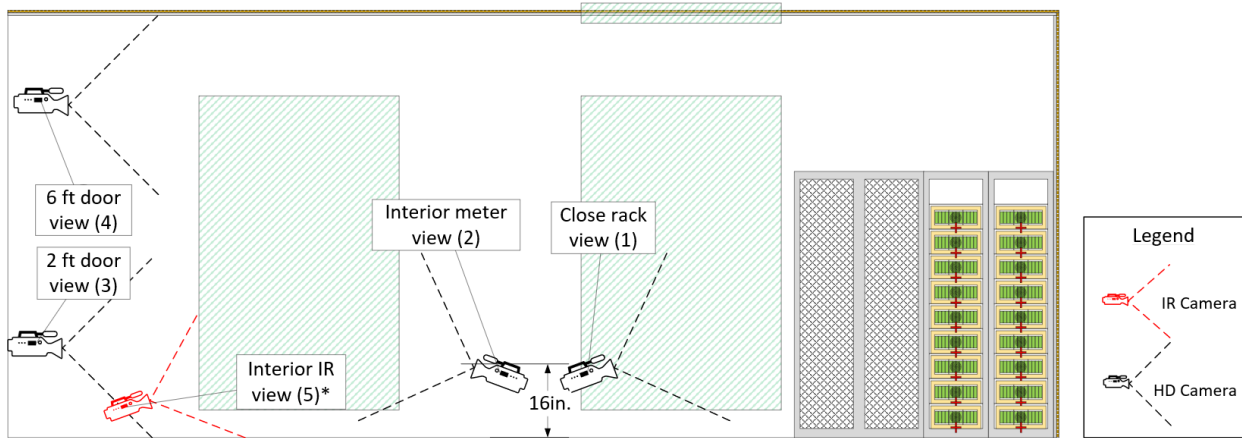


Figure 31 – Exterior camera locations.

## UL 9540A INSTALLATION LEVEL TESTS WITH OUTDOOR LITHIUM-ION ENERGY STORAGE SYSTEM MOCKUPS



**Figure 32 – Interior camera locations.**

**Table 9 – Camera numbering and locations.**

Number	Type	Location
1	HD	Interior container, view of Initiating Unit
2	HD	Inside container, view of meters
3	HD	2 ft above floor in doorway
4	HD	6 ft above floor in doorway
5*	IR	Floor level, inside doorway, view of Initiating Unit
6	HD	Side A (front)
7	HD	Side C (rear)
8	HD	Side B (left)
9	IR	Side B (left)
10	HD	Side D (right)
11	IR	Side D (right)
12	HD	A-B corner (front, right) Bird's-eye
13	IR	A-B corner (front, right) Bird's-eye
14	IR	Side C

HD cameras used in the experiments were HD-SDI CCTV cameras. In all three experiments, two HD cameras were placed on the interior of the container with views of the Initiating Module and the inside face of the door of the container. Two cameras were mounted to the outside of the container doors to view through glass-covered holes, located 2 ft and 6 ft above the floor. These two cameras captured views of the floor and ceiling. An additional six HD cameras were located on the laboratory floor to obtain views of each side of the exterior of the container, at locations shown in Figure 31.

Fire service thermal imaging cameras were co-located with the D-side and A-D side bird's-eye exterior cameras. In Test 1, a third thermal imaging camera was co-located with the B-side exterior camera. In Tests 2 and 3, this third IR camera was moved to a

## UL 9540A INSTALLATION LEVEL TESTS WITH OUTDOOR LITHIUM-ION ENERGY STORAGE SYSTEM MOCKUPS

location at floor level inside the doorway of the container, directed toward the Initiating Unit. The fire service thermal imaging cameras used were Bullard Model T3Xs.

FLIR model t450sc instrument-grade thermal imaging cameras were also used to measure the infrared thermal signature of the exterior of the container. One of these cameras was located on the C-side of the structure. In Test 1, the second camera was located on the A-side of the structure, co-located with the exterior HD camera. This camera was moved during Tests 2 and 3 to be co-located with the exterior HD camera on the B-side.



### 3 Procedure

Prior to each test, each analytical gas instrument was field calibrated. Every fire service gas meter and commercial gas detector was bump tested with appropriate calibration gases. New smoke detectors and commercial gas detectors were installed for each test.

Each test began by energizing a flexible film heater installed on one component 18650 cell within each mock-up cell. Power was automatically controlled to provide 6 °C/min of temperature rise on the initiating component cell surface. Heating continued at this rate until thermal runaway was observed, at which point the heater was de-energized.

Thermal runaway behavior was confirmed by a rapid increase in cell surface temperature exceeding 10 °C/s to a maximum temperature in excess of 500 °C for the 18650 cell at 100% state of charge. In contrast, cell venting was marked by temperature fluctuation on the cell surface of less than 10 °C within five seconds as the cell safety vent operates and relieves electrolyte vapor pressure within the cell case.

Following the initial thermal runaway event, thermal runaway propagation behavior of the ESS was monitored until actions were required to activate suppression systems. In Test 2, the Novec 1230 system was discharged with a solenoid valve upon activation of both smoke detectors installed in the container. In Test 3, the water suppression system was activated following the actuation of a 165 °F standard response sprinkler link and a 30 second delay to simulate pipe filling from a Siamese water connection. In Test 1, no suppression systems were utilized. After the deployment of suppression systems, as applicable, the behavior of the ESS was observed until test termination. While observing test progression, propagation of thermal runaway to additional modules in the Initiating Unit and Target Units was monitored. Thermal runaway behavior in these modules was marked by an immediate temperature increase of more than 400 °C and sustained temperatures above 300 °C. When thermal runaway activity subsided or module temperatures began decreasing, test termination procedures were initiated.

To begin test termination procedures, a carbon dioxide system was used to mitigate potential deflagration hazards. The system discharged 41 kg of CO<sub>2</sub> in order to develop a concentration of 62 v% CO<sub>2</sub> (less than 8.0 v% O<sub>2</sub> when including battery gas) before the doors were allowed to be opened. The operation of the system was verified before conducting the test series. Evaluation of this laboratory safety provision is outside the scope of this report. Following the deployment of the carbon dioxide system, the container doors were opened remotely utilizing electrically operated winches. Once the deflagration hazard was mitigated, manual extinguishment, overhaul, and disposal were conducted. This procedure was utilized for all three tests.

## 4 Results

### 4.1 Test 1 – Li-Ion ESS Installation without Fire Suppression System

Test 1 was conducted on June 19, 2020, at 9:40 AM Central time.

#### 4.1.1 Timeline

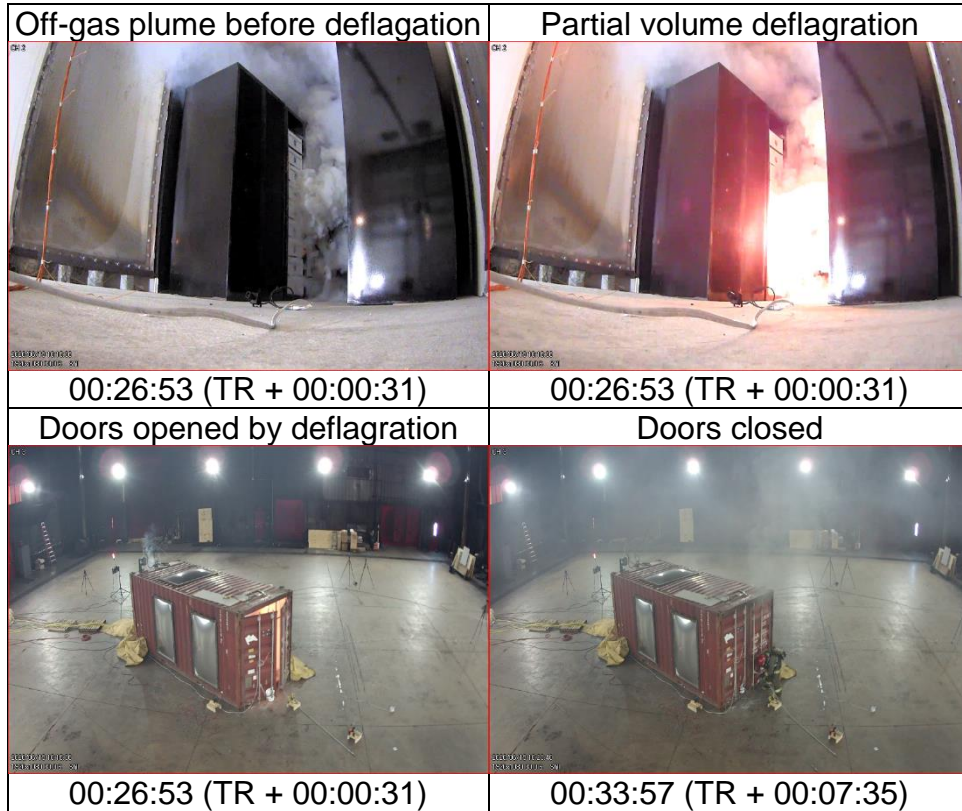
Figure 33 through Figure 35 show a visual sequence of the most significant events that occurred during Test 1.<sup>2</sup> Test 1 began when the flexible film heaters installed inside the Initiating Module were energized to begin heating. Power was automatically controlled to provide 6 °C/min of temperature rise on the initiating 18650 component cell surface. After 23 minutes and 43 seconds, venting of the heated cell was detected. Thermal runaway within the mockup Initiating Cell occurred 2 minutes and 39 seconds later, at 26 minutes and 22 seconds of test time. Smoke was first seen venting from the Initiating Module 15 seconds after thermal runaway. Within 30 seconds of thermal runaway, all of the wall-mounted gas detectors alarmed and an off-gas plume reached from the Initiating Module to the ceiling, as shown by Figure 33.

---

<sup>2</sup> A more detailed visual timeline is provided in Appendix A.



## UL 9540A INSTALLATION LEVEL TESTS WITH OUTDOOR LITHIUM-ION ENERGY STORAGE SYSTEM MOCKUPS



**Figure 33 – Sequence of events in Test 1 leading up to 34 minutes of test time.**

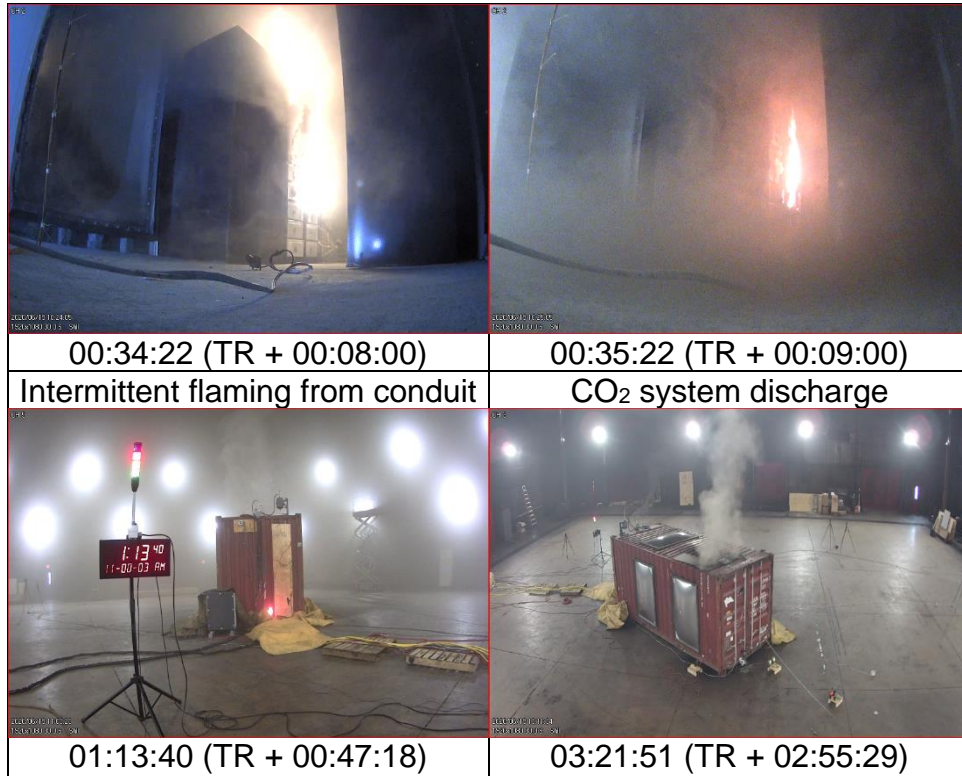
Thirty-one seconds after thermal runaway, the gas plume ignited at the initiating module and a partial volume deflagration<sup>3</sup> occurred inside the container.

Pressure generated by the deflagration exerted sufficient force to open the latched container doors but did not operate any of the deflagration pressure relief panels. Gas continued to vent from the Initiating Module and burn, which also caused ignition of the plastic faces of the modules in the Initiating Unit. Seven minutes and 35 seconds after thermal runaway, the doors were manually closed to re-establish the integrity of the container envelope. Smoke and combustion products accumulated with the doors closed, vitiating the flames. Flaming subsided within one minute and 25 seconds of the door closing. Without any further flaming inside the container, thermal runaway propagated to all modules in the Initiating Unit and to all modules in the Left Target Unit within two hours and 50 minutes of the first thermal runaway. Smoke and gases escaped a wiring conduit at the floor level. Unpiloted ignition of this escaping gas was observed several times during this three hour period, an example of which is shown in Figure 34.

Combustible materials ignited	Flaming subsides
-------------------------------	------------------

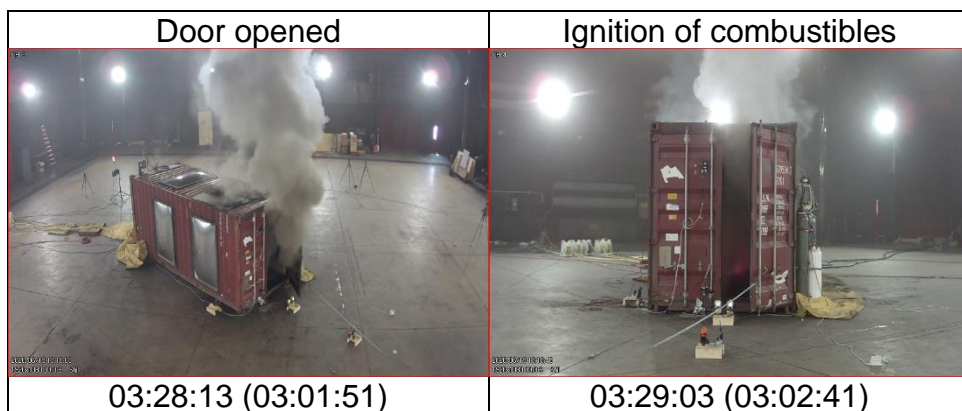
<sup>3</sup> A partial volume deflagration is the deflagration of a flammable mixture that occupies only a part of total confined volume.

# UL 9540A INSTALLATION LEVEL TESTS WITH OUTDOOR LITHIUM-ION ENERGY STORAGE SYSTEM MOCKUPS



**Figure 34 – Sequence of events in test 1 from 34 to 194 minutes of test time.**

The CO<sub>2</sub> system used as part of test termination procedures was discharged two hours and 55 minutes after the first thermal runaway. When the CO<sub>2</sub> system finished discharging, the container doors were immediately opened remotely using an electrically operated winch. Hot combustible materials ignited, but no further thermal runaways occurred. Final extinguishment was performed.



**Figure 35 – Sequence of events in test 1 from 194 to 209 minutes of test time.**

## UL 9540A INSTALLATION LEVEL TESTS WITH OUTDOOR LITHIUM-ION ENERGY STORAGE SYSTEM MOCKUPS

### 4.1.2 Comparison of Test 1 Results to UL 9540A Performance Metrics

**Table 10 – Test 1 performance .**

Ref.	UL 9540A Performance Metric	Assessment
10.5.1	“For BESS units intended for installation in locations with combustible construction, surface temperature measurements along instrumented wall surfaces shall not exceed a temperature rise of 97 °C (175 °F) above ambient...”	Not compliant
10.5.2	“The surface temperature of modules within the BESS units adjacent to the initiating BESS unit shall not exceed the temperature at which thermally initiated cell venting occurs...”	Not compliant
10.5.3	“The fire spread on the cables in the flame indicator shall not extend horizontally beyond the initiating BESS enclosure dimensions.”	N/A
10.5.4	“There shall be no flaming outside the test room.”	Not compliant*
10.5.5	“There is no observation of detonation. There is no observation of deflagration unless mitigated by an engineered deflagration protection system.”	Compliant†
10.5.6	“Heat flux in the center of the accessible means of egress shall not exceed 1.3 kW/m <sup>2</sup> .”	Not compliant
10.5.7	“There shall be no observation of re-ignition within the initiating unit after the installation test had been concluded and the sprinkler operation was discontinued.”	Compliant

† The deflagration pressure relief vents successfully prevented overpressure and maintained integrity of the ISO container.

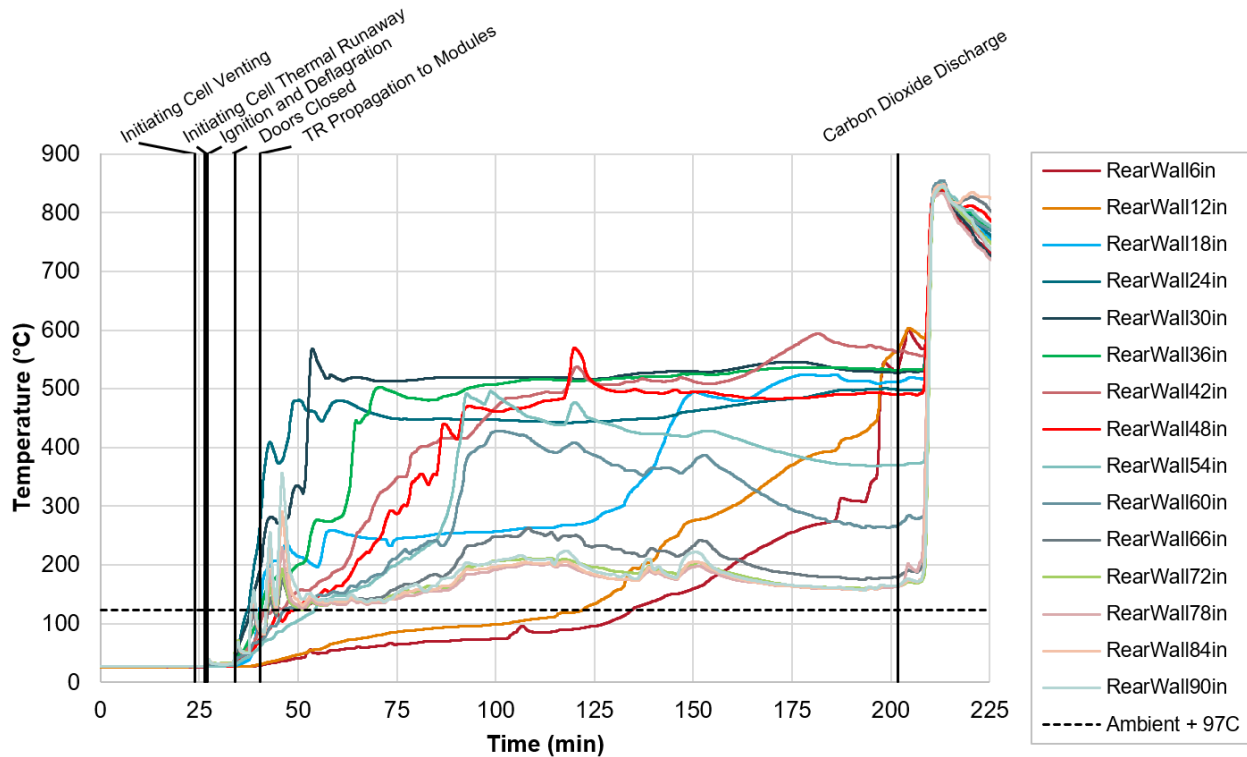
#### **Thermal Exposure to Walls**

All measurement locations on both the rear and side instrumented walls exceeded temperature performance criteria for combustible construction, as illustrated in Figure 36 and Figure 37. Except for the bottom locations 6 in and 12 in off the floor, all measurement locations exceeded the temperature performance criteria within 20 minutes of the first thermal runaway event. Measurement locations on the rear wall directly behind the Initiating Unit exceeded temperature performance criteria by nearly 400 °C. Measurement locations on the side wall exceeded temperature performance criteria by 100 °C. The difference in measurement magnitude is explained by the construction of the ESS. The module had vent openings symmetrically on the front and back of the module, which resulted in hot gases impinging directly on the back panel of the ESS unit. This back surface was hotter than the shielded side panel and emitted greater radiation toward the instrumented wall.



## UL 9540A INSTALLATION LEVEL TESTS WITH OUTDOOR LITHIUM-ION ENERGY STORAGE SYSTEM MOCKUPS

Temperatures measured on the rear wall spiked after the carbon dioxide system discharge during the test termination procedures. The doors of the container were remotely opened immediately after carbon dioxide system discharge, resulting in an influx of fresh air into the container. Increased oxygen in the container supported reignition of combustible materials in the Initiating Unit and Left Target Unit, as documented in Figure 43 in the next section, Thermal Exposure to ESS Targets.



**Figure 36 – Rear wall temperatures measured during Test 1.**

UL 9540A does not include a performance criterion based on incident heat flux to combustible materials. This data offers insight into the magnitude and duration of exposure and ignition risk to combustible materials. The rear wall exceeds  $12.5 \text{ kW/m}^2$  for the majority of the test, representing a critical threshold for ignition risk to combustible structures according to NFPA 80A [23]. The instrumented side wall received less incident heat flux due to the shielded unit design.

# UL 9540A INSTALLATION LEVEL TESTS WITH OUTDOOR LITHIUM-ION ENERGY STORAGE SYSTEM MOCKUPS

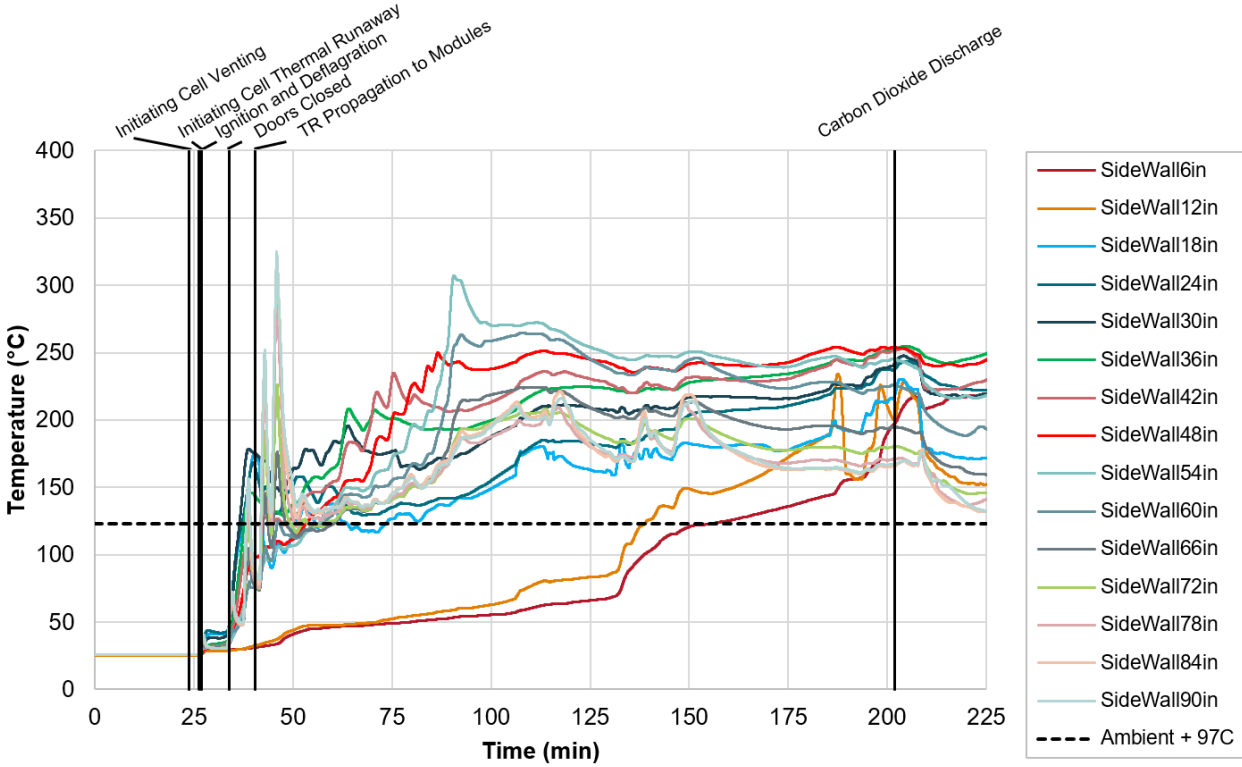
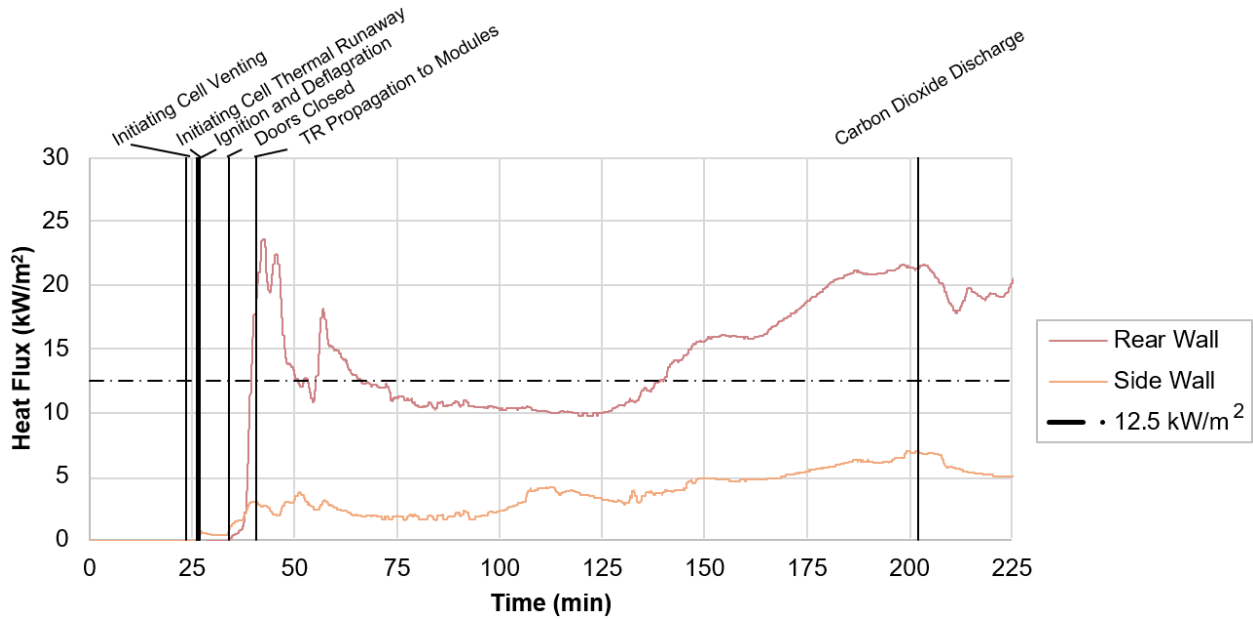


Figure 37 – Side wall temperatures measured in Test 1.





# UL 9540A INSTALLATION LEVEL TESTS WITH OUTDOOR LITHIUM-ION ENERGY STORAGE SYSTEM MOCKUPS



**Figure 38 – Incident heat fluxes to rear and side walls measured in Test 1.**

During overhaul of the test, the ESS units were moved aside to reveal the condition of the instrumented walls, as shown in Figure 39. The paper coatings were burned off both walls. Both walls were charred. The plywood layer beneath the gypsum board on the side wall was smoldering with damage penetrating to the bare steel behind the plywood.



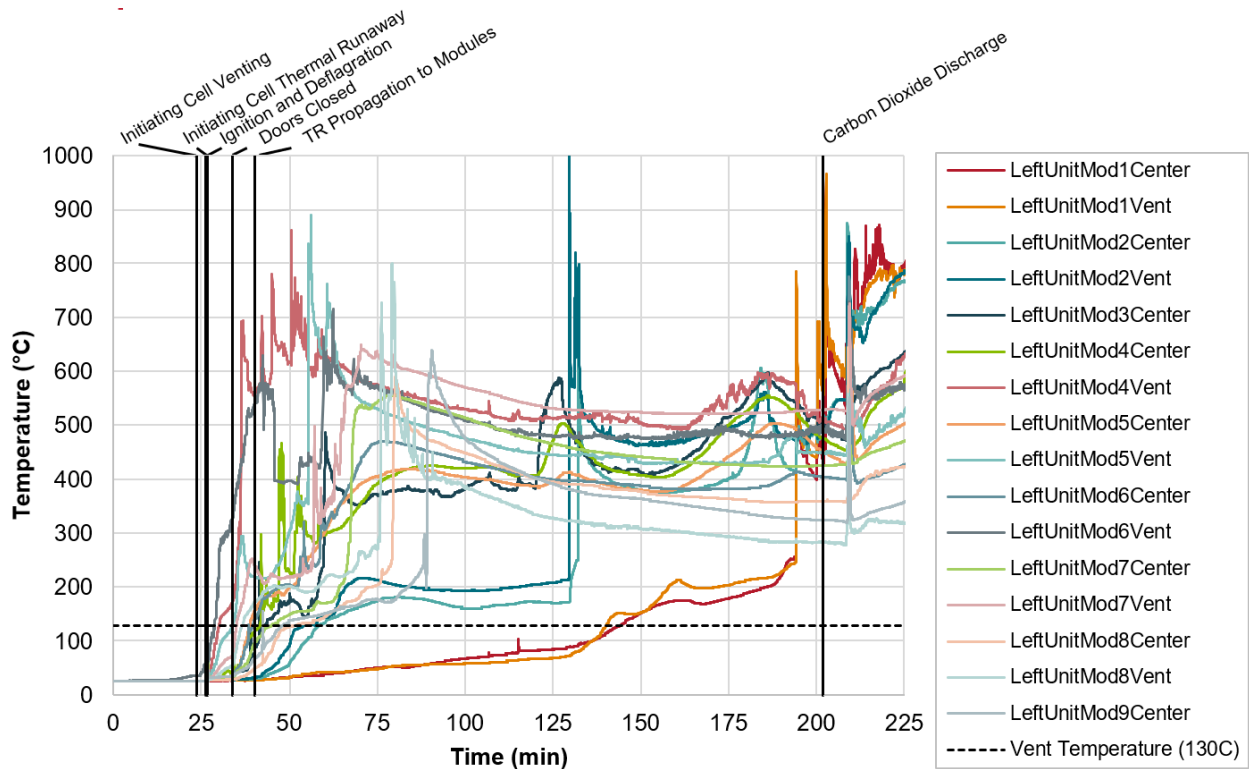
**Figure 39 – Thermal damage to walls photographed during test termination and overhaul after Test 1.**

# UL 9540A INSTALLATION LEVEL TESTS WITH OUTDOOR LITHIUM-ION ENERGY STORAGE SYSTEM MOCKUPS

## Thermal Exposure to ESS Targets

Both measurement locations in all target modules of the Left Target Unit exceeded the cell vent temperature (130 °C), and therefore the ESS was not compliant with the Target Unit temperature performance criteria. All modules of the Left Target Unit exceeded the cell vent temperature within 30 minutes of the first thermal runaway event, except for the bottom module (Module 1), as displayed in Figure 40.

Each target module of the Left Target Unit experienced thermal runaway during the test. Thermal runaway behavior is marked in Figure 40 by an immediate temperature increase of more than 400 °C, and a sustained temperature above 300 °C.

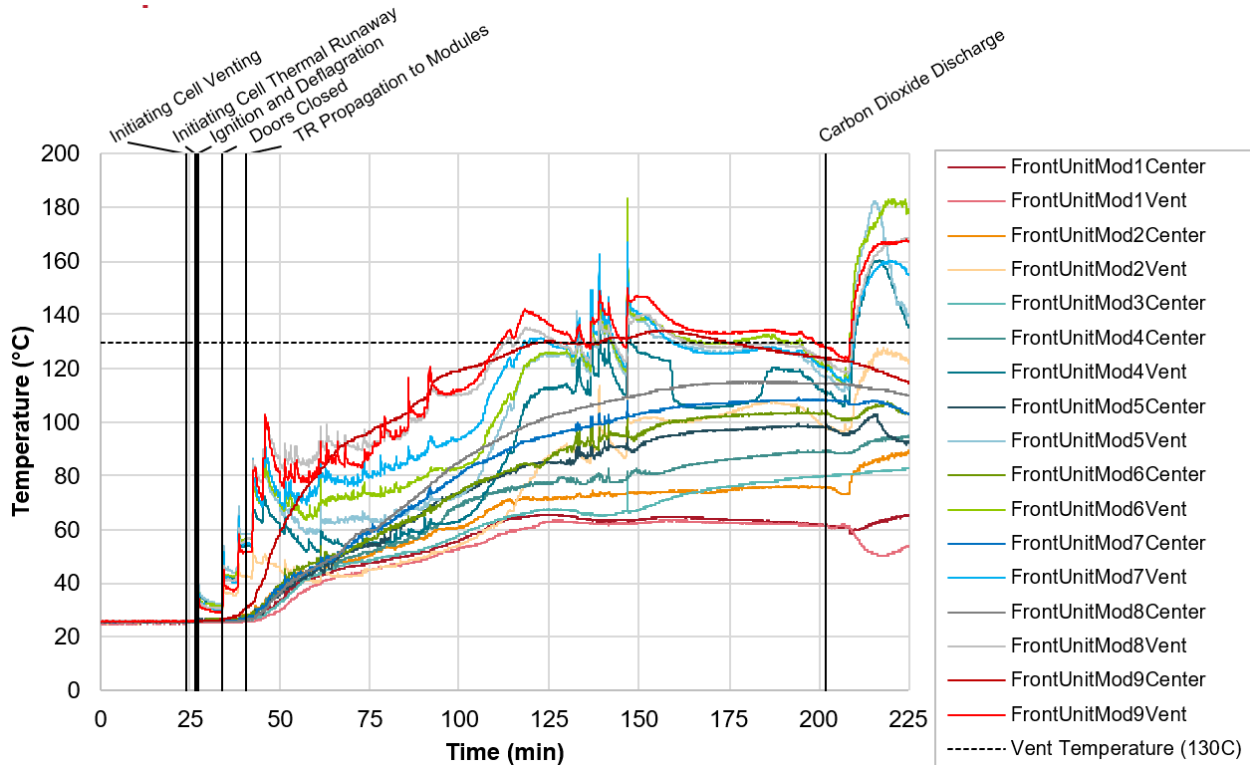


**Figure 40 – Temperatures measured in Left Target Unit during Test 1.**

Cell vent temperature was exceeded in five Front Target Unit modules, two hours after thermal runaway. None of the modules in the Front Target Unit experienced any thermal runaways.

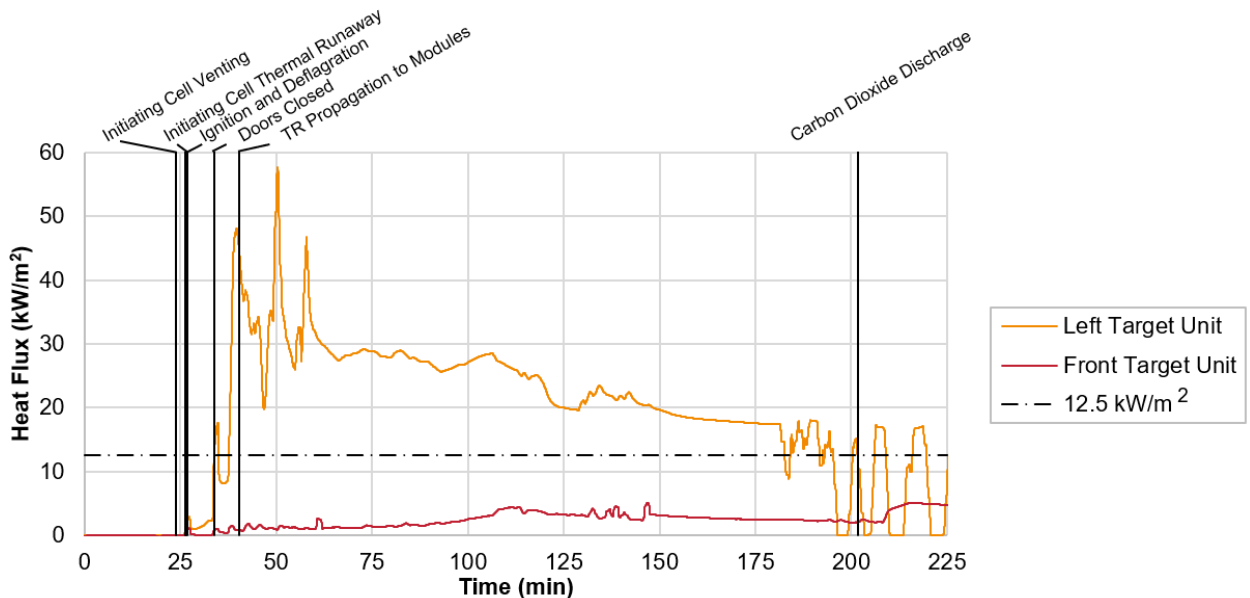


# UL 9540A INSTALLATION LEVEL TESTS WITH OUTDOOR LITHIUM-ION ENERGY STORAGE SYSTEM MOCKUPS



**Figure 41 – Temperatures measured in Front Target Unit during Test 1**

Figure 42 shows that less heat flux was imposed on the Front Target Unit than the Left Target Unit. Heat flux exposure was likely less for the Front Target Unit because of the separation distance provided by the aisle. The Left Target Unit experienced incident heat fluxes above the critical heat flux for ignition to many combustible materials,  $12.5 \text{ kW/m}^2$ . Heat flux measured at the Front Target Unit remained below  $12.5 \text{ kW/m}^2$  for the test duration.



## UL 9540A INSTALLATION LEVEL TESTS WITH OUTDOOR LITHIUM-ION ENERGY STORAGE SYSTEM MOCKUPS

**Figure 42 – Incident heat flux measured in Front and Left Target Units during Test 1.**

### Flaming Outside the Test Room

Intermittent flaming of gases escaping from an instrumentation cable conduit in the container wall was observed, as pictured in Figure 43. The intermittent flaming is an indication the gas mixture that accumulated inside the container lacked sufficient oxygen for complete combustion and may have been above the upper flammability limit (UFL).



**Figure 43 – Flaming outside the test container through cable conduit in Test 1.**

### Explosion Hazards

A partial volume deflagration occurred in the container 31 seconds after the first thermal runaway event. At the moment of this event, only the mockup Initiating Cell had undergone thermal runaway. The hydrocarbon concentration measured by the FID analyzers at the ceiling and the floor were both less than 0.5 v% at the time of the deflagration. The combustible gas detector at the floor registered 50% LEL.

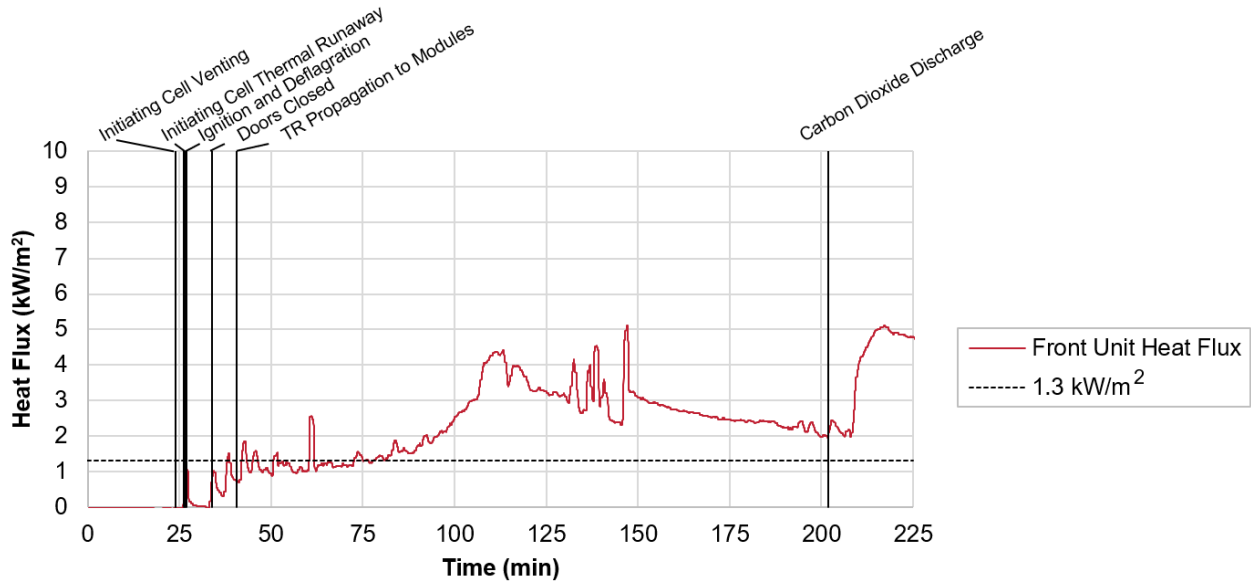
Potential sources of ignition included hot materials from the modules that experienced thermal runaway, and electrical components of wall-mounted gas detectors. Pressure generated by the deflagration was sufficient to open both latched doors to the container, as pictured in Figure 33. The force exerted was sufficient to unlatch and open the doors but did not rupture the deflagration vents. The force exerted on the container doors is estimated to have been 2300 lbf to 6900 lbf, based upon the deflagration vent panel operation pressure specifications [24].

### Egress Path Heat Flux

Measurements for egress path heat flux were taken from the heat flux gauge installed in the Front Target Unit, across the aisle from the Initiating Unit. UL 9540A prescribes this heat flux gauge be installed in the middle of the potential egress pathway, but the Front Target Unit measurement acted as a proxy for this test series. Heat flux measurements in Test 1 were noncompliant to the 1.3 kW/m<sup>2</sup> criteria for over two hours, as plotted in Figure 44. Heat flux was measured between 1 and 3 kW/m<sup>2</sup> from the time thermal runaway propagated outside the Initiating Module until the end of the test, with excursions as high as 5 kW/m<sup>2</sup>.



# UL 9540A INSTALLATION LEVEL TESTS WITH OUTDOOR LITHIUM-ION ENERGY STORAGE SYSTEM MOCKUPS



**Figure 44 – Heat flux measured in the egress path for Test 1.**

## Reignition Caused by Post-Test Thermal Runaways

Test termination safety procedures included discharging carbon dioxide gas for inerting the gas mixture inside the container immediately before opening the container doors. No thermal runaway events occurred after this test termination procedure. Because no additional thermal runaway events occurred, Test 1 complied with the UL 9540A, 4<sup>th</sup> edition, performance criteria for reignition.

While not considered re-ignition, opening the doors increased oxygen in the container, and notably enabled ignition of hot combustible materials in the Initiating Unit and Left Target Unit. A sequence of photos that capture the additional flaming are shown in Figure 45.



**Figure 45 – Sequence of reignition during overhaul of Test 1 (test time 03:29:21 to 03:57:00).**

## UL 9540A INSTALLATION LEVEL TESTS WITH OUTDOOR LITHIUM-ION ENERGY STORAGE SYSTEM MOCKUPS

A photo of the reignited mass of combustibles and cells is documented in Figure 46, which also illustrates the extent of thermal damage in Initiating, Left, and Front Target Units. All cells and most module materials were consumed in the Initiating and Left Target Units. The Front Target Unit shows soot deposition and some melting of module materials. Melted gas detectors positioned in the aisle demonstrated the thermal stress imposed on adjacent exposures.



**Figure 46 – Re-ignited fire observed during overhaul of Test 1 (four hours after test start).**

### 4.1.3 Thermal Runaway Propagation

Only one cell experienced thermal runaway before the partial volume deflagration occurred. The remainder of cells in the Initiating Module did not undergo thermal runaway until after the doors were closed again on the container, as illustrated in Figure 47. The remaining cells in the Initiating Module experienced thermal runaway within 30 seconds of each other.

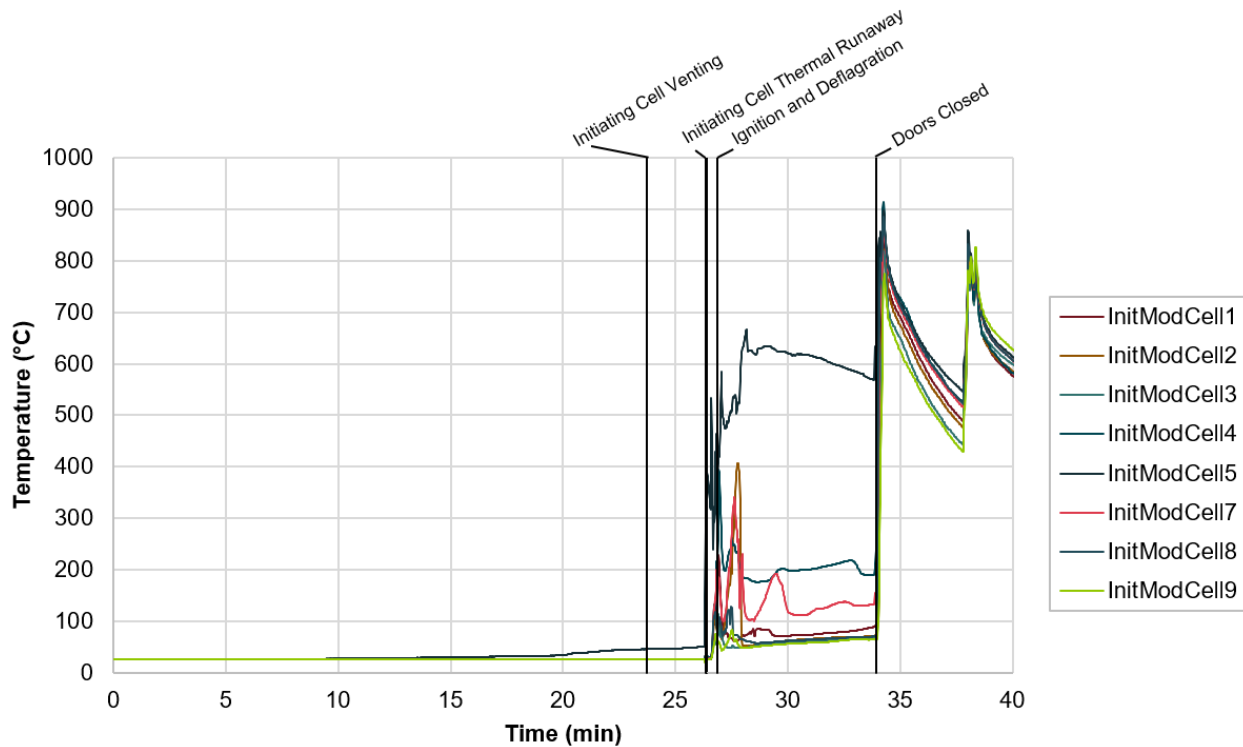


Figure 47 – Thermal runaway propagation within the Initiating Module in Test 1.

Figure 48 shows temperatures measured inside the Initiating Unit modules, which were analyzed to determine times and locations of thermal runaway propagation. Thermal runaway behavior in the Initiating Unit is marked in Figure 48 by an immediate temperature increase of more than 400 °C and a sustained temperature above 300 °C. Thermal runaway propagated module-to-module through all modules in the Initiating Unit and Left Target Unit. Upward thermal runaway propagation occurred at a rate of two to 10 minutes between events. Downward thermal runaway propagation also occurred with approximately one hour between thermal runaways. Propagation times and locations are summarized in Table 11 to aid in interpreting the data shown in Figure 48. Figure 46 above and Figure 49 below illustrate the extent of damage to the Initiating Unit. Most enclosure materials were consumed, and all cells experienced thermal runaway.

No thermal runaway behavior was observed in the Front Target Unit.

# UL 9540A INSTALLATION LEVEL TESTS WITH OUTDOOR LITHIUM-ION ENERGY STORAGE SYSTEM MOCKUPS

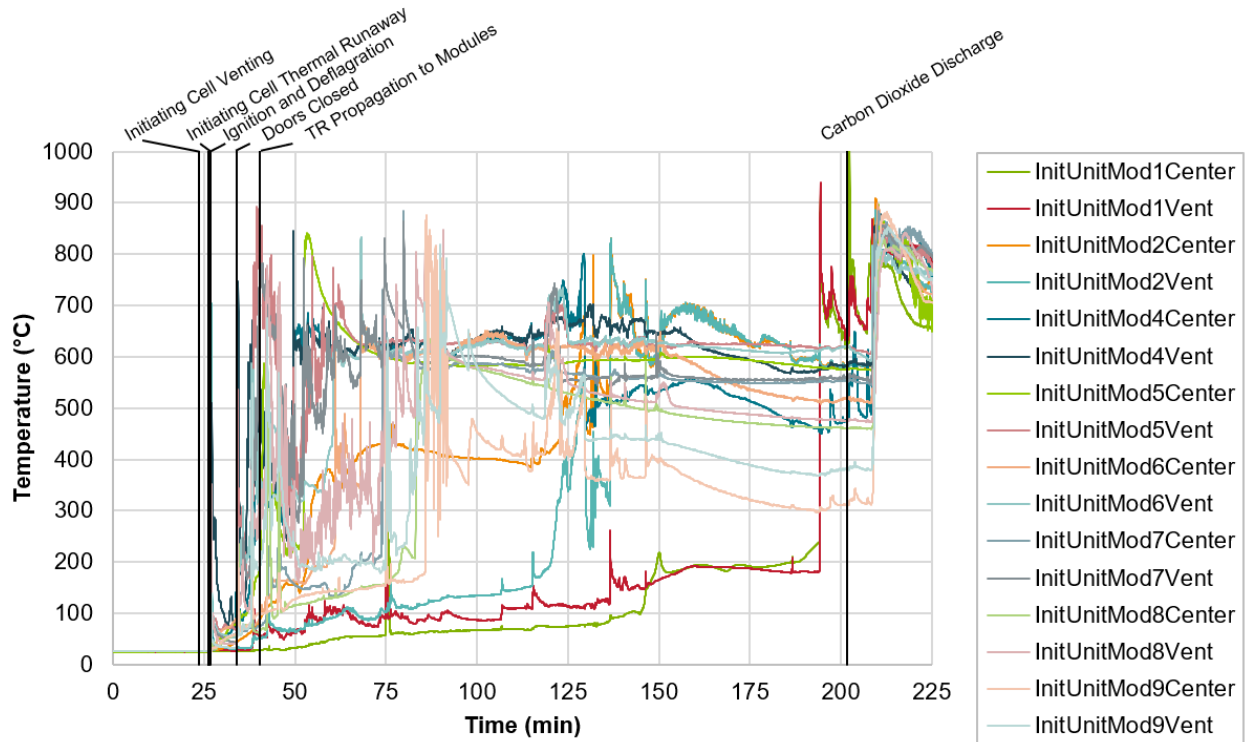


Figure 48 – Temperatures measured throughout the Initiating Unit during Test 1.

Table 11 – Thermal runaway propagation times for Test 1.

Test Time	Time Since TR	Location	Test Time	Time Since TR	Location
00:26:22	00:00:00	InitUnitMod3	01:13:37	00:47:15	InitUnitMod7
00:40:26	00:14:04	InitUnitMod5	01:15:10	00:48:48	LeftUnitMod8
00:46:57	00:20:35	LeftUnitMod4	01:22:57	00:56:35	InitUnitMod8
00:49:04	00:22:42	InitUnitMod4	01:25:48	00:59:26	InitUnitMod9
00:55:47	00:29:25	LeftUnitMod5	01:28:46	01:02:24	LeftUnitMod9
00:57:26	00:31:04	LeftUnitMod3	01:54:53	01:28:31	InitUnitMod2
00:58:41	00:32:19	LeftUnitMod6	02:08:06	01:41:44	LeftUnitMod2
01:00:55	00:34:33	InitUnitMod6	03:13:48	02:47:26	LeftUnitMod1
01:04:26	00:38:04	LeftUnitMod7	03:14:04	02:47:42	InitUnitMod1



**UL 9540A INSTALLATION LEVEL TESTS WITH OUTDOOR LITHIUM-ION ENERGY STORAGE SYSTEM MOCKUPS**



**Figure 49 – Condition of Initiating Unit after Test 1.**

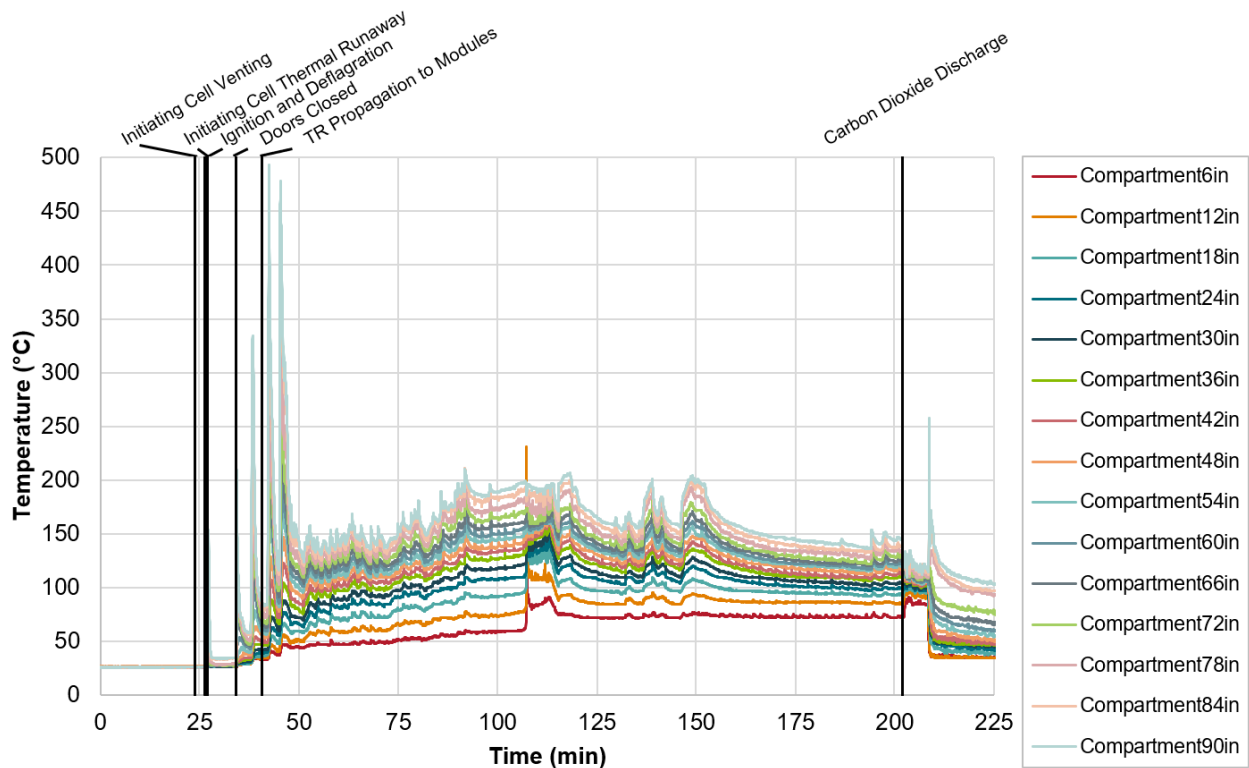


# UL 9540A INSTALLATION LEVEL TESTS WITH OUTDOOR LITHIUM-ION ENERGY STORAGE SYSTEM MOCKUPS

## 4.1.4 Test Conditions Inside ISO Container

### Gas Temperature

Gas temperatures measured in the center of the container increased rapidly when the container doors were shut after the partial volume deflagration. Once the container became under ventilated, flaming subsided and temperatures decreased. As more modules underwent thermal runaway, hot gases were vented from the modules into the container, resulting in temperatures ranging from 50 °C at the floor to 200 °C near the ceiling, as documented in Figure 50.



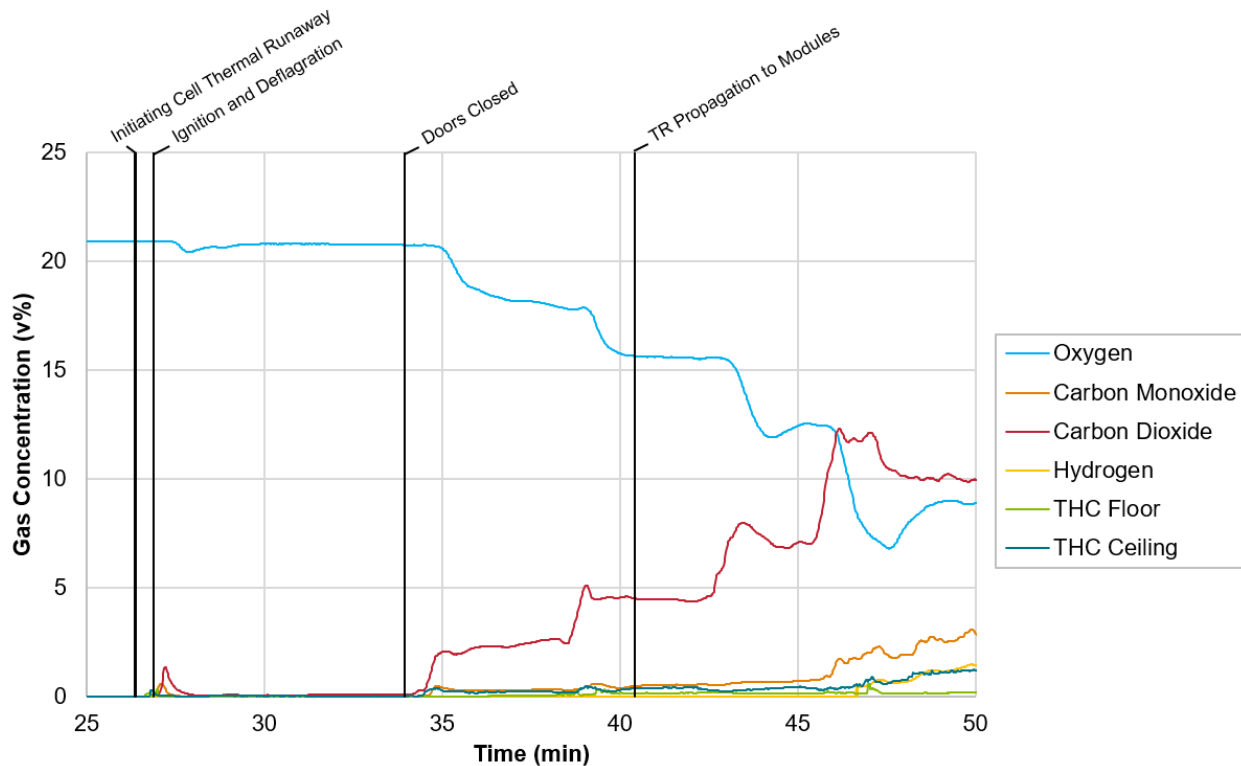
**Figure 50 – Container gas temperatures measured during Test 1.**

Temperatures observed in the container between 60 in and 90 in exceeded the cell vent temperature, 130 °C. Temperatures at the ceiling approached the cell thermal runaway temperature, 204 °C.



## Gas Concentrations

There was no indication of cell venting with the gas measurement instruments. After thermal runaway in the Initiating Cell, hydrocarbons were measured first and were followed by an increase in carbon monoxide and carbon dioxide concentrations, as shown in Figure 51. Hydrogen was not measured initially, though this is limited by a 0.4% concentration threshold applied within the meter.



**Figure 51 – Gases measured in the container from thermal runaway through propagation of thermal runaway to other modules in Test 14.**

Following the partial volume deflagration, flaming combustion was observed at the Initiating Unit. After the container doors were closed, carbon dioxide concentration increased while oxygen concentration decreased. The container became under ventilated and flaming subsided. Battery gases accumulated as thermal runaway propagated through the Initiating Module and adjacent modules. Step-like increases in gas concentrations are observed in Figure 51 as thermal runaway propagated through groups of cells. Carbon dioxide volume concentration increased the fastest, followed by carbon monoxide. Hydrogen was first measured above the 0.4% threshold at 47 minutes, 20 minutes after the first thermal runaway event.

<sup>4</sup> Gases are presented without 30 second averaging.

## UL 9540A INSTALLATION LEVEL TESTS WITH OUTDOOR LITHIUM-ION ENERGY STORAGE SYSTEM MOCKUPS

Between 60 and 90 minutes, a quasi-steady state condition was reached, as illustrated in Figure 52. Carbon dioxide, carbon monoxide, and hydrogen were all measured between 10 v% and 15 v%. At these concentrations, the atmosphere inside the container was comprised of 40–60 v% battery gas. Oxygen concentrations during this period were measured between 7 v% and 8 v%, corresponding to approximately 40% ambient air concentration by volume in the container. The upper flammability limit (UFL) of the battery gas is 40 v%, as was determined by ASTM E681 [25] during UL 9540A cell level testing. The majority of thermal runaway propagation activity subsided after 90 minutes. Between 90 minutes and 130 minutes, fresh air replaced battery gases as they leaked from the container, as illustrated by Figure 52. Increases in battery gas components were measured again near 130 minutes and 190 minutes, corresponding to thermal runaway events in Module 2 and Module 1. The decreasing concentration of battery gas and increasing concentration of oxygen demonstrates significant potential for flammable mixtures and a subsequent deflagration hazard. When the carbon dioxide system was discharged during test termination procedures, carbon dioxide concentration displaced other major gas components and enabled remote opening of the container doors with minimal risk of deflagration.

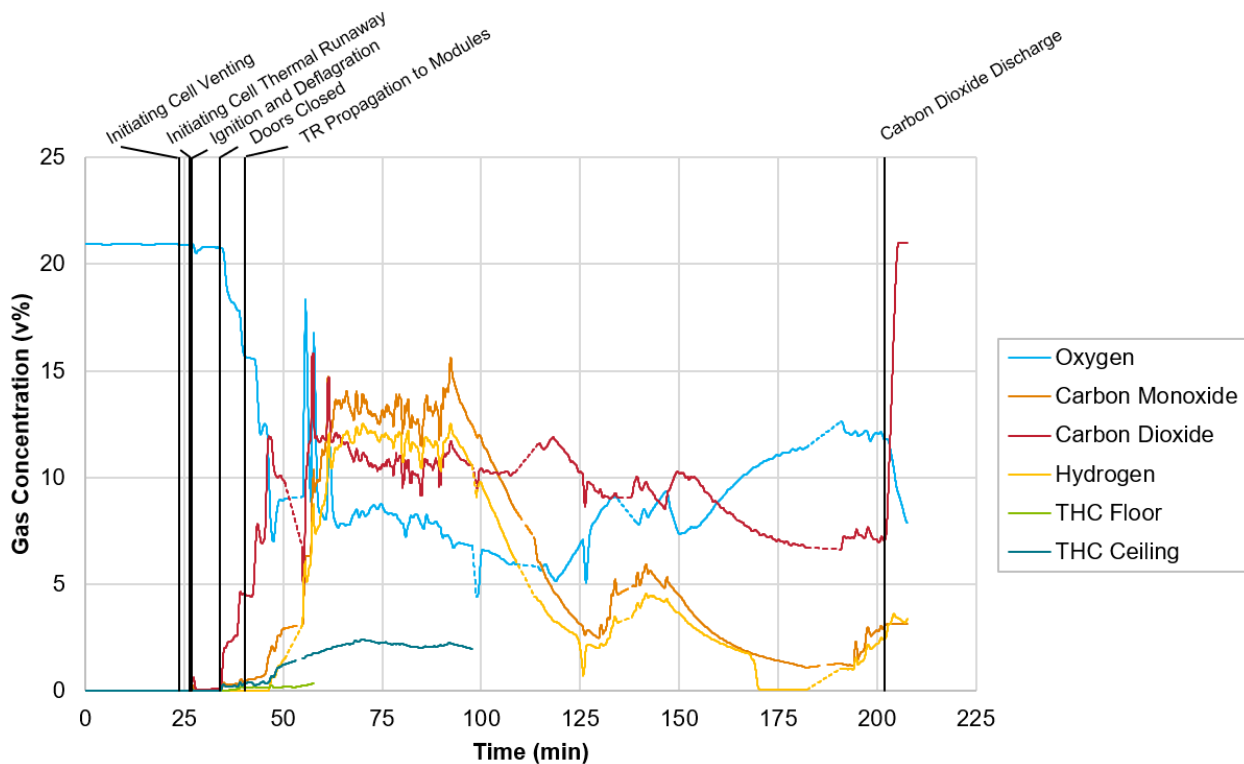


Figure 52 – Gas conditions measured in the container for the duration of Test 1<sup>5</sup>.

<sup>5</sup> Dashed portions are linearly interpolated for periods of equipment maintenance or adjustment between measurement ranges. Gases are presented with 30 second averaging.

# UL 9540A INSTALLATION LEVEL TESTS WITH OUTDOOR LITHIUM-ION ENERGY STORAGE SYSTEM MOCKUPS

## Post-Test

Thermal damage was limited primarily to the proximity of the Initiating and Left Target Units. The oriented strand board underneath the gypsum board and adjacent to the Initiating Unit was charred through its full thickness, as pictured in Figure 53. Some paper pyrolyzed off the gypsum wall board in a larger area, but most other apparent damage is actually soot deposition. All surfaces experienced heavy soot deposition, with the thickest layer of soot observed on the floor.



Figure 53 – Condition of container after Test 1 overhaul.

## 4.1.5 Smoke and Gas Detector Activation

### Smoke Detectors

Neither smoke detector alarmed prior to the partial volume deflagration. The smoke detector nearest the Initiating Unit alarmed 46 seconds after the first thermal runaway event. The smoke detector located further from the Initiating Unit alarmed one second later. Figure 54 shows the thickness of the smoke layer at the time of smoke detector activation.

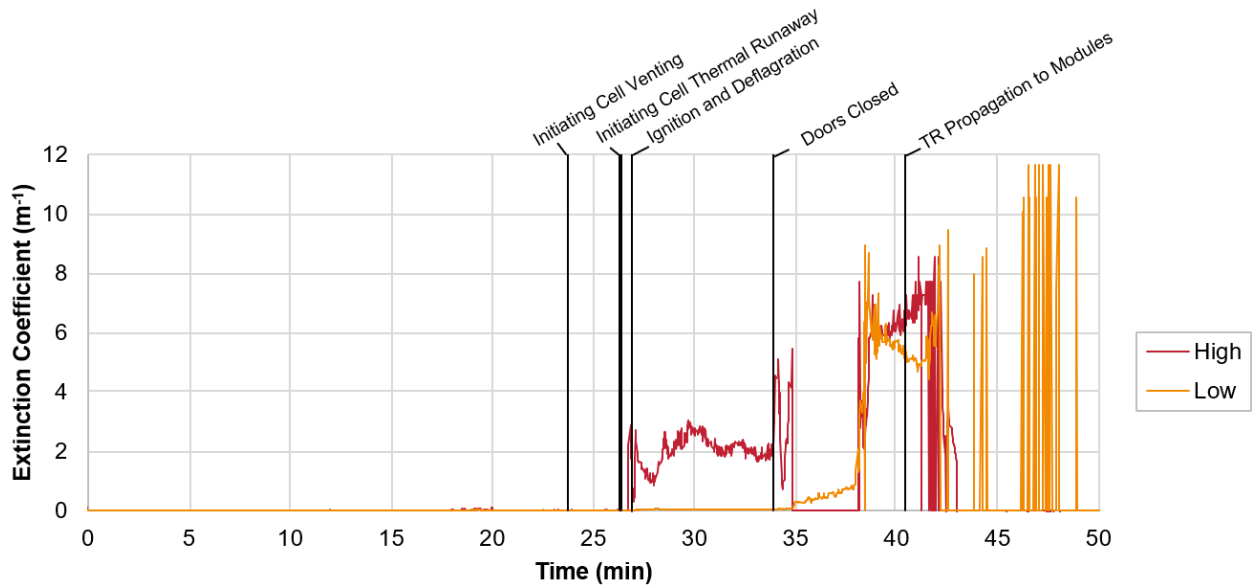


Figure 54 – Smoke layer condition upon activation of both smoke detectors in Test 1.

After thermal runaway, smoke obscuration increased at the ceiling level, as measured by the smoke meter near the ceiling (Figure 55). Smoke obscuration increased at the ceiling

## UL 9540A INSTALLATION LEVEL TESTS WITH OUTDOOR LITHIUM-ION ENERGY STORAGE SYSTEM MOCKUPS

level following ignition. When the door was closed after the deflagration, smoke obscuration continued to increase at the ceiling until flaming subsided. As the smoke layer lowered, obscuration was measured at the lower instrument location. A sharp spike is observed near 36 minutes when thermal runaway propagates through the Initiating Module and the container is filled with thermal runaway gases and particulate.



**Figure 55 – Extinction coefficient measurements made by smoke obscuration meter for Test 1 from the beginning of the test through the propagation of thermal runaway to additional modules.**

### Carbon Monoxide Detector

The carbon monoxide detector alarmed 20 seconds after the first thermal runaway event. This short response time was likely because of the proximity to the Initiating Unit.

### Combustible Gas Detectors

All three combustible gas detectors responded within 30 seconds of the first thermal runaway event, as summarized in Table 12. Initial responses occurred in the order of proximity to the Initiating Module.

**Table 12 – Combustible gas detector response summary for Test 1.**

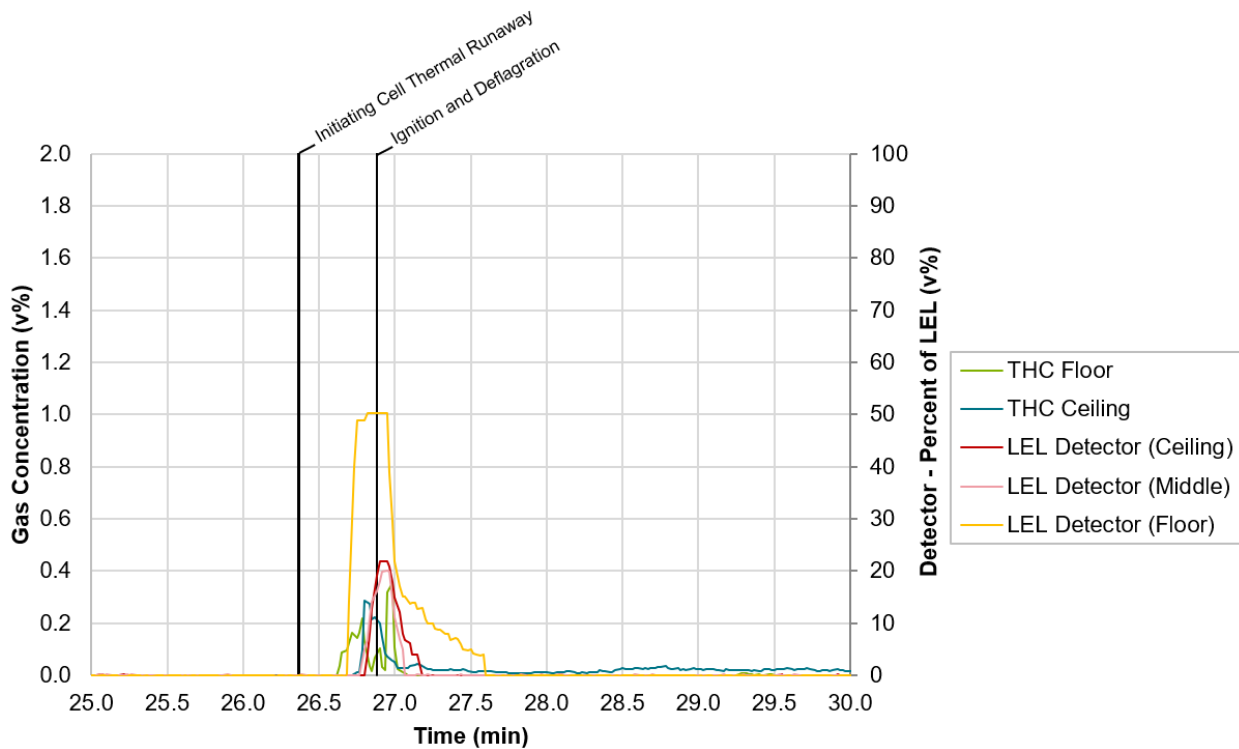
Location	Time of First Response	Time of 25% LEL	
		Limited Duration	Sustained Duration
Ceiling	TR + 27s	---	TR + 20 min 22 s
Middle	TR + 26s	---	TR + 22 min 32 s
Floor	TR + 20s	TR + 22s (13s duration)	TR + 22 min 10 s



## UL 9540A INSTALLATION LEVEL TESTS WITH OUTDOOR LITHIUM-ION ENERGY STORAGE SYSTEM MOCKUPS

The scales of the primary and secondary axes of Figure 57 have been adjusted to compare the general responses of the two types of instruments because direct comparison of Flame Ionization Detection (FID) total hydrocarbon measurements with combustible gas detector measurements are not possible. The FID was calibrated with propane; the combustible gas detectors were calibrated with methane; and the gas mixture they both measured was comprised of many hydrocarbon elements.

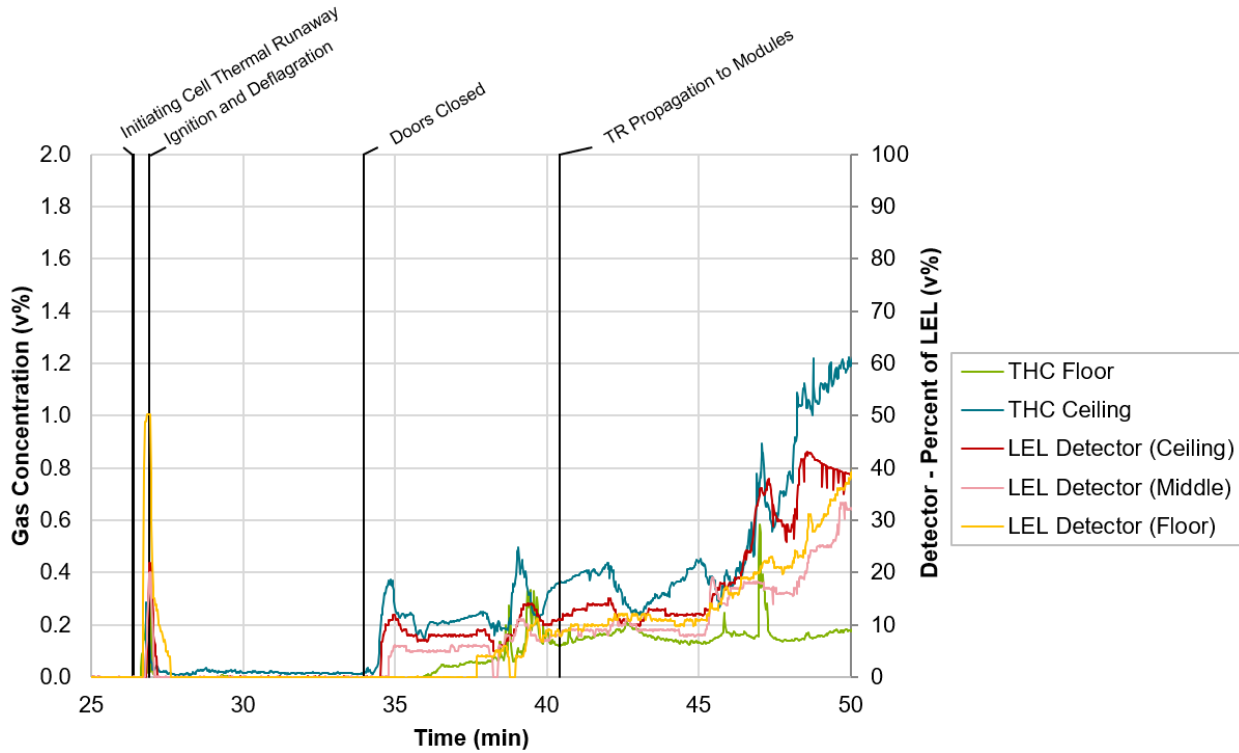
FID-based total hydrocarbon (THC) measurements are plotted from 0 to 2% based on 0 to 100% LEL of the calibration gas (propane). Catalytic bead-based combustible gas detector measurements are plotted from 0 to 100% LEL. The commercial combustible gas detectors all respond within 20 seconds of the FID hydrocarbon measurements, as shown in Figure 56. Both instruments show a similar magnitude response to gas mixtures they measured, as demonstrated in Figure 56 and Figure 57.



**Figure 56 – Total hydrocarbon concentration compared with commercial combustible gas detector response immediately after thermal runaway in Test 1 (test time 00:25:00 to 00:30:00).**



# UL 9540A INSTALLATION LEVEL TESTS WITH OUTDOOR LITHIUM-ION ENERGY STORAGE SYSTEM MOCKUPS



**Figure 57 – Total hydrocarbon concentration compared with commercial combustible gas detector response in Test 1 (test time 00:25:00 to 00:50:00).**

After the doors were closed following the partial volume deflagration, battery gas began to accumulate in the container. The THC analyzer near the ceiling, combustible gas detector at the ceiling, and the combustible gas detector in the middle of the wall all responded to the gas accumulation within seconds of each other after the doors were closed, as shown in Figure 57. All three instruments measured similar conditions in the upper half of the container.<sup>6</sup>

The combustible gas detector response at the floor level was delayed by three minutes after the door was closed. This delay was likely due to lighter hydrocarbon accumulation at the ceiling that steadily progressed downward.

<sup>6</sup> The product installation manual for the combustible gas detector recommends installing at the half height of the wall, or 1.6 m (5.25 ft) from the floor.





# UL 9540A INSTALLATION LEVEL TESTS WITH OUTDOOR LITHIUM-ION ENERGY STORAGE SYSTEM MOCKUPS

## Hydrogen Detector

The electrochemical hydrogen detector responded 20 minutes before the palladium-nickel hydrogen analyzer, as illustrated in Figure 58. The analytical hydrogen analyzer had a 0.4% measurement threshold, which prevents a comparison of response times. Furthermore, the electrochemical hydrogen detector had unspecified cross sensitivities. The proportional response of the electrochemical hydrogen detector, as compared with measurement from the Nondispersive infrared (NDIR) carbon monoxide analyzer, indicated cross sensitivity to carbon monoxide, as shown in Figure 58.

For the period between ignition and underventilation, hydrogen was likely consumed by flaming combustion as battery gases vented from the Initiating Module. Based on the carbon monoxide measurement and the palladium-nickel sensor measurement, it is likely hydrogen concentration was below 0.4 v% until after 45 minutes.

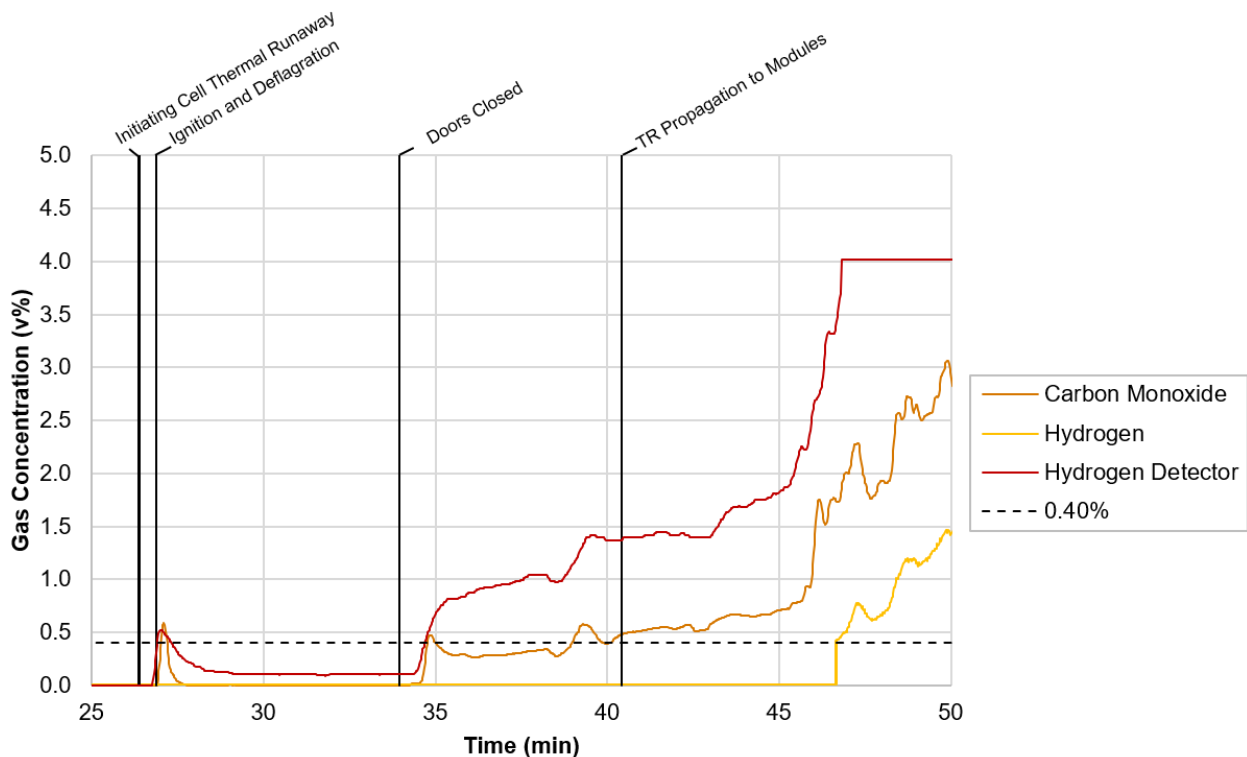


Figure 58 – Commercial hydrogen detector measurement compared with carbon monoxide and hydrogen concentrations measured in Test 1.

# UL 9540A INSTALLATION LEVEL TESTS WITH OUTDOOR LITHIUM-ION ENERGY STORAGE SYSTEM MOCKUPS

## 4.1.6 Fire Suppression System Operation

Active fire suppression systems were not deployed in Test 1.

## 4.1.7 Fire Service Size-up Equipment

### Thermal Imaging

Changes in the exterior thermal imaging views of the container closely followed the changes in exterior wall temperatures shown in Figure 59. Figure 60 shows the changes in the thermal signature over the first two hours of Test 1. Prior to the partial volume deflagration, the increase in exterior thermal signature was negligible. The bare metal (right) side of the container began to show visible changes in exterior thermal imaging views within 30 seconds of the partial volume deflagration, and it continued to increase to a steady state, which was maintained for the duration of the test. Exterior surface temperatures on the uninsulated wall indicated this steady state was reached 90 minutes after test start, with temperatures of 150 °C and 210 °C at 2 ft and 6 ft, respectively.

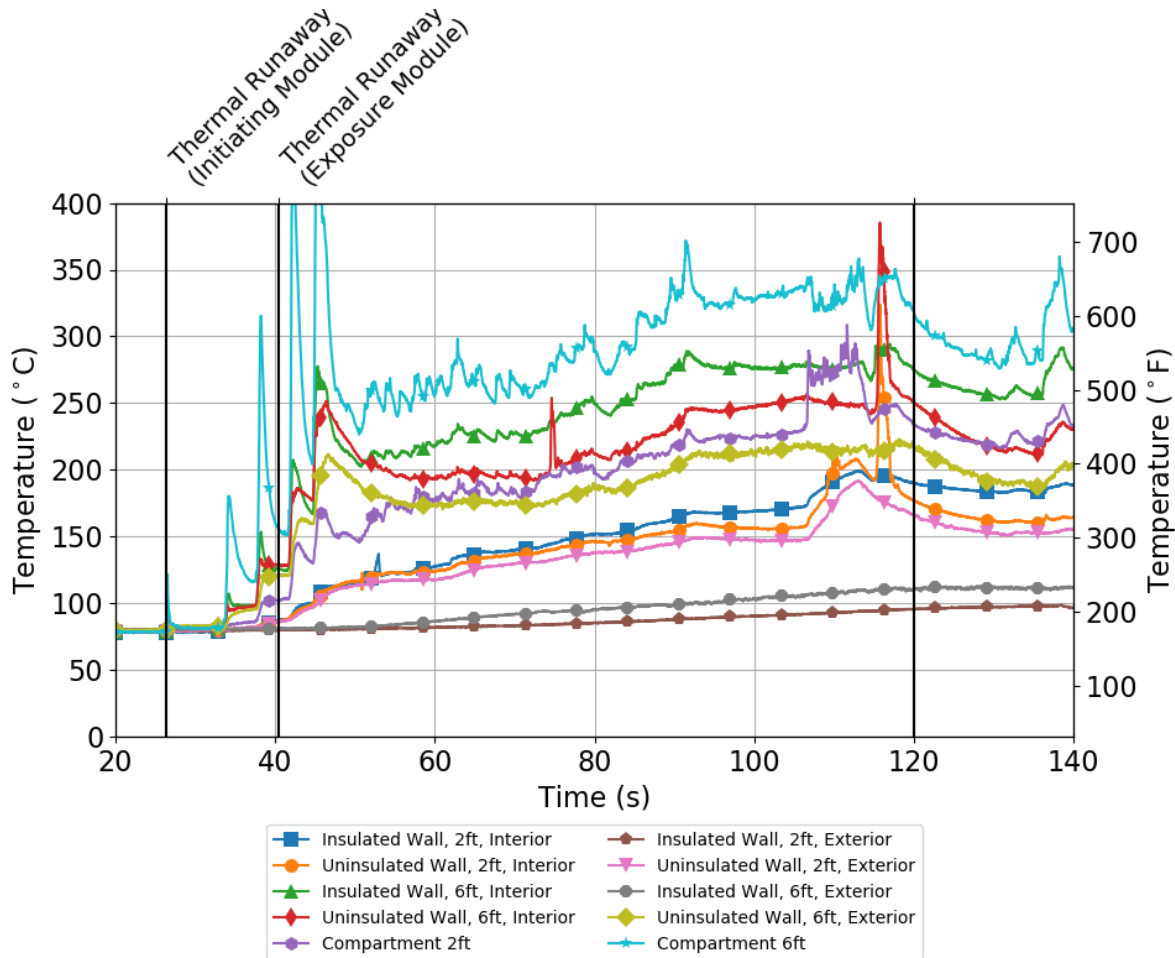
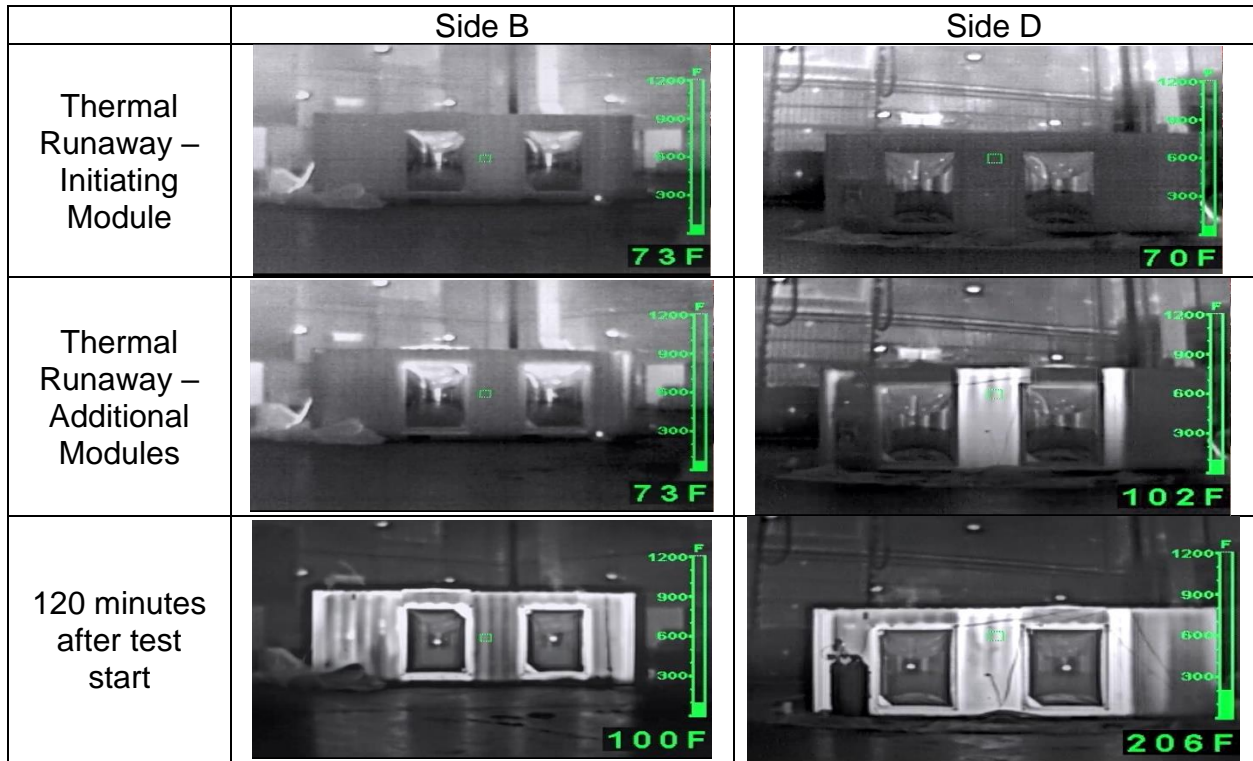


Figure 59 – Wall surface temperatures during Test 1. Vertical lines denote events corresponding to the images in the figure below.



## UL 9540A INSTALLATION LEVEL TESTS WITH OUTDOOR LITHIUM-ION ENERGY STORAGE SYSTEM MOCKUPS



**Figure 60 – Changes in thermal imaging view over the course of Test 1. Left column shows B-side of the container (insulated wall construction) and right column shows D-side of container (bare metal construction).**

Changes in thermal signature on the insulated B side of the container followed the trend of exterior surface temperatures. Figure 59 shows that while interior surface temperatures on the insulated side of the container began to increase at the same time as those on the uninsulated side of the container, exterior surface temperatures on the insulated side lagged behind. Exterior surface temperatures on the insulated side of the container slowly began to increase approximately 50 minutes after test start to steady temperatures of approximately 100 °C and 120 °C at 2 ft and 6 ft, respectively. This slower increase in exterior surface temperatures compared to the uninsulated side of the container resulted in less distinct visual changes in thermal signature on the insulated wall throughout the test, as shown in Figure 60.

The insulated wall construction did not immediately indicate an exterior temperature increase in response to the flaming that accompanied the partial volume deflagration. By the end of the test, the uninsulated deflagration vents were the primary area of the insulated wall where there was a visible change in thermal signature.

Figure 59 and Figure 60 show that uninsulated wall sections closely mirrored changes in the interior thermal environment, while insulated wall sections did not immediately reflect

## UL 9540A INSTALLATION LEVEL TESTS WITH OUTDOOR LITHIUM-ION ENERGY STORAGE SYSTEM MOCKUPS

changes in interior temperatures. This can be further visualized in Figure 61, which shows the temperature difference between the interior and exterior wall surfaces of the container over the course of the experiment. The temperature difference between the inside and outside surface of the uninsulated wall section on the B-side was typically less than 25 °C for the duration of the test. In contrast, the temperature differential between the inside and outside surfaces of the insulated wall section steadily increased over the course of the test. At the 6 ft measurement location, the temperature differential between the inside and outside surface reached 100 °C at several points throughout the test.

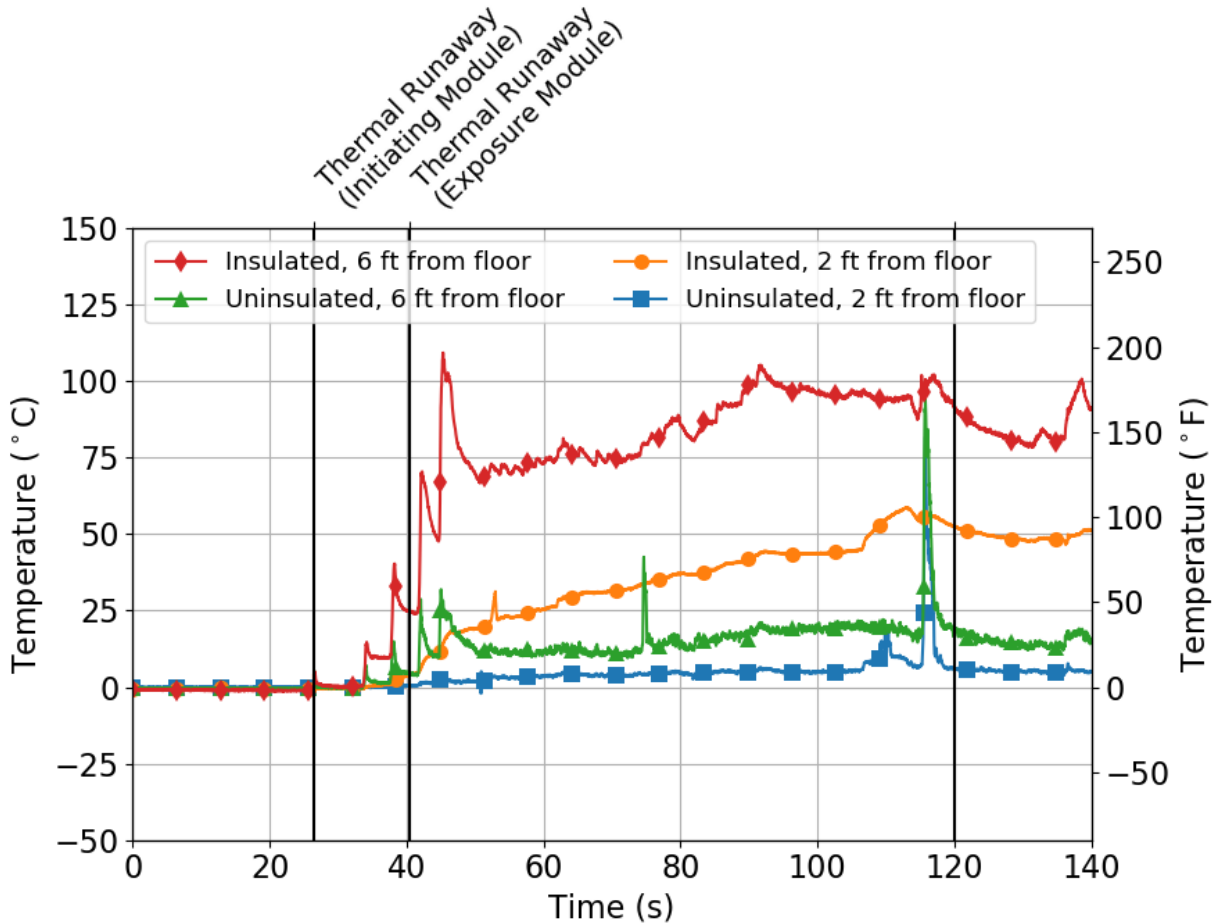
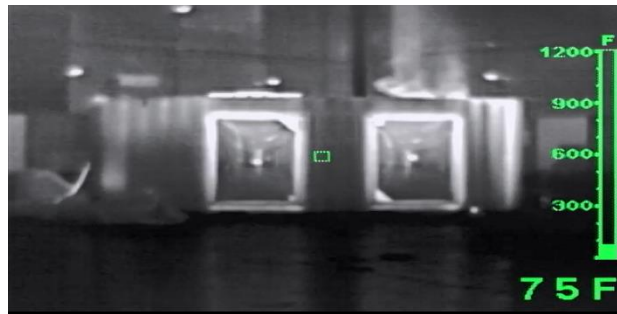


Figure 61 – Temperature difference between inside and outside surface of container during Test 1.

## UL 9540A INSTALLATION LEVEL TESTS WITH OUTDOOR LITHIUM-ION ENERGY STORAGE SYSTEM MOCKUPS

The insulated wall section adjacent to the Initiating Module showed an increase in thermal signature earlier than the insulated wall section between the deflagration panels. The insulated wall section adjacent to the Initiating Module received greater thermal input from the Initiating Unit and indicated the general location of the thermal runaway event. The insulated wall section between the deflagration panels did not indicate the temperature increase inside the compartment as quickly. Figure 62 shows a hot spot developing on the insulated wall behind the Initiating Unit 23 minutes after the initial thermal runaway; the region between the deflagration vents did not show an increased thermal signature at that time.











**Figure 62 – View of left side (B-side) of container 23 minutes after the initial thermal runaway (50 minutes after test start).**

As thermal runaway propagated through the Initiating Module and released hot gases within the container, a visible vapor cloud began to form on the exterior of the container. Figure 63 shows regular and thermal imaging camera views of the container and vapor cloud over the course of the test. The vapor cloud began to form 38 minutes into the test after a period of significant exhaust from the container. This cloud primarily clung close to the laboratory floor, although more buoyant gases were also observed over the course of the experiment.

The size of the cloud fluctuated over the course of the test, growing as additional modules went into thermal runaway and shrinking as exterior vapors were exhausted from the laboratory. Although the peak size of the cloud is difficult to assess in enclosed laboratory conditions, the period of peak cloud size corresponded to the period in which interior gas concentrations were at their peak, 60–90 minutes after the start of the test. After this peak period, the cloud gradually dissipated as thermal runaway activity inside the container subsided. The vapor cloud was visible to the naked eye, but it could not be distinguished in thermal imaging camera (TIC) views. Vapor was readily observed venting from the clean agent pressure relief vents, around the container door seams, and other small leakage points. The primary features of the TIC views during the period in which the vapor cloud was present were the elevated temperatures of uninsulated surfaces of the container and the bright colored (hot) gases exhausting through the roof vent of the container, as shown in Figure 63.



# UL 9540A INSTALLATION LEVEL TESTS WITH OUTDOOR LITHIUM-ION ENERGY STORAGE SYSTEM MOCKUPS

	AD Side (Standard)	AB Side (TIC)
Immediately Prior to Vapor Cloud Formation		
Vapor Cloud Formation (38:03)		
Peak Vapor Cloud (60:00)		
60 Minutes Post Peak		

**Figure 63 – Vapor cloud formation and development in standard (left) and thermal imaging (right) camera views during Test 1.**

## Portable Gas Meters

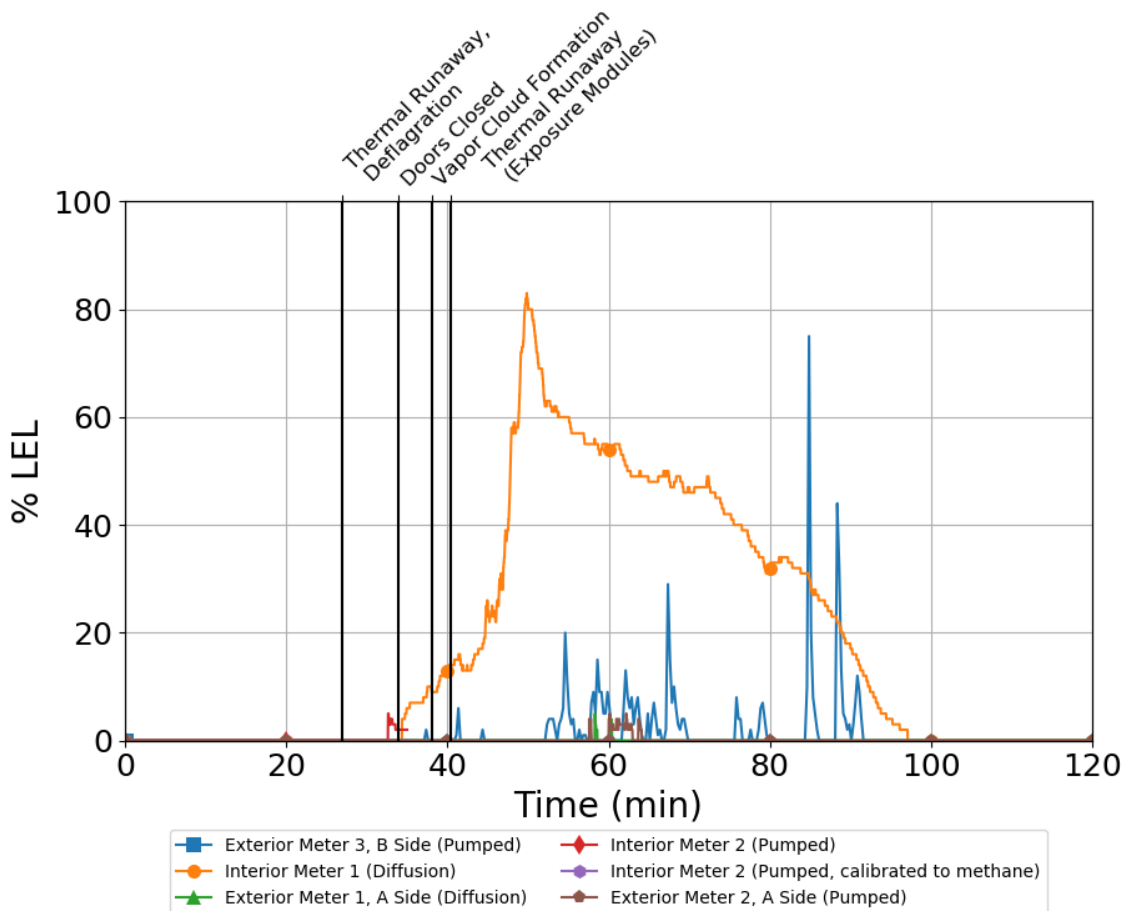
Portable gas meters inside the container first indicated an increase in combustible gas concentrations seven minutes after thermal runaway in the Initiating Unit (24 minutes after test start). This was consistent with the time that gas measurement instrumentation indicated an increase in carbon monoxide, carbon dioxide, and hydrocarbons (as described in Section 4.1.4 – Gas Concentrations). Prior to the partial volume deflagration, there was no increase in hydrogen concentration or LEL measured at the location of the two interior meters.

After the container doors were closed following the partial volume deflagration, the interior meters began to measure an increase in flammable gas measurements. Figure 64 shows the flammable gas measurement, expressed as a percentage of the lower explosive limit



## UL 9540A INSTALLATION LEVEL TESTS WITH OUTDOOR LITHIUM-ION ENERGY STORAGE SYSTEM MOCKUPS

(LEL) of their respective calibration gases (either pentane or methane) at all fire service gas meter locations. The interior diffusion style meter (Interior Meter 1) was the first interior meter to indicate an increase in flammable gas concentration after the container doors were closed. The peak value measured by Interior Meter 1 was 83% of LEL, 26 minutes after the initial thermal runaway event, before steadily decreasing to zero approximately 71 minutes after the first thermal runaway event. The highest LEL measurements were recorded after thermal runaway had started to propagate to target modules. Additionally, this period of elevated LEL measurement aligned with the period in which gas measurement instrumentation indicated elevated measurements of hydrogen and hydrocarbon gases.



**Figure 64 – LEL measurements from portable gas meters in Test 1.**

Combustible gas measurements greater than 0% of LEL were recorded by both exterior meters located 3 ft back from the door on the A-side and 1 ft from the B-side of the container, respectively. Exterior meters first indicated a sustained increase in LEL in the period following thermal runaway propagation to the additional modules in the Initiating Unit and Left Target Unit. The LEL measured by exterior meters in this period varied over time and between meters. The Exterior Meter 3 (located 1 ft offset from the B-side) recorded a peak of 75% of the LEL while both meters on the A-side recorded peaks of





## UL 9540A INSTALLATION LEVEL TESTS WITH OUTDOOR LITHIUM-ION ENERGY STORAGE SYSTEM MOCKUPS

5% of the LEL. Exterior Meter 4 was located 10 ft back from the A-side of the container and did not measure any elevated flammable gas concentrations during the test.

Interior Meter 1 and Exterior Meter 1 (located 3 ft offset from the A-side) were equipped to measure hydrogen gas ( $H_2$ ). The hydrogen concentrations measured inside the container began to increase 33 minutes after test start, at the same time the doors were closed, as plotted in Figure 65. The concentration measured at the interior location rose almost immediately to the measurement limit of the diffusion meter (1,000 ppm). The concentration remained at this level for the duration of the test. The hydrogen concentration measured by Exterior Meter 1 began to increase seven minutes after Interior Meter 1, 40 minutes after test start. The hydrogen measurement on Exterior Meter 1 aligned with carbon monoxide concentration measurements in the same meter. Both meters registered hydrogen gas concentration increases prior to the increase measured by gas measurement instrumentation within the container. The gas measurement instrumentation did not indicate the presence of hydrogen until approximately 46 minutes after test start. It is possible this discrepancy was a result of cross-sensitivities between hydrogen and carbon monoxide in the portable gas meters. Additionally, 1,000 ppm of hydrogen fell below the measurement threshold of the analytical hydrogen sensor (4,000 ppm).

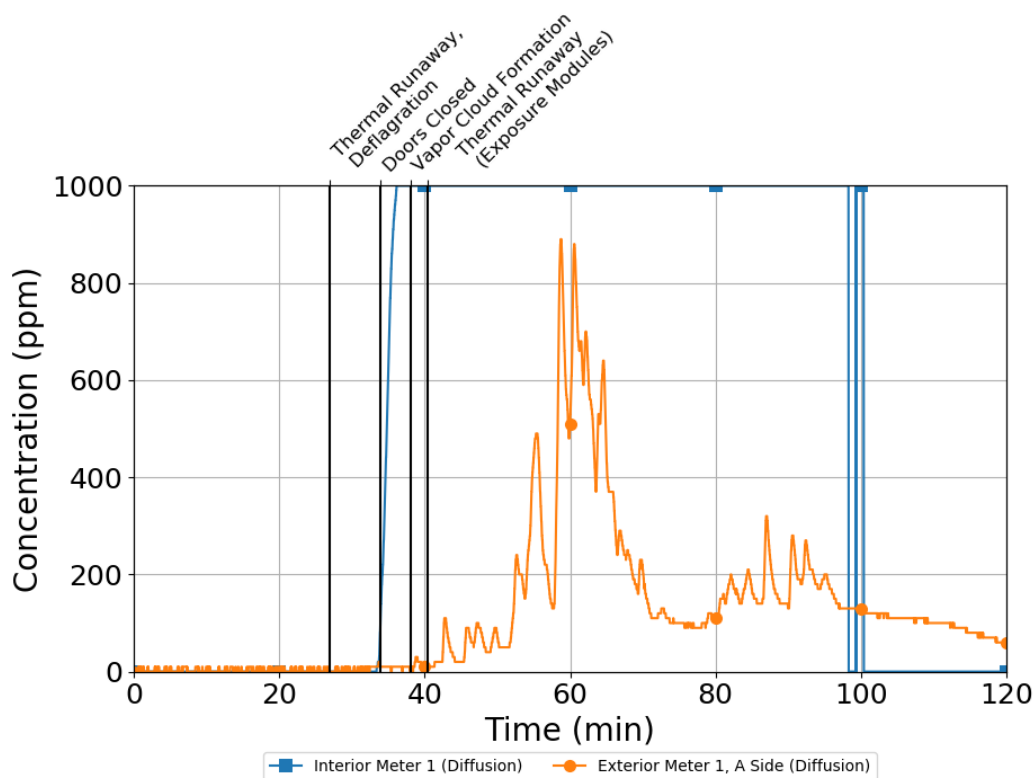


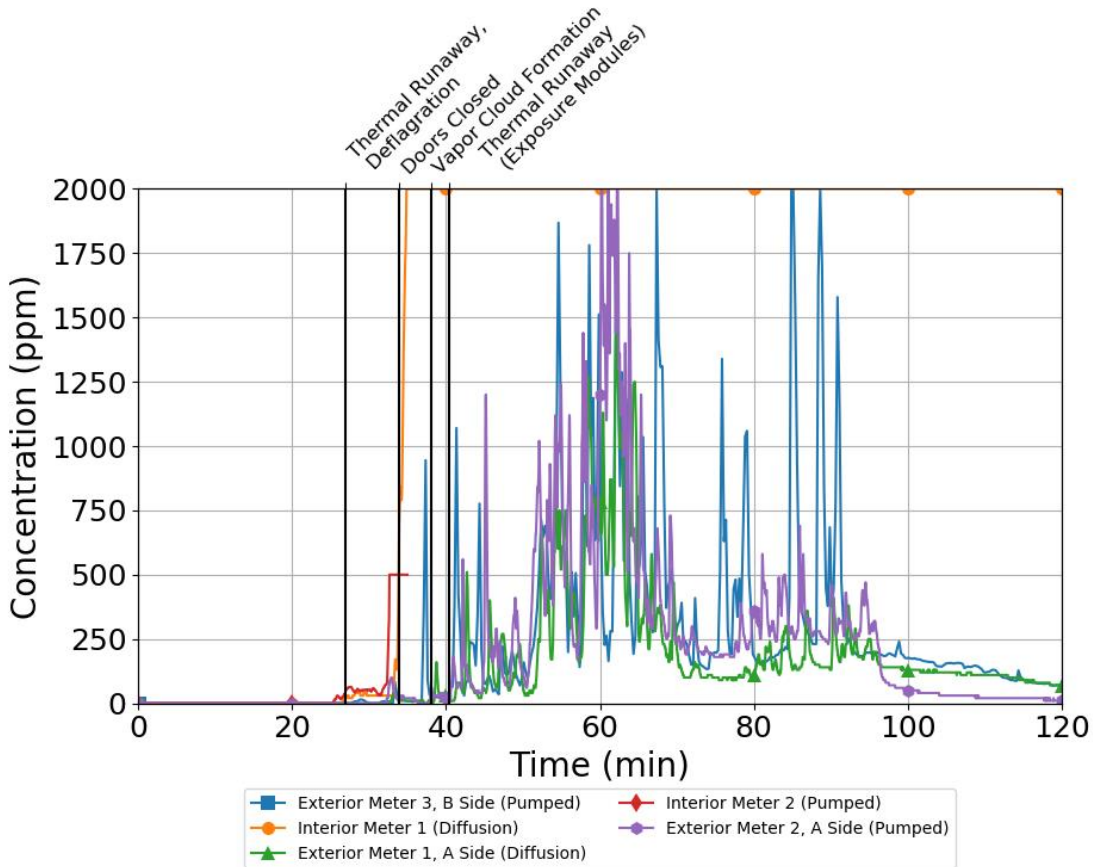
Figure 65 – Hydrogen gas concentration measured by Interior Meter 1 and Exterior Meter 1 in Test 1.

## UL 9540A INSTALLATION LEVEL TESTS WITH OUTDOOR LITHIUM-ION ENERGY STORAGE SYSTEM MOCKUPS

The peak hydrogen gas concentration recorded by Exterior Meter 1 was 890 ppm 60 minutes after test start. This corresponded to the time the scientific measurement equipment indicated hydrogen concentrations within the container were also approaching their maximum. The peak hydrogen gas concentration measured by the gas measurement instrumentation was above 12% (120,000 ppm), two orders of magnitude greater than the upper measurement threshold of the portable gas meters used in Test 1. Following the peak, the hydrogen gas concentrations on the exterior of the container decreased to negligible values 180 minutes after test start.

In addition to flammable gases, portable gas meters on the interior and exterior of the container measured elevated concentrations of carbon monoxide (CO) and hydrogen cyanide (HCN). Figure 66 shows the CO concentration measured by each of the fire service gas meters as a function of time. CO concentrations at both portable gas measurement locations within the container immediately began to increase after thermal runaway, and increased at a more rapid rate once the container doors were closed. Within nine minutes of the first cell venting, both meters had reached the upper threshold of their measurement capability (2,000 ppm) and remained at this limit for the duration of the test. This trend was consistent with the data recorded by gas measurement instrumentation in the container, which recorded CO concentrations several orders of magnitude higher than the peak CO concentrations measured within the container by the fire service meters.

# UL 9540A INSTALLATION LEVEL TESTS WITH OUTDOOR LITHIUM-ION ENERGY STORAGE SYSTEM MOCKUPS



**Figure 66 – Carbon monoxide (CO) concentration measured by fire service portable gas meters in Test 1.**

The CO concentration measured by meters outside the container first began to increase after a persistent vapor cloud began to form, 14 minutes after the Initiating Cell thermal runaway. The carbon monoxide concentrations measured outside the container fluctuated with the size of the vapor cloud over the course of the test, increasing as additional modules went into thermal runaway and decreasing as battery gases dissipated. Exterior CO concentrations increased to the saturation limit (2,000 ppm), a peak at 60 minutes corresponding to the beginning of the period in which gas measurement instrumentation measured peak CO concentrations within the container. The peak CO concentrations inside and outside the container exceeded the threshold for IDLH conditions, 1,200 ppm [26, 7].

Exterior Meter 4, located 10 ft offset from the A-side of the container, did not record time history data and is not shown in Figure 66. A video analysis of the gas concentrations measured by this meter indicated the CO concentrations followed a similar trend to the meters located closer to the container, but the magnitude of the peak CO concentrations was lower. The peak CO concentration recorded by this meter was 534 ppm.

The hydrogen cyanide (HCN) concentrations measured inside and outside the container followed a similar trend to the CO concentrations. The pumped style meters are cross

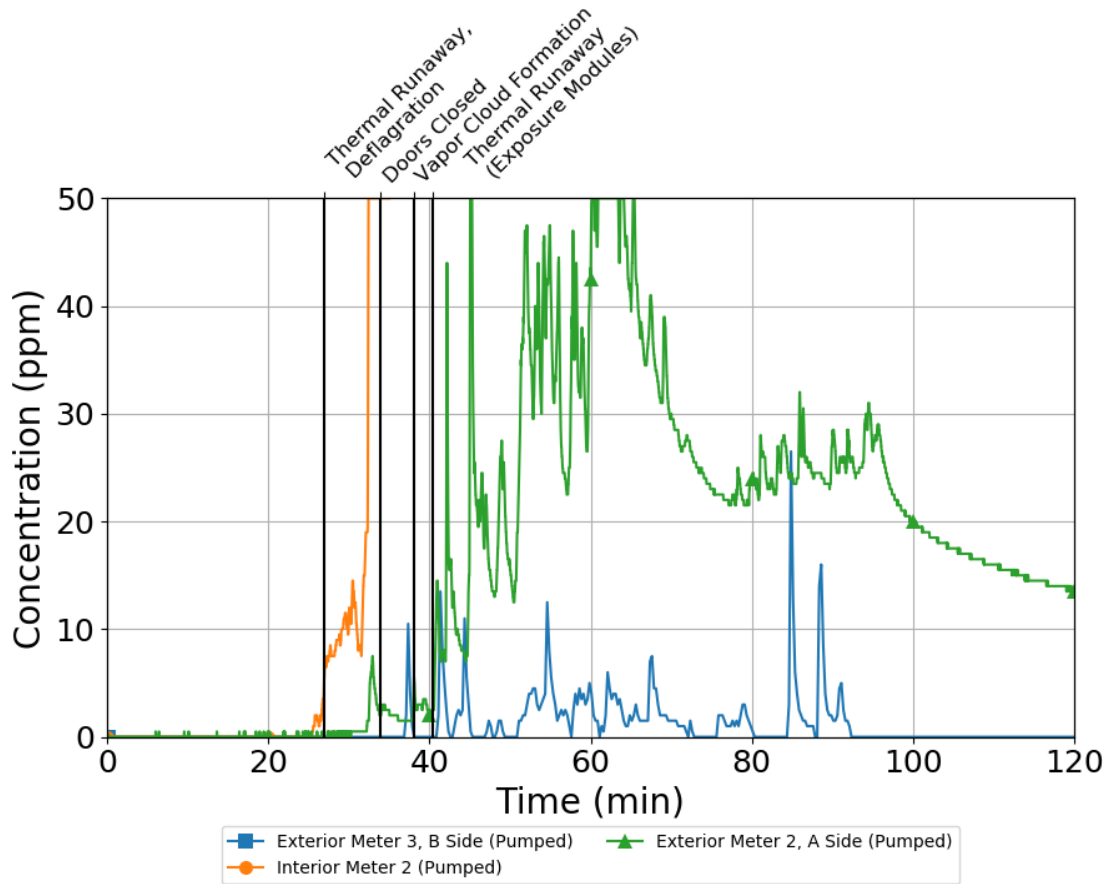


## UL 9540A INSTALLATION LEVEL TESTS WITH OUTDOOR LITHIUM-ION ENERGY STORAGE SYSTEM MOCKUPS

sensitive to hydrogen measurement as indicated in Table 7, but HCN was likely produced during the thermal decomposition of polyacrylonitrile component of the ABS plastic that made up the cell and module enclosures [27]. HCN is typically not measured in toxicity assessments of battery gas [28, 29, 30], but has been measured in low concentrations during vehicle fires [31], likely also due to polymeric material content.

HCN measured by Interior Meter 1 first began to increase after the doors were closed and reached the upper threshold of the measurement capability of the meter six minutes after thermal runaway, as illustrated in Figure 67. The meter then experienced a sensor error. The HCN measurements recorded by the exterior meters first began to increase seven minutes after the first thermal runaway event in parallel with the initial increase in exterior CO concentrations and the formation of the vapor cloud. The peak HCN concentrations measured by the meter on side A exceeded the upper limit of the measurement capability of the meter and the immediately dangerous to life or health (IDLH) concentration for HCN (50 ppm). The B-side meter indicated lower HCN concentrations, measuring a peak value of 16 ppm. Elevated concentrations of HCN were observed following propagation of thermal runaway to target modules until the end of the test. Critically, each of the HCN sensors used by these meters have listed cross-sensitivities with other gases, particularly CO and H<sub>2</sub>S, so it was not possible to decouple HCN concentration from CO concentration.

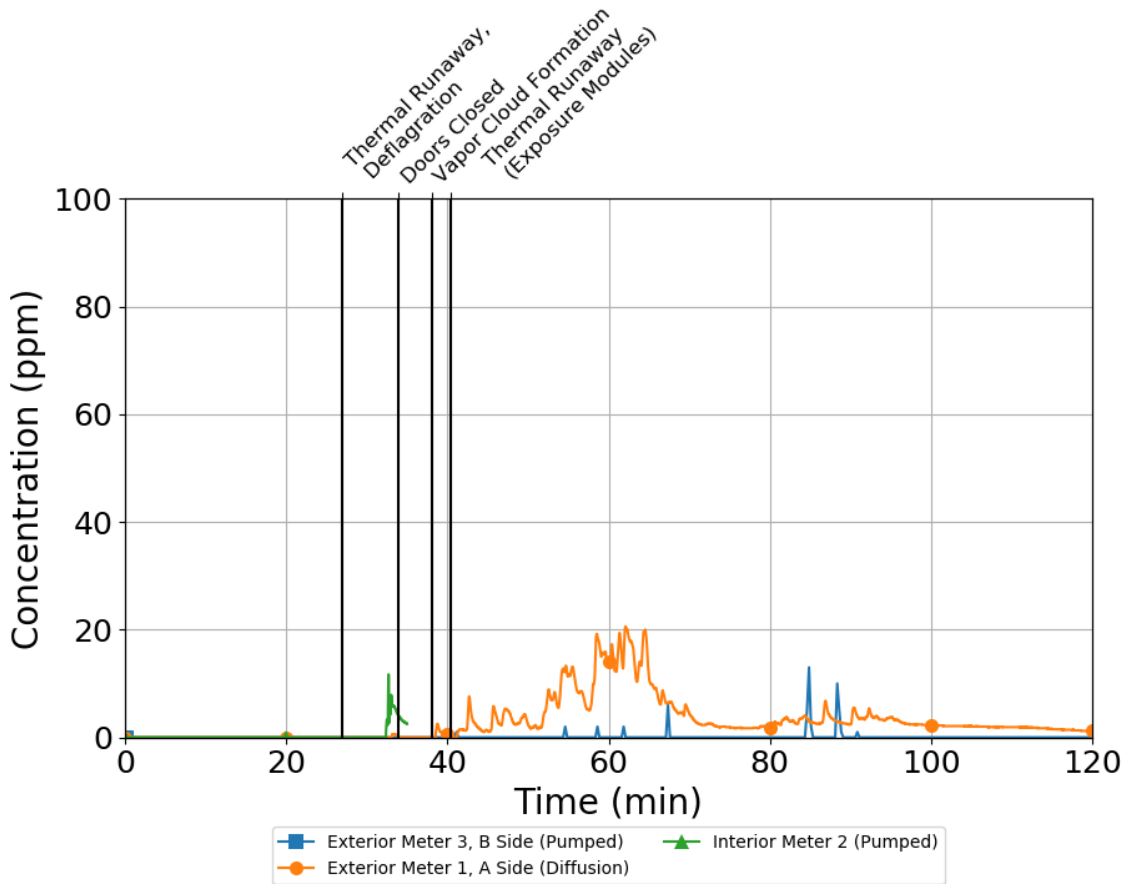
# UL 9540A INSTALLATION LEVEL TESTS WITH OUTDOOR LITHIUM-ION ENERGY STORAGE SYSTEM MOCKUPS



**Figure 67 – Hydrogen cyanide (HCN) concentration measured by fire service portable gas meters in Test 1.**

Other gases measured by the portable gas meters included hydrogen sulfide (H<sub>2</sub>S), oxygen (O<sub>2</sub>), and volatile organic compounds (VOCs). Hydrogen sulfide was measured in concentrations less than 20 ppm at all three meters capable of measuring H<sub>2</sub>S, as shown in Figure 68. H<sub>2</sub>S was first measured by Interior Meter 2 just prior to the doors closing, at the same time portable gas meters indicated an increase in CO, flammable gases, and HCN in the container. The exterior meters on the A and B sides measured concentrations of H<sub>2</sub>S later in the test. The peak exterior H<sub>2</sub>S concentration was measured 60 minutes after test start, matching the time at which peak exterior CO and HCN concentrations were observed and interior gas concentrations plateaued.

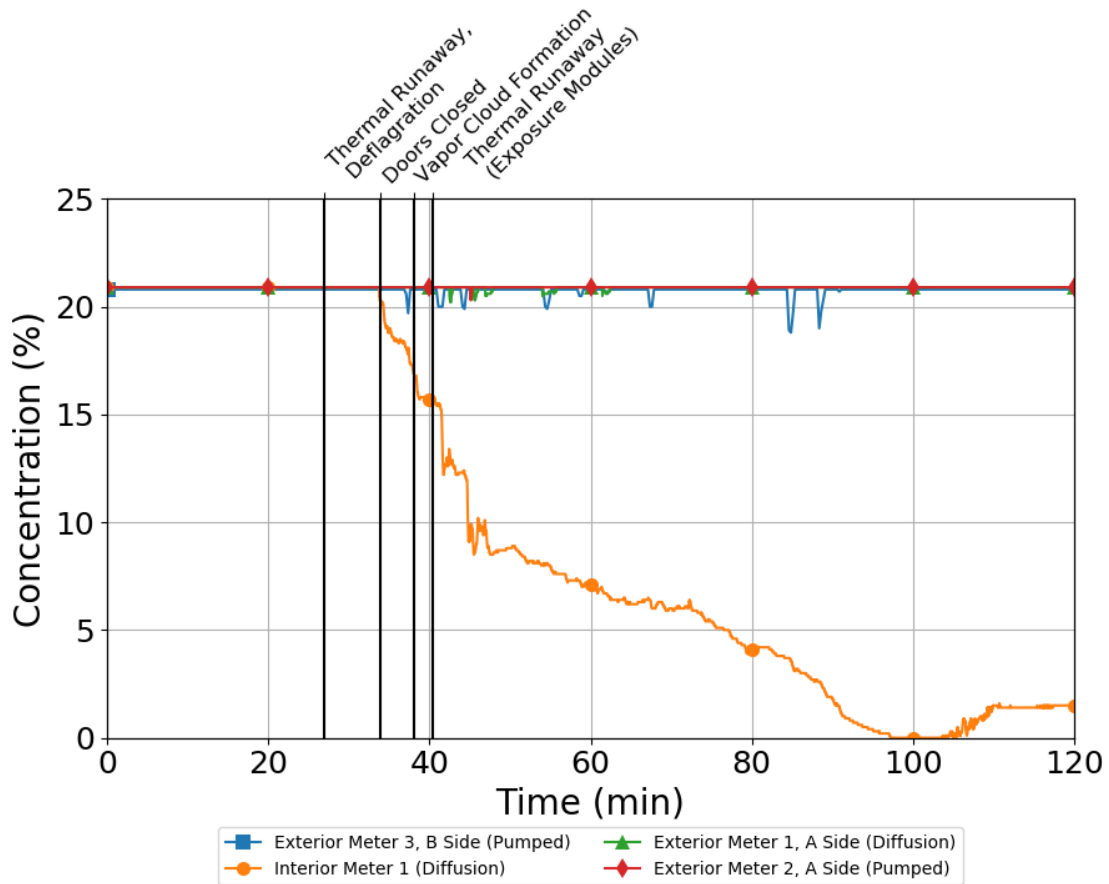
# UL 9540A INSTALLATION LEVEL TESTS WITH OUTDOOR LITHIUM-ION ENERGY STORAGE SYSTEM MOCKUPS



**Figure 68 – Hydrogen sulfide (H<sub>2</sub>S) concentration measured by fire service portable gas meters in Test 1.**

Oxygen concentrations measured by interior Meter 1 began to decrease after the container door was closed, which mirrored the increase in concentration for products of thermal runaway. Figure 69 shows the oxygen concentration in the container decreased to a minimum value of 0% approximately 100 minutes after test start. This contrasts with the oxygen concentration measured by the gas measurement instrumentation, which indicated a minimum value of approximately 5 v%, although the minimum value in both cases was observed 100 minutes after test start. Oxygen concentrations outside of the container, including Exterior Meter 4, remained at ambient concentration for the duration of the test, with the exception of a few brief decreases as thermal runaway started to propagate through the Initiating Unit.

# UL 9540A INSTALLATION LEVEL TESTS WITH OUTDOOR LITHIUM-ION ENERGY STORAGE SYSTEM MOCKUPS



**Figure 69 – Oxygen (O<sub>2</sub>) concentration measured by fire service portable gas meters in Test 1.**

Volatile organic compound (VOC) concentration was measured by the pumped meter on the A-side of the container. VOC concentrations followed a similar trend to the other exterior gas concentrations and increased as thermal runaway propagated to the target modules. The VOC concentration exceeded the upper limit of the measurement capability of the meter (100 ppm) 60 minutes after test start, which aligned with the peak exterior CO, HCN, and H<sub>2</sub>S concentrations. The VOC concentration dropped to zero 100 minutes after test start.





# UL 9540A INSTALLATION LEVEL TESTS WITH OUTDOOR LITHIUM-ION ENERGY STORAGE SYSTEM MOCKUPS

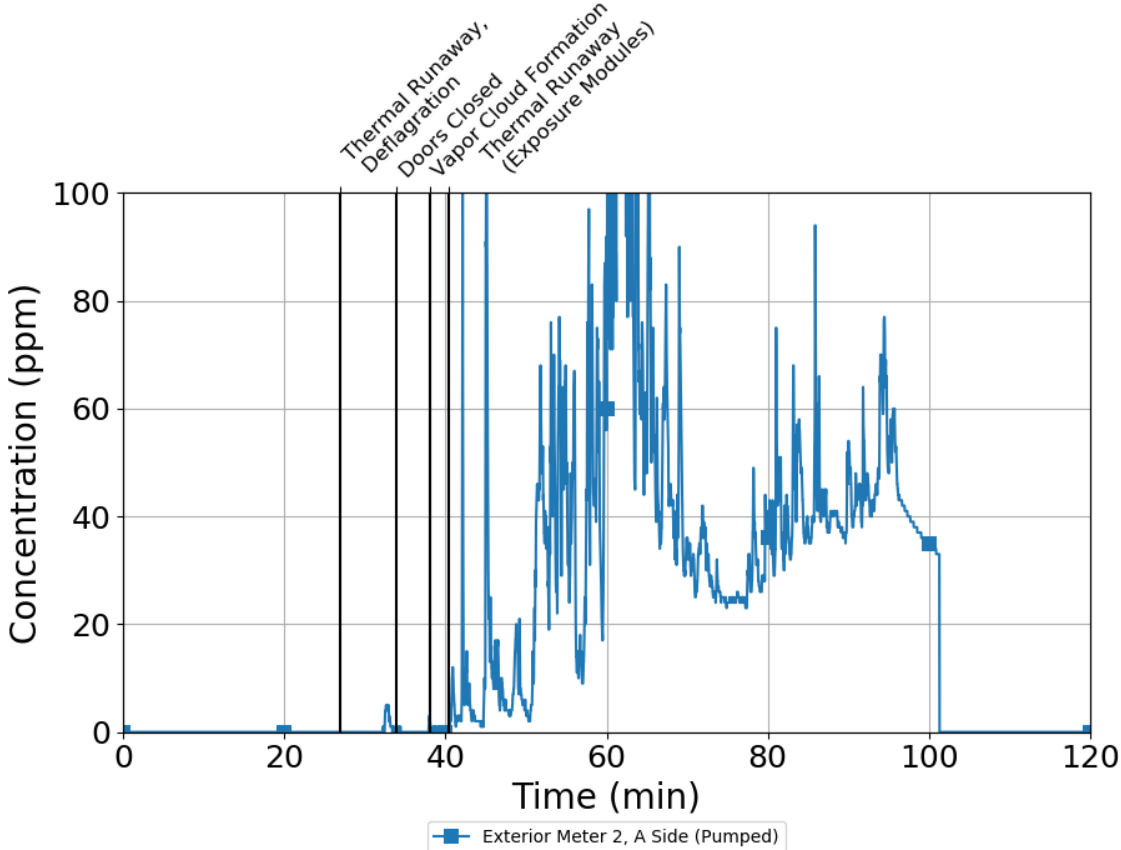


Figure 70 – Volatile organic compound (VOC) concentration measured by fire service portable gas meters in Test 1.



## 4.2 Test 2 – Li-Ion ESS Installation with Novec 1230 Clean Agent System

Test 2 was conducted on June 25, 2020, at 9:05 AM Central time.

### 4.2.1 Timeline

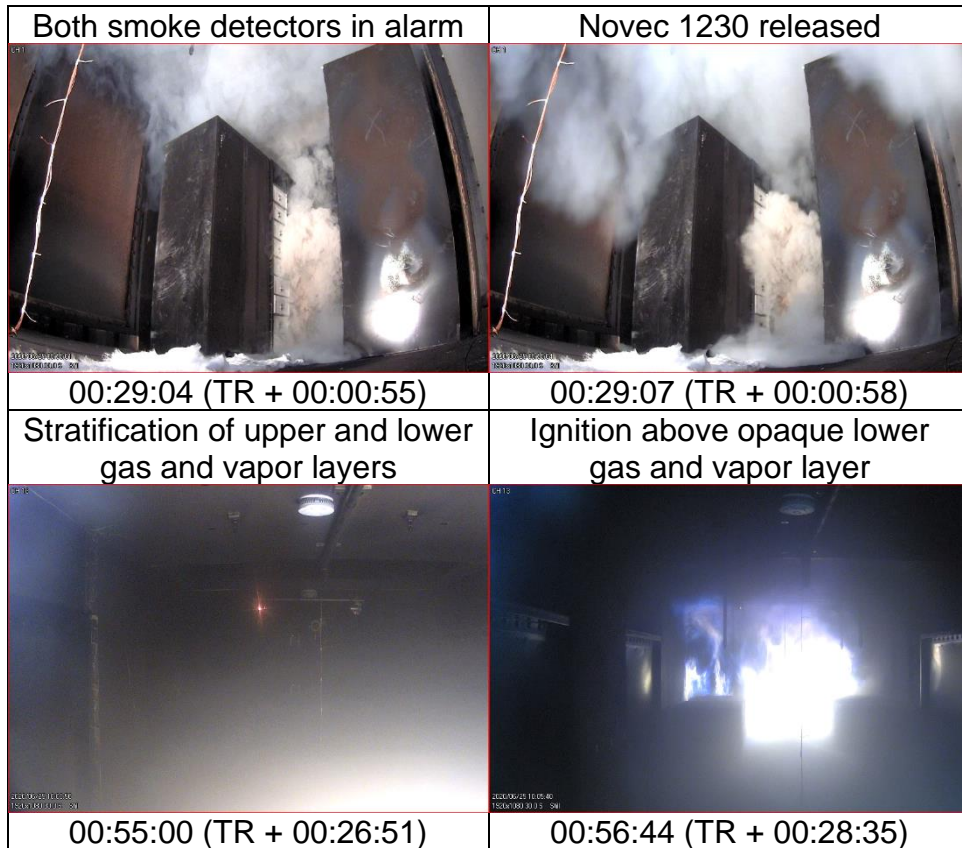
Figure 71 through Figure 72 show a visual sequence of the most significant events that occurred during Test 2.<sup>7</sup> Test 2 began when flexible film heaters installed inside the initiating module were energized to begin heating. Power was automatically controlled to provide 6 °C/min of temperature rise on the initiating 18650 component cell surface. After 22 minutes and 30 seconds, venting of the heated cell was detected by temperature measurements. Thermal runaway of the Initiating Cell occurred five minutes and 39 seconds later, at 28 minutes and nine seconds of test time. Smoke was first seen venting from the Initiating Module one second later. Within 30 seconds of the first thermal runaway event, thermal runaway occurred in another cell of the Initiating Module, the carbon monoxide detector was saturated with 250 ppm CO, and all three combustible gas detectors responded. The first smoke detector alarmed 53 seconds after thermal runaway, and the second smoke detector alarmed two seconds later. The activation of both smoke detectors triggered the release of Novec 1230 to a designed concentration of 8 v%.

Seven minutes after the Novec 1230 discharge, thermal runaway propagation was observed through the remainder of the Initiating Module. For 27 minutes after Novec 1230 discharge, stratification developed between the upper gas layer and the lower gas and vapor layer. Ignition occurred in the upper gas layer, and flaming did not penetrate the lower layer, at 56 minutes and 41 seconds of test time, 28 minutes and 32 seconds after the first thermal runaway. Flames flashed from the tops of the units to the ceiling, and shortly thereafter appeared to come from a flammable gas mixture accumulated within the top of the unit enclosures. Flaming ceased within 30 seconds.

---

<sup>7</sup> A more detailed visual timeline is provided in Appendix B: Detailed Visual Timeline of Test 2 Events.

## UL 9540A INSTALLATION LEVEL TESTS WITH OUTDOOR LITHIUM-ION ENERGY STORAGE SYSTEM MOCKUPS



**Figure 71 – Sequence of events in Test 2 leading up to 57 minutes of test time.**

Sixteen minutes after the ignition of gases in the upper layer, flammable gases reaccumulated and a deflagration occurred. At the time of this event, only one module had undergone thermal runaway. Pressure generated by the deflagration caused the operation of the top and one side of the deflagration vent panels. Flaming was observed at the vent locations as shown in the top left of Figure 72.

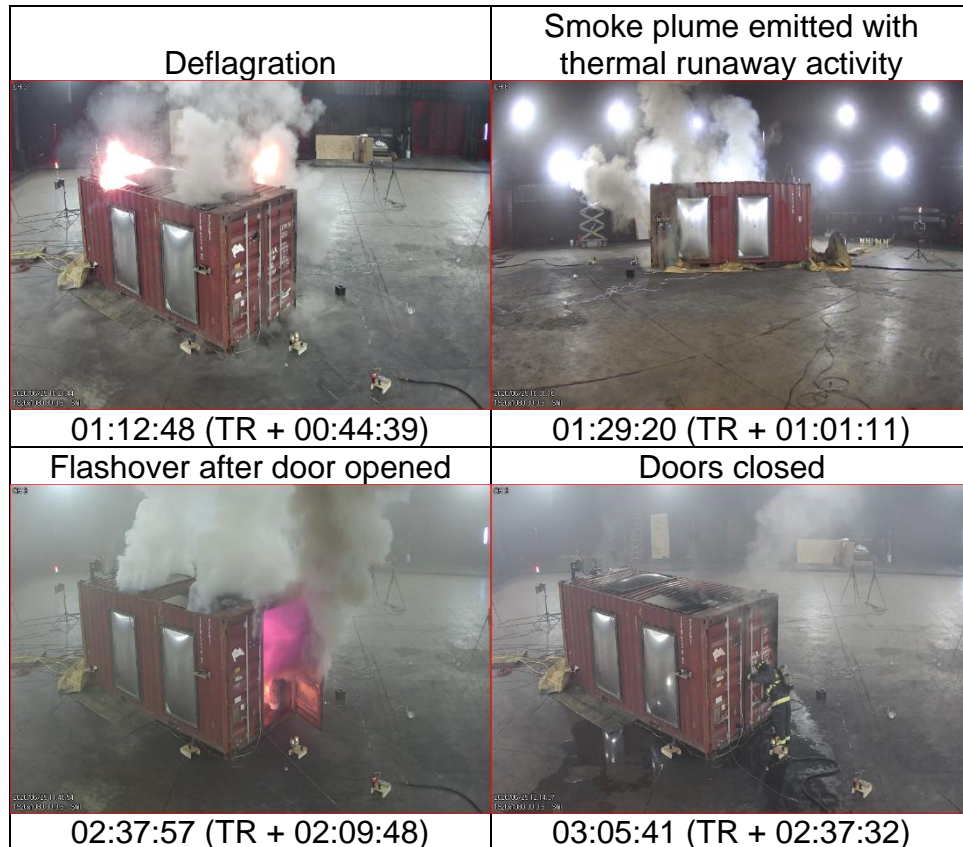
Two minutes after the deflagration, thermal runaway began to propagate upward through the Initiating Unit, starting with Module 4. Three minutes and 30 seconds later, the first response of the commercial hydrogen detector was recorded. Thermal runaway was observed in the Left Target Unit for the first time one hour and one minute after the initiating thermal runaway event. Thermal runaway continued to propagate upward through both units with one to 12 minutes between events. Thermal runaway was coupled with a release of gas and smoke from the container.

Starting at two hours and 17 minutes, unpiloted and intermittent ignition of gases occurred at a floor level wiring conduit.

One hour and 54 minutes after the first thermal runaway event, thermal runaway had propagated to the top module in both the Initiating Unit and the Left Target Unit. Fifteen minutes later, one door of the container was opened remotely to simulate fire department

## UL 9540A INSTALLATION LEVEL TESTS WITH OUTDOOR LITHIUM-ION ENERGY STORAGE SYSTEM MOCKUPS

response to an event in which thermal runaway activity had appeared to subside. A plume of smoke and gas were vented from the container and flashover of the container contents occurred within 21 seconds of opening the door. The flashover behavior continued for approximately 30 seconds, at which point gas measurements indicate that accumulated flammable gases were consumed and flaming was limited to the remaining solid combustible materials. Two minutes after flaming subsided, the bottom two modules of the Initiating Unit experienced thermal runaway. Thermal runaway had propagated through all modules of the Initiating Unit within two hours and 13 minutes of the initial cell thermal runaway.



**Figure 72 – Sequence of events in Test 2 from 72 to 185 minutes of test time.**

Intermittent hose stream application suppressed the remainder of flaming materials. During the period of intermittent hose stream application, thermal runaway was observed in Module 2 in the Left Target Unit, below the elevation of the Initiating Module. Thirty minutes after the door was opened, the door was manually closed. The carbon dioxide system was discharged one minute later to mitigate explosion hazards for test termination procedures. Thermal runaway occurred in the bottom module of the Left Target Unit nearly 28 minutes after the discharge of the carbon dioxide system. Thermal runaway had propagated through all modules of the Left Target Unit within three hours and six minutes of the first thermal runaway event in the Initiating Unit, and within two hours and six minutes of the first thermal runaway event in the Left Target Unit.

## UL 9540A INSTALLATION LEVEL TESTS WITH OUTDOOR LITHIUM-ION ENERGY STORAGE SYSTEM MOCKUPS

The doors remained closed for another hour and a half before overhaul procedures began. No further thermal runaway activity or flaming occurred. Thermal runaway behavior was never observed within the Front Target Unit.

### 4.2.2 Comparison of Test 2 Results to UL 9540A Performance Metrics

**Table 13 – Test 2 Performance**

Ref.	UL 9540A Performance Metric	Assessment
10.5.1	For BESS units intended for installation in locations with combustible construction, surface temperature measurements along instrumented wall surfaces shall not exceed a temperature rise of 97 °C (175 °F) above ambient. Surface temperature rise is not applicable if the intended installation is composed completely of noncombustible materials in which wall assemblies, cables, wiring, and any other combustible materials are not to be present in the BESS installation. In this case, the report shall note that the installation shall contain no combustible materials.	Not compliant
10.5.2	The surface temperature of modules within the BESS units adjacent to the initiating BESS unit shall not exceed the temperature at which thermally initiated cell venting occurs.	Not compliant
10.5.3	The fire spread on the cables in the flame indicator shall not extend horizontally beyond the initiating BESS enclosure dimensions.	N/A
10.5.4	There shall be no flaming outside the test room.	Not compliant
10.5.5	There is no observation of detonation. There is no observation of deflagration unless mitigated by an engineered deflagration protection system.	Compliant <sup>†</sup>
10.5.6	Heat flux in the center of the accessible means of egress shall not exceed 1.3 kW/m <sup>2</sup> .	Not compliant
10.5.7	There shall be no observation of re-ignition within the initiating unit after the installation test had been concluded and the sprinkler operation was discontinued.	Not compliant

<sup>†</sup> The deflagration venting successfully vented overpressure, potentially preventing dangerous loss of integrity/rupture of the ISO container.

### Thermal Exposure to Walls

Most temperature measurement locations on both the rear- and side-instrumented walls exceeded the temperature performance criteria within 30 minutes after the propagation of thermal runaway outside the Initiating Unit, as illustrated in Figure 73 and Figure 74. As with Test 1, the temperatures measured on the rear wall exceeded the side wall because hot battery gases impinged directly on the rear panel of the Initiating Unit enclosure. Despite an initial difference in temperature development, potentially due to Novec 1230 inhibiting the flaming combustion of battery off-gas, the peak temperatures



# UL 9540A INSTALLATION LEVEL TESTS WITH OUTDOOR LITHIUM-ION ENERGY STORAGE SYSTEM MOCKUPS

observed on the instrumented walls were consistent with Test 1. Novec 1230 did not prevent noncompliant temperature rise results.

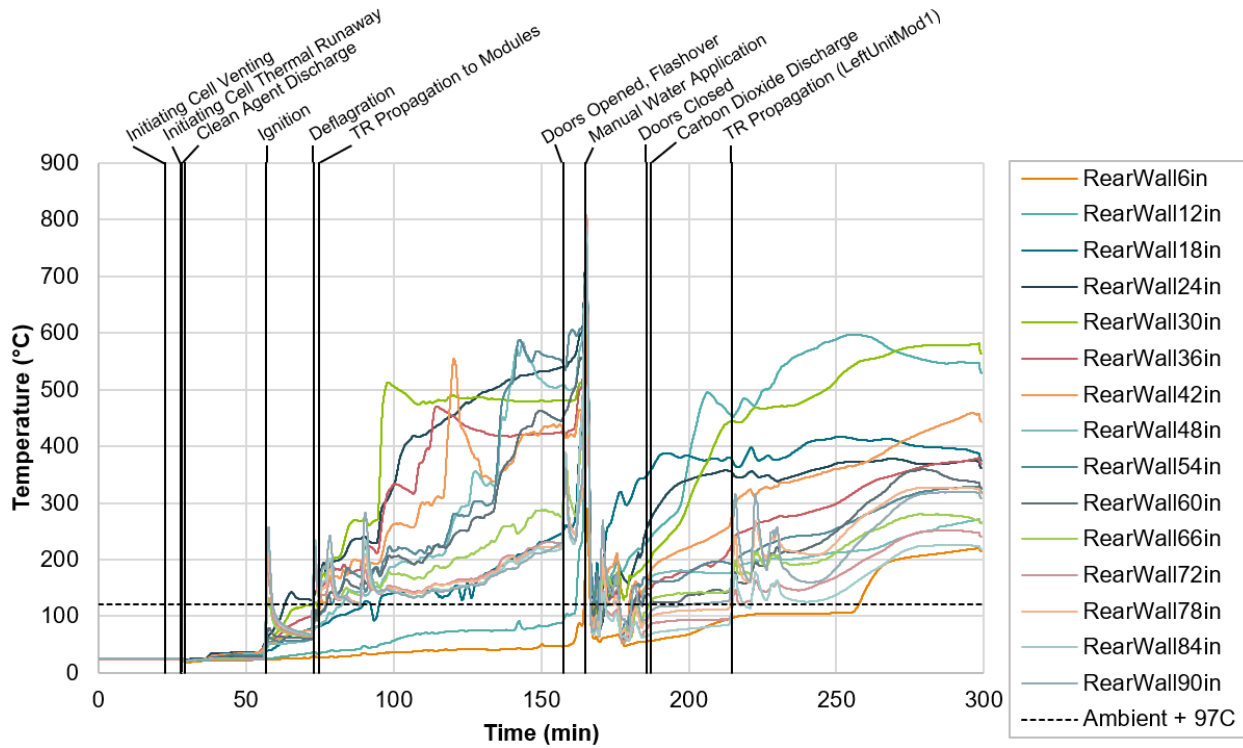
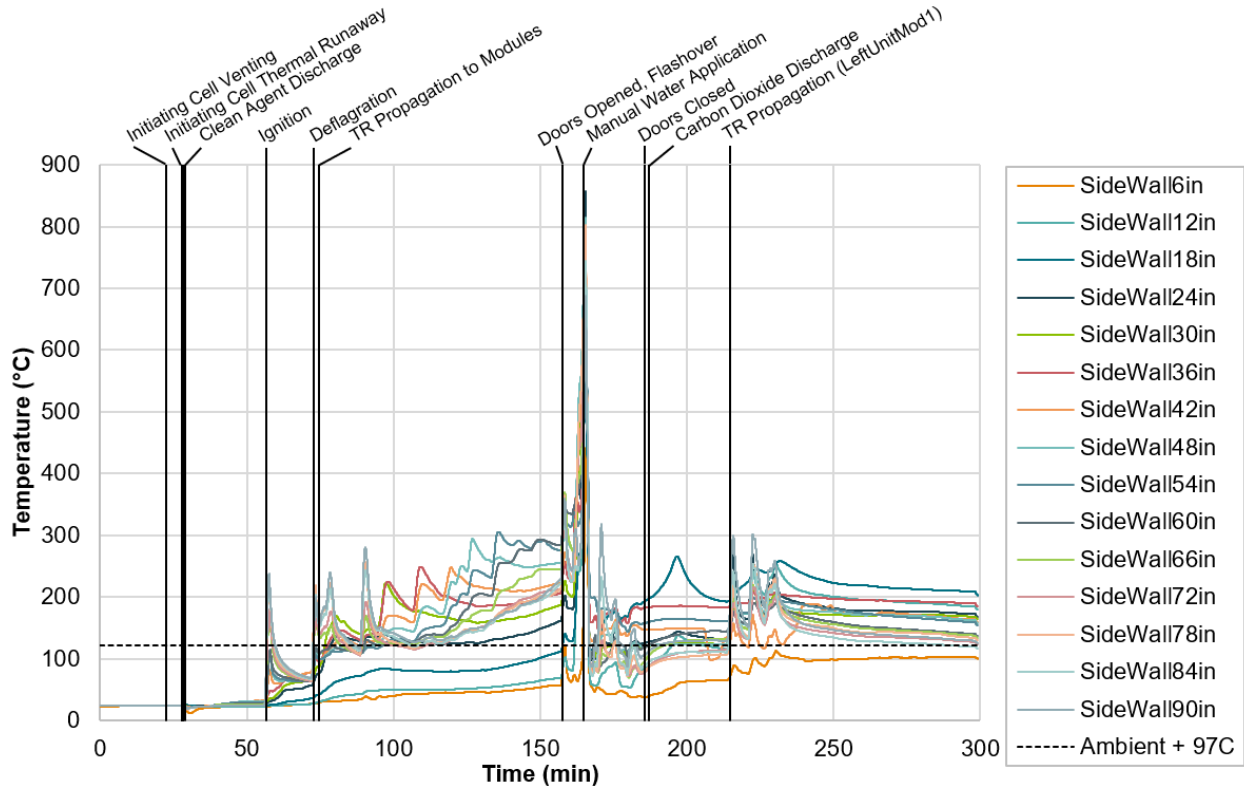


Figure 73 – Rear wall temperatures measured during Test 2.



## UL 9540A INSTALLATION LEVEL TESTS WITH OUTDOOR LITHIUM-ION ENERGY STORAGE SYSTEM MOCKUPS



**Figure 74 – Side wall temperatures measured during Test 2,**

During manual water application, wall surface temperatures on both walls dropped from flashover temperatures above 600 °C to an average of 100 °C in two minutes, as shown in Figure 73. Intermittent manual water application resulted in average rear wall temperature fluctuations between 90 °C and 160 °C, and side wall temperature fluctuations between 100 °C and 145 °C. When manual water application was discontinued and the doors were closed, the carbon dioxide system was discharged. The carbon dioxide system discharge, meant only to reduce deflagration hazards, did not have any observable impact on wall surface temperatures. The rear wall surface temperatures continued to rise for an additional two hours after the doors were closed and the carbon dioxide system was discharged. Propagation of thermal runaway to an additional module was observed after carbon dioxide system discharge, which further contributed to temperature rise on both instrumented walls. After thermal runaway activity was complete, wall surface temperatures on the rear wall stabilized and temperatures on the side wall temperatures gradually decreased.

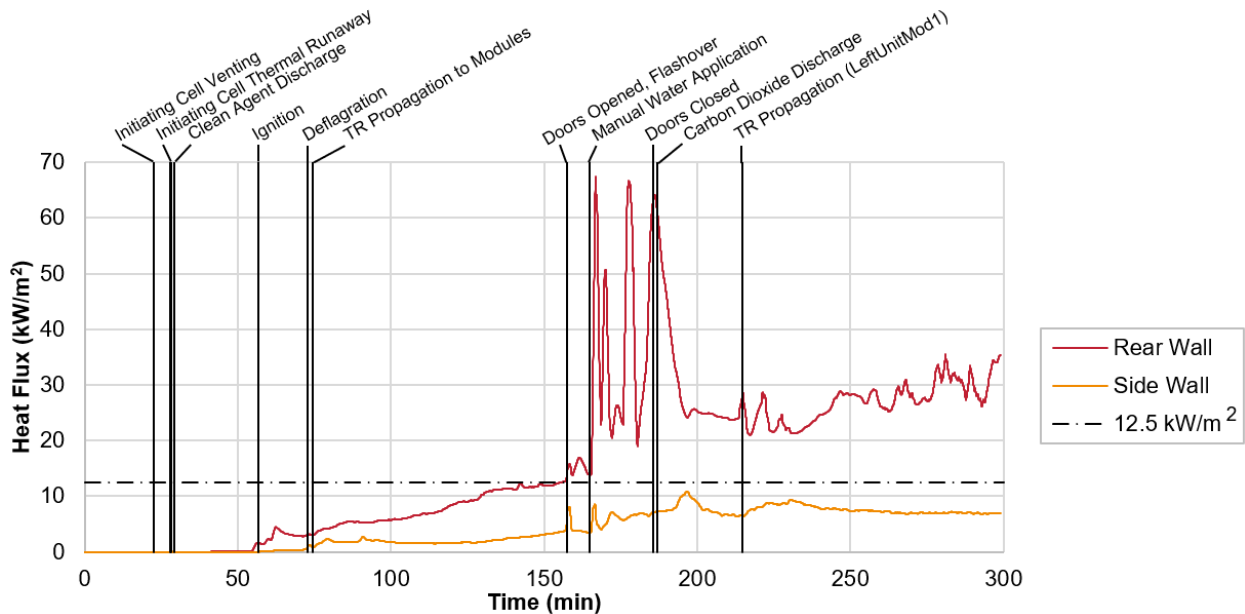
UL 9540A does not include a performance criterion based on incident heat flux to combustible materials. Heat flux measured in Test 2 offers insight into the magnitude and duration of exposure and subsequent ignition risk to combustible materials. Heat flux measured on rear wall was less than 12.5 kW/m<sup>2</sup>, a critical threshold for ignition risk to combustible structures according to NFPA 80A [23], until 150 minutes. Manual water application caused a rapid increase in the heat flux at the rear wall. Rear wall heat flux fluctuated between 20 kW/m<sup>2</sup> and 65 kW/m<sup>2</sup> until water application was terminated, likely





## UL 9540A INSTALLATION LEVEL TESTS WITH OUTDOOR LITHIUM-ION ENERGY STORAGE SYSTEM MOCKUPS

due to gas turbulence induced by the hose stream and phase change of suppression water. After carbon dioxide system discharge, heat flux at the rear wall was between 20 kW/m<sup>2</sup> and 35 kW/m<sup>2</sup> for two hours. The instrumented side wall heat flux was less than 12.5 kW/m<sup>2</sup> for the duration of Test 2. Side wall heat flux was not as significantly impacted as the rear wall by the gas ignition after the doors were opened, or manual water application, which may have been due to its shielded location.

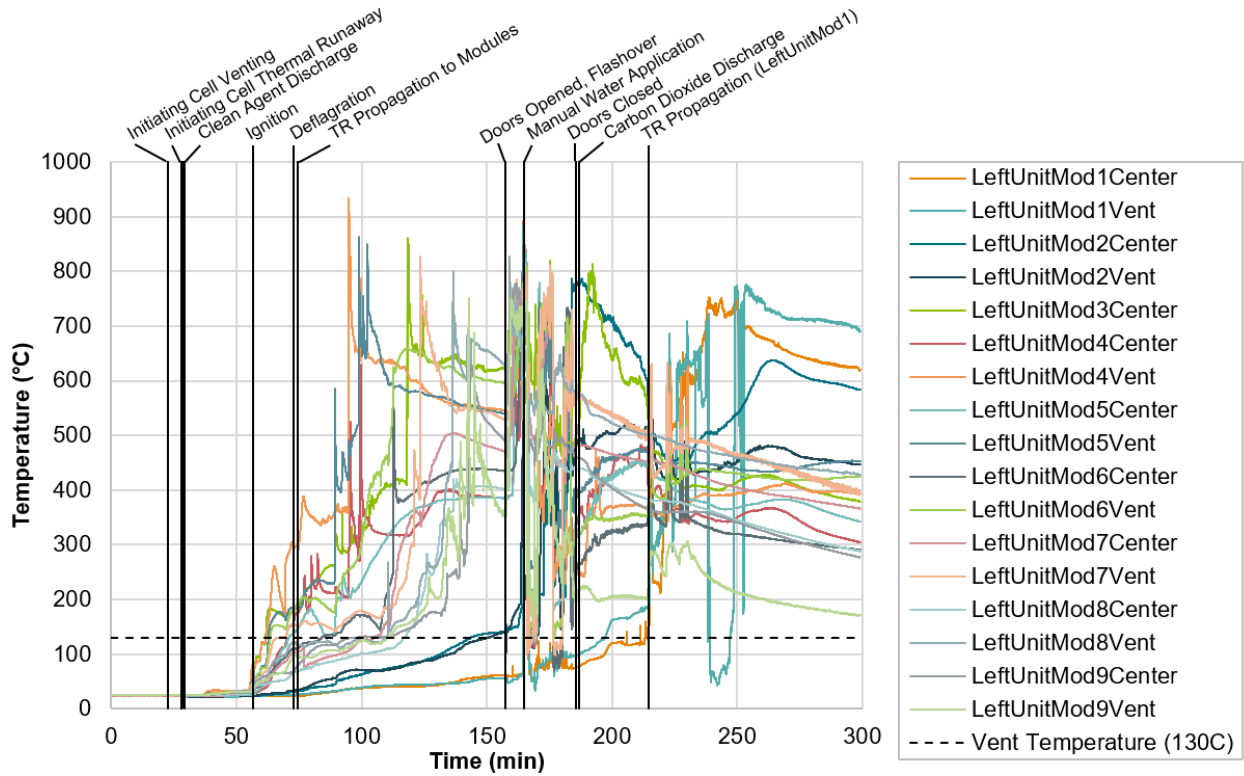


**Figure 75 – Incident heat flux measured to rear and side walls during Test 2.**

### Thermal Exposure to ESS Targets

All temperature measurements in all target modules of the Left Target Unit exceeded the cell vent temperature, 130 °C. Therefore, temperature measurements demonstrated the ESS configuration was not compliant with the Target Unit temperature performance criteria. Most modules of the Left Target Unit exceeded the cell vent temperature within 60 minutes of ignition (90 minutes from the first thermal runaway event), as displayed in Figure 76. Novec 1230 may have impacted initial hazard development by preventing an early ignition, but the Target Unit temperatures developed to the same magnitudes as Test 1 over the duration of Test 2.

# UL 9540A INSTALLATION LEVEL TESTS WITH OUTDOOR LITHIUM-ION ENERGY STORAGE SYSTEM MOCKUPS



**Figure 76 – Temperatures measured in Left Target Unit during Test 2.**

All target modules in the Left Target Unit experienced thermal runaway during the test. Thermal runaway behavior is marked in Figure 76 by an immediate temperature increase of more than 400 °C and a sustained temperature above 300 °C. Seven modules experienced thermal runaway before the doors of the container were opened. One module experienced thermal runaway after doors were opened and manual water application began. One final module experienced thermal runaway after the doors of the container were closed and the carbon dioxide system was discharged. Figure 77 illustrates the extent of extent of damage to the Left Target Unit.



## UL 9540A INSTALLATION LEVEL TESTS WITH OUTDOOR LITHIUM-ION ENERGY STORAGE SYSTEM MOCKUPS

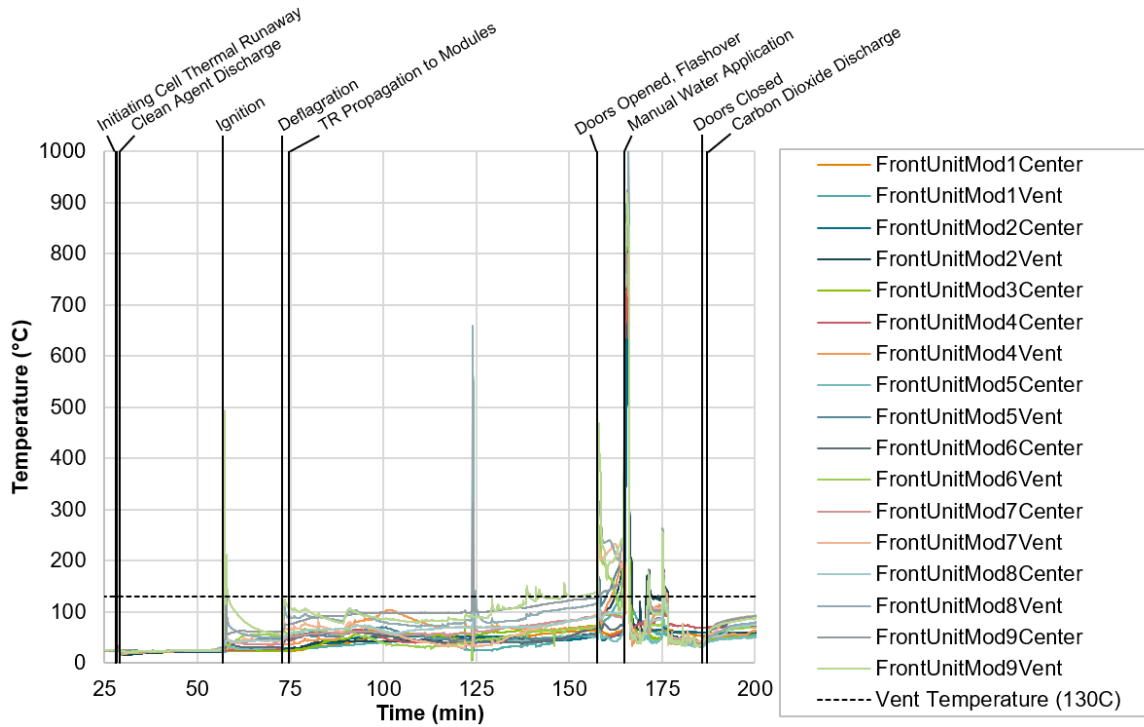


**Figure 77 – Condition of Left Target Unit after Test 2.**

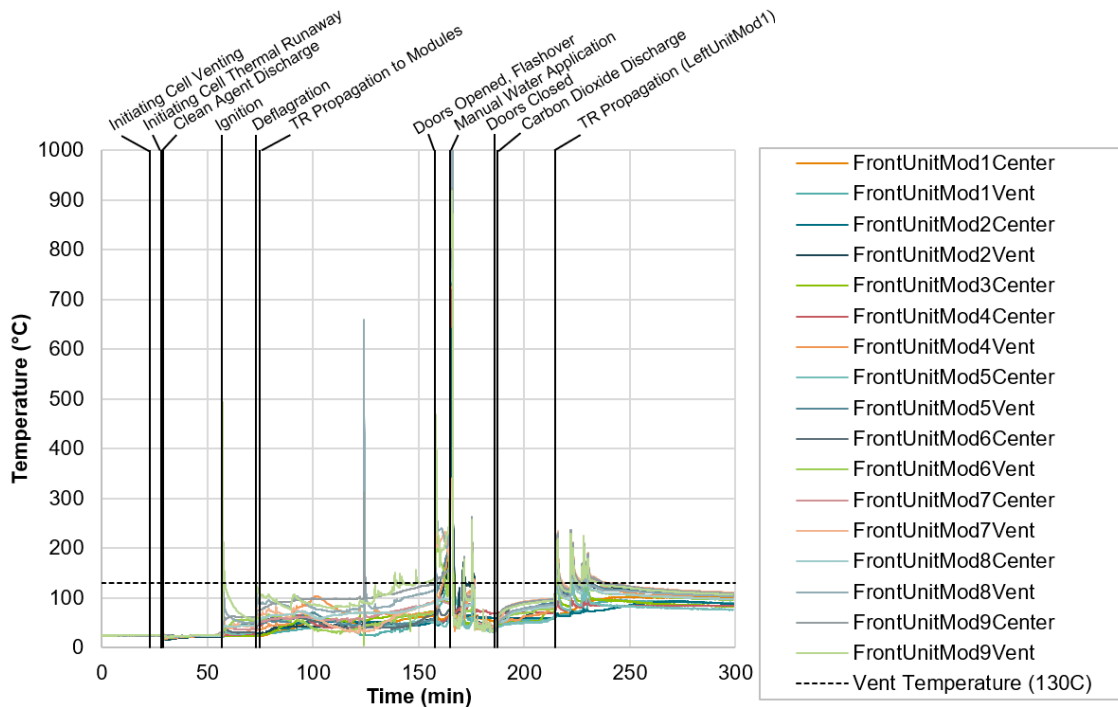
Before the container doors were opened and the accumulated gases ignited, three modules in the Front Target Unit were noncompliant with the target unit temperature performance criteria, as shown in Figure 78. Once the doors were opened and the container experienced flashover and the container was subjected to manual water application, cell vent temperature was exceeded in all nine Front Target Unit modules, as documented in Figure 79.

None of the modules in the Front Target Unit experienced any thermal runaways in Test 2.

# UL 9540A INSTALLATION LEVEL TESTS WITH OUTDOOR LITHIUM-ION ENERGY STORAGE SYSTEM MOCKUPS



**Figure 78 – Temperatures measured in Front Target Unit from thermal runaway to carbon dioxide system discharge during Test 2.**



**Figure 79 – Temperatures measured in Front Target Unit during Test 2.**



## UL 9540A INSTALLATION LEVEL TESTS WITH OUTDOOR LITHIUM-ION ENERGY STORAGE SYSTEM MOCKUPS

Figure 80 shows that heat flux exposure to the Front Target Unit was nominally 2 kW/m<sup>2</sup> over the duration of Test 2 after the deflagration. Short-duration rapid increases in heat flux exposure exceeded 12.5 kW/m<sup>2</sup> when the doors were opened and during manual water application. Figure 81 shows the extent of thermal damage to a Front Target Unit module, including melting, deformation, and heavy soot deposition.

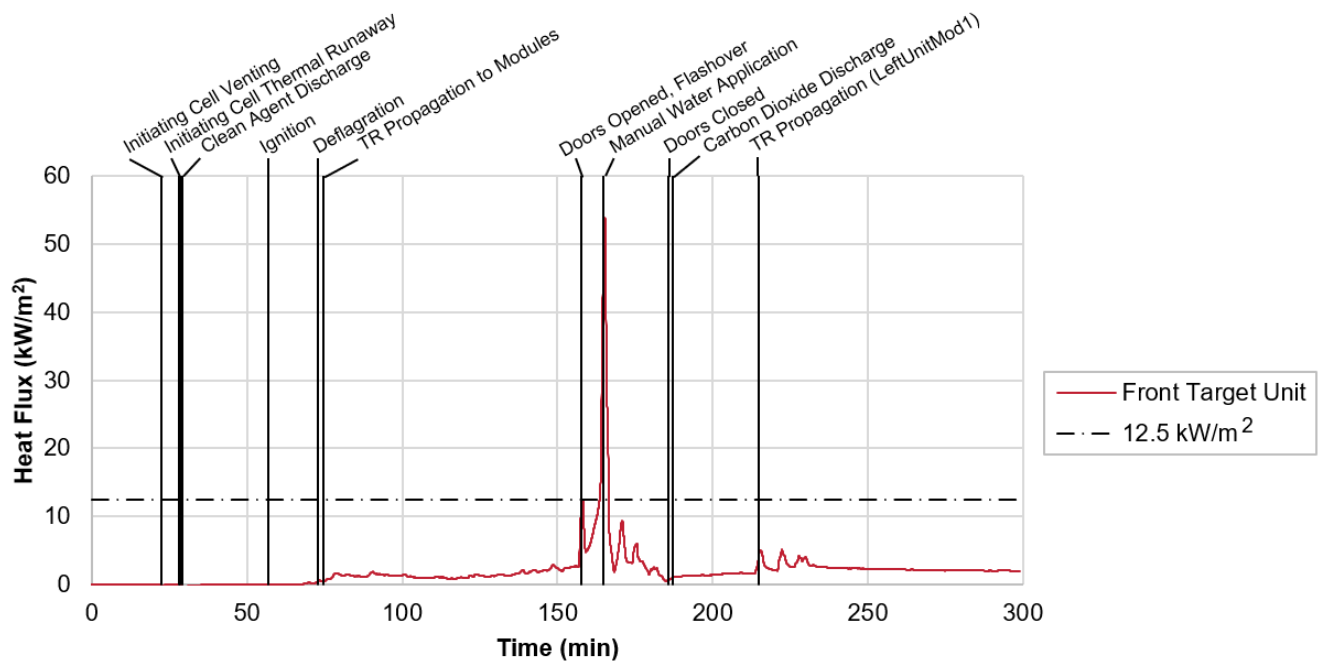


Figure 80 – Incident heat flux measured in Front Target Unit during Test 2.





# UL 9540A INSTALLATION LEVEL TESTS WITH OUTDOOR LITHIUM-ION ENERGY STORAGE SYSTEM MOCKUPS

**Figure 81 – Condition of a module in Front Target Unit after Test 2.**

## Flaming Outside the Test Room

Intermittent flaming of gases escaping from an instrumentation cable conduit in the container wall was observed, as pictured in Figure 82. The intermittent flaming is an indication the gas mixture accumulated inside the container lacked sufficient oxygen for complete combustion and may have been above the upper flammability limit (UFL).



**Figure 82 – Flaming observed intermittently through instrumentation opening in container wall in Test 2.**

Flames were vented from the container during the deflagration, as pictured in Figure 83. Though the deflagration was safely vented, flaming observed through the deflagration vents must be considered during siting.



**Figure 83 – Short duration flaming observed from deflagration vents.**

## UL 9540A INSTALLATION LEVEL TESTS WITH OUTDOOR LITHIUM-ION ENERGY STORAGE SYSTEM MOCKUPS

When the container door was opened for test termination, ambient air was exchanged with gases inside the container. Flashover occurred within 21 seconds, as illustrated by Figure 84. Flaming materials included flammable gases and vapors, battery enclosure materials, and container surface paint.



**Figure 84 – Flaming of container contents after door opening in Test 2.**



# UL 9540A INSTALLATION LEVEL TESTS WITH OUTDOOR LITHIUM-ION ENERGY STORAGE SYSTEM MOCKUPS

## Explosion Hazards

A deflagration occurred in the container 44 minutes after thermal runaway and 43 minutes after Novec 1230 discharge. At this time, only one module had undergone thermal runaway. Potential ignition sources include hot materials from the modules that experienced thermal runaway, and electrical components of wall-mounted gas detectors. Pressure generated by the deflagration caused the operation of the top and one side of the deflagration vent panels, as pictured in Figure 85.



Figure 85 – Deflagration images from Test 2.

# UL 9540A INSTALLATION LEVEL TESTS WITH OUTDOOR LITHIUM-ION ENERGY STORAGE SYSTEM MOCKUPS

## Egress Path Heat Flux

Measurements for egress path heat flux were taken from the heat flux gauge installed in the Front Target Unit, across the aisle from the Initiating Unit.

Heat flux measurements were noncompliant with the 1.3 kW/m<sup>2</sup> criteria for the remainder of the test after 75 minutes, as plotted in Figure 86. Heat flux measurements were nominally 1.9 kW/m<sup>2</sup> after the deflagration and until the doors were opened and the container experienced flashover. Additionally, the deflagration likely produced a brief peak heat flux much greater than 1.3 kW/m<sup>2</sup>, that was not captured due to the 1 Hz data collection rate. Immediately prior to water application, heat flux at the Front Target Unit reached 50 kW/m<sup>2</sup>.

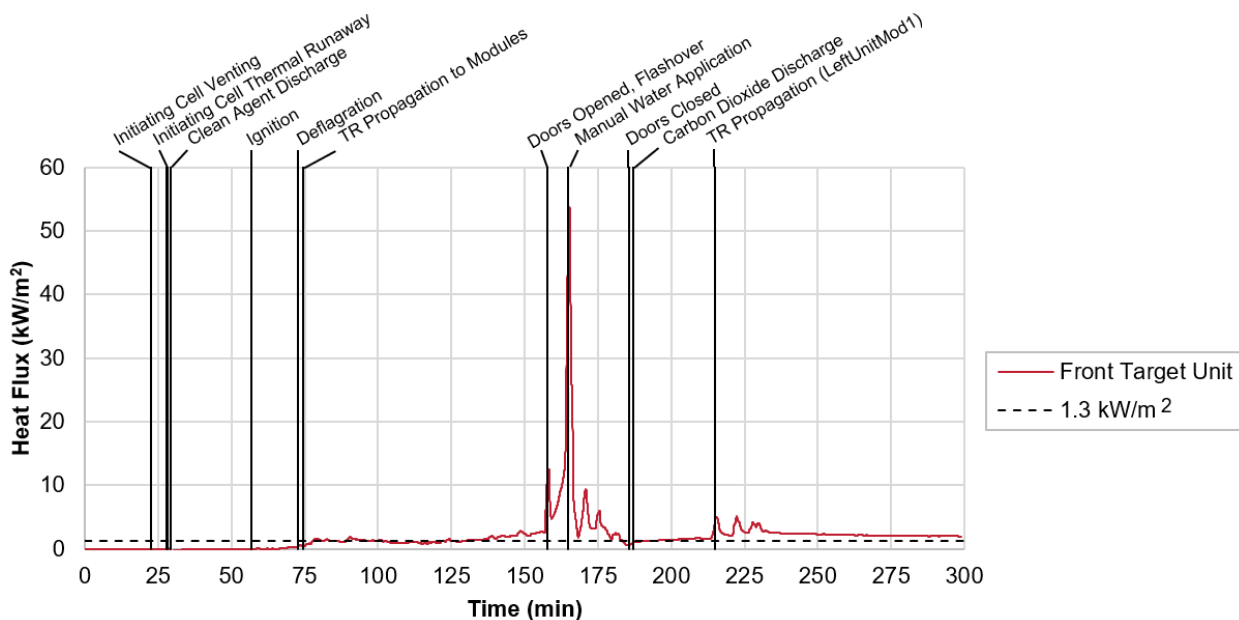


Figure 86 – Heat flux measured in the egress path during Test 2.<sup>8</sup>

## Reignition Caused by Post-Test Thermal Runaways

Opening the door of the container was considered the first step of test termination procedures. This influx of air resulted in flashover conditions. After flashover, two more modules in the Initiating Unit experienced thermal runaway. During the following period of intermittent manual water application, one additional module in the Left Target Unit experienced thermal runaway. Once the doors were closed again and a carbon dioxide gas system was discharged, one more module in the Left Target Unit underwent thermal runaway. Thermal runaway behavior after test termination procedures demonstrated a

<sup>8</sup> Plot includes 60 second averaging.

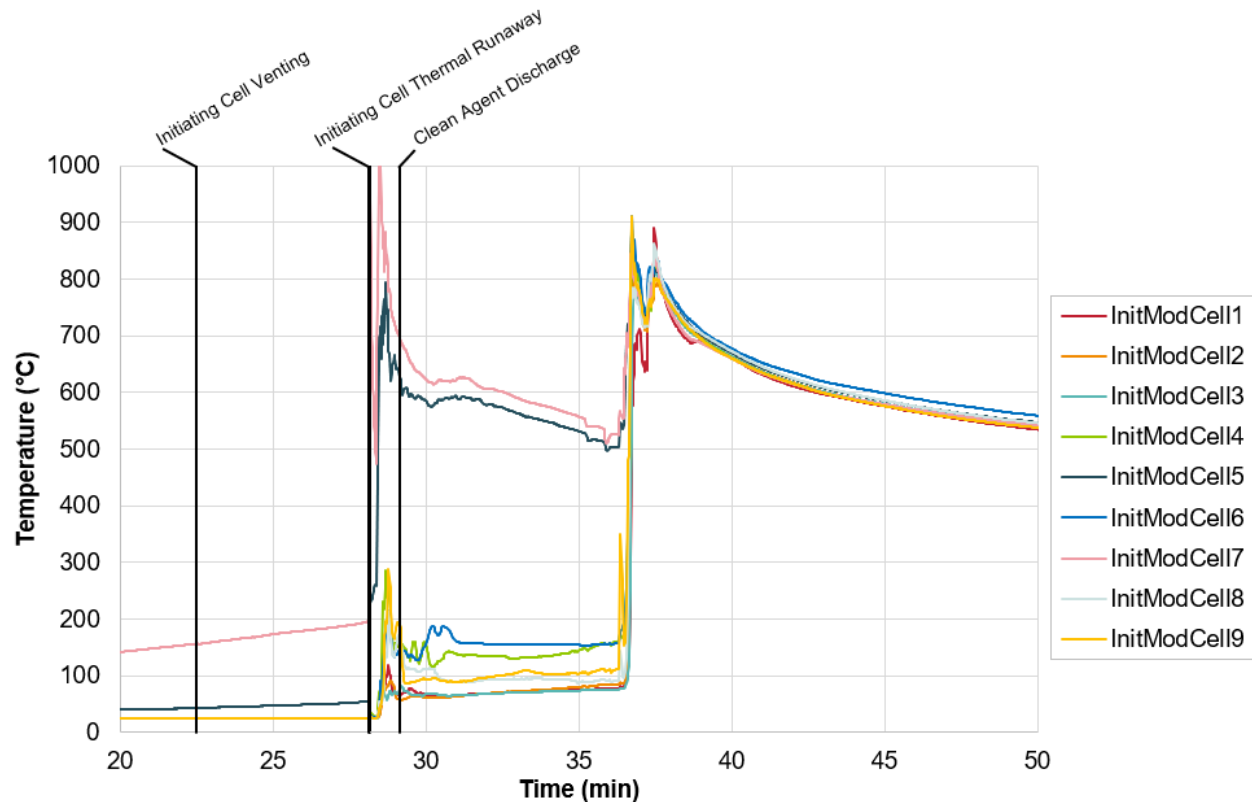


## UL 9540A INSTALLATION LEVEL TESTS WITH OUTDOOR LITHIUM-ION ENERGY STORAGE SYSTEM MOCKUPS

reignition hazard for incident managers and other responders and, therefore, is not compliant with UL 9540A, 4<sup>th</sup> edition, criteria for re-ignition.

### 4.2.3 Thermal Runaway Propagation

Cell 7 went into thermal runaway within 30 seconds of the initiating cell (Cell 5), as documented in Figure 87. Within another 30 seconds, both smoke detectors alarmed, and the clean agent system was discharged. Eight minutes later, the remainder of cells in the Initiating Module underwent thermal runaway. Temperatures measured throughout the Initiating Module do not show a clear impact of Novec 1230 discharge. The rate of temperature dissipation on Cell 5 and Cell 7 was not impacted by Novec 1230 discharge.

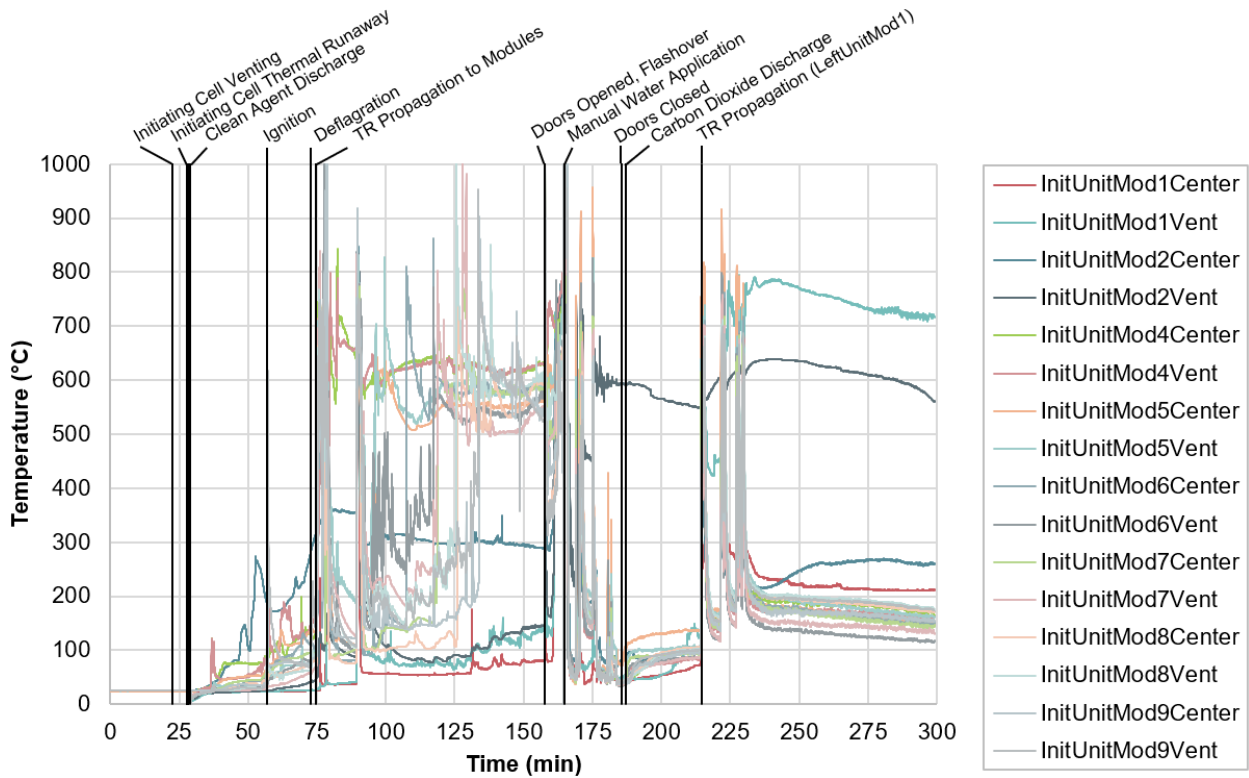


**Figure 87 – Temperatures measured throughout the Initiating Module indicate propagation of thermal runaway in Test 2.**

Thermal runaway propagated module-to-module through all modules in the Initiating Unit and the Left Target Unit. Thermal runaway propagated from the Initiating Module upward to Module 4 after the deflagration occurred. Thermal runaway behavior in the Initiating Unit is marked in Figure 88 by an immediate temperature increase of more than 400 °C and a sustained temperature above 300 °C. After the initial propagation event, thermal runaway propagation occurred similarly to Test 1. After Module 4, upward thermal runaway propagation occurred at a rate of one to 12 minutes between events.

## UL 9540A INSTALLATION LEVEL TESTS WITH OUTDOOR LITHIUM-ION ENERGY STORAGE SYSTEM MOCKUPS

Downward thermal runaway propagation also occurred with two hours and 12 minutes for propagation between the Initiating Module and lower modules in the Initiating Unit; thermal runaway occurred in both modules after the container door was opened and flashover occurred, and before any water application. Downward thermal runaway propagation was observed in the Left Target Unit with an average of one hour between each event. In the Left Target Unit, propagation of thermal runaway to Module 2 happened after water application, and propagation of thermal runaway to Module 1 happened after the door was closed and the carbon dioxide system was discharged. A summary of propagation times is given in Table 14.



**Figure 88 – Temperatures measured throughout the Initiating Unit during Test 2.**



**UL 9540A INSTALLATION LEVEL TESTS WITH OUTDOOR LITHIUM-ION ENERGY STORAGE SYSTEM MOCKUPS**

**Table 14 – Thermal runaway propagation times for Test 2.**

<b>Test Time</b>	<b>Time Since TR</b>	<b>Location</b>	<b>Test Time</b>	<b>Time Since TR</b>	<b>Location</b>
00:28:09	00:00:00	InitUnitMod3	02:13:18	01:45:09	InitUnitMod9
00:29:07	00:00:58	Novec 1230	02:16:30	01:48:21	LeftUnitMod8
01:12:48	00:44:39	Deflagration	02:22:05	01:53:56	LeftUnitMod9
01:14:35	00:46:26	InitUnitMod4	02:37:36	02:09:27	Door Opened
01:29:09	01:01:00	LeftUnitMod5	02:37:57	02:09:48	Flashover
01:34:29	01:06:20	InitUnitMod5	02:40:29	02:12:20	InitUnitMod1
01:34:40	01:06:31	LeftUnitMod4	02:41:01	02:12:52	InitUnitMod2
01:47:06	01:18:57	InitUnitMod6	02:44:56	02:16:47	Waterflow Begins
01:47:29	01:19:20	LeftUnitMod6	02:51:09	02:23:00	LeftUnitMod2
01:57:36	01:29:27	InitUnitMod7	03:05:41	02:37:32	Door Closed
01:57:43	01:29:34	LeftUnitMod3	03:07:01	02:38:52	CO <sub>2</sub> Discharge
02:00:01	01:31:52	LeftUnitMod7	03:34:45	03:06:36	LeftUnitMod1
02:05:42	01:37:33	InitUnitMod8			

Figure 89 illustrates the extent of damage to the Initiating Unit. Most enclosure materials were consumed and all cells experienced thermal runaway.

No thermal runaway behavior was observed in the Front Target Unit.



**Figure 89 – Condition of Initiating Unit after Test 2.**

# UL 9540A INSTALLATION LEVEL TESTS WITH OUTDOOR LITHIUM-ION ENERGY STORAGE SYSTEM MOCKUPS

## 4.2.4 Test Conditions Inside ISO Container

### Gas Temperature

There was no change in container gas temperatures between initial thermal runaway and Novec 1230 discharge. The phase change of the discharging Novec 1230 caused gas temperatures in the container to drop below ambient, as illustrated in Figure 90. Gas temperatures increased rapidly 56 minutes after flammable gases ignited in the upper half of the container, above an opaque gas layer that had formed in the bottom portion of the container. Flaming, however, was limited to the accumulated flammable gases and lasted 50 seconds. Subsequently, container temperatures cooled, and gas temperatures returned to less than 75 °C within five minutes of the gas ignition. Gas temperatures increased again after the deflagration occurred and more modules underwent thermal runaway. Hot gases were vented from the modules into the container, resulting in temperatures from 60 °C at the floor level to 205 °C at the ceiling before the door was opened at 157 minutes.

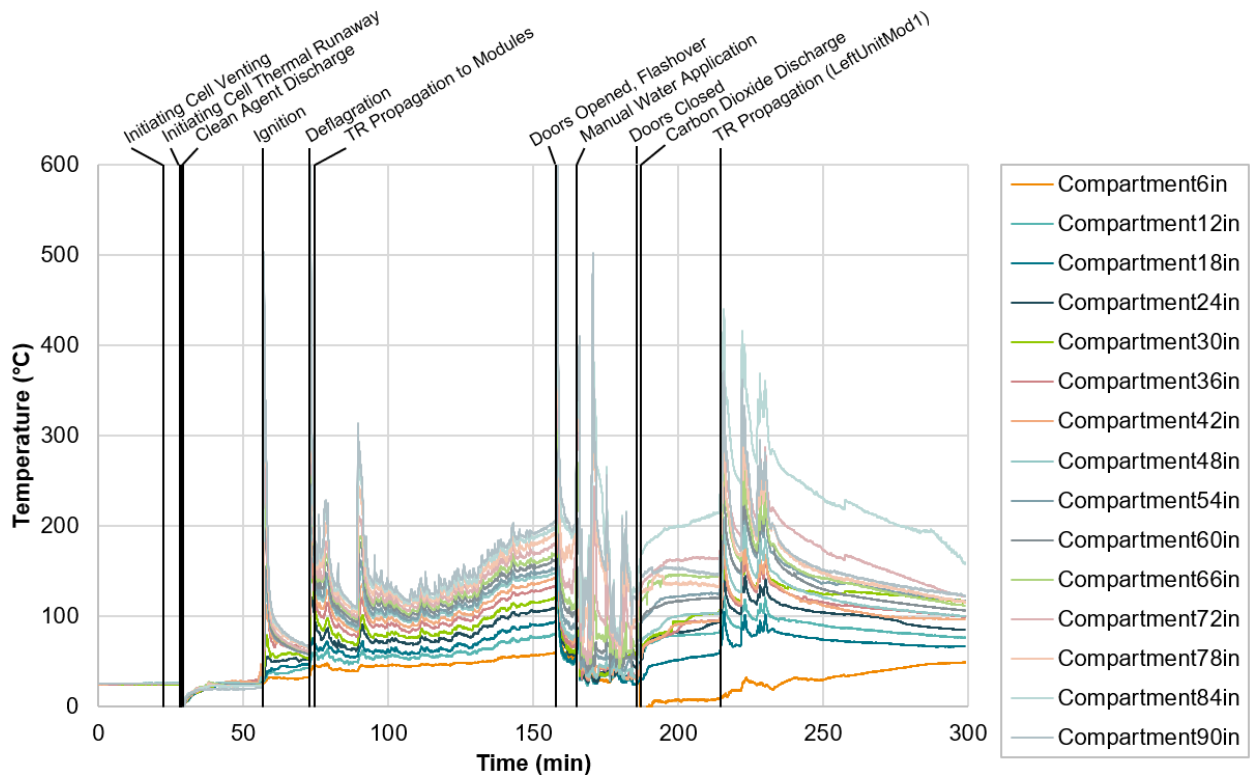


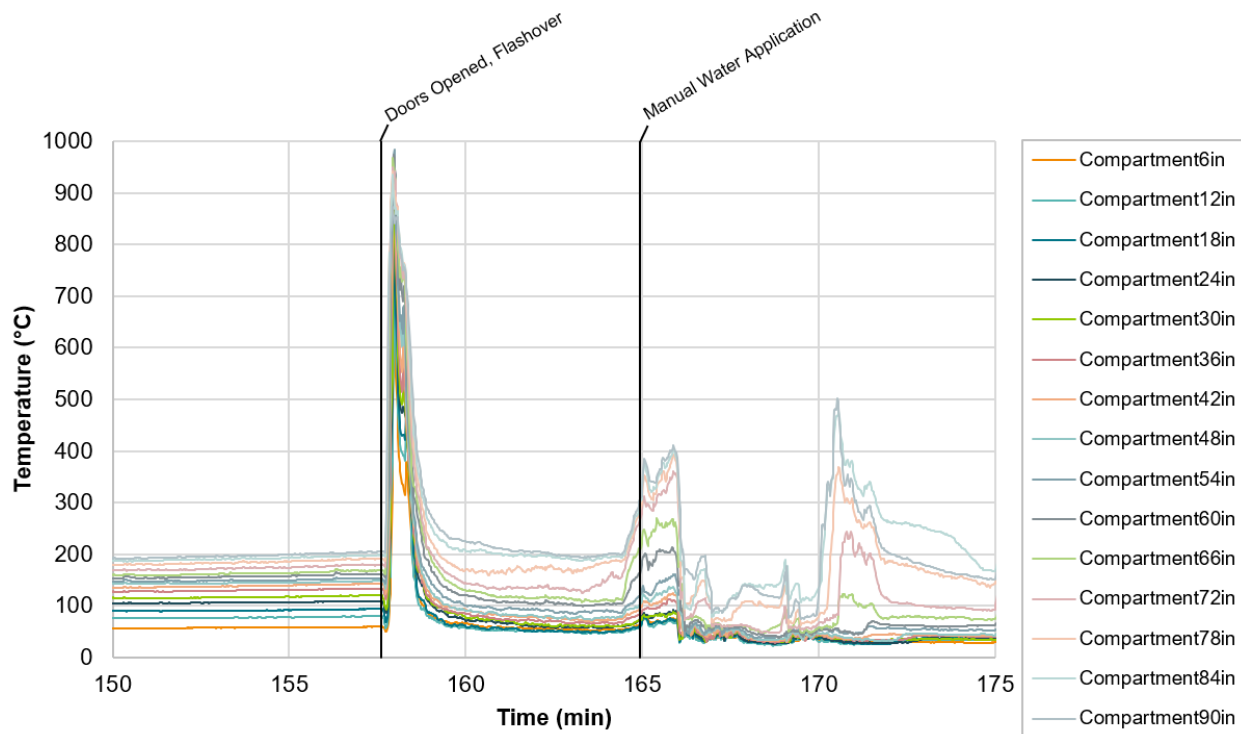
Figure 90 – Container gas temperatures measured during Test 2.

From thermal runaway until the door was opened, the temperatures observed in the container between 30 in and the ceiling exceeded the cell vent temperature, 130 °C. Temperatures observed in the container between 36 in and the ceiling exceeded the cell thermal runaway temperature, 204 °C.



## UL 9540A INSTALLATION LEVEL TESTS WITH OUTDOOR LITHIUM-ION ENERGY STORAGE SYSTEM MOCKUPS

Before opening the door to the container, the gas temperatures in the container ranged from 60 °C to 205 °C, as shown in Figure 91. After the doors were opened, all measurement locations exceeded the cell thermal runaway temperature. Within 21 seconds of opening the door, a flashover occurred, as pictured sequentially in Figure 92. Typical flashover conditions are preceded by temperatures near 600 °C [32]; gas temperatures inside the container were at least 400 °C lower than this benchmark prior to the rapid influx of air with the open door. The flashover conditions occurred for approximately 30 seconds, at which point accumulated flammable gases were consumed, as shown by gas concentration measurements in Figure 94.. Compared with Test 1, gas temperatures were similar before the door was opened; the difference between Test 1 and Test 2 was the discharge of the carbon dioxide system before opening the container door.



**Figure 91 – Container gas temperatures measured before and after opening of the container door during Test 2.**





## UL 9540A INSTALLATION LEVEL TESTS WITH OUTDOOR LITHIUM-ION ENERGY STORAGE SYSTEM MOCKUPS

### **Figure 92 – Sequence of reignition in Test 2 (test time 02:37:36 to 02:38:01).**

For the remainder of the data collection period after flashover, the temperatures observed in the container between 24 in and the ceiling exceeded the cell vent temperature (130°C), as shown in Figure 90. Temperatures observed in the container between 54 in and the ceiling exceeded the cell thermal runaway onset temperature, 204 °C.



## UL 9540A INSTALLATION LEVEL TESTS WITH OUTDOOR LITHIUM-ION ENERGY STORAGE SYSTEM MOCKUPS

### Gas Concentrations

There was no indication of cell venting with the gas measurement instruments installed in the container, likely because of the small volume of vapors emitted from the initiating 18650 cells, and confinement of the cell and module enclosures. After thermal runaway in the Initiating Cell, hydrocarbons were measured first and were followed by an increase in carbon monoxide concentrations, as described in Figure 93. Hydrogen was not measured with this initial group of gases, as the concentration was likely too low for the sensitivity of the hydrogen sensor. Hydrogen concentrations increased above 0.5 v% approximately 1 hour into the test, after additional thermal runaways resulted in further hydrogen release.

When the Novec 1230 was discharged, oxygen concentration dropped from 21 v% to 1 v% over a one-minute period, returned to nearly 21 v% and then steadily decreased to 18 v% when the remaining cells in the Initiating Module went into thermal runaway at 36 minutes. The rapid decrease and increase in oxygen was likely due to impingement of Novec 1230 upon the ceiling-mounted sample probe that supplied the oxygen analyzer.

Carbon monoxide, carbon dioxide, and hydrogen concentrations were unaffected by Novec 1230 discharge and remained less than 1 v% until thermal runaway propagation occurred in the rest of the module at 36 minutes, at which point the concentrations of these three gases increased to 2 v%.

Total hydrocarbon concentration at the ceiling increased to 2 v% one minute after Novec 1230 discharge and slowly decreased over 32 minutes until the ignition of the upper gas layer. Total hydrocarbon concentration at the floor level increased from 1 v% to 6 v% within 10 seconds of Novec 1230 discharge, and stayed relatively constant, even during the ignition and burning of the upper gas layer.

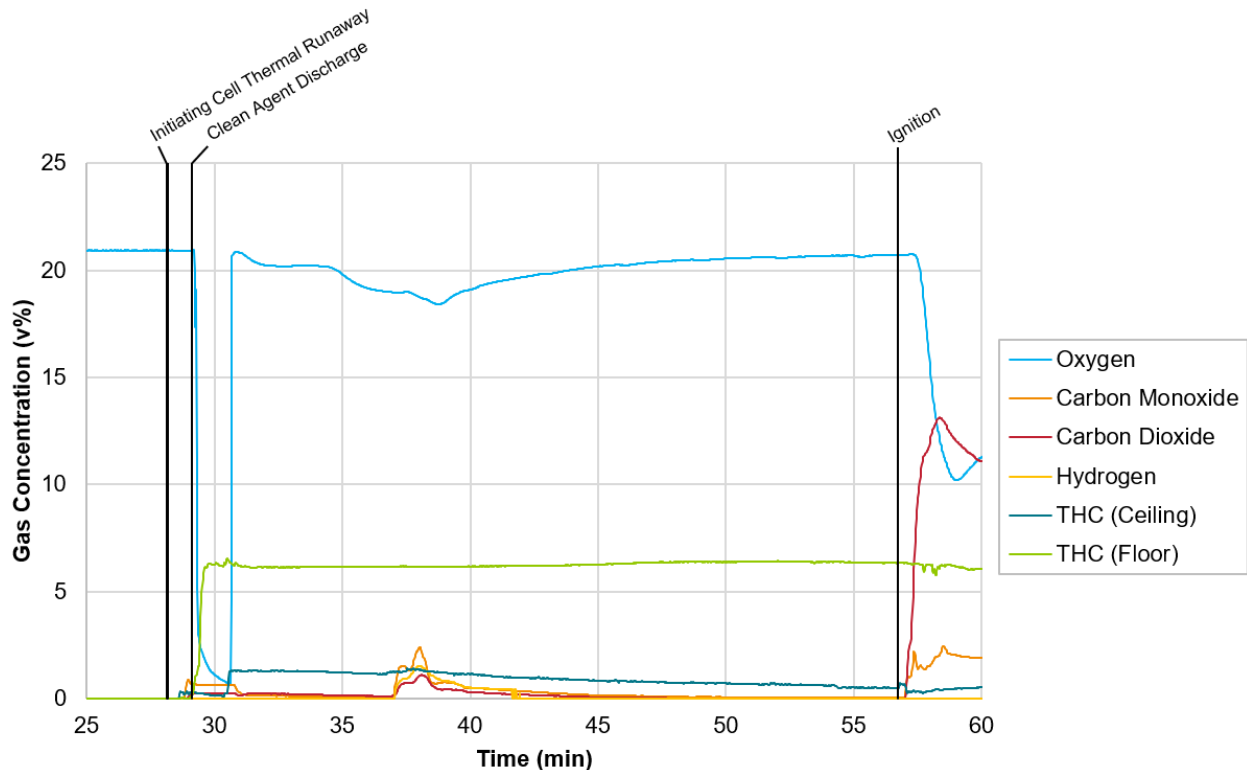
Total hydrocarbon measurements were influenced by Novec 1230 discharge because of the measuring principal of flame ionization detection; based on the carbon composition of the Novec 1230 molecule, the molecule will register above zero on an FID analyzer. Exact concentrations of Novec 1230 cannot be determined from this FID data because the analyzer was calibrated with propane, and the measurement is inseparable with other hydrocarbons in the battery gas.

Comparison of the total hydrocarbon concentration at the ceiling and floor level reflects visual observations that separate upper and lower layers formed within the container. The measurements show the upper layer contained mostly air and a small concentration of hydrocarbons, and that the lower layer contained a mixture of Novec 1230 and battery gases. Still images from video of the upper half of the container visually demonstrate the layer formation, or stratification, behavior. Flammable gases that accumulated within the ESS unit enclosures, and between the initiating unit and the wall, ignited at approximately 56 minutes. The ignition occurred near the Initiating Module. Buoyancy lofted the flames from the unit openings to the ceiling. Flaming was limited to these confined volumes and flaming otherwise did not occur in the semi-opaque lower layer.



## UL 9540A INSTALLATION LEVEL TESTS WITH OUTDOOR LITHIUM-ION ENERGY STORAGE SYSTEM MOCKUPS

Hydrocarbon concentration in the lower layer remained constant. After ignition, oxygen concentration decreased to 10 v% and carbon monoxide and carbon dioxide concentrations increased to 3 v% and 13 v% in the upper layer, respectively.



**Figure 93 – Gases measured in the container from thermal runaway to ignition in Test 2.**

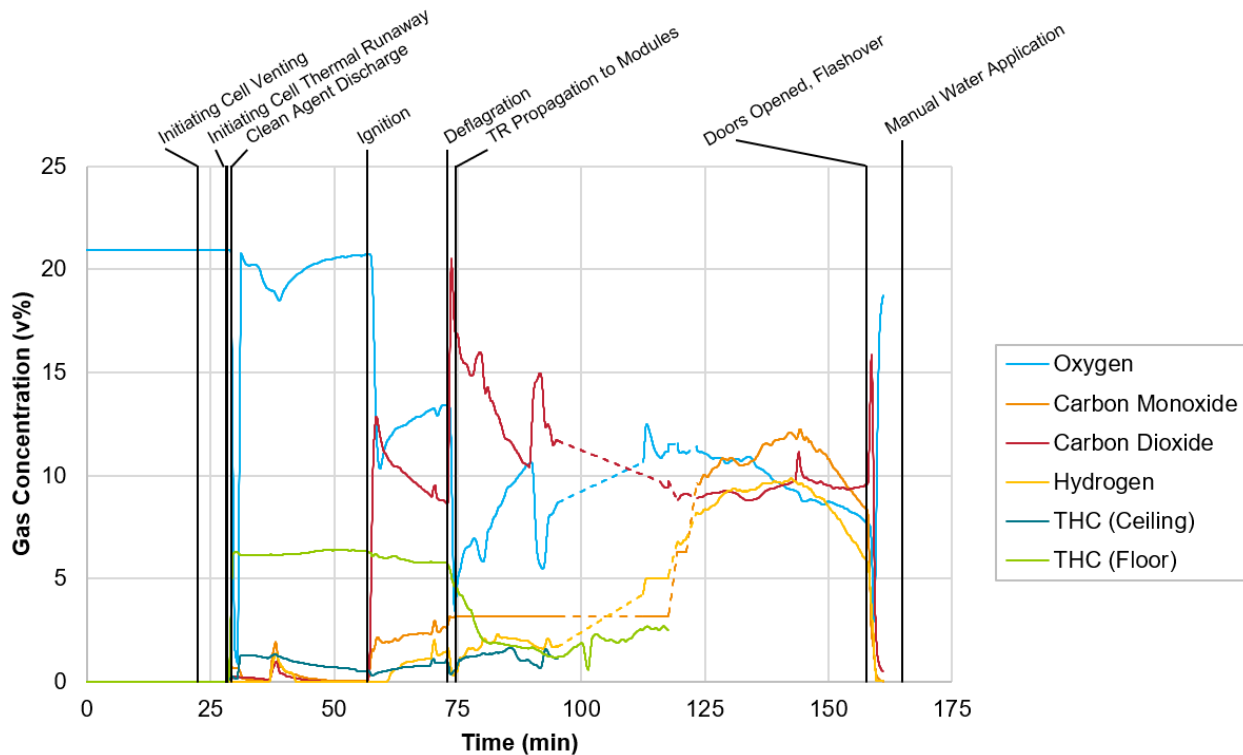
After the upper gas layer burning subsided, oxygen concentration increased to 13 v% before the deflagration occurred, as plotted in Figure 94. The deflagration resulted in a rapid increase in carbon dioxide concentration to 20 v% and a decrease in oxygen concentration to less than 5 v%. Flammable gases, including hydrogen and hydrocarbons, were consumed by this reaction.

Thermal runaway behavior was observed in other modules of the Initiating Unit and Left Target Unit immediately following the deflagration, and battery gases began accumulating again inside the container. Between 120 and 150 minutes, a quasi-steady state condition was reached, as plotted in Figure 94. Carbon monoxide, carbon dioxide, and hydrogen were all measured within 8 v% to 13 v%. At these concentrations, the atmosphere inside the container was comprised of approximately 40–50 v% battery gas. The UFL of the battery gas is 40 v%, as determined by ASTM E681 during UL 9540A cell level testing<sup>9</sup>. For the period between 120 and 150 minutes, the gas mixture exceeded the UFL. Though

<sup>9</sup> UL 9540A, 4<sup>th</sup> Edition requires use of ASTM E918. The referenced cell level testing was conducted with the 3<sup>rd</sup> edition of UL 9540A, which required ASTM E681.

## UL 9540A INSTALLATION LEVEL TESTS WITH OUTDOOR LITHIUM-ION ENERGY STORAGE SYSTEM MOCKUPS

the initial gas conditions developed more slowly than Test 1, long term steady-state conditions (potentially above the UFL) were still achieved in Test 2. Oxygen concentration was between 8 v% and 12 v% corresponding to 40–60 v% ambient air concentration inside the container. It should be considered that the limiting oxygen concentrations for methane and ethylene are 11.1 %O<sub>2</sub> and 8.5 %O<sub>2</sub>, respectively [33].



**Figure 94 – Gas conditions measured in the container for the duration of Test 2.**

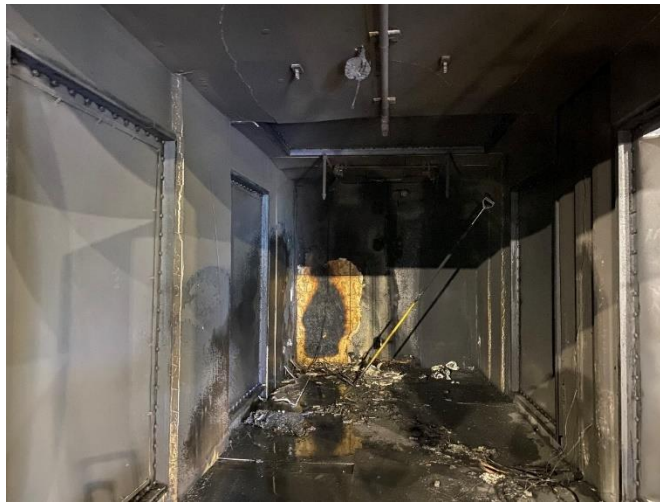
Note: Dashed portions are linearly interpolated for periods of gas sampling equipment maintenance or adjustment between measurement ranges. Gases are presented with 30 second averaging. The carbon monoxide analyzer was saturated between 75 and 120 minutes, indicating a real concentration higher than 3 v%.

After the door was opened, a rapid ignition of accumulated gases occurred, leading to flashover-like conditions. Carbon dioxide concentration rose to 15 v%, while fuel gases including carbon monoxide and hydrogen were consumed by sustained flaming out the container doorway. When manual water application began, gas measurements were discontinued.

## UL 9540A INSTALLATION LEVEL TESTS WITH OUTDOOR LITHIUM-ION ENERGY STORAGE SYSTEM MOCKUPS

### Post-Test

Most thermal damage was observed within the proximity of the Initiating and Left Target Units. The oriented strand board underneath the gypsum board and adjacent to the Initiating Unit was charred, as photographed in Figure 95. Most other apparent damage was actually soot deposition. All surfaces experienced heavy soot deposition with the thickest layer observed on the floor.



**Figure 95 – Condition of container after Test 2 overhaul.**

Two deflagration vents (on the side (Figure 96) and ceiling) were opened by the deflagration. Other deflagration vents experienced thermal damage, indicated by deformed gaskets and membrane layers.



**Figure 96 – Condition of deflagration vent after Test 2.**

## 4.2.5 Smoke and Gas Detector Activation

### Smoke Detectors

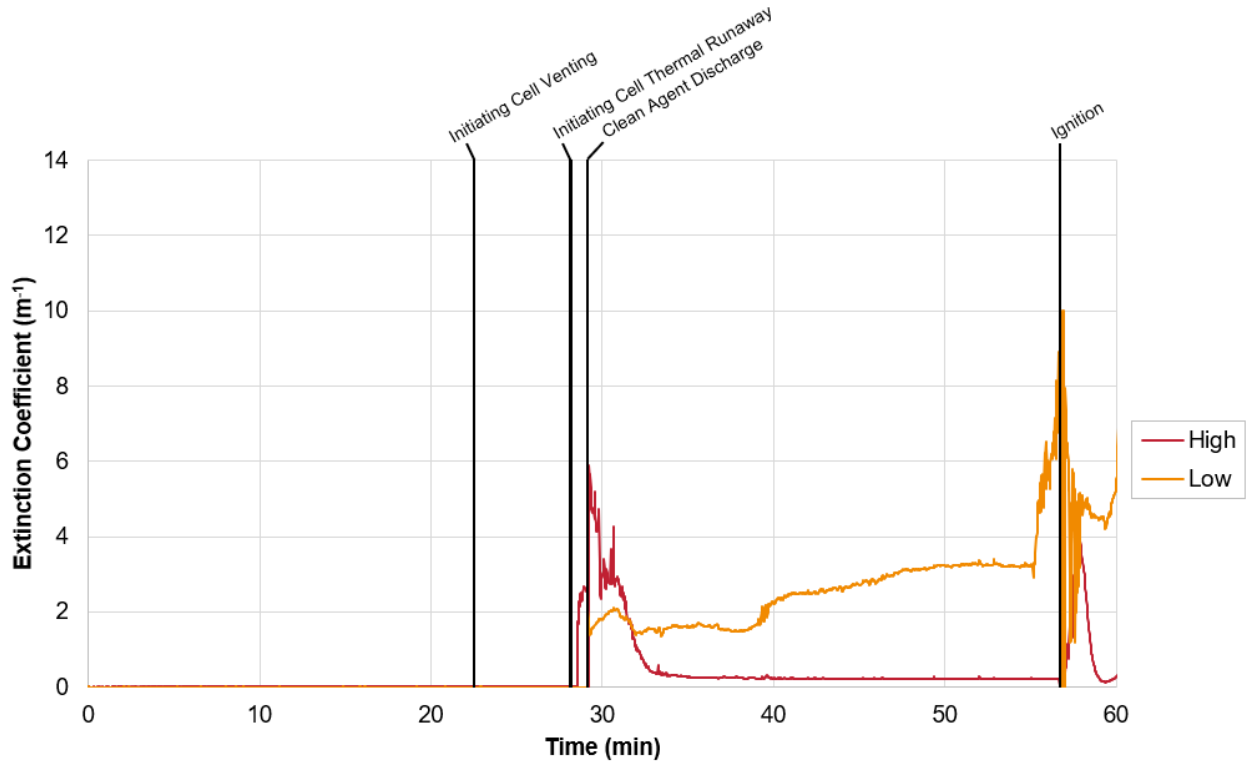
The smoke detector nearest to the Initiating Unit alarmed 53 seconds after the first thermal runaway. The smoke detector located further from the Initiating Unit alarmed two seconds later. Figure 97 shows the thickness of the smoke layer at the time of smoke detector activation. The confirmation of alarm by both smoke detectors was used as a signal to activate the Novec 1230 system.



**Figure 97 – Smoke layer condition upon activation of near (left) and far (right) smoke detectors in Test 2.**

After thermal runaway, smoke obscuration increased at the ceiling level, as measured by the smoke meter near the ceiling (Figure 98). Following Novec 1230 discharge, the contents of the room were stirred, and obscuration at the high and low position approached equal levels. The extinction coefficient at the ceiling was near zero within 10 minutes of Novec 1230 discharge, indicating a clear path between the light source and receiver. The steady measurement near  $3 \text{ m}^{-1}$  for the low position measurement indicated the presence of an opaque lower gas and vapor layer. Visually, the smoke and vapors appeared to separate into layers that formed at the ceiling and at the floor, respectively.

# UL 9540A INSTALLATION LEVEL TESTS WITH OUTDOOR LITHIUM-ION ENERGY STORAGE SYSTEM MOCKUPS



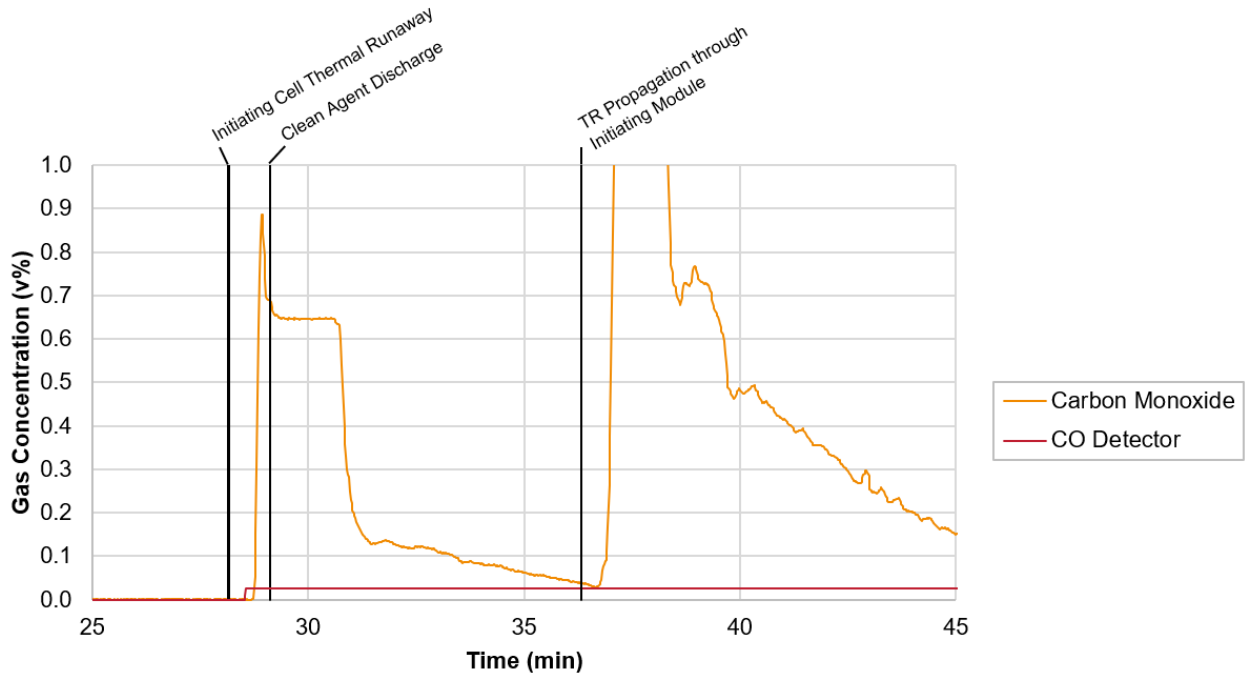
**Figure 98 – Extinction coefficient measurements made by smoke obscuration meter for Test 2 from the beginning of the test through ignition.**

## Carbon Monoxide Detector

The carbon monoxide detector alarmed 23 seconds after thermal runaway and was saturated at 250 ppm (20% IDLH [34]) two seconds later, as illustrated by Figure 99. The detector remained saturated above this level for the duration of the test. The NDIR CO analyzer measured carbon monoxide concentration two magnitudes higher than the commercial electrochemical CO detector. The carbon monoxide detector did not appear to be impacted by the Novec 1230 discharge.



# UL 9540A INSTALLATION LEVEL TESTS WITH OUTDOOR LITHIUM-ION ENERGY STORAGE SYSTEM MOCKUPS



**Figure 99 – Commercial carbon monoxide detector response compared with carbon monoxide concentrations measured in Test 2.<sup>10</sup>**

## Combustible Gas Detectors

All three combustible gas detectors responded within 30 seconds of the first thermal runaway event as summarized in Table 15. Initial responses occurred in the order of proximity to the Initiating Module. This response pattern was consistent with Test 1.

**Table 15 – Combustible gas detector response summary for Test 2.**

Location	Time of First Response	Time of 25% LEL	
		Limited Duration	Sustained Duration
Ceiling	TR + 30 s	TR + 49 s	TR + 8 min 42 s
Middle	TR + 28 s	TR + 48 s	TR + 8 min 31 s
Floor	TR + 21 s	TR + 23 s	TR + 15 min 35 s

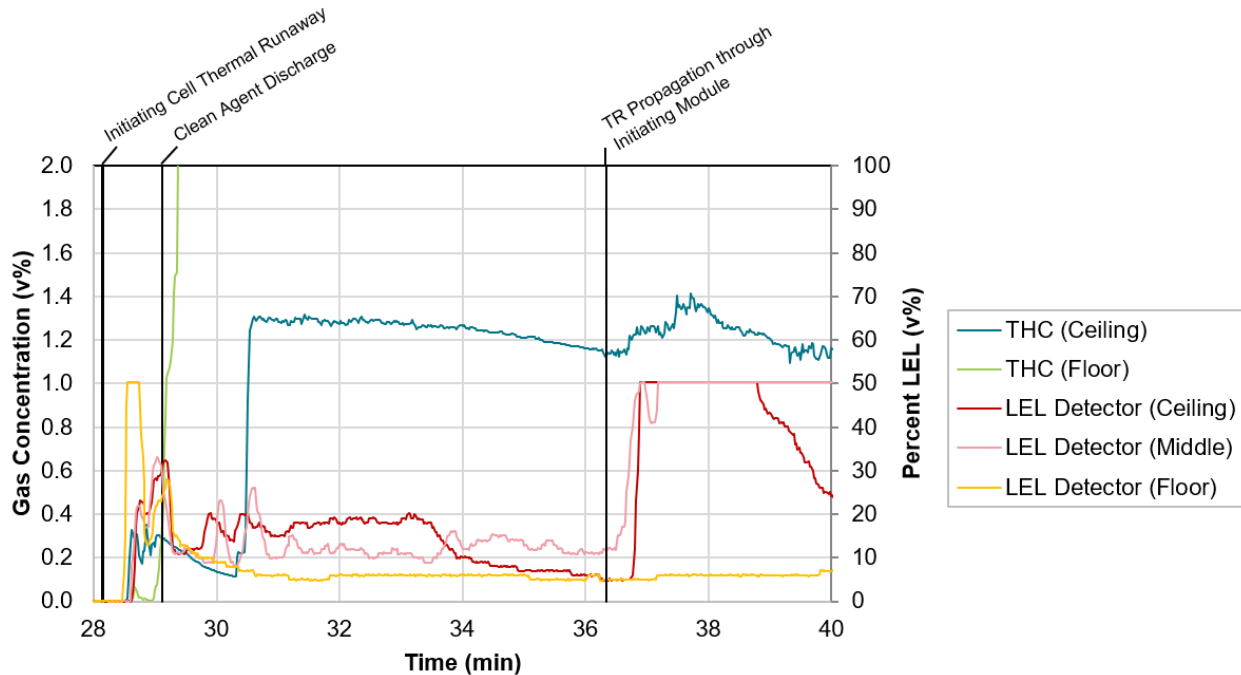
The scales of the primary and secondary axes of Figure 100 have been adjusted to compare the general responses of the two different types of instrument because direct comparison of FID total hydrocarbon measurements with combustible gas detector measurements are not possible. The FID was calibrated with propane, the combustible

<sup>10</sup> Carbon monoxide concentration measurements are plotted without 30 second averaging.

## UL 9540A INSTALLATION LEVEL TESTS WITH OUTDOOR LITHIUM-ION ENERGY STORAGE SYSTEM MOCKUPS

gas detectors were calibrated with methane, and the gas mixture they both measured was comprised of many hydrocarbon elements.

FID-based total hydrocarbon (THC) measurements are plotted from 0 to 2% based on 0 to 100% LEL of the calibration gas (propane). Catalytic bead-based combustible gas detector measurements are plotted from 0 to 100% LEL. The commercial combustible gas detectors all responded within 10 seconds of the THC analyzers, as documented in Figure 100.



**Figure 100 – Total hydrocarbon concentration<sup>11</sup> compared with commercial combustible gas detector response in Test 2 (test time 00:28:00 to 00:40:00).**

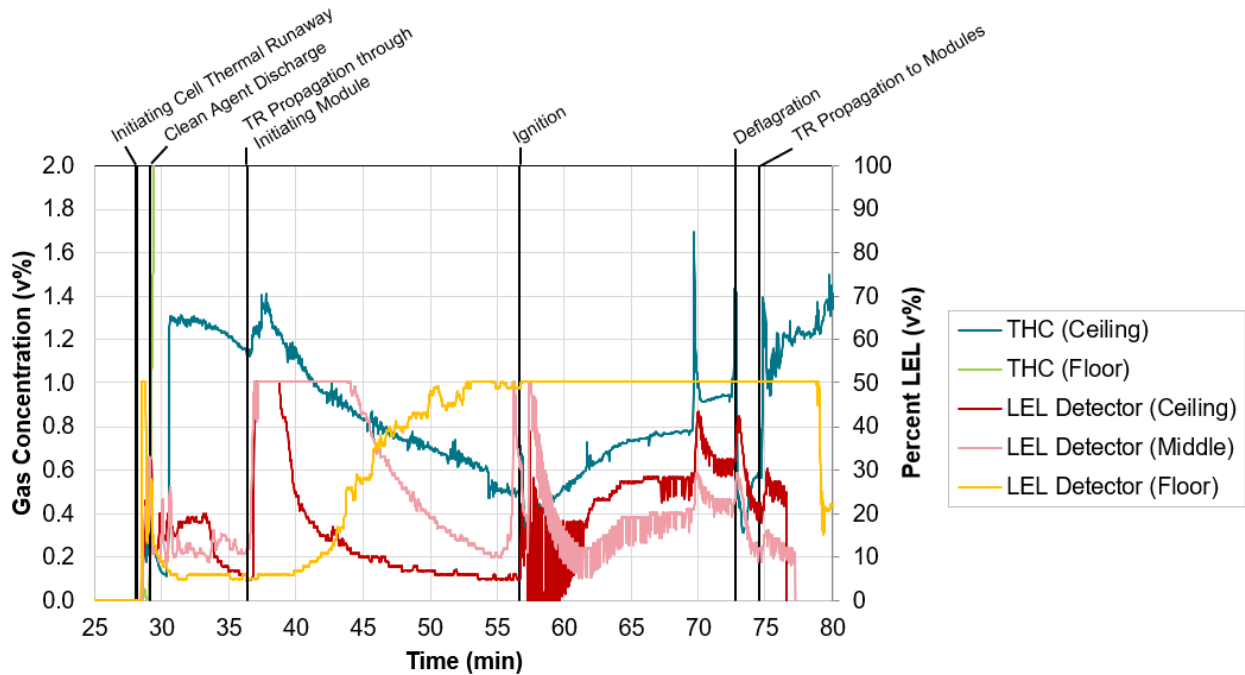
The sensitivity of FID and catalytic bead measurements to the Novec 1230 molecule are not known. After Novec 1230 discharge, total hydrocarbon measurements by FID increased rapidly.

When thermal runaway propagated to other cells in the Initiating Module after 36 minutes, the combustible gas detectors at the middle and ceiling levels responded to the increase in hydrocarbon gases within 30 seconds, as shown above in Figure 100. The combustible gas detector at the floor did not respond to the influx of hydrocarbon gases. This delay was likely due to lighter hydrocarbon accumulation at the ceiling. Unlike Test 1, hydrocarbon concentrations measured at the floor level did not increase along with the ceiling and middle combustible gas detector locations. Novec 1230 may have displaced

<sup>11</sup> Total hydrocarbon concentration is plotted without 30 second averaging.

## UL 9540A INSTALLATION LEVEL TESTS WITH OUTDOOR LITHIUM-ION ENERGY STORAGE SYSTEM MOCKUPS

lighter hydrocarbons because the combustible gas detector at the floor level was immersed in a Novec 1230 environment.



**Figure 101 – Total hydrocarbon concentration<sup>12</sup> compared with commercial combustible gas detector response in Test 2 (test time 00:25:00 to 00:80:00).**

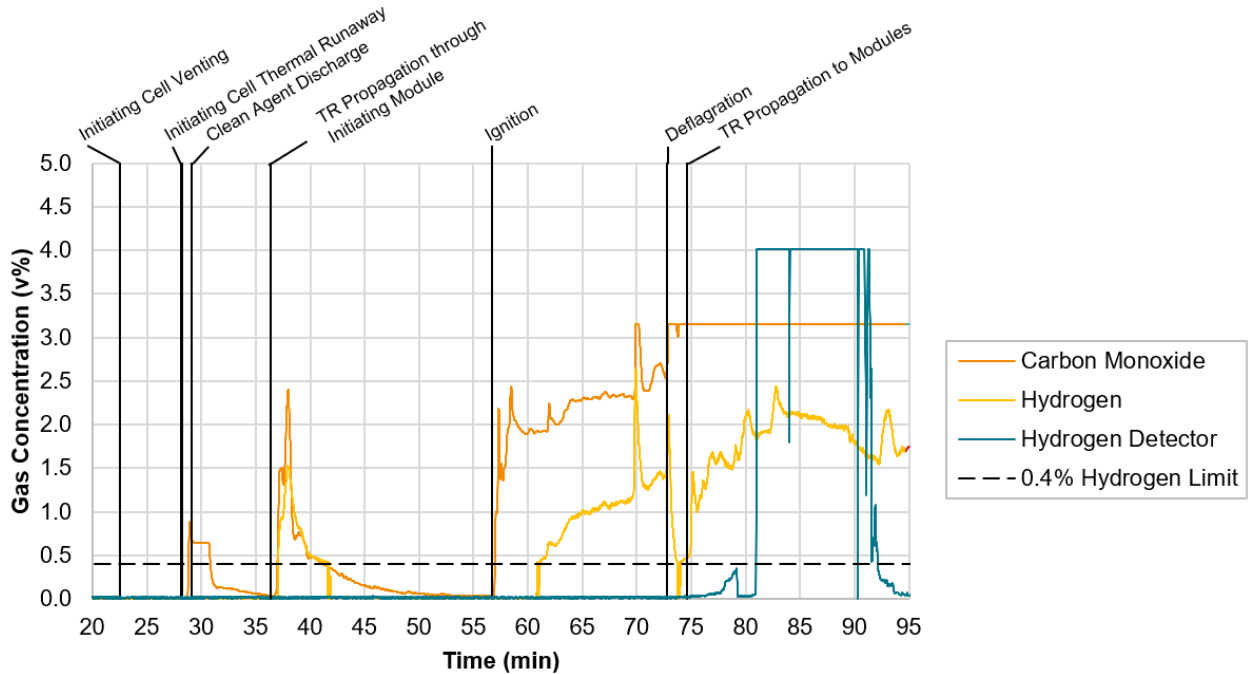
### Hydrogen Detector

Delayed response of the hydrogen detector measurement suggests Novec 1230 interrupted the operation of the sensor. The hydrogen detector did not respond until 76 minutes into Test 2, as shown in Figure 102. However, hydrogen was measured above the 0.4 v% threshold for the palladium-nickel hydrogen sensor after 35 minutes when thermal runaway occurred within a second module. Hydrogen was measured above the 0.4 v% threshold again after ignition and after the deflagration took place.

After nearly an hour of exposure to battery gases, particulate, and direct flame impingement during two periods of upper layer burning, it is likely the hydrogen detector was no longer providing valid measurement. Inspection after Test 2 confirmed that the wiring within the hydrogen detector was destroyed by thermal exposure.

<sup>12</sup> Total hydrocarbon concentration is plotted without 30 second averaging.

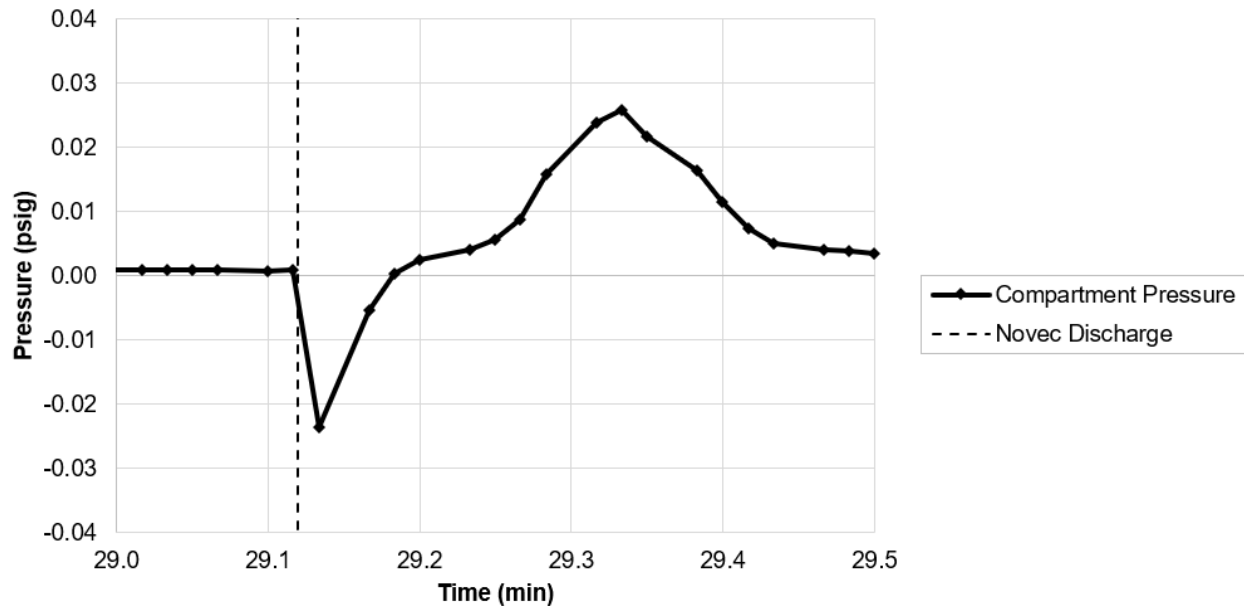
# UL 9540A INSTALLATION LEVEL TESTS WITH OUTDOOR LITHIUM-ION ENERGY STORAGE SYSTEM MOCKUPS



**Figure 102 – Commercial hydrogen detector measurement compared with carbon monoxide and hydrogen concentrations measured in Test 2.**

## 4.2.6 Fire Suppression System Operation

The Novec 1230 system operated as intended. Both positive and negative pressure relief vents operated appropriately, and kept the container pressure within the operating specifications of the 0.5 psig deflagration vent panels, as illustrated in Figure 103.



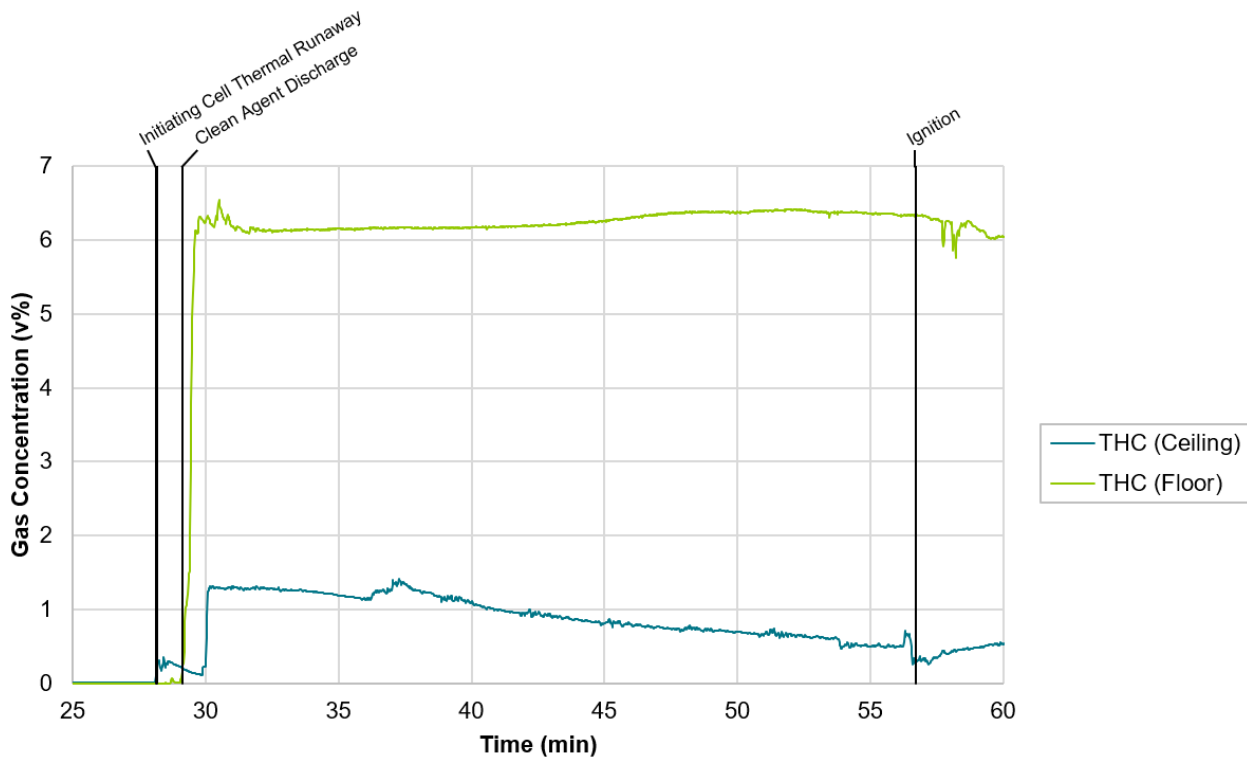
**Figure 103 – Container pressure measured during Novec 1230 discharge in Test 2.**



## UL 9540A INSTALLATION LEVEL TESTS WITH OUTDOOR LITHIUM-ION ENERGY STORAGE SYSTEM MOCKUPS

Novec 1230 concentrations were constant up to the ceiling for the first eight minutes after discharge, as documented in Figure 104. Eight minutes after discharge, gas and vapor stratification was starting to be observed visually (Figure 105) as well as in the steady decline of hydrocarbons measured at the ceiling level. After 20 minutes of stratification, ignition occurred and combusted gases that had accumulated in the upper layer of the container, as pictured in Figure 106. No burning was measured or visually observed in the gas and vapor mixture of the lower layer.

Compared with Test 1, it is likely Novec 1230 delayed ignition of battery gases, given its principles of operation. Also compared with Test 1, this likely prevented flames involving adjacent combustible module enclosure material. However, Novec 1230 did not provide long term protection for the ESS installation as configured in this test. Novec 1230 cooled the container as the agent changed phase during discharge, but did not deliver sufficient cooling to remove heat from the batteries to prevent propagation of thermal runaway. Over the long duration of the test, the Novec 1230 dissipated, gases accumulated in adequate concentration for a deflagration, and eventually thermal runaway propagated through the Initiating Unit and Left Target Unit.



**Figure 104 – THC measurements at floor and ceiling after Novec 1230 deployment show progressive stratification in Test 2.**

# UL 9540A INSTALLATION LEVEL TESTS WITH OUTDOOR LITHIUM-ION ENERGY STORAGE SYSTEM MOCKUPS



**Figure 105 – Visual stratification aligned with steady decrease in THC concentrations at ceiling in Test 2 (test time 43:00, 48:00, and 53:00).**



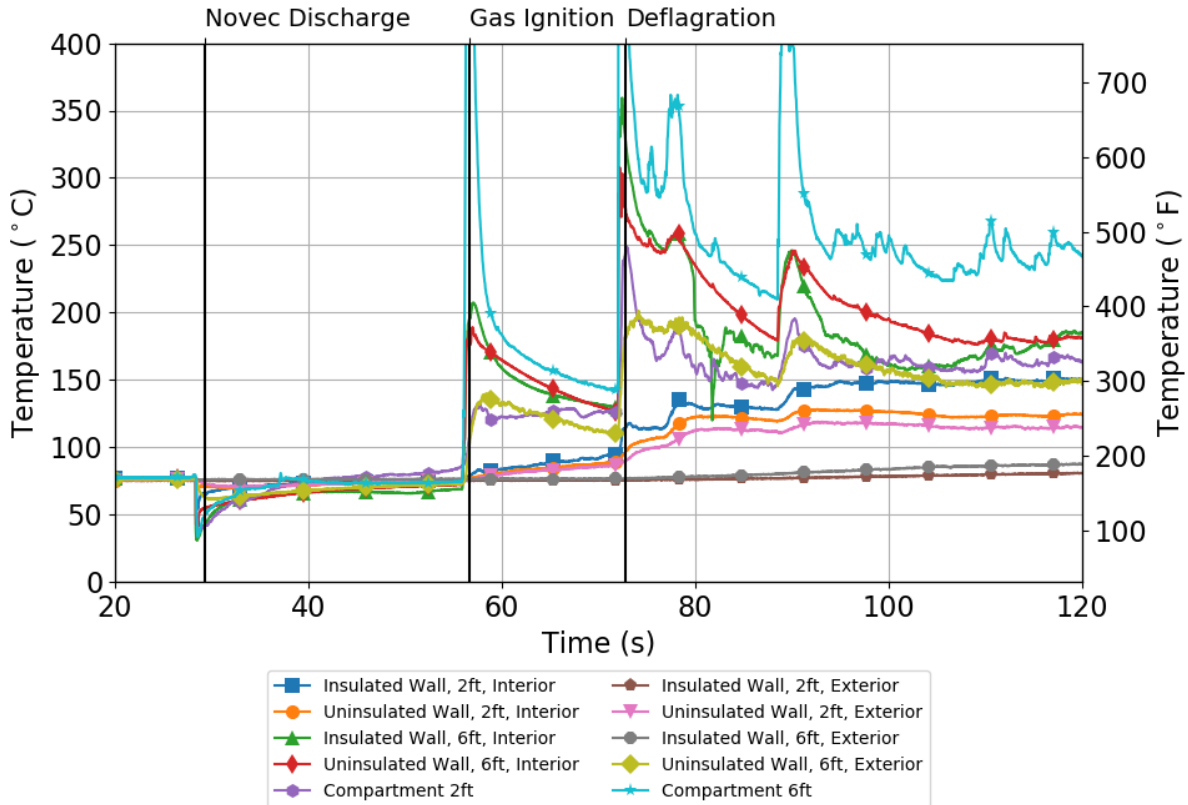
**Figure 106 – Images of combustion in upper layer at 56:44 (left) and 56:48 (right) in Test 2.**



### 4.2.7 Fire Service Size-up Equipment

#### Thermal Imaging

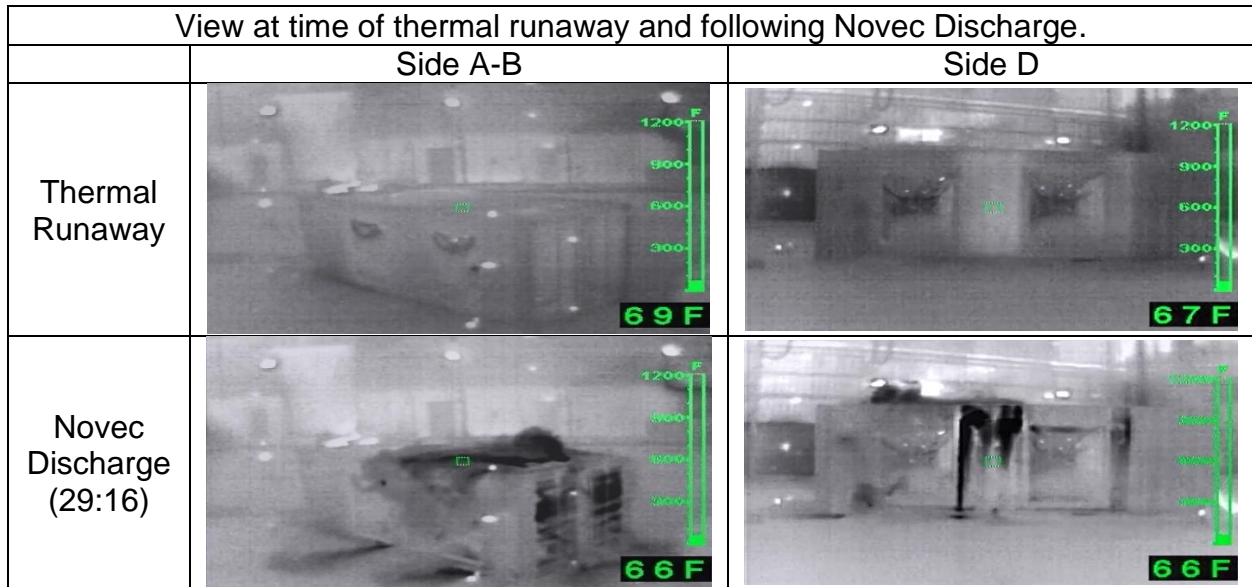
Changes in the exterior thermal imaging camera (TIC) views of the container generally mirrored the changes in the exterior surface temperatures of the container. Figure 107 shows the interior and exterior surface temperatures during the period between the first thermal runaway event and propagation of thermal runaway to adjacent modules.



**Figure 107 – Wall surface temperatures during the period from the first thermal runaway event until propagation of thermal runaway to additional modules. Vertical lines denote events corresponding to the images in Figure 108, Figure 109, and Figure 110 below.**

## UL 9540A INSTALLATION LEVEL TESTS WITH OUTDOOR LITHIUM-ION ENERGY STORAGE SYSTEM MOCKUPS

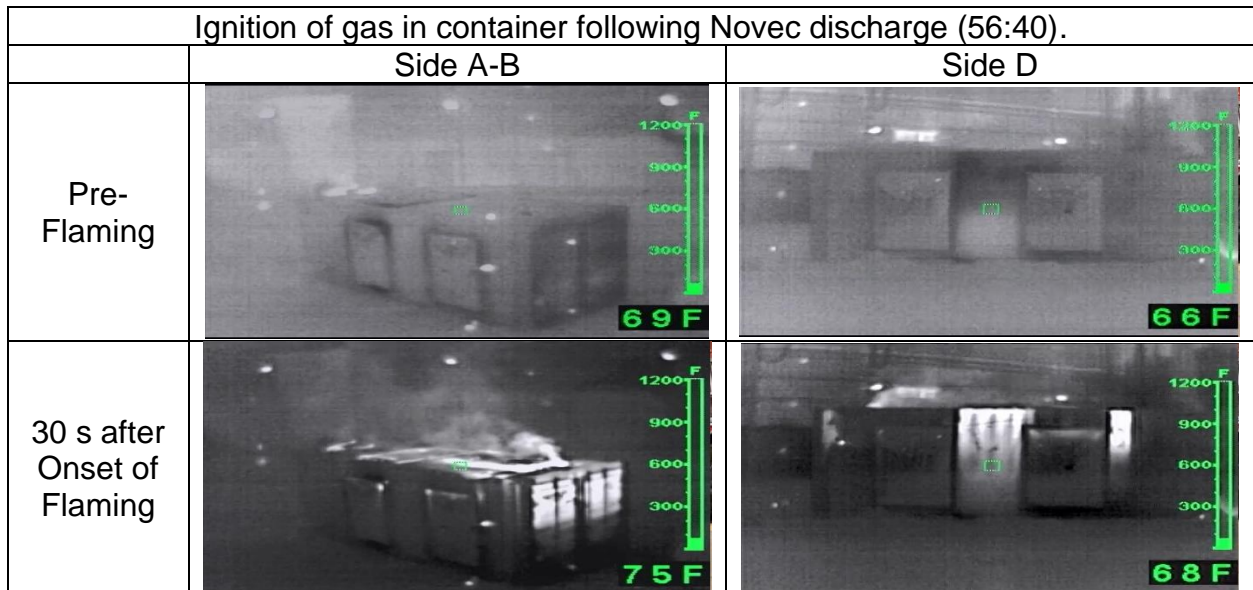
Prior to the discharge of Novec 1230, the surface temperatures and thermal imaging views remained near ambient. Following Novec 1230 discharge, interior and exterior surface temperatures decreased, which corresponded to visible cooling in the exterior thermal imaging cameras. The thermal imaging cameras were able to visually differentiate both the cooling of container surfaces and the presence of cooler vapor clouds of Novec 1230 fluid that vented through leakage points in the container, as shown in Figure 108. This contrast was most apparent in bare metal portions of the container, such as the D-side wall.



**Figure 108 – Changes in IR view from thermal runaway in Initiating Module to Novec 1230 discharge in Test 2. Left column shows A-B corner of the container (insulated wall construction) and right column shows D-side of container (bare metal construction).**

## UL 9540A INSTALLATION LEVEL TESTS WITH OUTDOOR LITHIUM-ION ENERGY STORAGE SYSTEM MOCKUPS

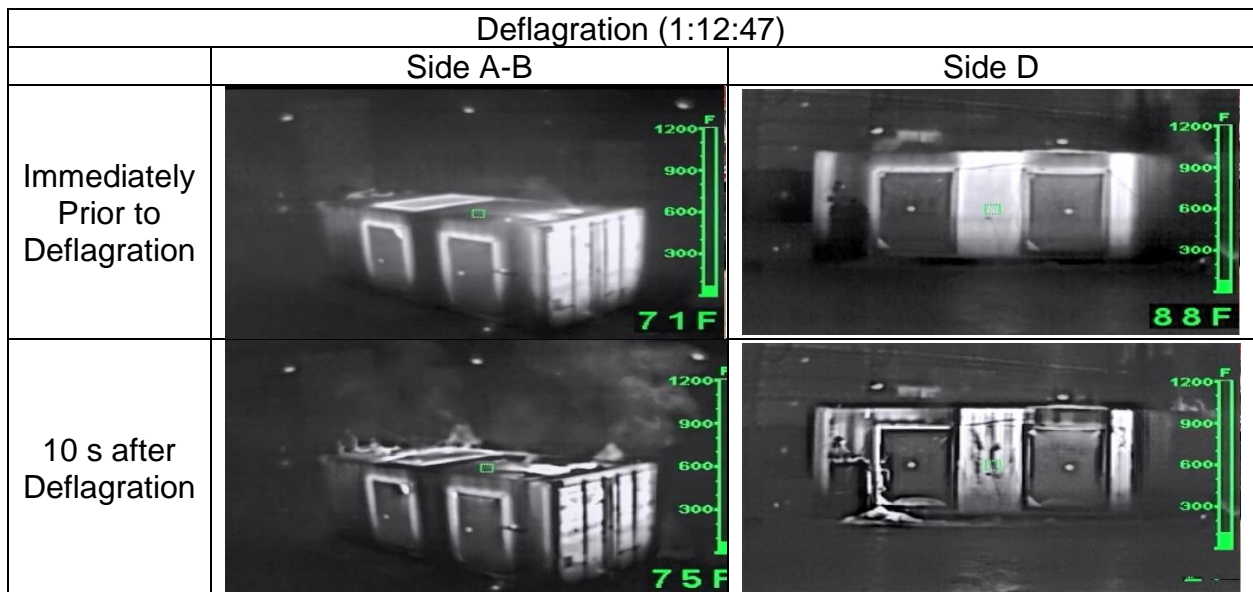
In the period between the Novec 1230 discharge and the first flaming event, 56 minutes and 40 seconds after the start of the test, surface temperatures remained relatively steady, while the exterior TIC views trended slowly toward pre-discharge conditions. A period of temperature increase was measured in the uninsulated exterior surface temperature data following the initial flaming event in the container (Figure 107). The bare metal portions of the container experienced a higher rate and magnitude of temperature increase, and that was also reflected in the quick response of thermal imaging views to the event. Insulated portions of the container experienced minimal temperature rise, and therefore the presence of temperature rise inside the container was not visible on thermal imaging views of these locations, as shown in Figure 109.



**Figure 109 – Changes in thermal imaging view before and after initial flaming in the container in Test 2. Left column shows A-B corner of the container (insulated wall construction) and right column shows D-side of container (bare metal construction).**

## UL 9540A INSTALLATION LEVEL TESTS WITH OUTDOOR LITHIUM-ION ENERGY STORAGE SYSTEM MOCKUPS

In the time between the first flaming event (56:40 after test start) and the deflagration event (1:12:47 after test start), uninsulated exterior wall temperatures gradually decreased while insulated exterior wall temperatures remained constant. Following the deflagration event, a second distinct surface temperature increase was observed at all four interior measurement locations and the uninsulated exterior measurement locations. Although the thermocouples indicated a temperature increase on the uninsulated side, the thermal signature of the container on TIC views did not change meaningfully following the deflagration, because exterior surface temperatures were already elevated following the initial flaming event. The relative lack of change following the deflagration can be seen in Figure 110.

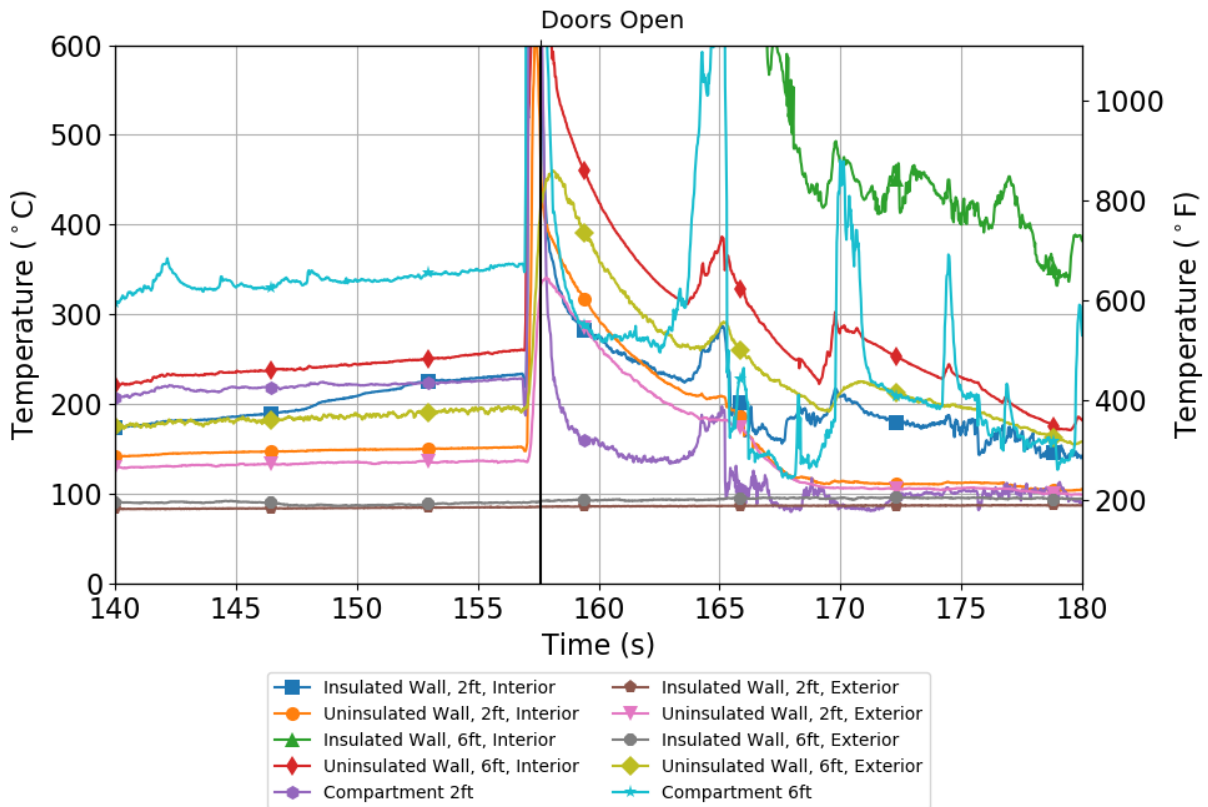


**Figure 110 – Changes in thermal imaging view before and after deflagration in Test 2. Left column shows A-B corner of the container (insulated wall construction) and right column shows D-side of container (bare metal construction).**

Following the deflagration event, interior surface temperatures and uninsulated exterior surface temperatures steadily decreased. This period of overall decrease was punctuated by two distinct increases that occurred approximately 75 minutes and 90 minutes after test start and corresponded to additional modules entering thermal runaway.

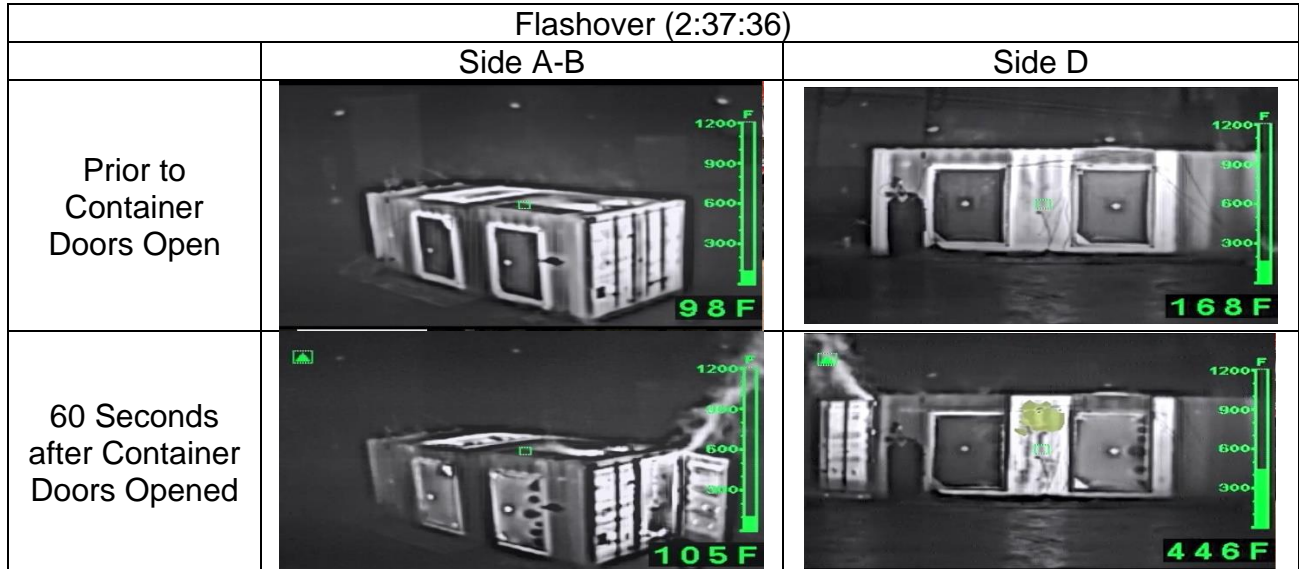
## UL 9540A INSTALLATION LEVEL TESTS WITH OUTDOOR LITHIUM-ION ENERGY STORAGE SYSTEM MOCKUPS

Prior to the doors opening, the exterior and interior surface temperatures were relatively steady, as shown in Figure 111. Opening the container doors two hours and 37 minutes after the test began provided oxygen to the fuel-rich environment within the container. Within 30 seconds of opening the doors, the container transitioned through flashover, and flames were observed venting from the container door. This resulted in a 300 to 400 °C increase in interior surface temperatures at all four interior measurement locations, and at both uninsulated exterior measurement locations. The two exterior measurements on the insulated side remained steady. The views from the exterior thermal imaging cameras mirrored the behavior of the surface temperature measurements.



**Figure 111 – Wall surface temperatures during the period before and after the container doors were opened in Test 2. Vertical lines denote events corresponding to the images in Figure 112 below.**

## UL 9540A INSTALLATION LEVEL TESTS WITH OUTDOOR LITHIUM-ION ENERGY STORAGE SYSTEM MOCKUPS



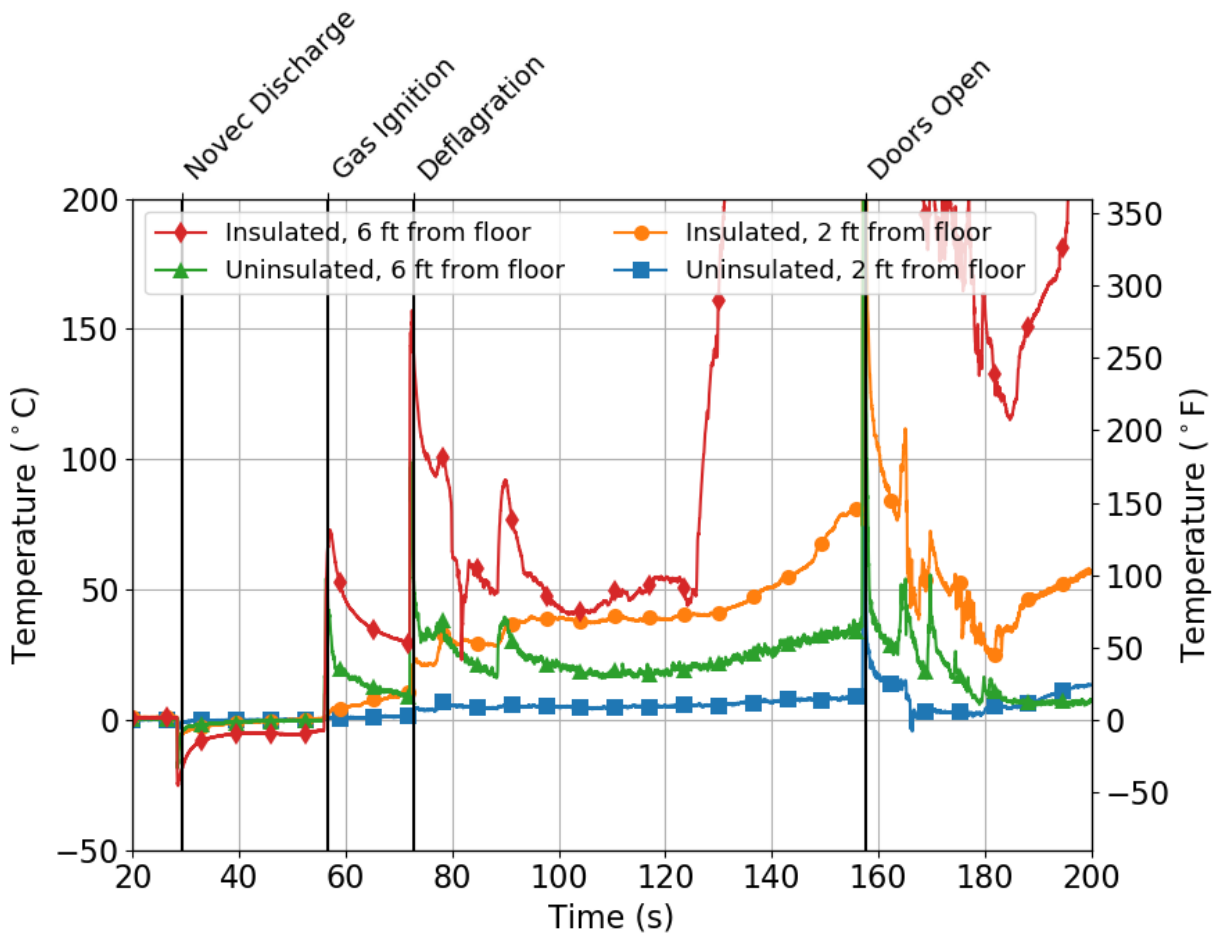
**Figure 112 – Changes in thermal imaging view immediately before and 60 seconds after the container doors were opened, which occurred 2:37:36 after test start in Test 2. Left column shows A-B corner of the container (insulated wall construction) and right column shows D-side of container (bare metal construction).**

As in Test 1, the uninsulated wall sections tended to closely mirror changes in the interior thermal environment, while insulated wall sections did not respond quickly to changes in interior temperatures. This was apparent during periods where compartment temperatures were decreasing (Figure 108) and increasing (Figure 109 and Figure 110). Figure 113 shows the temperature differential between the interior and exterior wall surfaces of the container over the course of the test. The temperature differential between the uninsulated wall section on the B-side remained lower than 50 °C for the majority of the experiment. This indicates exterior surface temperatures provide a reasonable estimate of interior surface temperatures.

In contrast, the temperature differential across the wall thickness of the insulated upper portion of the container was typically two to five times higher, especially during rapid temperature increase events such as the gas ignition and deflagration. The temperature differential across the lower insulated wall section steadily increased over the course of the test. At the 6 ft measurement location, the temperature difference between the inside and outside surface was as high as 200 °C at several points throughout the test. The temperature differential at 2 ft measurement location reached 80 °C before the flashover occurred. Because of these discrepancies and variations, thermal imaging views of the insulated wall section may provide an incomplete understanding of thermal conditions inside of the container.











## UL 9540A INSTALLATION LEVEL TESTS WITH OUTDOOR LITHIUM-ION ENERGY STORAGE SYSTEM MOCKUPS



**Figure 113 – Temperature difference between inside and outside surface of container during Test 2.**

Over the course of Test 2, standard and thermal imaging cameras observed emission of vapors from the container starting with the discharge of Novec 1230 (29:16), as illustrated in Figure 114. The discharge of Novec 1230 from the container was distinct from the exhaust of battery gases, particularly when viewed with a thermal imaging camera. The dark-colored (cold) agent that was apparent immediately after Novec 1230 discharge stood in stark contrast to the bright colored (hot) battery gas later in the test. Additionally, the visible exhaust of gas from the container following Novec 1230 discharge was visible for seconds, while the vapor cloud that formed following thermal runaway propagation was present for hours.

## UL 9540A INSTALLATION LEVEL TESTS WITH OUTDOOR LITHIUM-ION ENERGY STORAGE SYSTEM MOCKUPS

	A Side (Standard)	AB Side (TIC)
Novec 1230 Discharge (29:16)		
Vapor Cloud Development (56:55)		
Peak Vapor Cloud (80:00)		
Immediately Before Door Opened (2:37:36)		

**Figure 114 – Vapor cloud formation and development in standard (left) and thermal imaging (right) camera views during Test 2.**





A visible vapor cloud began to form as Novec 1230 began to dissipate and thermal runaway within the container continued to propagate, as in Test 1. The vapor cloud slowly increased in size in the period between agent discharge and gas ignition. The cloud became more easily discernable following the gas ignition at 56:55, as shown in the second row of images in Figure 114. The size of the cloud fluctuated over the course of the experiment, growing as additional modules went into thermal runaway and decreasing as exterior vapors were exhausted from the laboratory.

After the deflagration event (1:12:47), the size of the cloud grew substantially. This was impacted by additional propagation of thermal runaways and gas leakage points from the opened deflagration vents. Although the peak size the cloud could reach outdoors is

## UL 9540A INSTALLATION LEVEL TESTS WITH OUTDOOR LITHIUM-ION ENERGY STORAGE SYSTEM MOCKUPS

difficult to reliably assess in enclosed and ventilated laboratory conditions, the period of peak cloud size in Test 2 corresponded to the period in which interior gas concentrations were at their peak, approximately 60–90 minutes after the test began. After this peak period, the vapor cloud gradually began to dissipate. Prior to the container door opening, the cloud had mostly dissipated in the immediate area of the container, although vapors were still visible within the larger laboratory.

In Test 2, one of the fire service TICs was relocated to the interior of the container to assess its ability to provide an entry crew with information. Although the thermal imaging camera was initially able to distinguish the hot gases venting from the Initiating Unit following thermal runaway, the camera’s view was obscured within 10 seconds of Novec 1230 discharge due to the stirring of room contents and additional vapor presence. The TIC remained obscured in the heavy gas layer formed by the Novec 1230 for the majority of the test. This optically dense gas layer inhibited the view of the TIC during the initial flaming event (56:40 after test start). Figure 115 shows the interior thermal imaging view compared to the HD camera placed 6 ft above the floor in the doorway. Although the standard camera could easily distinguish the increase in flaming close to the ceiling of the container, there was no noticeable change in the thermal imaging view.

Thermal imaging camera view of gas ignition at 56:40.		
	Standard Camera - 6 ft Container Door	IR camera
Initial View (No Smoke)		
Immediately after Gas Ignition.		

**Figure 115 – Interior view of gas ignition 56:40 after test start. Note the lack of thermal signature in the thermal imaging camera compared to the visible burning in the standard camera view.**

## UL 9540A INSTALLATION LEVEL TESTS WITH OUTDOOR LITHIUM-ION ENERGY STORAGE SYSTEM MOCKUPS

### Portable Gas Meters

Interior Meter 1 was not utilized for O<sub>2</sub> and CO measurements in Test 2 due to faults in the O<sub>2</sub> and CO sensors caused by Test 1. Interior Meter 2 was utilized for the first 48 minutes of Test 2 and discontinued after the sample pump failed.

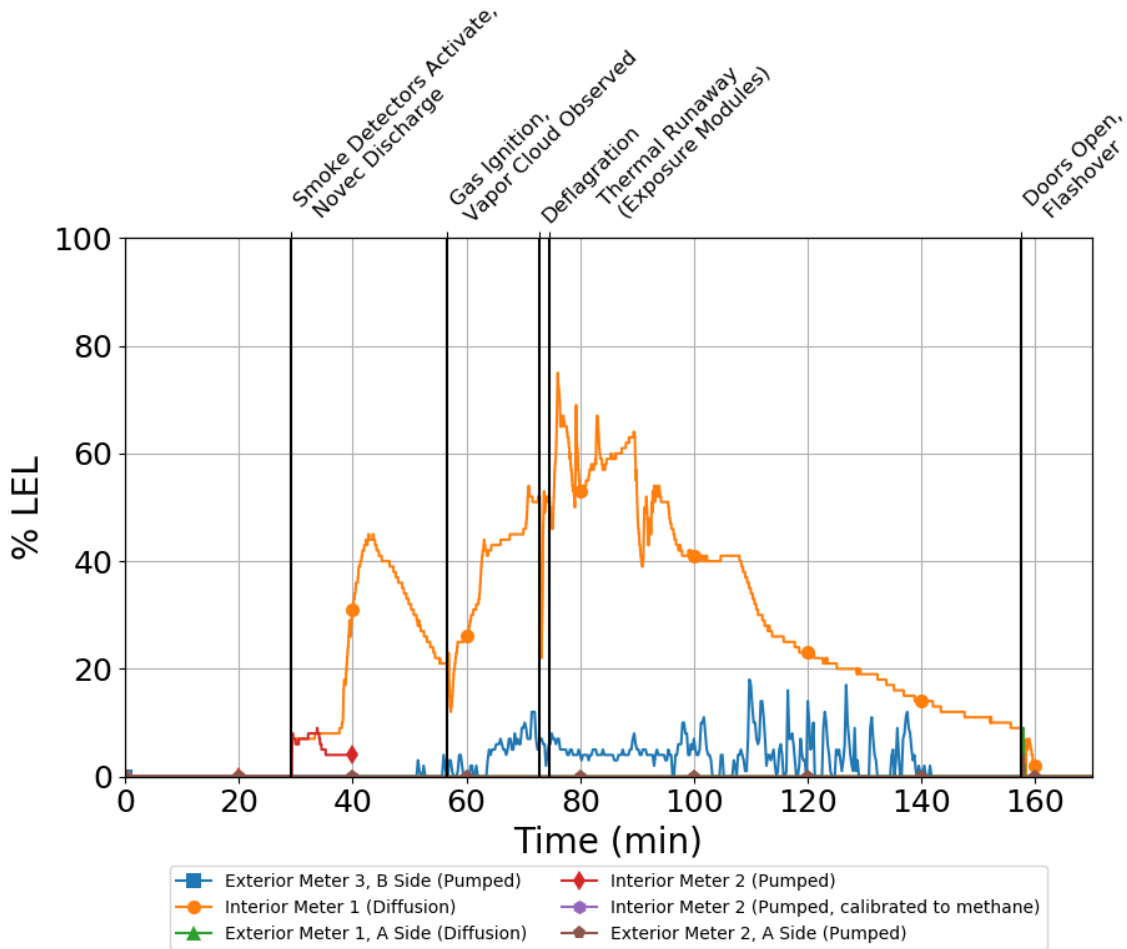
Figure 116 displays the time histories of the flammable gas concentrations measured by the five portable gas meters. The portable gas meters first indicated an increase in flammable gas concentrations (LEL and H<sub>2</sub>) immediately after the Novec 1230 discharge, 29:16 after test start. The flammable gas concentrations measured by both meters inside the container plateaued for eight minutes after Novec 1230 was discharged. The plateau following Novec 1230 discharge aligned with the THC concentrations measured by gas measurement instrumentation (described in Figure 93).

The flammable gas concentration measured by the interior diffusion meter began to increase again 36 minutes after test start. The peak flammable gas concentration measurement recorded prior to the deflagration event was 44%, measured 42 minutes after test start. After reaching this peak, the flammable gas concentration decreased until the gas ignition was observed 56:40 after test start. Following the ignition event, the flammable gas concentration measured by the Interior Meter 1 continued to increase until a deflagration was observed 1:12:47 after test start. This behavior contrasts with THC concentration measured by FID at the floor, which remained steady until the deflagration event.

At the time of this deflagration, Interior Meter 1 indicated the combustible gas concentrations reached 51% of the LEL of pentane. Following the deflagration, the flammable gas concentration measured by Interior Meter 1 continued to increase, reaching an absolute peak of 75% of the LEL 76 minutes after test start. This peak was observed at the same time thermal runaway propagated beyond the Initiating Module. After the peak at 76 minutes, the flammable gas concentration measured by Interior Meter 1 decreased for the remainder of the test. This contrasts with the data from gas measurement instrumentation, which indicated a steady peak period between 120 and 150 minutes.



# UL 9540A INSTALLATION LEVEL TESTS WITH OUTDOOR LITHIUM-ION ENERGY STORAGE SYSTEM MOCKUPS



**Figure 116 – Flammable gas concentration measurements from portable gas meters in Test 2.**

The only exterior portable gas meter that registered elevated flammable gas concentration readings was Exterior Meter 3, which first indicated the presence of flammable gases 51 minutes after test start. The flammable gas concentration measured by this meter continued to increase until the deflagration. At the time of the deflagration, Exterior Meter 3 reported a value of 11% of the LEL of pentane. This increase was measured simultaneously with the formation of a visible vapor cloud.

The deflagration operated the deflagration vent immediately adjacent to the B-side exterior meter. After the deflagration, flammable gas concentration measurements at this location began to increase. The flammable gas concentration values at this location remained above 0% from 60 minutes after test start to approximately 105 minutes after test start, which covered the period in which thermal runaway propagated through the Initiating Unit and Left Target Unit. Following this period, elevated flammable gas concentrations were observed, but they fluctuated between 0% of the LEL and peaked as high as 16% of the LEL. The period in which these peak measurements were recorded matched the period in which gas concentrations within the container had reached a

## UL 9540A INSTALLATION LEVEL TESTS WITH OUTDOOR LITHIUM-ION ENERGY STORAGE SYSTEM MOCKUPS

steady state. Exterior Meter 4, located 10 ft back from the A-side of the container, did not measure any elevated flammable gas concentrations during the test.

Hydrogen gas concentrations measured by the diffusion meter inside of the container, Interior Meter 1, began to increase at the same time as the flammable gas concentration measured in the container, as shown in Figure 117. In contrast to Test 1, in which the H<sub>2</sub> concentration grew rapidly to the upper measurement threshold (1,000 ppm), the interior H<sub>2</sub> concentration in Test 2 plateaued when Novec 1230 was discharged into the container. This increase in hydrogen gas concentrations early in the test did not match the trend observed with the gas measurement instrumentation, which first indicated an increase approximately 38 minutes after test start. Additionally, the magnitude of this increase was higher than that recorded by the portable gas meter. The H<sub>2</sub> concentration measured by the portable gas meter did not exhibit any further increase prior to the deflagration event. After the delagration, the interior H<sub>2</sub> concentration briefly decreased, before gradually increasing to the upper measurement threshold (1,000 ppm).

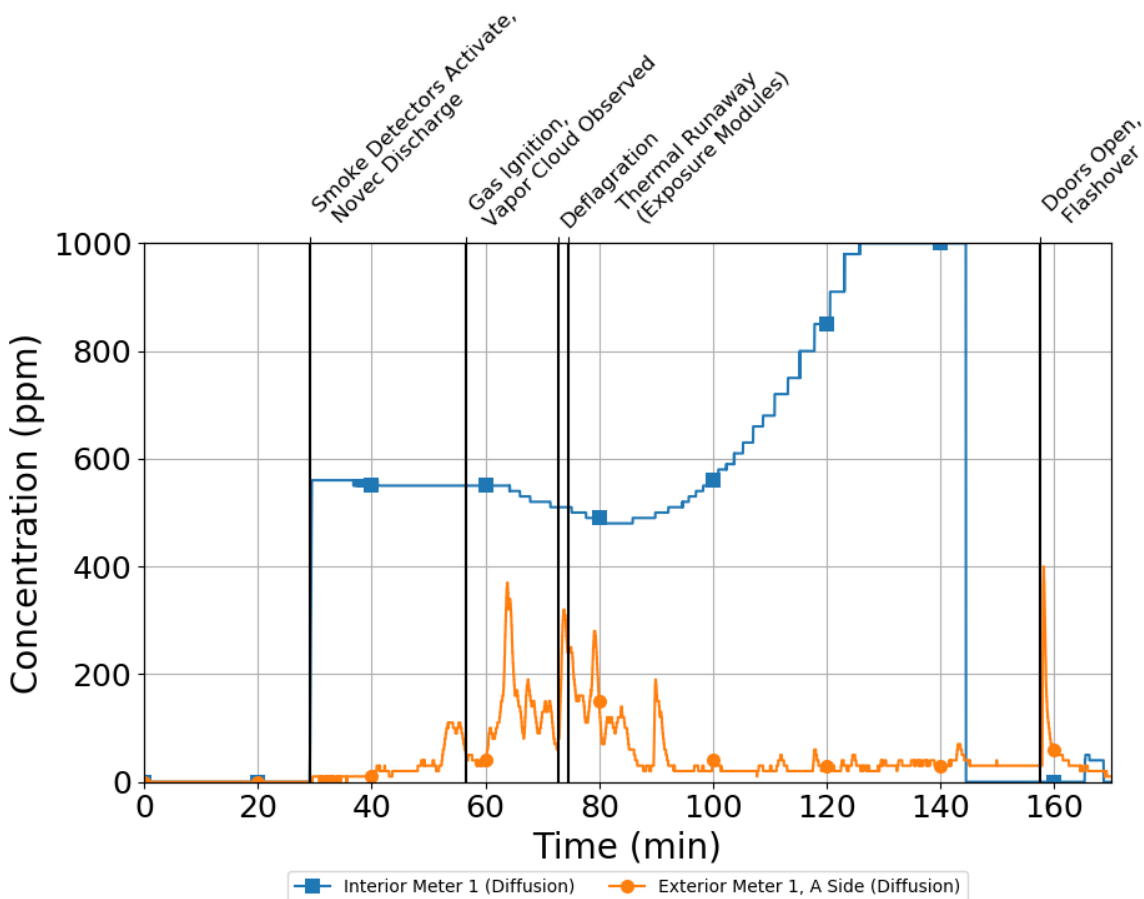


Figure 117 – Hydrogen gas concentration measured by MultiRAE Lite Diffusion meters inside and outside of container in Test 2.



## UL 9540A INSTALLATION LEVEL TESTS WITH OUTDOOR LITHIUM-ION ENERGY STORAGE SYSTEM MOCKUPS

Exterior Meter 1 (3 ft from A-side) first indicated an increase in H<sub>2</sub> concentrations between 50 and 60 minutes after test start. This coincided with the formation of a visible vapor cloud. It is possible the additional leakage from the container following the deflagration precipitated the venting of products of thermal runaway from the container, and therefore resulted in higher concentrations of H<sub>2</sub> as thermal runaway propagated through the Initiating Unit and Left Target Unit. H<sub>2</sub> concentrations remained elevated from 60 to 90 minutes after test start. This corresponded to the period in which hydrogen gas concentrations measured by gas measurement instrumentation in the container were beginning to increase. Although Exterior Meter 1 recorded elevated H<sub>2</sub> concentrations during this period, it did not measure elevated H<sub>2</sub> concentrations later on when gas measurement instrumentation indicated concentrations of H<sub>2</sub> within the container were at their peak (120–150 minutes after test start).

The toxic gas concentrations (CO and HCN) within the container began to increase at the same time as the flammable gases. Figure 118 shows the CO concentrations recorded by each meter. Although a sensor error prevented the interior diffusion meter from collecting usable CO data, the interior pumped meter indicated the CO concentration within the container rapidly increased to the upper measurement threshold simultaneous with Novec 1230 discharge.

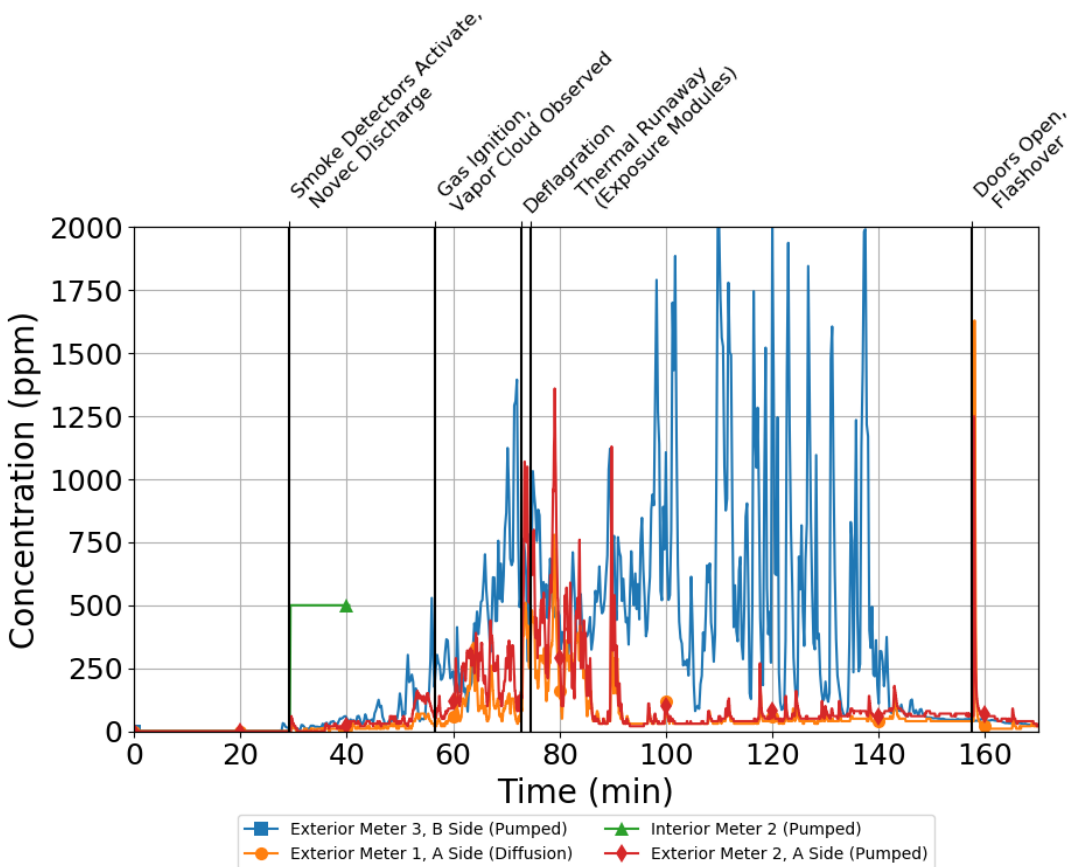


Figure 118 – Carbon monoxide (CO) concentration measured by fire service portable gas meters in Test 2.



## UL 9540A INSTALLATION LEVEL TESTS WITH OUTDOOR LITHIUM-ION ENERGY STORAGE SYSTEM MOCKUPS

CO concentrations measured by portable gas meters located on the exterior of the container began to increase immediately after Novec 1230 was discharged. The release of Novec 1230 into the container may have displaced CO that was previously in the container through the roof vent and other points of leakage. The CO concentration measured by the exterior meters slowly increased in the period between Novec 1230 discharge and the gas ignition. Exterior CO concentrations began to increase more rapidly after this flaming event. Each meter indicated a peak in CO concentrations between 70 and 75 minutes, coincident with the deflagration and propagation of thermal runaway beyond the Initiating Module. This matched the period when gas measurement instrumentation indicated a substantial increase in CO concentrations within the container itself.

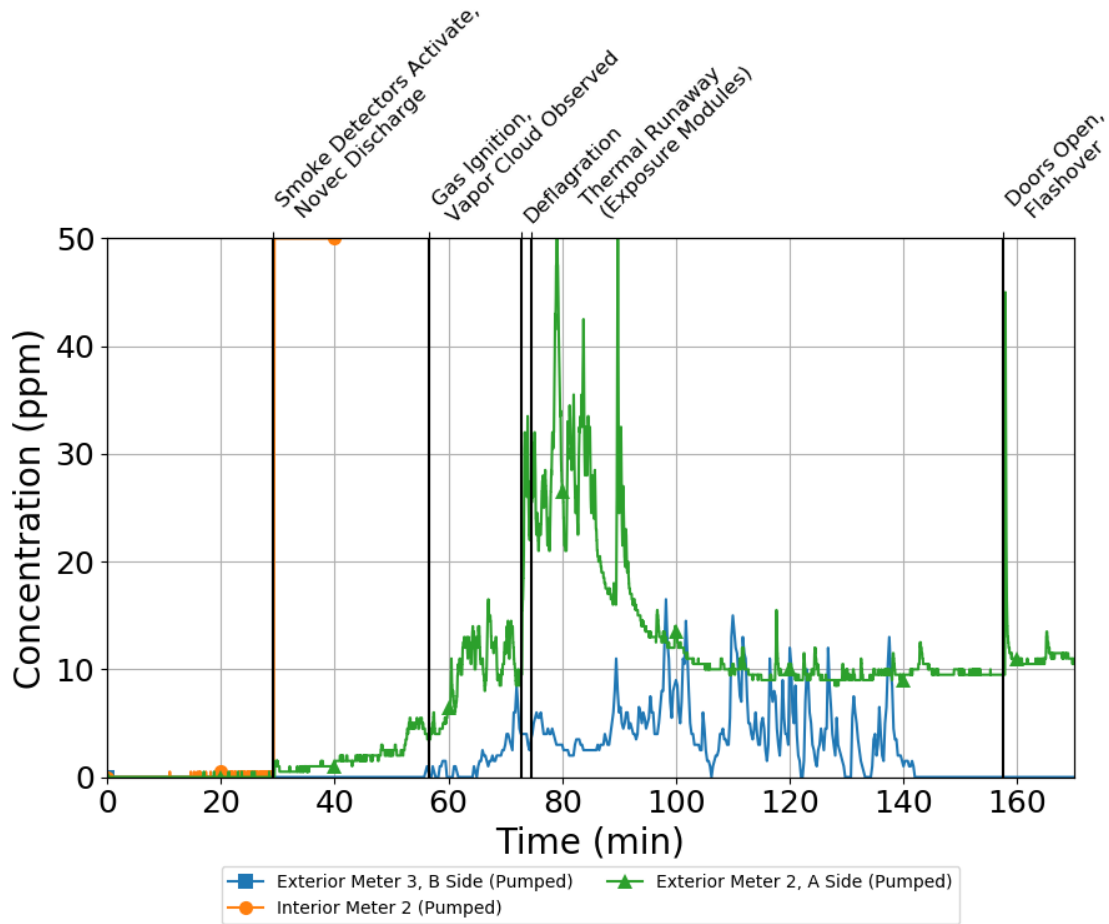
Following the deflagration, additional leakage points were created by the ruptured deflagration panels. This was particularly apparent in the data measured by Exterior Meter 3, located directly adjacent to the opened deflagration panel on the B-side. Following the deflagration, Exterior Meter 3 measured CO concentrations that fluctuated between baseline values and peaks as high as 2,000 ppm. The timing of these fluctuations matched the period in which steady, peak CO concentrations were measured in the container (130–150 min). In contrast, the two exterior meters on the A-side did not measure CO concentrations above 150 ppm after 90 minutes. Exterior Meter 4, located 10 ft offset from the A-side of the container, did not record time history data and is not shown in Figure 118. A video analysis of the gas concentrations measured by this meter indicated the CO concentrations followed a similar trend to the meters located closer to the container, but the magnitude of the peak CO concentrations was lower. The peak CO concentration recorded by this meter was 430 ppm. The peak CO concentrations observed at Exterior Meters 2 and 3 exceeded IDLH values, although concentrations were below this threshold for the majority of the test.

The HCN concentrations, shown in Figure 119, followed a similar trend to the CO concentrations. The HCN concentration measured inside of the container increased after venting and reached the upper measurement threshold six minutes later, before a sensor error occurred in that meter.

The HCN concentration measured by exterior meters began to increase after Novec 1230 discharge aligned with CO concentrations. The HCN concentration measured by Exterior Meter 2 (A-side, 3 ft) peaked between approximately 70 minutes and 90 minutes.



## UL 9540A INSTALLATION LEVEL TESTS WITH OUTDOOR LITHIUM-ION ENERGY STORAGE SYSTEM MOCKUPS

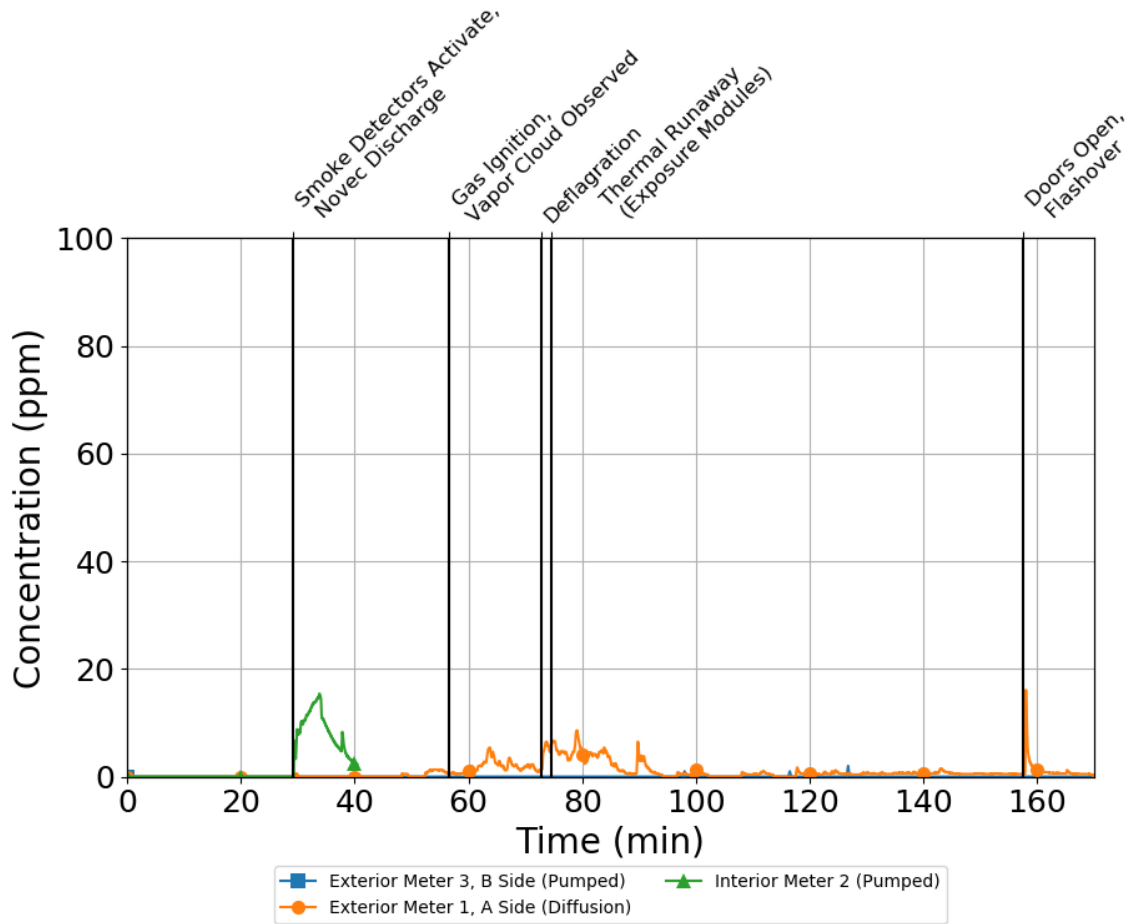


**Figure 119 – Hydrogen cyanide (HCN) concentration measured by fire service portable gas meters in Test 2.**

Other gases measured by the portable gas meters included hydrogen sulfide (H<sub>2</sub>S), oxygen (O<sub>2</sub>), and volatile organic compounds (VOCs), as shown in Figure 120, Figure 121, and Figure 122, respectively.

H<sub>2</sub>S was first measured by the portable gas meter on the interior of the structure, which indicated an increase after Novec 1230 discharge. There is no known source of sulfur in the materials in these tests, so the response may be due to Novec or HCN cross-sensitivity. Following the Novec 1230 discharge, the H<sub>2</sub>S concentration measured by the meter decreased and remained at negligible values for the remainder of the test. The exterior meter on the A-side of the container measured concentrations of H<sub>2</sub>S less than 10 ppm from 60 minutes to 90 minutes, corresponding to the period of peak CO values. Although the exterior meter on the B-side of the container was equipped to measure H<sub>2</sub>S, it did not record any elevated concentrations over the course of the test.

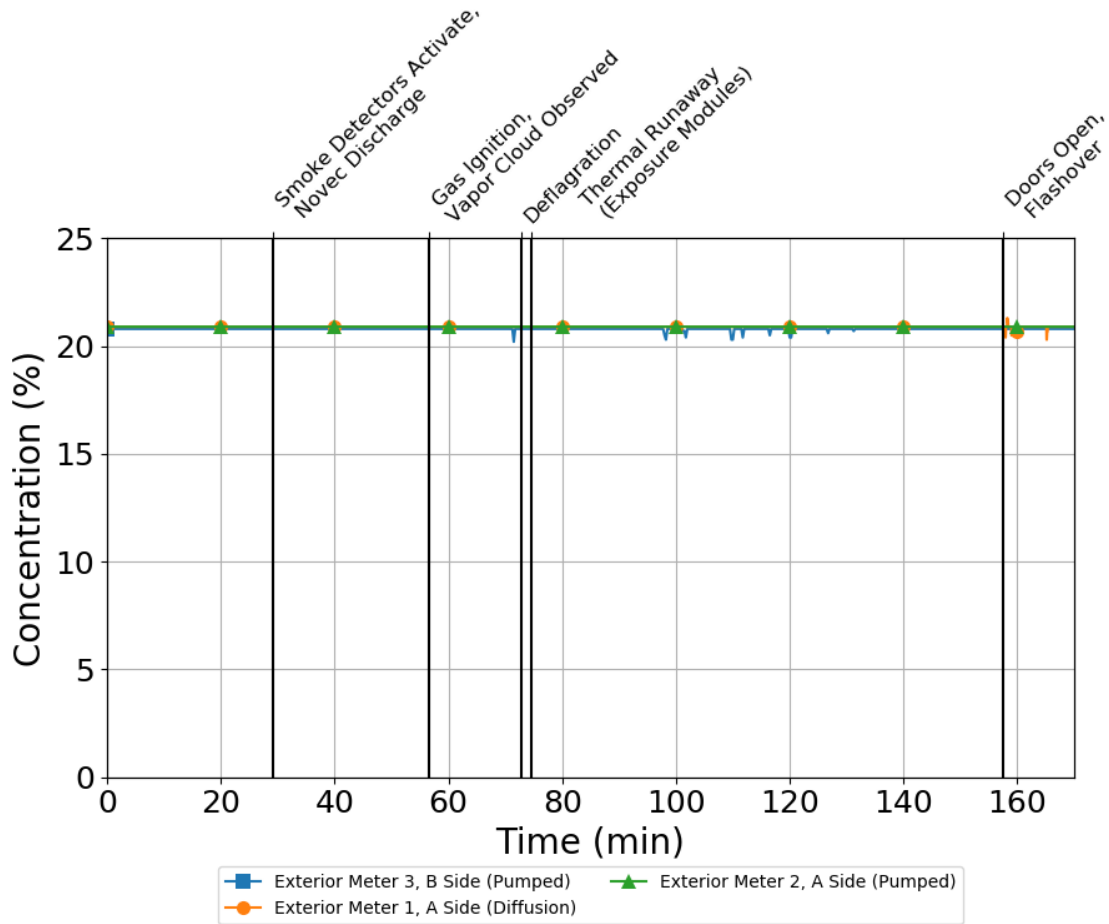
# UL 9540A INSTALLATION LEVEL TESTS WITH OUTDOOR LITHIUM-ION ENERGY STORAGE SYSTEM MOCKUPS



**Figure 120 – Hydrogen sulfide (H<sub>2</sub>S) concentration measured by fire service portable gas meters in Test 2.**

Figure 121 shows the time histories of oxygen concentration for the three meters that recorded viable data. All of these meters were located on the exterior of the container. With the exception of a few minor dips, oxygen concentrations remained at ambient concentrations for the duration of the test.

## UL 9540A INSTALLATION LEVEL TESTS WITH OUTDOOR LITHIUM-ION ENERGY STORAGE SYSTEM MOCKUPS



**Figure 121 – Oxygen (O<sub>2</sub>) concentration measured by fire service portable gas meters in Test 2.**

The VOC concentrations measured by the exterior meter on the A-side of the container are shown in Figure 122. VOC concentrations increased after thermal runaway and Novec 1230 discharge. This is consistent with increases in other exterior gas concentrations. A more rapid increase was observed after the deflagration event and further thermal runaways. The peak VOC concentrations were observed from 70 minutes to 90 minutes. After 90 minutes, VOC concentrations decreased to less than 20 ppm for the duration of the test. VOCs were likely produced from the vaporization and thermal decomposition of the electrolytes contained in the cells.

# UL 9540A INSTALLATION LEVEL TESTS WITH OUTDOOR LITHIUM-ION ENERGY STORAGE SYSTEM MOCKUPS

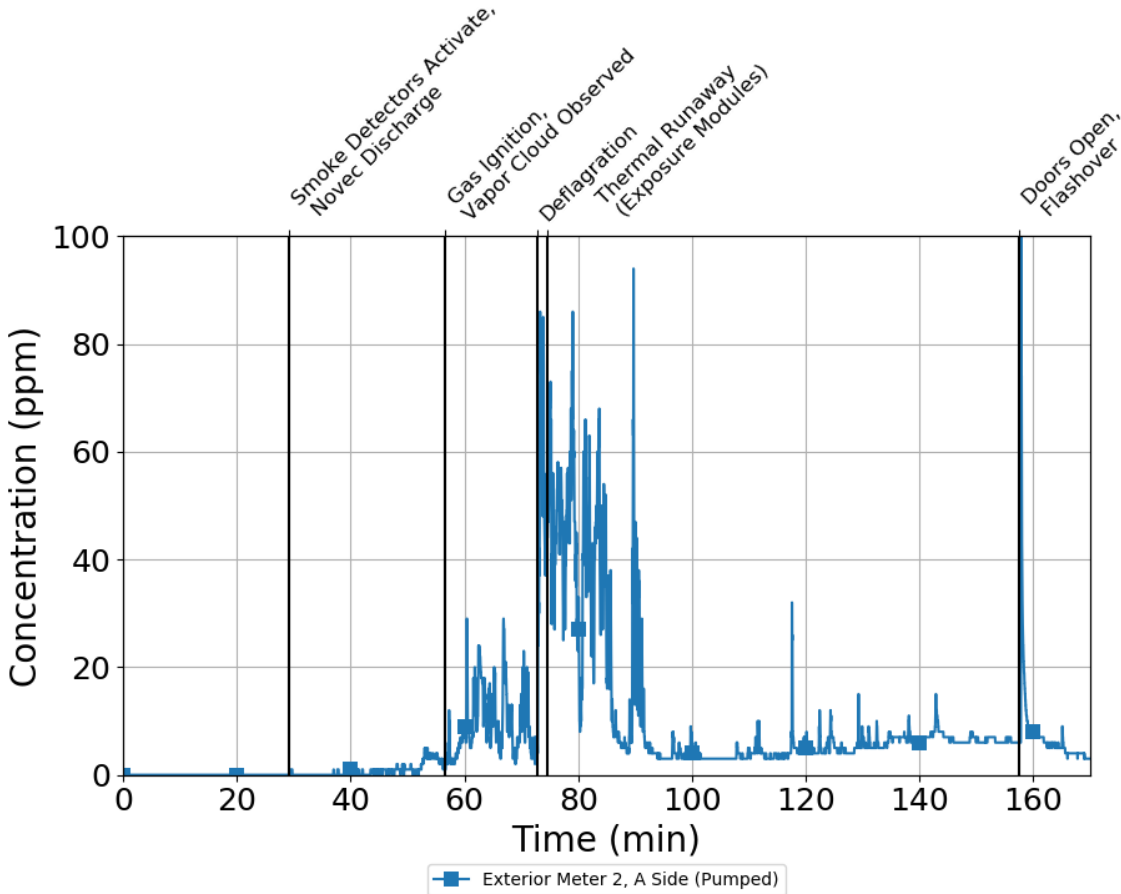


Figure 122 – Volatile organic compound (VOC) concentration measured by fire service portable gas meters in Test 2.








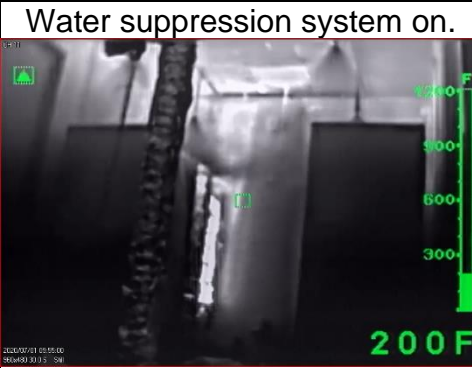
**UL 9540A INSTALLATION LEVEL TESTS WITH OUTDOOR LITHIUM-ION ENERGY STORAGE SYSTEM MOCKUPS**

**4.3 Test 3 - Li-Ion ESS Installation with 0.5 gpm/ft<sup>2</sup> Actual Delivered Density Water Spray**

Test 3 was conducted on July 1st, 2020, at 9:01 AM Central time.

**4.3.1 Timeline**

Figure 123 through Figure 125 show a visual sequence of the most significant events that occurred during Test 3. Test 3 began when the flexible film heaters installed inside the Initiating Cell were energized to begin heating. Power was automatically controlled to provide 6 °C/min of temperature rise on the Initiating Cell surface. After 21 minutes and 37 seconds, venting of the heated cell occurred. Thermal runaway of the Initiating Cell occurred two minutes and 39 seconds later, at 29 minutes and 53 seconds of test time. Smoke was first seen venting from the Initiating Module within one second of thermal runaway. All the wall-mounted gas detectors alarmed within 30 seconds of thermal runaway, and an off-gas fire plume reached from the Initiating Module to the ceiling, as shown by Figure 123. Both smoke detectors activated within 60 seconds of thermal runaway. Eight minutes and 49 seconds passed after thermal runaway of the first cell before complete propagation occurred in the Initiating Module. The generated gas ignited and initiated flaming up the vertical face of the Initiating Unit as the thermal runaway propagated through the cells in the Initiating Module.

<p>Both smoke detectors activated.</p>  <p>00:30:53 (TR + 00:01:00)</p>	<p>Ignition, sustained flaming.</p>  <p>00:38:42 (TR+ 00:08:49)</p>
<p>Sprinkler link activation.</p>  <p>00:39:27 (TR + 00:09:34)</p>	<p>Water suppression system on.</p>  <p>00:40:06 (TR + 00:10:13)</p>

**Figure 123 – Sequence of events in Test 3 leading up to 40 minutes of test time.**

## UL 9540A INSTALLATION LEVEL TESTS WITH OUTDOOR LITHIUM-ION ENERGY STORAGE SYSTEM MOCKUPS

Venting gases during thermal runaway had a negligible effect on gas temperatures at the container ceiling. By contrast, the ceiling jet of the fire plume rapidly increased ceiling temperatures. The sprinkler link activated nine minutes and 34 seconds after thermal runaway. Water was supplied to the suppression system after a 30-second delay to simulate pipe-filling from a fire department connection. Water spray from the open nozzles began 39 seconds later, as shown in the thermal image in the bottom right corner of Figure 123. Flaming combustion ceased within five seconds of suppression system flow. There was no immediately observable cooling within the Initiating Unit, as the overhead water spray impinged on and did not penetrate the Initiating Unit enclosure. Operation of the suppression system immediately reduced container gas and wall surface temperatures and reduced the thermal exposure to the Target Units. Partial thermal runaway was observed in three additional modules in the Initiating Unit while the suppression system was operating. A deflagration occurred simultaneously when the third additional module entered thermal runaway. Gas measurements near the ceiling, shown in Figure 143, demonstrate that the gas accumulating near the ceiling exceeded the LFL of the mixture during the 2<sup>nd</sup> or 3<sup>rd</sup> module thermal runaway.

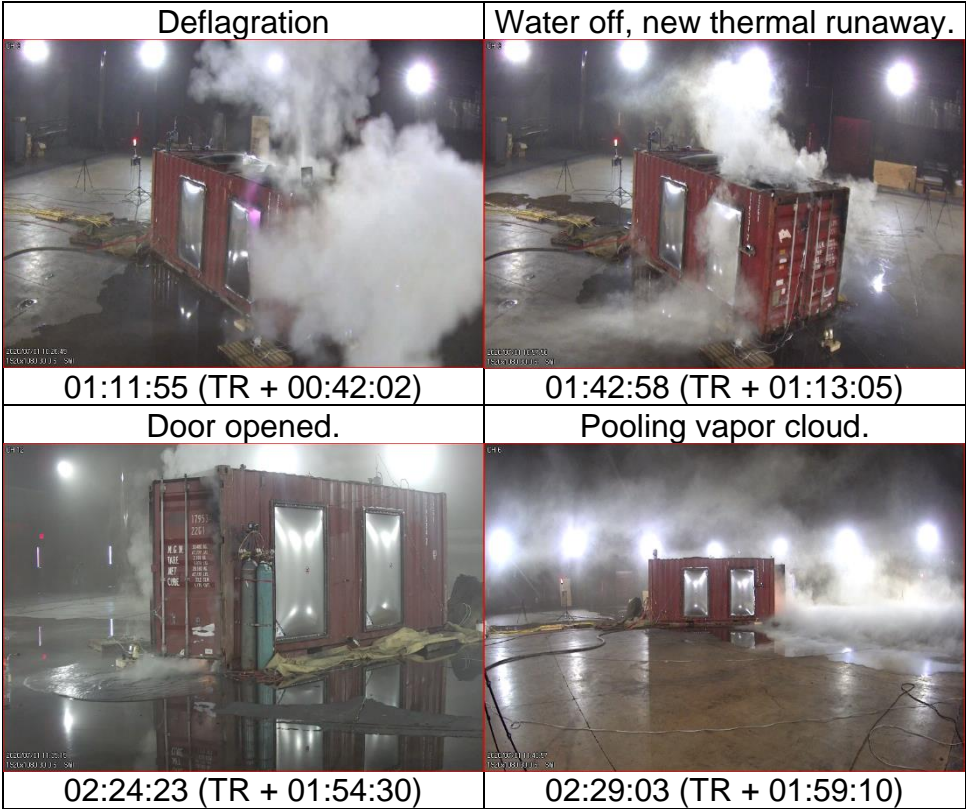
Having observed that 1) thermal exposure measurements demonstrated noncompliance with UL 9540A temperature performance criteria prior to suppression system operation; 2) all temperatures and heat fluxes measured within the container and target units returned to ambient conditions; 3) high temperatures were still indicated in the Initiating Unit but were steadily decreasing; and 4) a deflagration had breached the envelope of the container, waterflow was discontinued 25 minutes after the last observed thermal runaway, one hour and 36 minutes into the test. This time was considered the potential end to the test.

Module-to-module propagation of thermal runaway resumed in the Initiating Unit eight minutes after waterflow was discontinued, as two additional modules experienced thermal runaway. One hour and 42 minutes after the initial thermal runaway, thermal runaway propagated into a module in the Left Target Unit. Waterflow was re-initiated one minute later to determine if the suppression system could limit further propagation of thermal runaway. Gas concentration measurements indicated an accumulation of battery gases in a potentially flammable atmosphere lacking oxygen, so the container doors were opened at two hours and 29 minutes of test time in order to compare subsequent fire behavior with Test 2. The suppression system operation was maintained and no ignition occurred. Steam, a vapor cloud, and accumulated water vented at a low velocity from the open doors, pooling within a 20 ft radius of the open container end. One final module at the top of the Initiating Unit entered thermal runaway. No further thermal runaways were observed.

The test was terminated after three hours and 44 minutes.



**UL 9540A INSTALLATION LEVEL TESTS WITH OUTDOOR LITHIUM-ION ENERGY STORAGE SYSTEM MOCKUPS**



**Figure 124 – Sequence of events in test 1 from 72 to 149 minutes of test time.**



**Figure 125 – Final thermal runaway at 02:39:22 (TR + 01:59:30).**

**UL 9540A INSTALLATION LEVEL TESTS WITH OUTDOOR LITHIUM-ION ENERGY STORAGE SYSTEM MOCKUPS**

**4.3.2 Comparison of Test 3 Results to 9540A Performance Metrics**

**Table 16 – Test 3 Performance**

<b>Ref.</b>	<b>UL 9540A Performance Metric</b>	<b>Assessment</b>
10.5.1	For BESS units intended for installation in locations with combustible construction, surface temperature measurements along instrumented wall surfaces shall not exceed a temperature rise of 97 °C (175 °F) above ambient. Surface temperature rise is not applicable if the intended installation is composed completely of noncombustible materials in which wall assemblies, cables, wiring, and any other combustible materials are not to be present in the BESS installation. In this case, the report shall note that the installation shall contain no combustible materials.	Not compliant
10.5.2	The surface temperature of modules within the BESS units adjacent to the initiating BESS unit shall not exceed the temperature at which thermally initiated cell venting occurs.	Left: Not compliant Front: Compliant
10.5.3	The fire spread on the cables in the flame indicator shall not extend horizontally beyond the initiating BESS enclosure dimensions.	N/A
10.5.4	There shall be no flaming outside the test room.	Compliant <sup>†</sup>
10.5.5	There is no observation of detonation. There is no observation of deflagration unless mitigated by an engineered deflagration protection system.	Compliant
10.5.6	Heat flux in the center of the accessible means of egress shall not exceed 1.3 kW/m <sup>2</sup> .	Not compliant
10.5.7	There shall be no observation of re-ignition within the initiating unit after the installation test had been concluded and the sprinkler operation was discontinued.	Not compliant

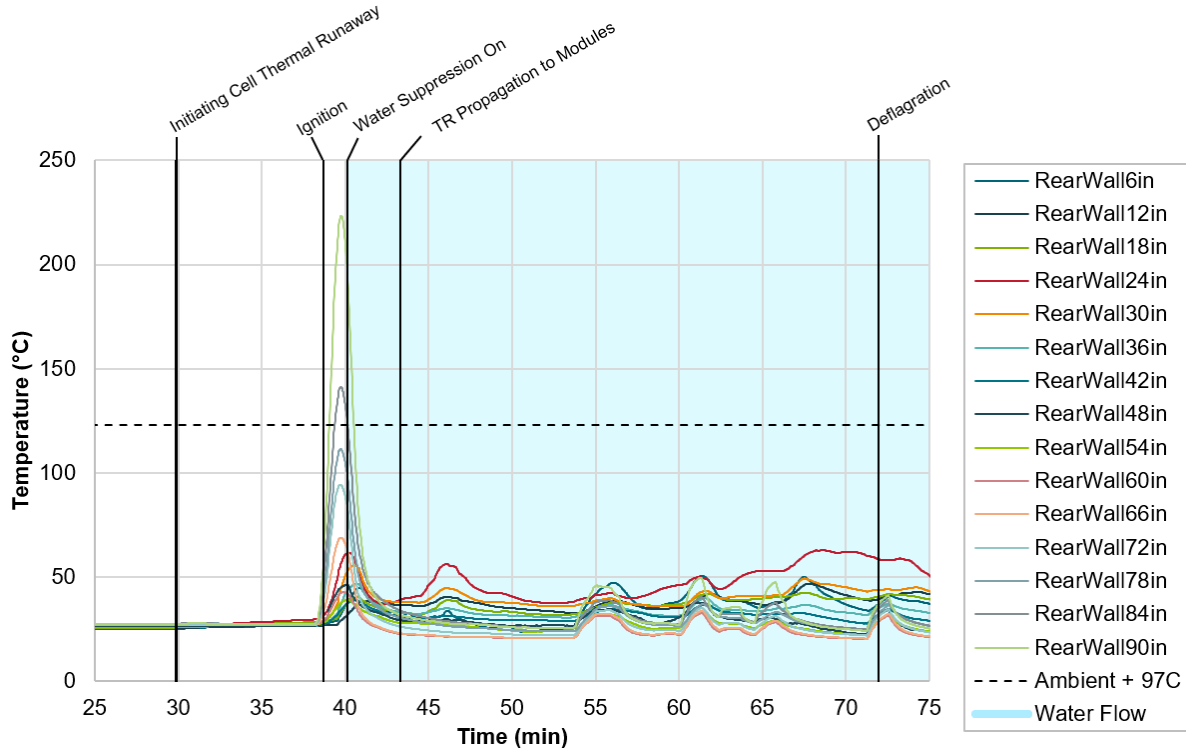
<sup>†</sup> The deflagration venting successfully vented overpressure, potentially preventing dangerous loss of integrity/rupture of the ISO container.

**Thermal Exposure to Walls**

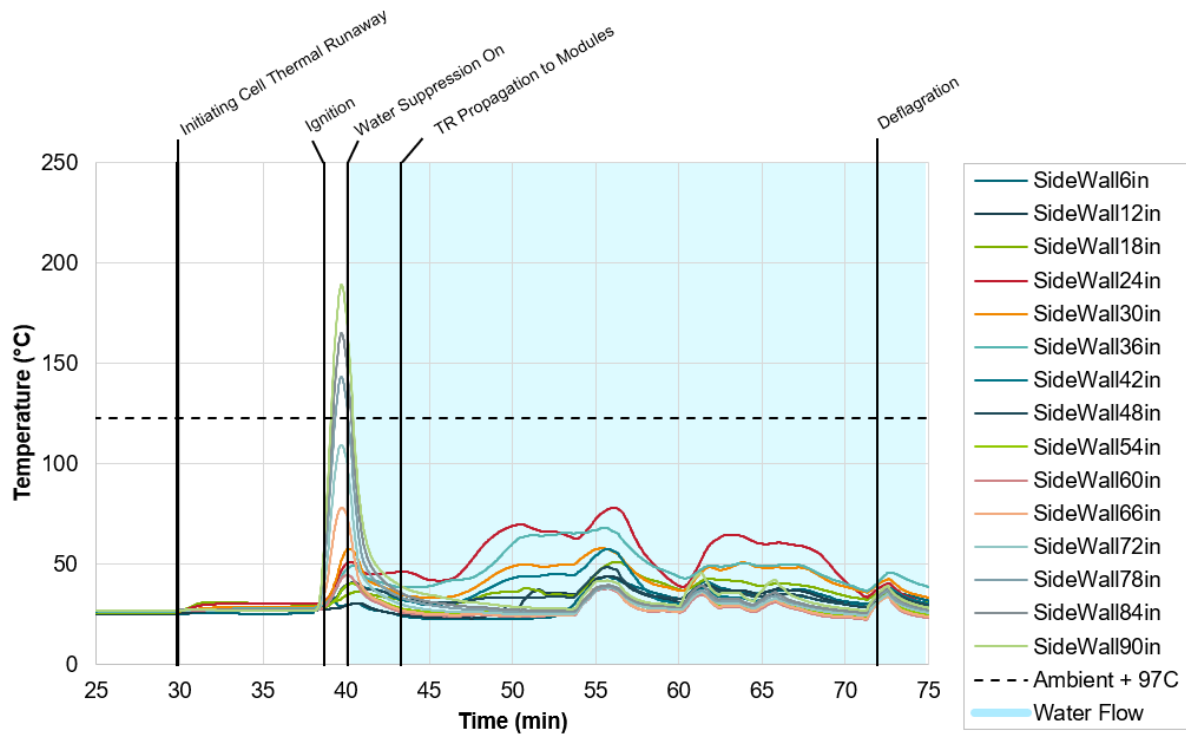
During the period between the initial thermal runaway and activation of the water suppression system, rear wall temperatures between 84 in and 90 in exceeded the temperature performance criteria within one minute of ignition, as described in Figure 126. For this same period, side wall temperatures between 78 in and 90 in exceeded the temperature performance criteria within one minute of ignition, as shown in Figure 127. Activation of the water suppression system rapidly reduced temperatures on both walls to near ambient temperatures. Temperatures measured on both walls remained below the temperature performance criteria despite ongoing thermal runaways, until the waterflow was discontinued.



# UL 9540A INSTALLATION LEVEL TESTS WITH OUTDOOR LITHIUM-ION ENERGY STORAGE SYSTEM MOCKUPS



**Figure 126 – Temperatures measured on the rear wall during Test 3 from the Initiating Cell thermal runaway through the deflagration.**



**Figure 127 – Temperatures measured on the side wall during Test 3 from the Initiating Cell thermal runaway through the deflagration.**



## UL 9540A INSTALLATION LEVEL TESTS WITH OUTDOOR LITHIUM-ION ENERGY STORAGE SYSTEM MOCKUPS

Figure 128 and Figure 129 show the walls were negligibly heated by the deflagration that occurred at 72 minutes, while the suppression system was operating. Wall surface temperatures measured on both instrumented walls steadily increased to a peak of 240 °C after waterflow was discontinued at 95 minutes. Two modules in the Initiating Unit and one module in the Left Target Unit experienced thermal runaways during this time, contributing to wall heating. As the waterflow was restarted, temperature measurements from 24 in to 66 in on the rear wall and 42 in to 60 in on the side wall exceeded the temperature performance criteria. These measurement locations corresponded to locations adjacent to the modules that experienced thermal runaway in the Initiating Unit. Additional waterflow decreased wall surface temperatures beneath the temperature performance criteria within seconds and maintained wall surface temperatures below this threshold for the remainder of the test.

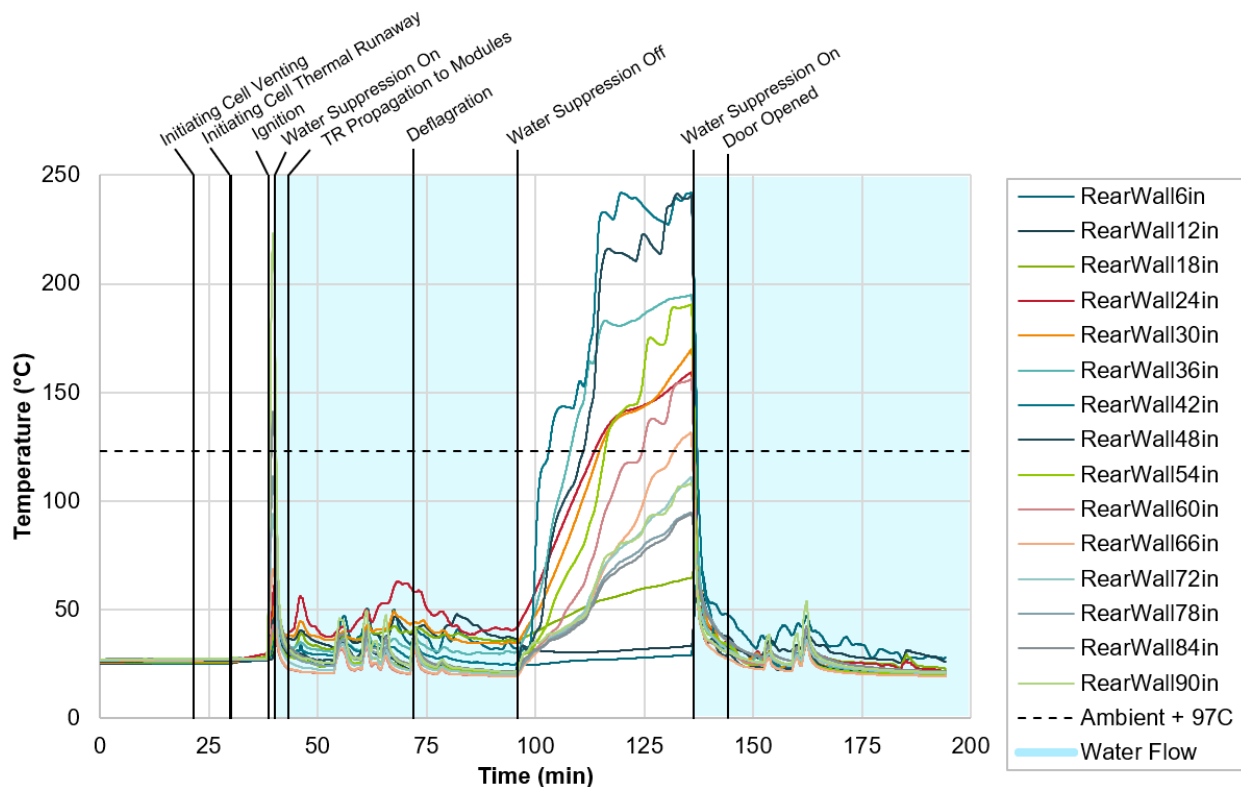
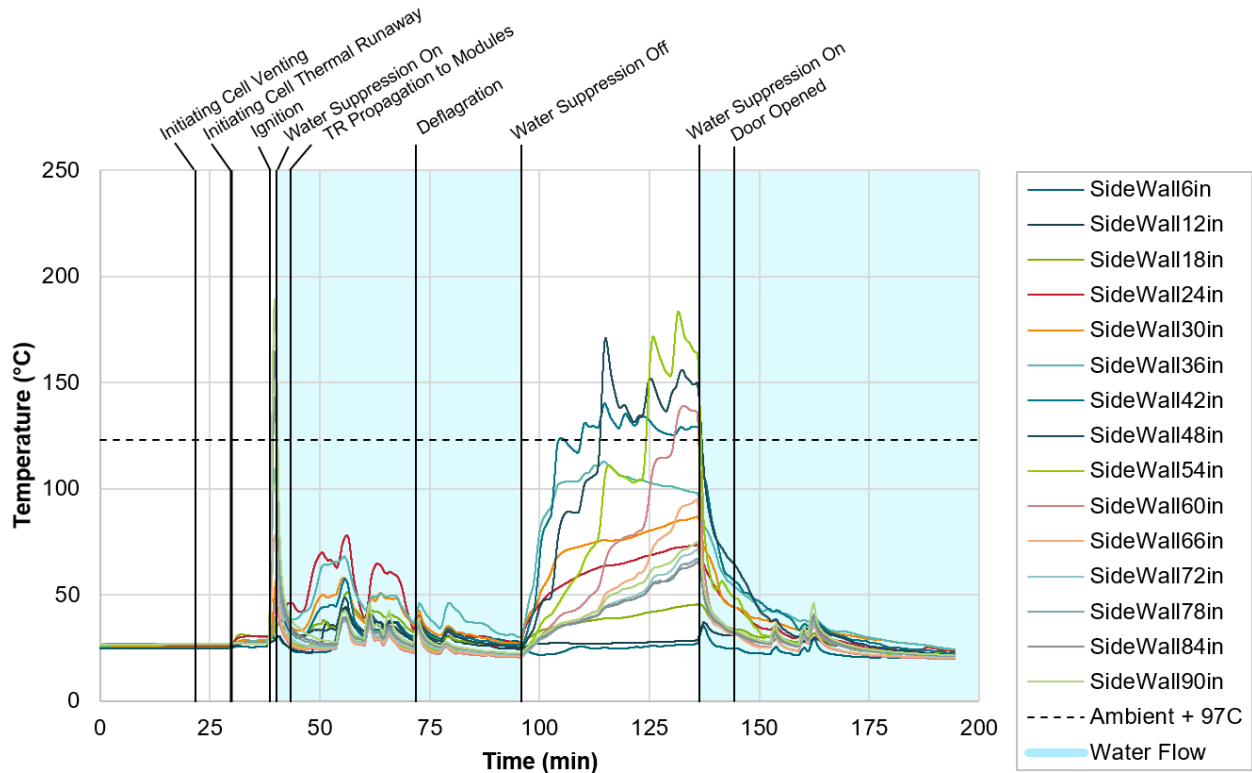


Figure 128 – Temperatures measured on the rear wall during Test 3.



## UL 9540A INSTALLATION LEVEL TESTS WITH OUTDOOR LITHIUM-ION ENERGY STORAGE SYSTEM MOCKUPS



**Figure 129 – Temperatures measured on the side wall during Test 3.**

UL 9540A does not include a performance criterion based on incident heat flux to combustible materials. Heat flux measured in Test 3 describes the magnitude, duration, and subsequent risk of ignition for combustible materials. Figure 130 illustrates that the heat flux measured at the side wall was less than  $12.5 \text{ kW/m}^2$ , a critical threshold for ignition risk to combustible structures according to NFPA 80A [23]. The rear wall also remained below  $12.5 \text{ kW/m}^2$  except for brief peak of  $14 \text{ kW/m}^2$  for a period of three minutes after the restart of the water suppression system. The heat from the Initiating Unit may have caused a phase change in water which resulted in a rapid increase in heat flux. Heat flux measurements on the side wall also increased at this point, but to a peak of  $3 \text{ kW/m}^2$ . Once the unit doors were opened, incident heat flux decreased until reaching ambient heat flux.

# UL 9540A INSTALLATION LEVEL TESTS WITH OUTDOOR LITHIUM-ION ENERGY STORAGE SYSTEM MOCKUPS

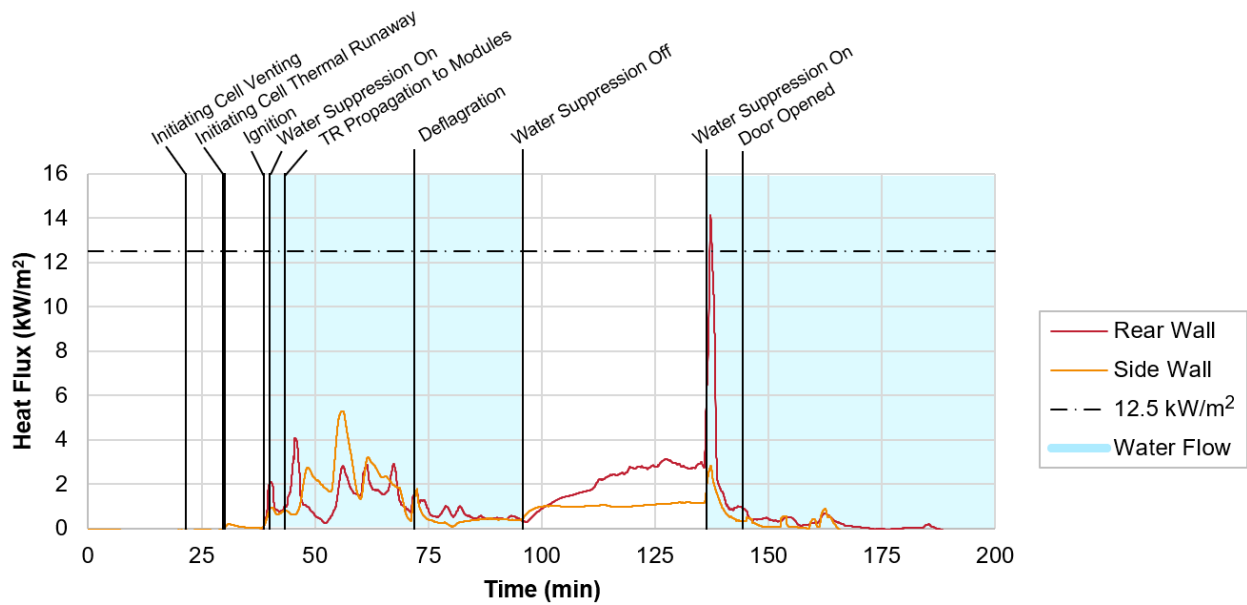
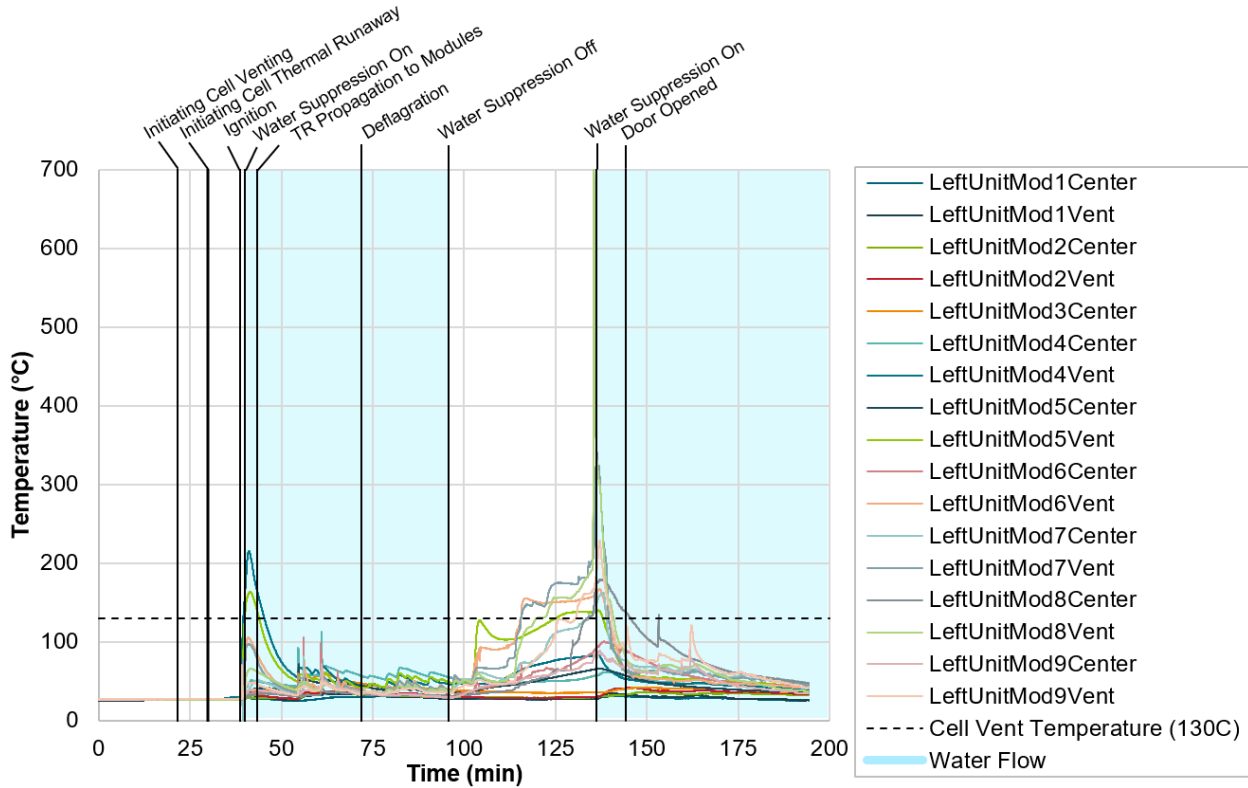


Figure 130 – Incident heat flux to rear and side walls measured during Test 3.

## Thermal Exposure to ESS Targets

In the Left Target Unit, temperatures measured in Module 4 and Module 5 exceeded the cell vent temperature (130 °C) for a short duration after waterflow first began, as shown in Figure 131. Therefore, temperature measurements demonstrated the ESS configuration was not compliant with the Target Unit temperature performance criteria for the spacing specified to the Left Target Unit. Module 4 and Module 5 were directly adjacent to the region of flaming at the front of the Initiating Unit. Once the flames were suppressed by waterflow, the temperatures measured in the Left Target Unit decreased below the cell vent temperature threshold and decreased until waterflow was discontinued at 95 minutes. Left Target Unit temperatures were not impacted by the deflagration.

## UL 9540A INSTALLATION LEVEL TESTS WITH OUTDOOR LITHIUM-ION ENERGY STORAGE SYSTEM MOCKUPS

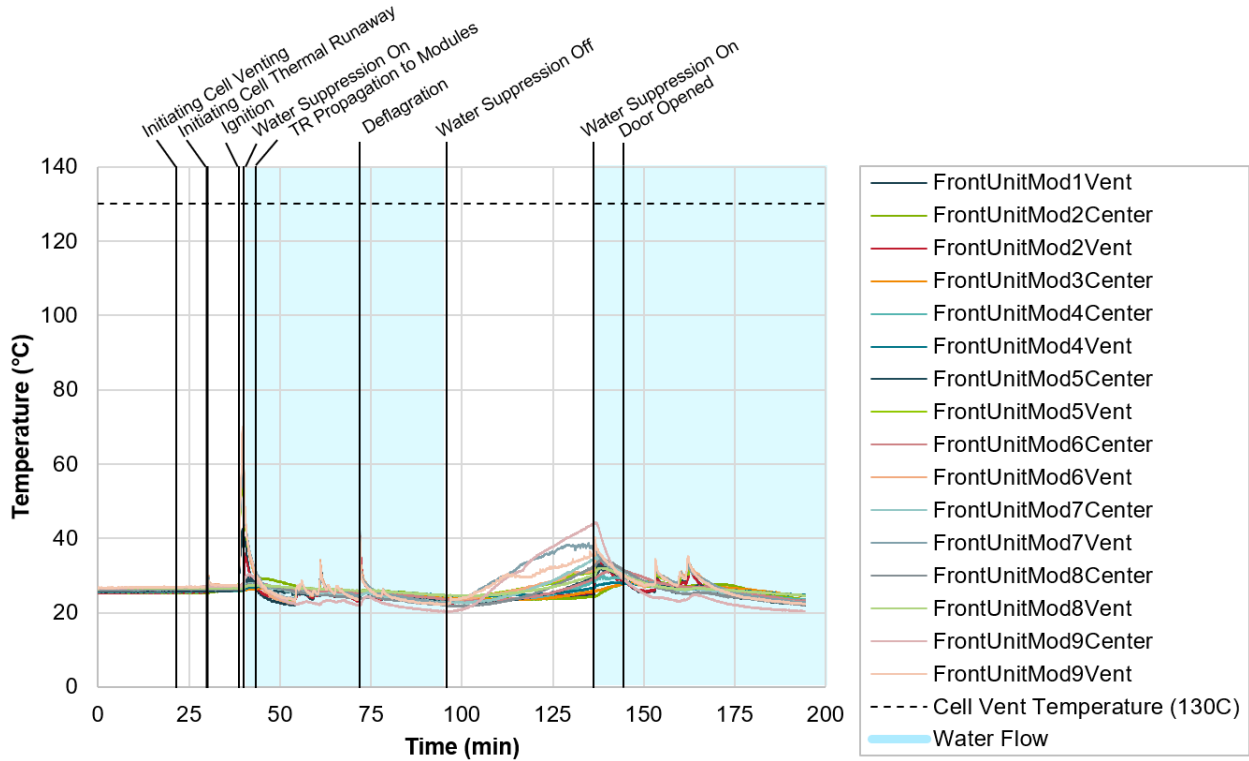


**Figure 131 – Temperatures measured in Left Target Unit during Test 3.**

When waterflow was discontinued, temperatures in the Left Target Unit steadily increased. During the period of discontinued waterflow, Module 5 through Module 9 of the Left Target Unit exceeded the cell vent temperature, as shown in Figure 131. Thermal runaway occurred within Module 8 at 135 minutes, one minute before waterflow was restarted. When waterflow resumed at 136 minutes, temperatures measured throughout the Left Target Unit decreased below the cell vent temperature. Thermal runaway did not occur within any modules of the Left Target Unit during periods of active waterflow.

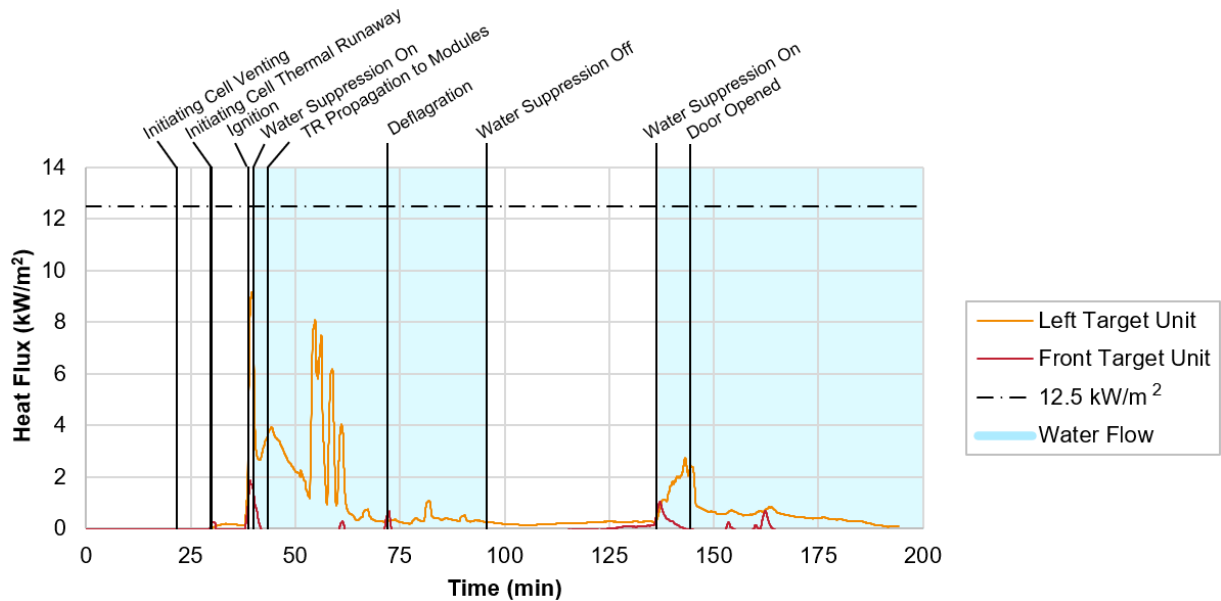
Unlike Test 1 and Test 2, all temperatures measured in the Front Target Unit were compliant to the target temperature performance criteria for the duration of Test 3, as indicated in Figure 132. Temperatures in the Front Target Unit initially rose as high as 70 °C before waterflow was activated. Once waterflow was activated, the Front Target Unit temperatures decreased to near ambient. Front Target Unit temperatures were not significantly increased by the deflagration. When waterflow was discontinued, temperatures rose slowly, but remained nearly 100 °C below the cell vent temperature. When waterflow was resumed, temperatures returned near ambient. No modules in the Front Target Unit experienced thermal runaway in Test 3.

# UL 9540A INSTALLATION LEVEL TESTS WITH OUTDOOR LITHIUM-ION ENERGY STORAGE SYSTEM MOCKUPS



**Figure 132 – Temperatures measured in Front Target Unit during Test 3.**

After ignition, incident heat flux on the Left Target Unit exceeded  $12.5 \text{ kW/m}^2$ . Heat flux reached  $9 \text{ kW/m}^2$  after the initial ignition event and intermittently  $8 \text{ kW/m}^2$  during the first period of water suppression system activation. Incident heat flux measured on the Front Target Unit remained below  $3 \text{ kW/m}^2$  for the duration of Test 3, as plotted in Figure 133.



**Figure 133 – Incident heat flux to Left and Front Target Units measured during Test 3.**



## UL 9540A INSTALLATION LEVEL TESTS WITH OUTDOOR LITHIUM-ION ENERGY STORAGE SYSTEM MOCKUPS

Figure 134 illustrates the extent of thermal damage to both Target Units. The magnitude of damage to the Left Target Unit and Front Target Unit are markedly improved from Test 1 and Test 2. The Target Units both experienced deposition of particulate from the battery thermal runaway events, but no indication of severe melting or deformation. By contrast, significant melting and deformation were observed on the front face of the Initiating Unit.



**Figure 134 – Condition of Left Target Unit (left), Initiating Unit (left), and Front Target Unit (right) after Test 3.**

### Flaming Outside the Test Room

Flames were only vented from the container during the deflagration, as pictured in Figure 135. Intermittent flaming of gases escaping from the instrumentation cable conduits were not observed in Test 3, unlike Test 2 and Test 1.

### Explosion Hazards

A deflagration occurred in the container 42 minutes after the initial thermal runaway and 32 minutes after activation of the water suppression system. At this time, four modules in the Initiating Unit had experienced thermal runaway and water was flowing at 0.5 gpm/ft<sup>2</sup>. Potential sources of ignition included hot materials from the modules that experienced thermal runaway, and electrical components of wall-mounted gas detectors.



## UL 9540A INSTALLATION LEVEL TESTS WITH OUTDOOR LITHIUM-ION ENERGY STORAGE SYSTEM MOCKUPS

Pressure generated by the deflagration partially operated one deflagration vent on the side of the container, as pictured in Figure 135. This panel was likely weakened in test 2. After test 2, the seam on this panel appeared distorted but the panel did not lose its sealing integrity when inspected. Smoke, gas, steam, and flames were emitted from the deflagration vent and the positive pressure vent intended for the Novec 1230 system.



**Figure 135 – Deflagration and side vent operation in Test 3 (test time 01:11:55).**

### **Egress Path Heat Flux**

Measurements for egress path heat flux were taken from the heat flux gauge installed in the Front Target Unit, across the aisle from the Initiating Unit. Figure 136 shows heat flux measurements were briefly noncompliant to the  $1.3 \text{ kW/m}^2$  performance criteria for only the 84 second period between ignition and activation of the water suppression system.



## UL 9540A INSTALLATION LEVEL TESTS WITH OUTDOOR LITHIUM-ION ENERGY STORAGE SYSTEM MOCKUPS

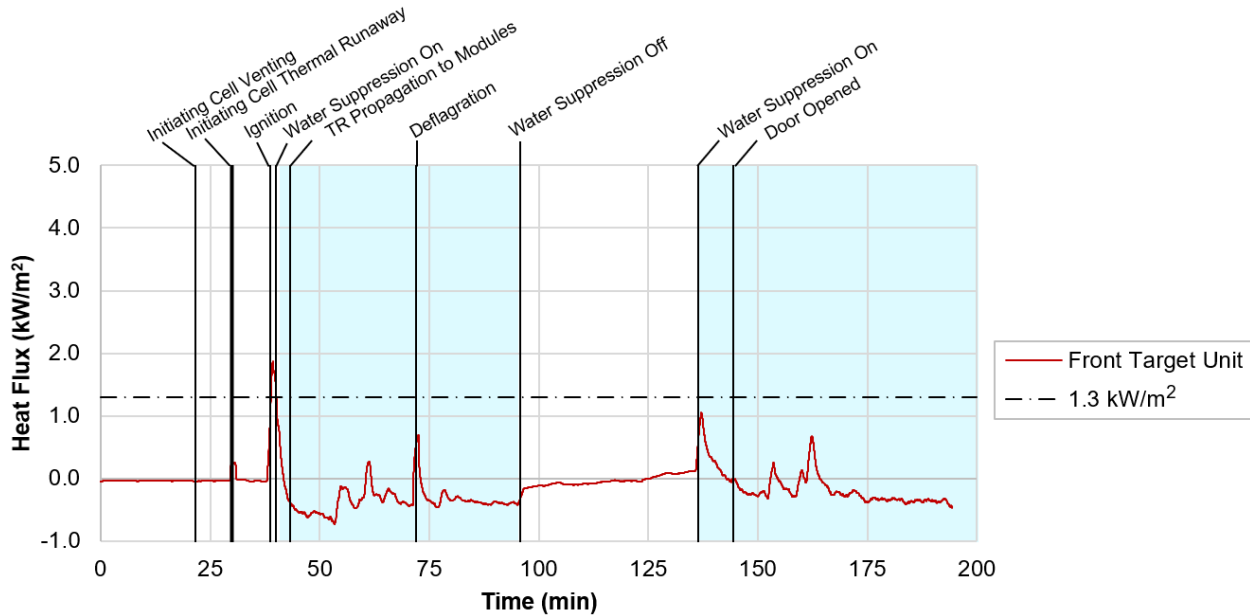


Figure 136 – Heat flux measured in the egress path during Test 3.

### Reignition Caused by Post-Test Thermal Runaways

Two periods were evaluated for reignitions in Test 3: when the waterflow was discontinued the first time at one hour and 36 minutes of test time, and when waterflow was discontinued at the conclusion of the test.

Thermal runaway occurred in Module 7 of the Initiating Unit eight minutes after waterflow was discontinued. Subsequent propagation of thermal runaway occurred above Module 7, in Module 8, followed by propagation of thermal runaway to Module 8 of the Left Target Unit. Although it is unclear if flaming occurred during this time, previous module thermal runaways were shown to ignite in this test series, and Figure 125 demonstrates possible flaming behavior in the thermal image. The observed behavior is considered a re-ignition hazard for this ESS configuration. This result is not compliant with UL 9540A performance criteria, but it is possible a longer duration waterflow would have improved this performance. Waterflow duration must be taken into account during installation siting conditions.

There were no re-ignitions from post-test thermal runaways when the waterflow was discontinued the second and final time. At the termination of the test, all modules above the Initiating Module in the Initiating Unit had been consumed by thermal runaway. The bottom two modules filled with water. Only one module experienced thermal runaway in the Left Target Unit, and there were no thermal runaways in the Front Target Unit. Though some cells may have been thermally damaged, no thermal runaways occurred during disassembly or disposal.



### 4.3.3 Thermal Runaway Propagation

Thermal runaway was initiated in Cell 5 of the Initiating Module. The rest of the cells in the Initiating Module experienced thermal runaway eight minutes later and within a span of 30 seconds, as shown in Figure 137. Thermal runaway in the second cell (Cell 4) of the Initiating Module and ignition of battery gases and surrounding materials were observed within one second of each other. Sufficient heat was generated to activate the sprinkler link 45 seconds after ignition. Waterflow reached the container 39 seconds later. Temperatures measured throughout the Initiating Module demonstrated there was no impact of water suppression inside the Initiating Module; the rate of temperature dissipation on Cell 1 through Cell 9 were not impacted by waterflow.

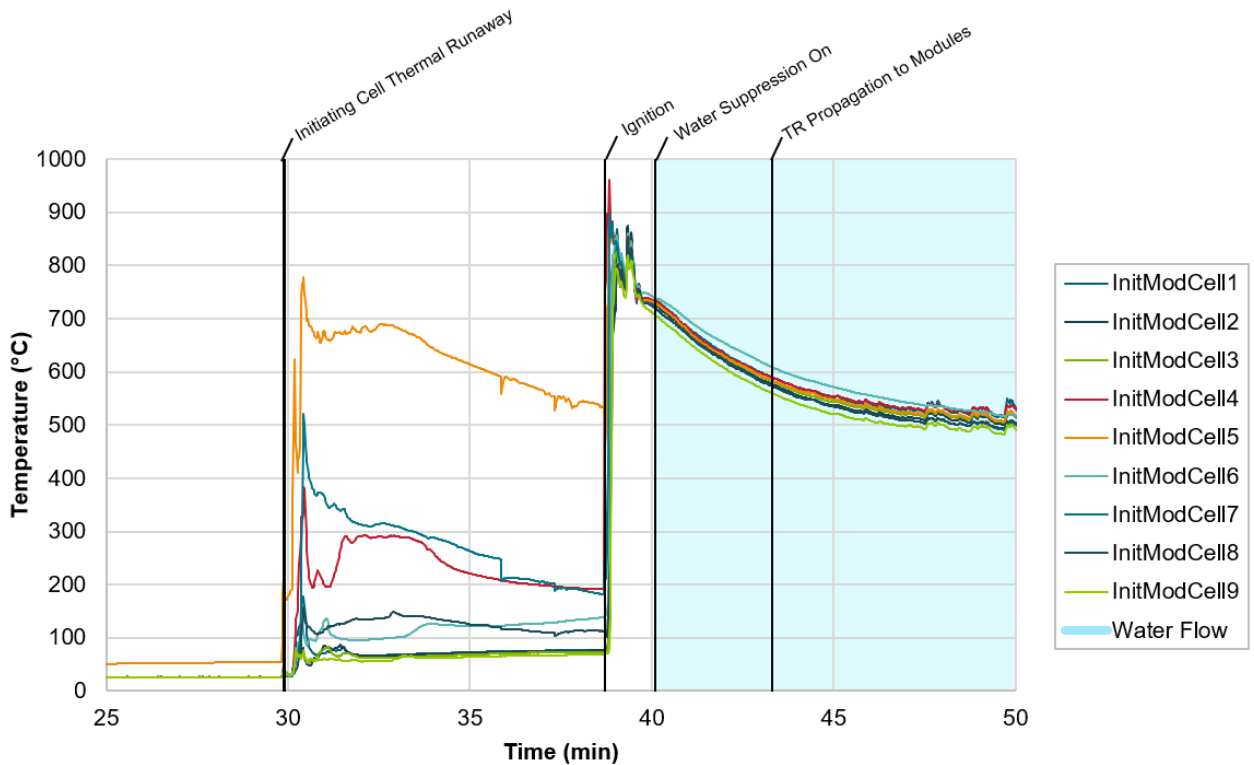
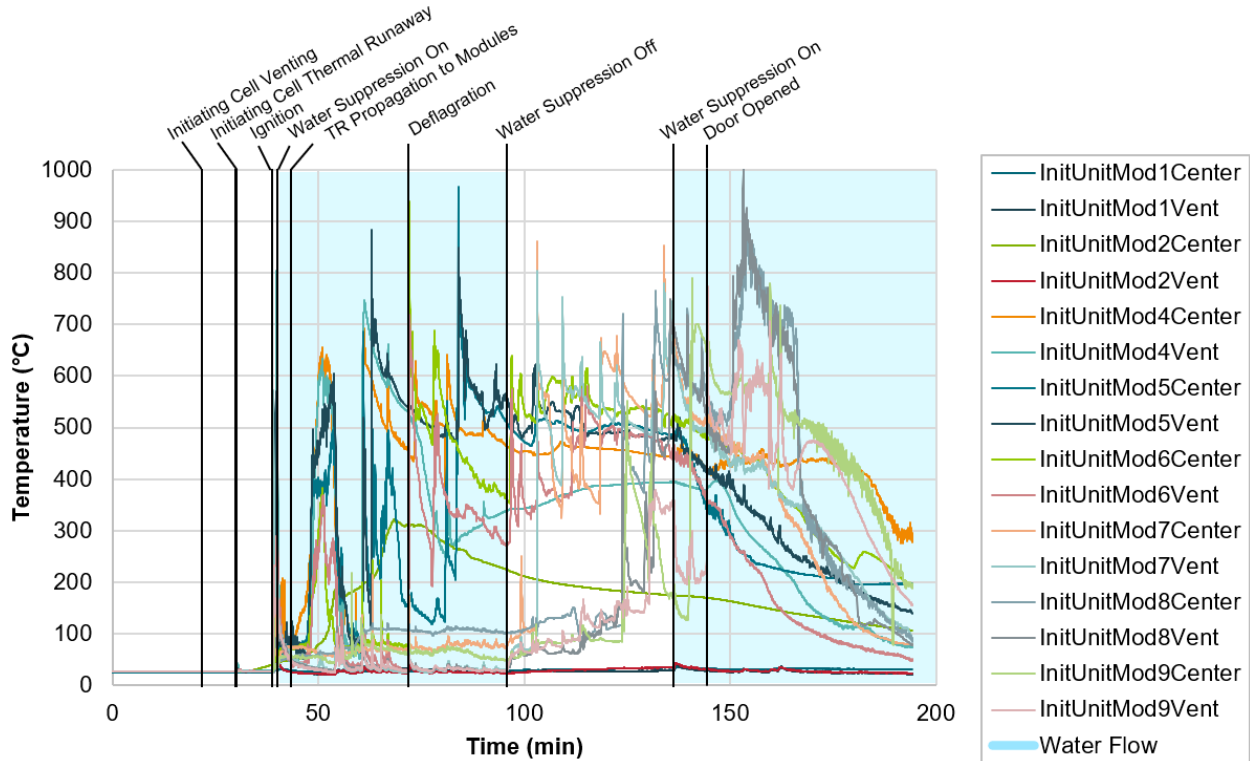


Figure 137 – Temperatures of cells in the Initiating Module from the first thermal runaway through propagation of thermal runaway to other modules in Test 3.

## UL 9540A INSTALLATION LEVEL TESTS WITH OUTDOOR LITHIUM-ION ENERGY STORAGE SYSTEM MOCKUPS



**Figure 138 – Temperatures measured inside Initiating Unit modules.**

Figure 138 shows temperatures measured inside the Initiating Unit modules, which were analyzed to determine times and locations of thermal runaway propagation. Thermal runaway behavior in the Initiating Unit is marked in Figure 138 by an immediate temperature increase of more than 400 °C and a sustained temperature above 300 °C. Propagation times and locations are summarized in Table 17 to aid in interpreting the data shown in Figure 138.

Within eight minutes of suppression system activation, thermal runaway progressed upward through three more modules within the Initiating Unit. Waterflow was discontinued after 55 minutes of operation. Two modules within the Initiating Unit experienced thermal runaway after waterflow was discontinued. The first module experienced thermal runaway seven minutes after water flow was discontinued and the second module experienced thermal runaway 28 minutes after water flow was discontinued. Thermal runaway was first observed in the Left Target Unit, in Module 8, 40 minutes after waterflow was discontinued. One minute later, waterflow was resumed. After three minutes and 30 seconds of waterflow, the top module of the Initiating Module (Module 9) experienced thermal runaway. Additional thermal runaway behavior was observed within these modules after the doors of the container were opened. Over the course of the test, thermal runaway propagation occurred at a rate of four to 30 minutes between events. No downward propagation of thermal runaway was observed in Test 3. A summary of propagation times is included in Table 17.

**UL 9540A INSTALLATION LEVEL TESTS WITH OUTDOOR LITHIUM-ION ENERGY STORAGE SYSTEM MOCKUPS**

**Table 17 – Thermal runaway propagation times for Test 3.**

<b>Test Time</b>	<b>Time Since TR</b>	<b>Location</b>	<b>Test Time</b>	<b>Time Since TR</b>	<b>Location</b>
00:29:53	00:00:00	InitUnitMod3	01:42:58	01:13:05	InitUnitMod7
00:40:06	00:10:13	Water On	02:03:49	01:33:56	InitUnitMod8
00:43:18	00:13:25	InitUnitMod4 <sup>13</sup>	02:15:06	01:45:13	LeftUnitMod8
00:47:02	00:17:09	InitUnitMod5 <sup>1</sup>	02:16:16	01:46:23	Water On
01:11:55	00:42:02	InitUnitMod6	02:19:47	01:49:54	InitUnitMod9
01:35:48	01:05:55	Water Off			

Over the course of Test 3, thermal runaway propagated from Module 3 through Module 9 in the Initiating Unit. The bottom two modules were submerged in water by the end of the test and did not experience thermal runaway. The top of Module 2 experienced thermal damage from the Initiating Module above prior to submersion, as pictured in Figure 139. Minimal thermal damage occurred to the Left Target Unit and Front Target Unit, as shown in Figure 134. The accumulation of water from the suppression system did not compound hazards in test 3, but may introduce significant hazards in an actual installation. Water may cause additional shorting of batteries, may create unintended ground paths that pose electrical shock hazards, and may accumulate in sufficient quantity to damage and disable other equipment as well as contribute significant weight to the installation. Installations should be designed to account for water drainage if a water suppression system is installed.



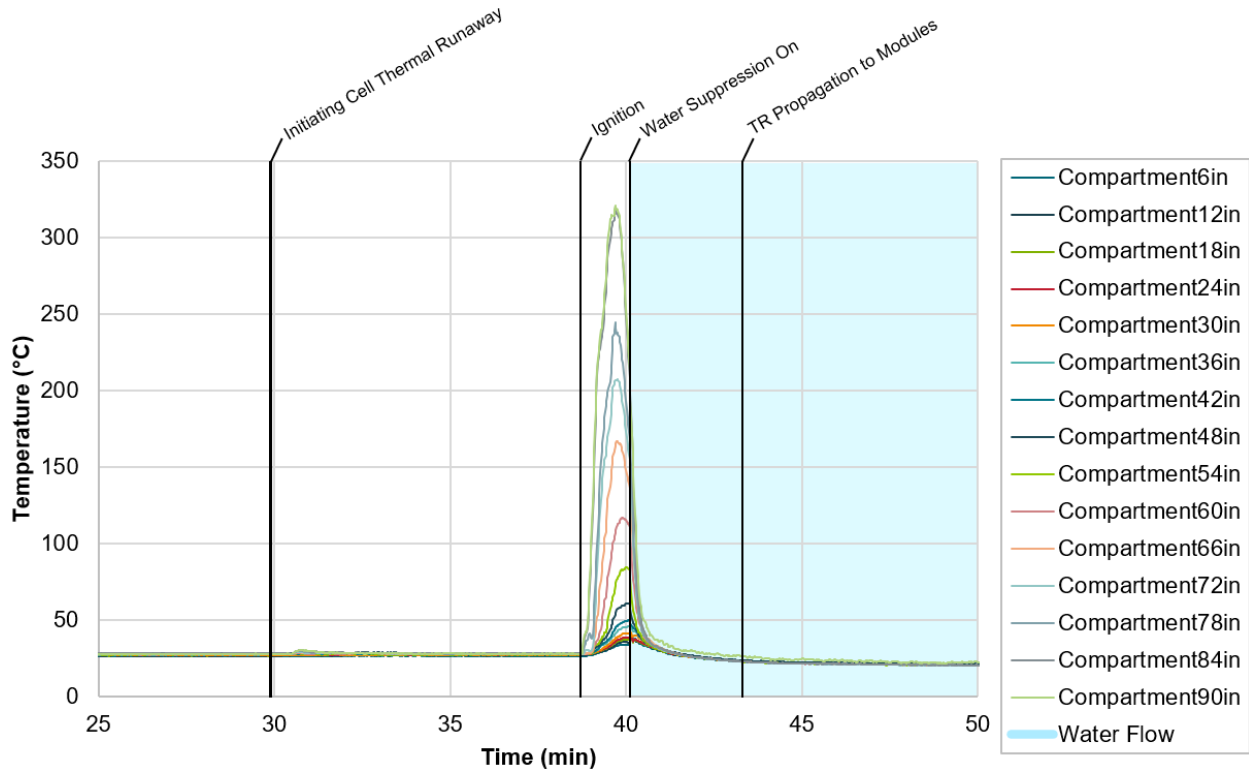
**Figure 139 – Condition of InitUnitMod2 with waterline visible after Test 3.**

<sup>13</sup> Time of initial thermal runaway in module. Thermal runaway did not completely propagate through all cells in the module at one time.

### 4.3.4 Test Conditions Inside ISO Container

#### Gas Temperature

There was no change in container gas temperatures between the initial thermal runaway event and ignition, as shown in Figure 140. A rapid temperature increase to 320 °C at the ceiling was observed after ignition and further thermal runaway in the Initiating Module. Temperatures measured above 72 in exceeded the cell thermal runaway temperature, 204 °C. Once the suppression system was activated, the gas temperatures measured in center of the container declined to initial ambient in less than 30 seconds.



**Figure 140 – Container gas temperatures measured from the initiating cell thermal runaway through the propagation of thermal runaway to other modules in Test 3.**

Figure 141 documents a steady increase in gas temperatures for the period while waterflow was discontinued. Just before waterflow was restarted, gas temperatures ranged from 32 °C at 12 in off the floor to 94 °C at the ceiling; the thermocouple 6 in off the floor was submerged in water. Gas temperatures returned to initial ambient levels when waterflow resumed.

Overall, gas temperatures were near ambient while the water suppression system was active. Rapid increases and decreases in temperature were observed when thermal runaway events occurred. While the water suppression system was not active, gas temperatures increased.



# UL 9540A INSTALLATION LEVEL TESTS WITH OUTDOOR LITHIUM-ION ENERGY STORAGE SYSTEM MOCKUPS

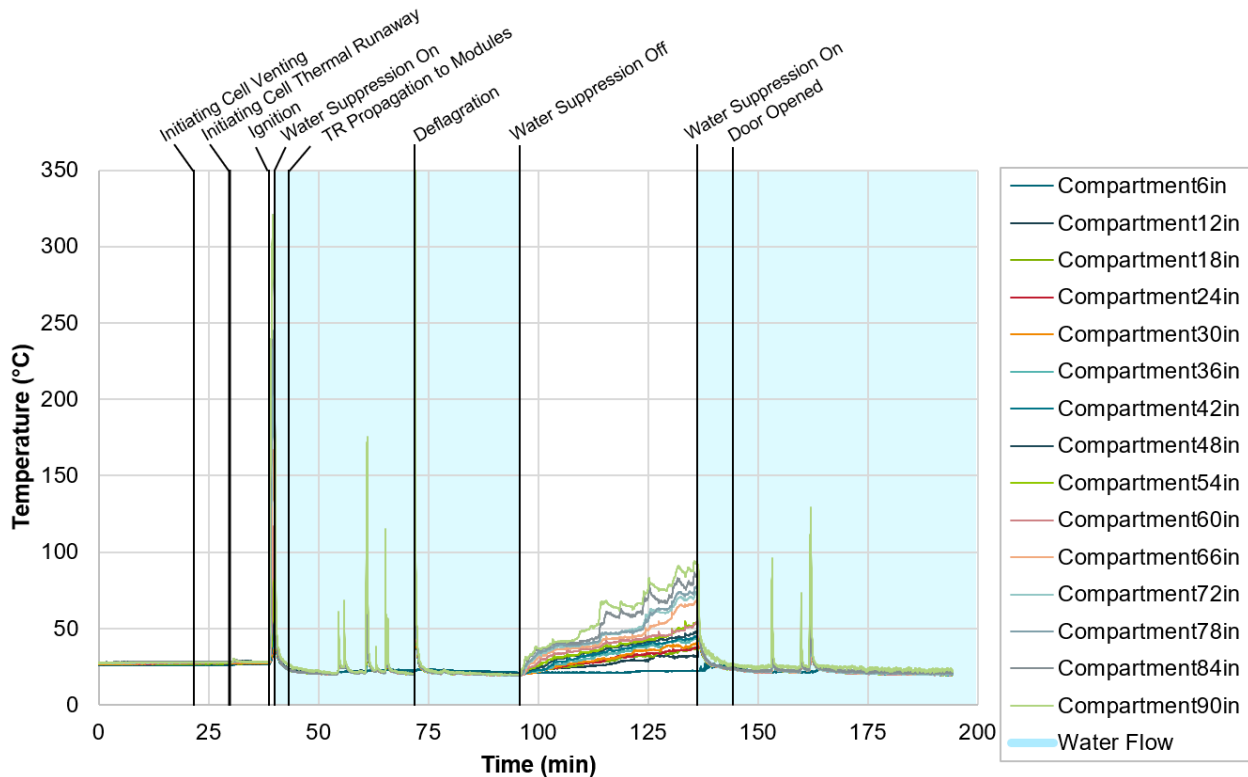


Figure 141 – Container gas temperatures measured during Test 3.

## Gas Concentrations

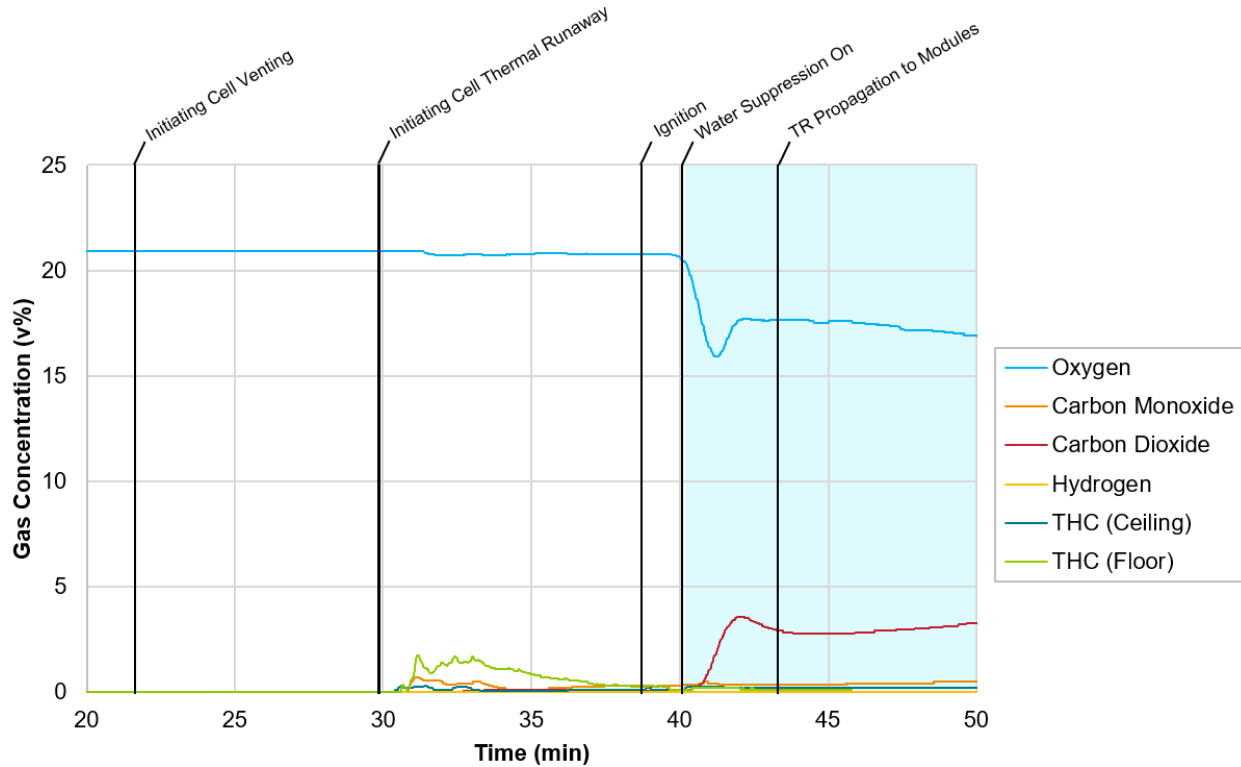
There was no indication of cell venting with the gas measurements installed in the container. Hydrocarbons were first measured 25 seconds after thermal runaway of the Initiating Cell. Carbon monoxide was first measured 51 seconds after thermal runaway, as plotted in Figure 142.

Oxygen concentration began to decrease after ignition and was coupled with an increase in carbon dioxide concentration. After the water suppression system was activated, flaming slowly subsided. The decrease in oxygen concentration when the water suppression system activated was likely due to dilution of the sampled atmosphere with water vapor and the formation of CO<sub>2</sub>. Oxygen concentration reached 16 v% and carbon dioxide concentration reached 4 v%. When flaming subsided at 40 minutes of test time, oxygen concentration returned to 18 v%. Other gas components were measured less than 1 v% during this period.





## UL 9540A INSTALLATION LEVEL TESTS WITH OUTDOOR LITHIUM-ION ENERGY STORAGE SYSTEM MOCKUPS



**Figure 142 – Gases measured in the container from Initiating Cell venting through thermal runaway propagation to additional modules in Test 3.**

Thermal runaway partially propagated within Modules 4 and 5 in the Initiating Unit starting at 43 minutes. A gradual increase in the concentration of carbon dioxide, carbon monoxide, and hydrocarbons was observed alongside a gradual decrease in oxygen concentration, as illustrated in Figure 143. Hydrocarbon concentration remained less than 0.5 v%. The measurement of THC at the floor level was discontinued after 45 minutes when the sample probe was submerged under water. A faster increase in battery gas components started at 54 minutes, which may have been due to additional thermal runaway off-gassing or flaming combustion of off-gases. However, flaming typically consumes battery gases and oxygen and yields only CO and CO<sub>2</sub>, and hydrogen and hydrocarbons both increased at 54 minutes. Figure 144 shows a snapshot from the thermal imaging camera video at 54 minutes.

# UL 9540A INSTALLATION LEVEL TESTS WITH OUTDOOR LITHIUM-ION ENERGY STORAGE SYSTEM MOCKUPS

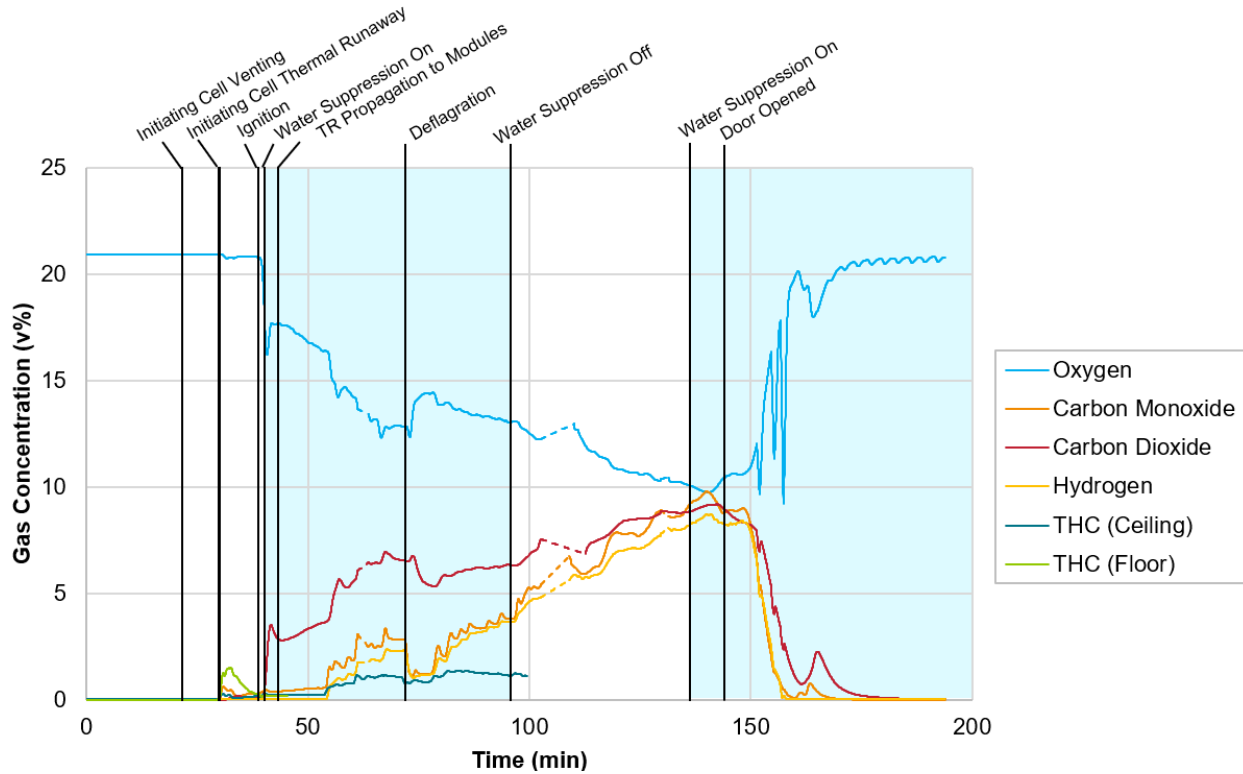


Figure 143 – Gas conditions measured in the container for the duration of Test 3.<sup>14</sup>



Figure 144 – Snapshot of thermal imaging camera facing the Initiating Unit suggesting additional off-gassing or flaming (test time 00:54:06).

<sup>14</sup> Dashed portions are linearly interpolated for periods of equipment maintenance or adjustment between measurement ranges. Gases are presented with 30 second averaging.

## UL 9540A INSTALLATION LEVEL TESTS WITH OUTDOOR LITHIUM-ION ENERGY STORAGE SYSTEM MOCKUPS

Immediately prior to deflagration at one hour and 12 minutes, oxygen, carbon dioxide, carbon monoxide, and hydrogen concentrations measured 13 v%, 7 v%, 3 v%, and 2 v%, respectively. It should be noted that 13 v% O<sub>2</sub> is marginally above the limiting oxygen concentration for methane. Following the deflagration, concentrations of carbon dioxide, carbon monoxide, and hydrogen reduced by 1–2 v%. Oxygen concentration increased 2 v%. The change in gas composition is attributed to combustion of flammable gases and ventilation of the container through the open deflagration vent.

After the deflagration, carbon monoxide, carbon dioxide, and hydrogen concentrations increased, while oxygen decreased. When the water flow was discontinued, carbon monoxide and hydrogen were measured at 4 v%; carbon dioxide concentration was 6 v%; and oxygen concentration was 13 v%. In the period while there was no water flow, three modules experienced thermal runaway. When waterflow was resumed, carbon monoxide and carbon dioxide measured 8 v%; hydrogen concentration measured 7 v%; and oxygen measured 10 v%. The operation of the water suppression system did not appear to impact gas concentrations. At these concentrations, the environment was composed of 30–50 v% battery gas and approximately 50 v% ambient air. The UFL of the battery gas is 40 v%, as determined by ASTM E681 during UL 9540A cell level testing. The container gas environment may have exceeded the UFL for the battery gas mixture.

When the water suppression system was reactivated, gas concentrations were unaffected for five minutes. After 5 minutes, the container door was opened to ventilate the container. Concentrations of carbon monoxide, carbon dioxide, and hydrogen decreased toward zero, and oxygen concentration returned to ambient over 20 minutes. No flaming of the potentially flammable gas mixture occurred.

### Post-Test

Less thermal damage was observed in Test 3 than Test 1 or Test 2. Most thermal damage was observed within proximity to the Initiating Unit. Figure 145 shows the gas detector housings were not melted as they had been in Test 1 or Test 2. Water damage was observed throughout the container, including flooding of the container volume up to approximately 12 in off of the floor, as pictured in Figure 146. All surfaces experienced heavy soot deposition.



**UL 9540A INSTALLATION LEVEL TESTS WITH OUTDOOR LITHIUM-ION ENERGY STORAGE SYSTEM MOCKUPS**



**Figure 145 – Condition of side wall next to the Initiating Unit after Test 3.**



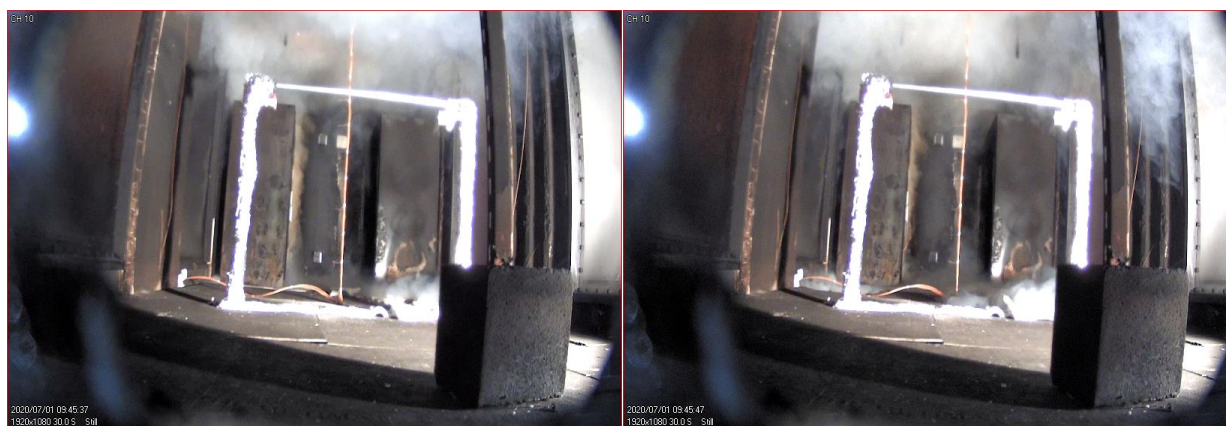
**Figure 146 – Photograph of Target Units and container after Test 3.**

# UL 9540A INSTALLATION LEVEL TESTS WITH OUTDOOR LITHIUM-ION ENERGY STORAGE SYSTEM MOCKUPS

## 4.3.5 Smoke and Gas Detector Activation

### Smoke Detectors

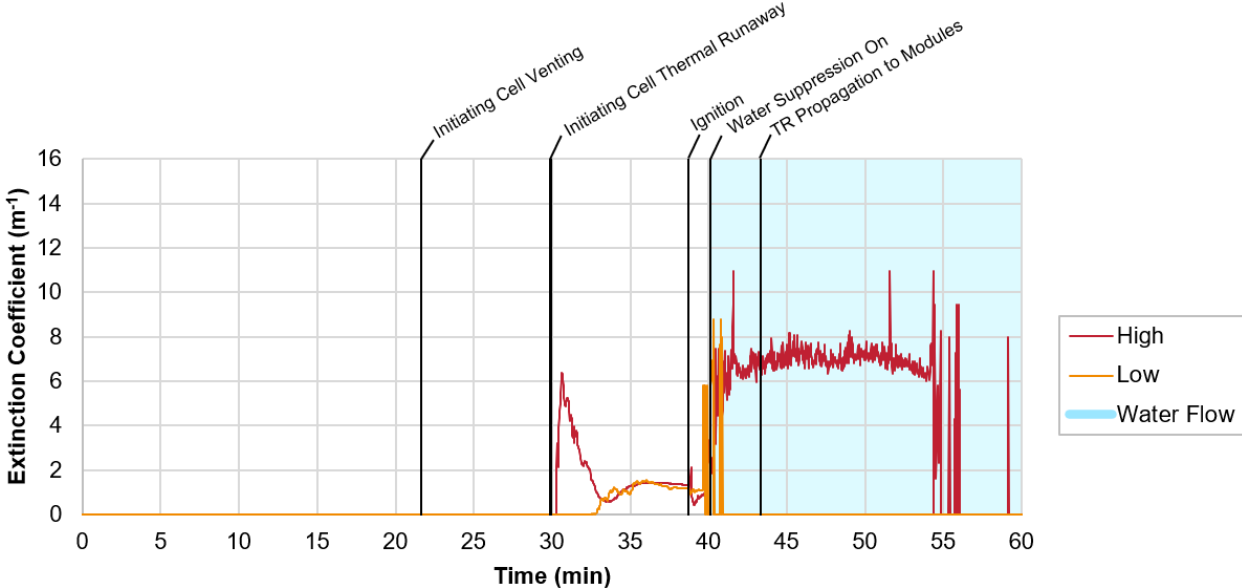
The smoke detector nearest to the Initiating Unit alarmed 50 seconds after the first thermal runaway. The smoke detector located further from the Initiating Unit alarmed 10 seconds later. Figure 147 shows the thickness of the smoke at the time of smoke detector activation.



**Figure 147 – View from floor up toward smoke layer when the near (left) and far (right) smoke detectors alarmed in Test 3.**

After thermal runaway, smoke obscuration rapidly increased at the ceiling level, as measured by the smoke meter near the ceiling (Figure 148). The smoke plume from the Initiating Module dispersed in the 10 minutes that followed, which was represented by a decreasing extinction coefficient at the high smoke meter location and an increasing extinction coefficient at the low smoke meter location. Ignition and further thermal runaway of the Initiating Module slightly reduced smoke obscuration before water suppression system operation heavily occluded visibility in the container. Waterflow shorted the electrical connections at the low smoke meter location. As long as waterflow was in operation, visibility was limited, as indicated by the high smoke meter location.

# UL 9540A INSTALLATION LEVEL TESTS WITH OUTDOOR LITHIUM-ION ENERGY STORAGE SYSTEM MOCKUPS



**Figure 148 – Extinction coefficient measurements made by smoke obscuration meter for Test 3 from the beginning of the test through thermal runaway propagation into additional modules.**

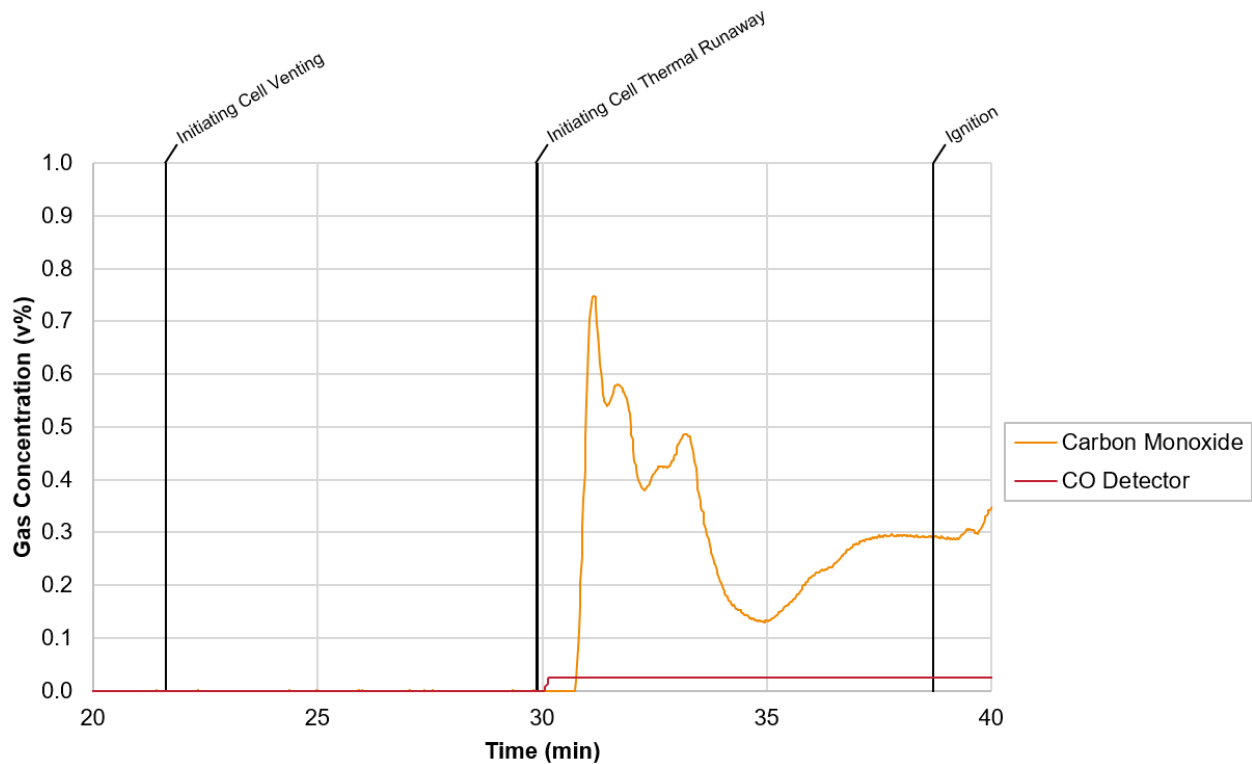




# UL 9540A INSTALLATION LEVEL TESTS WITH OUTDOOR LITHIUM-ION ENERGY STORAGE SYSTEM MOCKUPS

## Carbon Monoxide Detector

The carbon monoxide detector alarmed 10 seconds after the initial thermal runaway and was saturated at 250 ppm (20% IDLH [34]) six seconds later, as illustrated by Figure 149. The detector remained saturated above this level for the duration of the test. The short response time was aided by proximity to the Initiating Unit.



**Figure 149 – Commercial carbon monoxide detector response compared with carbon monoxide concentrations measured in Test 3.<sup>15</sup>**

<sup>15</sup> Carbon monoxide concentration measurements are plotted without 30 second averaging.



## UL 9540A INSTALLATION LEVEL TESTS WITH OUTDOOR LITHIUM-ION ENERGY STORAGE SYSTEM MOCKUPS

### Combustible Gas Detectors

All three combustible gas detectors responded within 30 seconds of the first thermal runaway event, as summarized in Table 18 and shown in Figure 150. Initial responses occurred in order of proximity to the Initiating Module. This response pattern was consistent with Test 1 and Test 2.

**Table 18 – Combustible gas detector response summary for Test 3.**

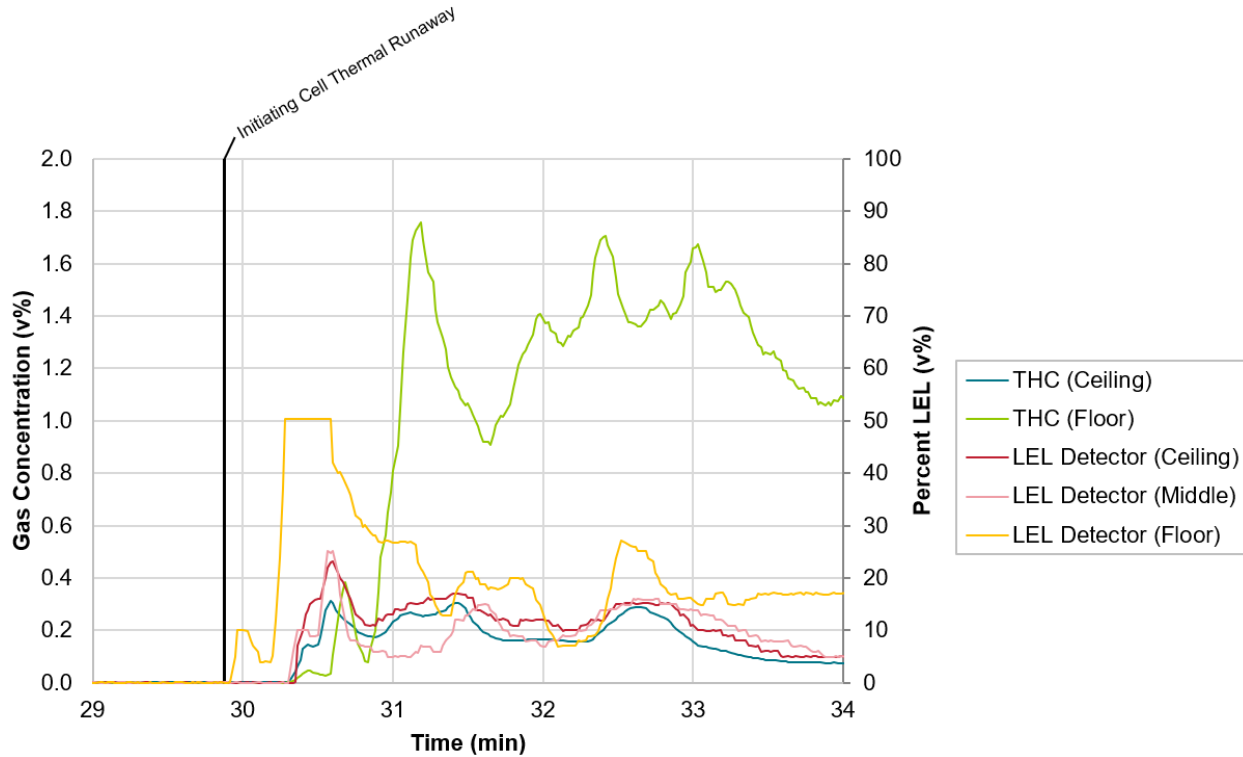
Location	Time of First Response	Time of 25% LEL	
		Limited Duration	Sustained Duration
Ceiling	TR + 29 s	--	TR + 24 min 34 s
Middle	TR + 27 s	--	TR + 24 min 34 s
Floor	TR + 4 s	TR + 23 s; TR + 2 min 38 s	TR + 25 min 11 s

The scales of the primary and secondary axes of Figure 150 and Figure 151 have been adjusted to compare the general responses of the two different types of instrument because direct comparison of FID total hydrocarbon measurements with combustible gas detector measurements were not possible. The FID was calibrated with propane, the combustible gas detectors were calibrated with methane, and the gas mixture they both measured was comprised of many hydrocarbon elements.

FID-based total hydrocarbon (THC) measurements were plotted from 0 to 2% based on 0 to 100% LEL of the calibration gas (propane). Catalytic bead-based combustible gas detector measurements were plotted from 0 to 100% LEL. Though the comparison was approximate, the combustible gas detector outputs were proportional to the FID measurements at the floor and ceiling.



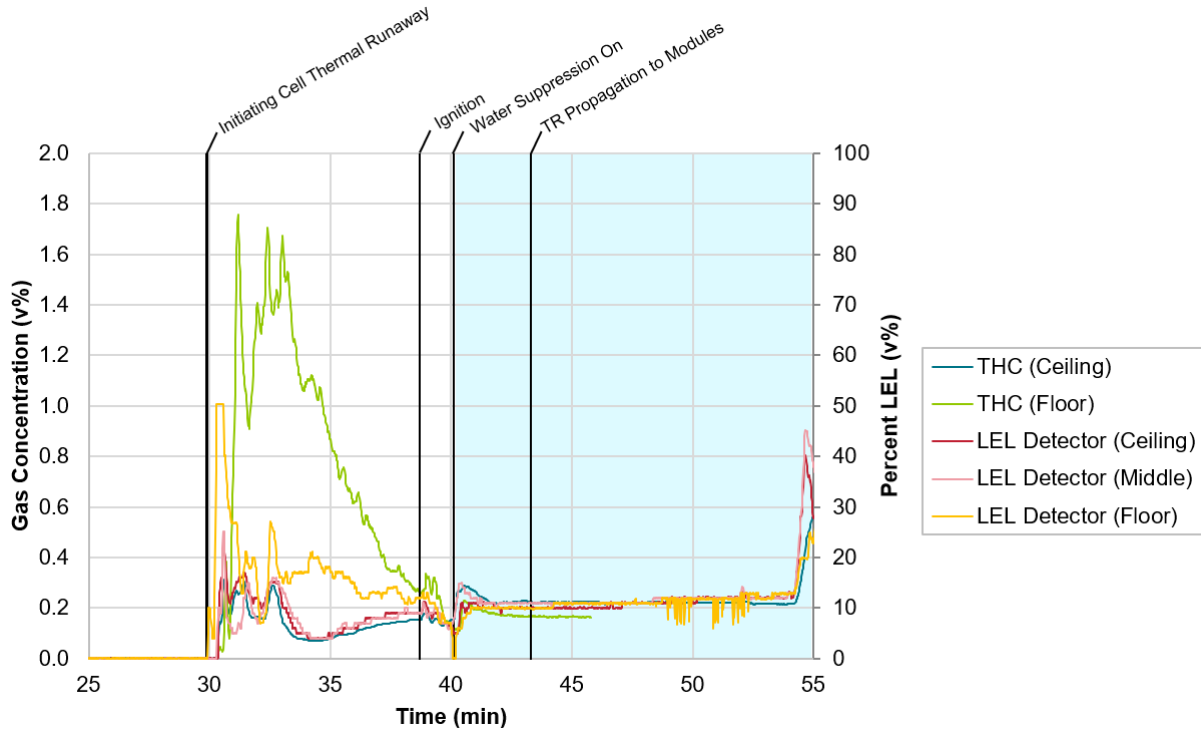
# UL 9540A INSTALLATION LEVEL TESTS WITH OUTDOOR LITHIUM-ION ENERGY STORAGE SYSTEM MOCKUPS



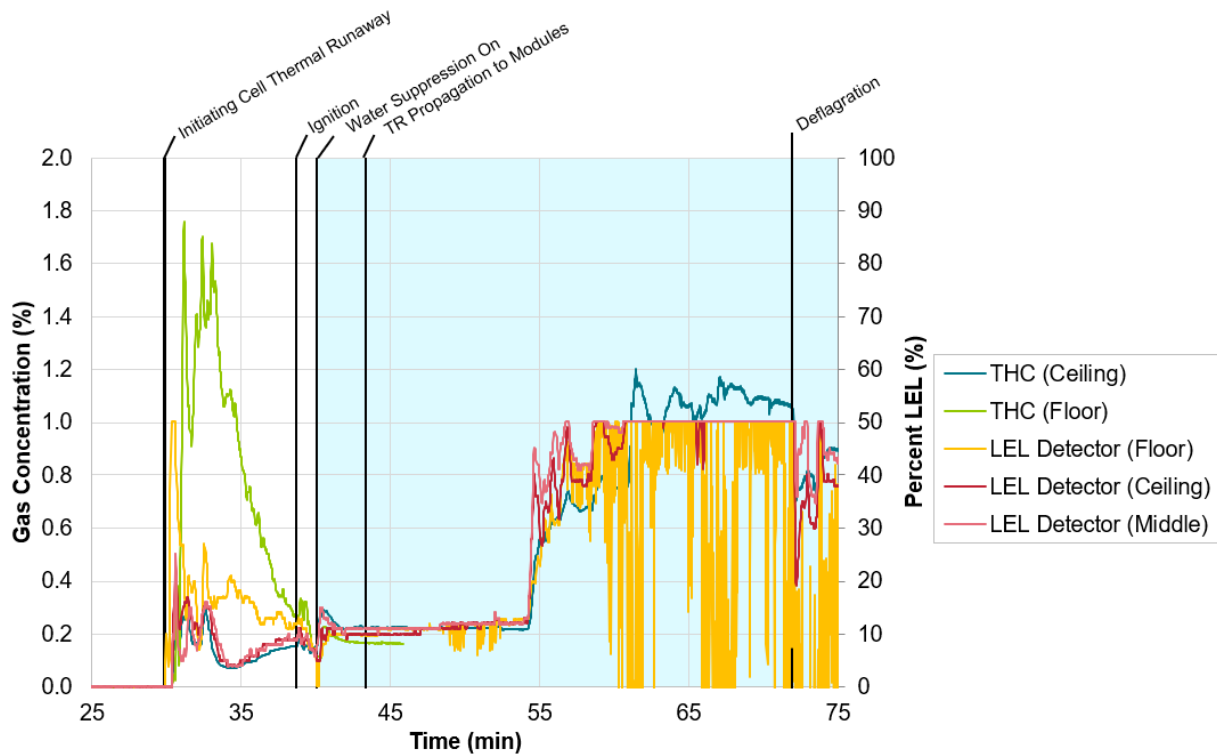
**Figure 150 – Total hydrocarbon concentration compared with commercial combustible gas detector response in Test 3 (test time 00:29:00 to 00:34:00).**

After ignition, combustion consumed most of the flammable gases, as documented in Figure 151. After suppression water was flowing, measurements on both the THC analyzers and combustible gas detectors were constant, as described by Figure 151. The measurement of THC at the floor level was discontinued after 45 minutes when the probe was submerged under water, but at 54 minutes, an increase in hydrocarbon concentration was measured by FID at the ceiling. The increase in hydrocarbons was also measured by all three combustible gas detectors. This event aligned with additional thermal runaway observed at the Initiating Unit, as documented by the thermal imaging camera in Figure 144.

# UL 9540A INSTALLATION LEVEL TESTS WITH OUTDOOR LITHIUM-ION ENERGY STORAGE SYSTEM MOCKUPS



**Figure 151 – Total hydrocarbon concentration compared with commercial combustible gas detector response in Test 3 (test time 00:25:00 to 00:55:00).**



**Figure 152 – Total hydrocarbon concentration compared with commercial combustible gas detector response in Test 3 (test time 00:25:00 to 00:75:00).**



# UL 9540A INSTALLATION LEVEL TESTS WITH OUTDOOR LITHIUM-ION ENERGY STORAGE SYSTEM MOCKUPS

## Hydrogen Detector

The commercial hydrogen detector not used in Test 3.

### 4.3.6 Fire Suppression System Operation

The 165 °F standard response sprinkler link located in the center of the container activated 10 minutes and 13 seconds after the initial thermal runaway event, before thermal runaway propagated to any additional modules. Waterflow reached the ESS container 39 seconds after the operation of the sprinkler link. Water flowed from four nozzles above the ESS units at a rate of 32 gpm, corresponding to 0.5 gpm/ft<sup>2</sup> for the protected area. Total flow volumes during both periods of suppression system operation are summarized in Table 19.

**Table 19 – Summary of water flow volumes for Test 3.**

Period	Duration (MM:SS)	Total Flow (gal)
1	55:42	1782
2	58:04	1858

While the suppression system was active, the coverage of the nozzle spray pattern caused water to impinge on the instrumented walls and the tops of the unit enclosures. Less water impinged on the faces of the units because of the angle of the nozzle spray pattern.

Water that impinged on the container walls was effective in limiting the thermal exposure to a performance acceptable by UL 9540A performance metrics. Water that impinged on the tops of the unit enclosures had little impact on the temperatures inside the enclosures, but water that cascaded down the sides of the units from the top was likely effective in reducing thermal exposure to the target units. Thermal runaway was observed in the Left Target Unit only while waterflow was discontinued. The Front Target Unit remained below the Target Unit performance criteria for the duration of the test. Water impinging across the faces of the Initiating Unit was effective in limiting flaming. Waterflow did not significantly impact gas concentrations or prevent deflagration.

### 4.3.7 Fire Service Size-up Equipment

#### Thermal Imaging

The surface temperatures and exterior thermal imaging views of the container were not impacted by cell venting and remained ambient prior to thermal runaway. After the onset of thermal runaway, surface temperatures in the container began to increase, as shown in Figure 153. Surface temperatures increased in the period between the gas ignition (38:42) and the suppression system activation (39:27). This surface temperature increase was accompanied by a visible change in the thermal signature of uninsulated portions of the container wall, as seen in the exterior thermal imaging views in Figure 154.

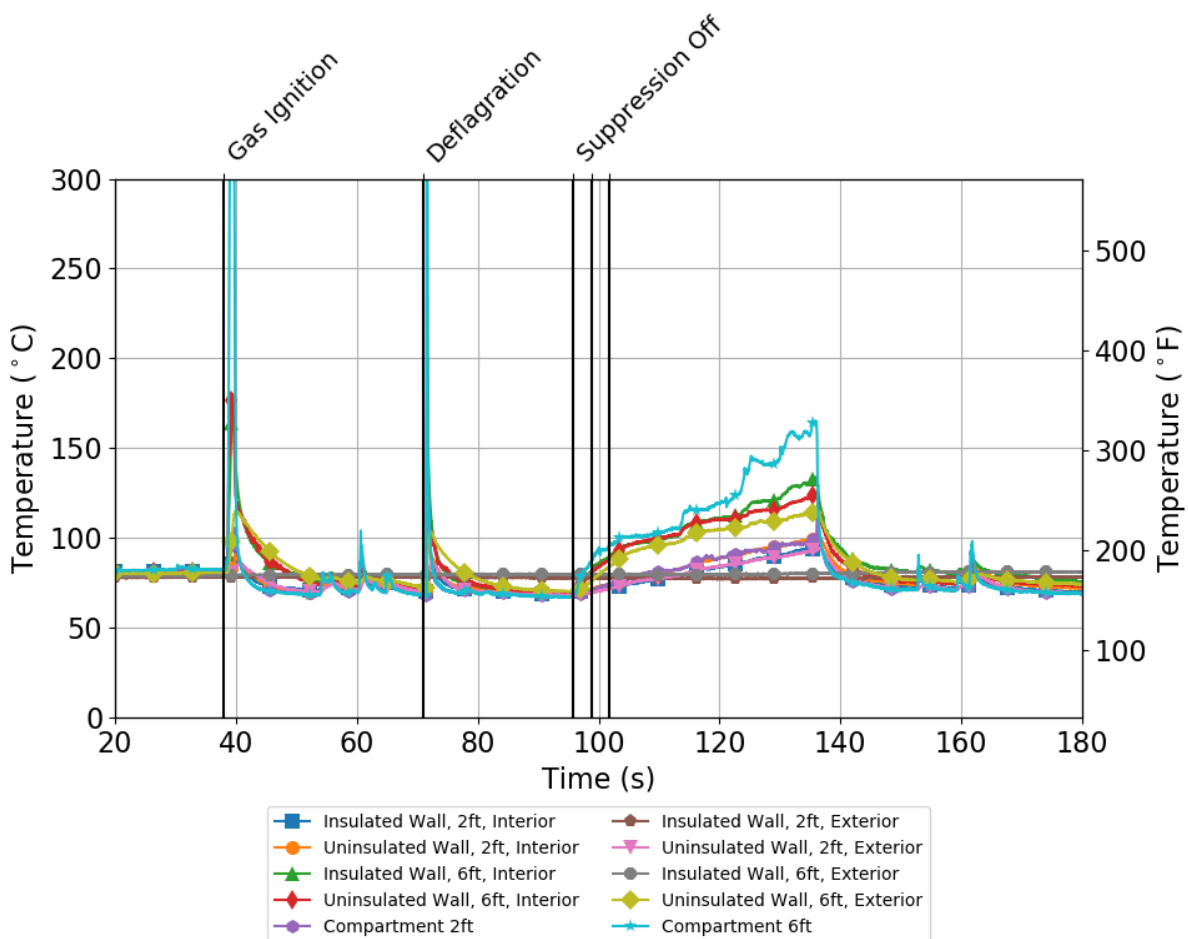

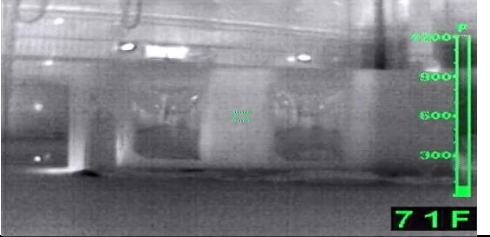

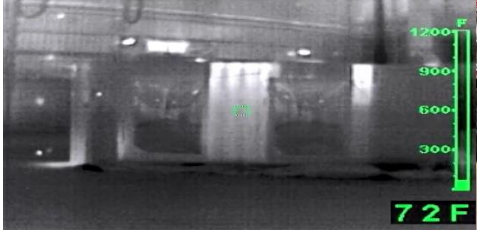


Figure 153 – Wall surface temperatures during Test 3. Vertical lines denote events corresponding to the images in Figure 154, Figure 155, and Figure 156.



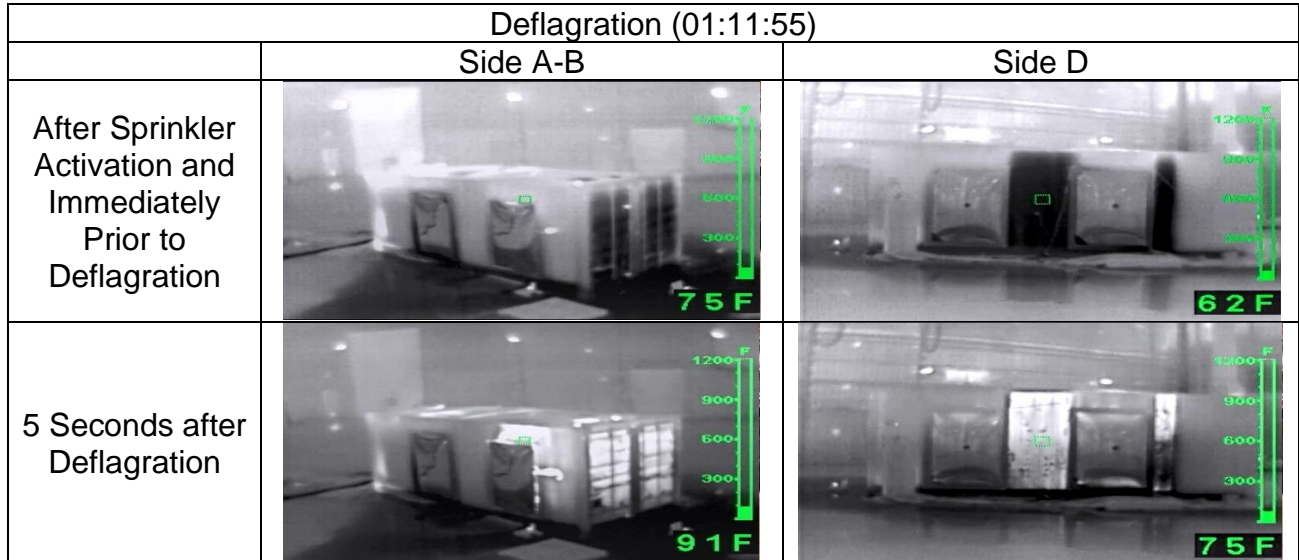
**UL 9540A INSTALLATION LEVEL TESTS WITH OUTDOOR LITHIUM-ION ENERGY STORAGE SYSTEM MOCKUPS**

Gas Ignition (38:00)		
	Side A-B	Side D
Immediately Prior to Flaming		
10 Seconds after Flaming		

**Figure 154 – Changes in thermal imaging view immediately before and 10 seconds after the initial flaming in Test 3. Left column shows A-B corner of the container (insulated wall construction) and right column shows D-side of container (bare metal construction).**

Following sprinkler activation, the elevated exterior surface temperatures on the uninsulated wall decreased towards ambient over the course of 10 minutes. This period of elevated exterior surface temperatures was mirrored by the thermal signature recorded in the exterior thermal imaging cameras. Uninsulated areas of the upper portion of the container exhibited elevated thermal signatures for several minutes after sprinkler activation. Lower portions of the container received more water flux, and cooling was visible earlier for these sections than the upper wall sections. Cooling of the lower wall sections can be seen in the top row of images in Figure 155. Although insulated areas of the container did not exhibit any substantial change as a result of water flow, a hot spot was visible in the area of the Initiating Unit, as pictured in both A-B side images of Figure 155.

## UL 9540A INSTALLATION LEVEL TESTS WITH OUTDOOR LITHIUM-ION ENERGY STORAGE SYSTEM MOCKUPS

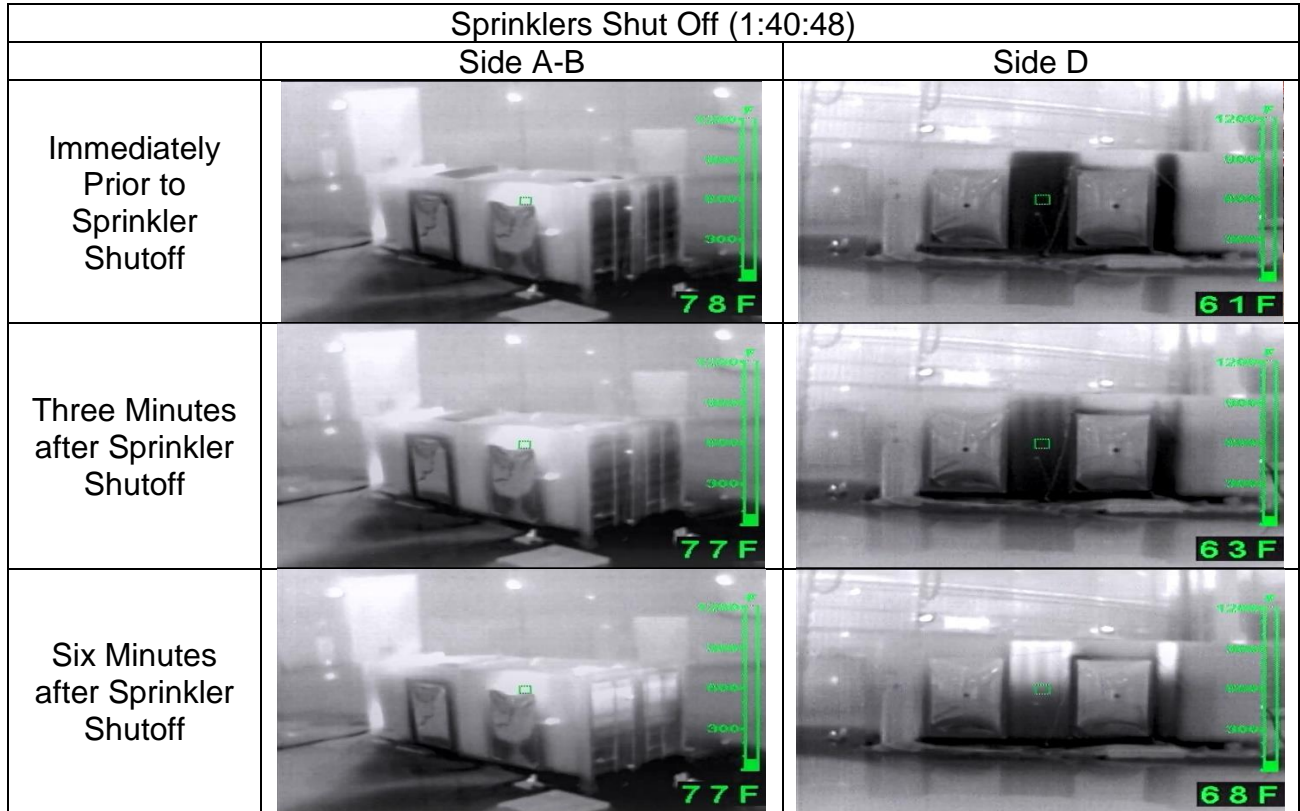


**Figure 155 – Changes in thermal imaging view immediately before and five seconds after the deflagration and second temperature peak of Test 3. Left column shows A-B corner of the container (insulated wall construction) and right column shows D-side of container (bare metal construction).**

A second distinct period of surface temperature increase was observed 1:11:55 after the start of the test, simultaneous with a deflagration event. Prior to the flaming event, the exterior thermal imaging views of uninsulated surfaces indicated cooling due to suppression, as shown in Figure 155. Within five seconds of the deflagration event, uninsulated surface temperatures increased and exterior thermal imaging cameras indicated elevated thermal signature. A thermal response on the insulated portions of the container was not discernable in thermal imaging views.

Interior container temperatures increased steadily after the suppression system was shut off 1:40:48 after test start, as illustrated above in Figure 153. Interior and uninsulated exterior temperatures reached peaks between 90 °C and 170 °C approximately 135 minutes after test start. The measured temperature increase was reflected in exterior thermal imaging views, as shown in Figure 156. Before waterflow was discontinued, the dark portions of the thermal imaging views of the A- and D-sides of the container indicated cooling. The middle and bottom rows of Figure 156 show the exterior of the container three and six minutes after the sprinklers were shut off, respectively. The images show the exterior thermal imaging cameras first began to indicate heating of the container on uninsulated areas within three minutes of the sprinkler system being shut down. Heating was more apparent within six minutes. The insulated surface of the container did not exhibit a substantial change during this period. Two hot spots were visible on the insulated wall section at this time: one adjacent to the Initiating Unit, and one at the A-B deflagration vent. The latter hot spot was a result of hot gases venting from the top-front corner of the deflagration vent after that panel had operated.

## UL 9540A INSTALLATION LEVEL TESTS WITH OUTDOOR LITHIUM-ION ENERGY STORAGE SYSTEM MOCKUPS

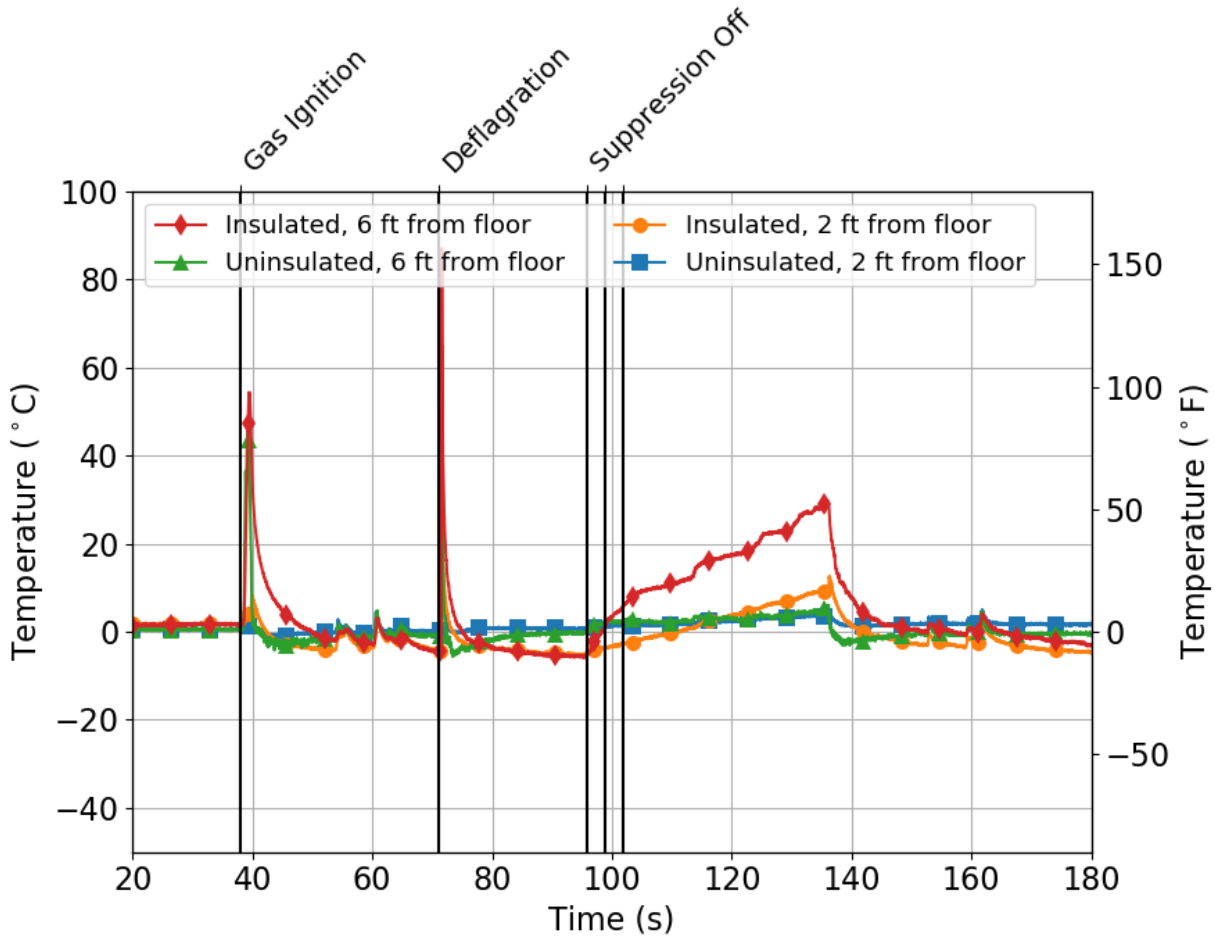


**Figure 156 – Changes in thermal imaging view immediately before, three minutes after, and six minutes after the sprinklers were shut off in the container in Test 3. Left column shows A-B corner of the container (insulated wall construction) and right column shows D-side of container (bare metal construction).**

As in the first two tests, uninsulated wall sections tended to closely track changes in the interior thermal environment, while insulated wall sections did not reflect changes in interior temperatures. This behavior can be visualized in Figure 157, which shows the temperature differential between the interior and exterior wall surfaces of the container over the course of the test. Uninsulated wall temperatures responded with a temperature differential less than 5 °C to both heating and cooling. Temperature differences greater than 5 °C were only observed on the insulated wall locations during the gas ignition and flaming events, which represented rapid, short duration heating events inside the container.

In contrast, temperature differentials on the insulated wall locations were of a greater magnitude and longer duration than on the uninsulated side. Additionally, the temperature difference between the interior and exterior surface of the insulated wall section steadily increased after the suppression system was deactivated.

UL 9540A INSTALLATION LEVEL TESTS WITH OUTDOOR LITHIUM-ION ENERGY STORAGE SYSTEM MOCKUPS













**Figure 157 – Temperature differential between inside and outside surface of container during Test 3.**

Exterior standard cameras indicated the development of a visible vapor cloud on the exterior of the container following the flaming ignition of battery gas observed 38 minutes into the test. The vapor cloud was formed by leakage through the clean agent vents at the roof and from around the door seams. Figure 158 documents the formation and development of the vapor cloud over the course of the test. The size of the vapor cloud increased as additional modules went into thermal runaway and decreased as vapors dissipated; this behavior was consistent with Test 1 and Test 2. The visual appearance of the vapors in Test 3 was lighter and more buoyant than in the previous two tests, as shown in Figure 63 and Figure 114. Although the peak size of the cloud is difficult to assess in enclosed laboratory conditions, the cloud appeared to increase during the period in which interior gas concentrations were increasing, starting with the deflagration at 1:11:55 and continuing through the time the suppression system was shut down.



**UL 9540A INSTALLATION LEVEL TESTS WITH OUTDOOR LITHIUM-ION ENERGY STORAGE SYSTEM MOCKUPS**

	A Side (Standard)	AB Side (TIC)
Gas Ignition (38:00)		
Deflagration (1:11:55)		
Container Doors Open (2:25:00)		
Container Doors Open +60 seconds (2:26:00)		
Container Doors Open +180 seconds (2:28:00)		

**Figure 158 – Vapor cloud formation and development in standard (left) and thermal imaging (right) camera views during Test 3.**

## UL 9540A INSTALLATION LEVEL TESTS WITH OUTDOOR LITHIUM-ION ENERGY STORAGE SYSTEM MOCKUPS

The bottom three rows of Figure 158 show the A-side camera view at the time the doors were opened 60 seconds after opening and 180 seconds after opening. The images show a vapor cloud spilled out of the container and spread out across the laboratory floor. This cloud appeared to be heavier than ambient air because the vapors were not buoyant. These vapors were cooled by water spray from the suppression system, which was operating when the doors were opened. Exterior thermal imaging views (shown in the right column of Figure 158) were able to discern hot vapors venting from the container, but they were not able to discern the exterior vapor cloud that extended from the container after the doors were opened.

### Portable Gas Meters

Interior Meter 1 was not used for O<sub>2</sub> and CO measurements in Test 3 due to sensor faults that occurred during Test 1. Additionally, a fault occurred in Interior Meter 2 meter 42 minutes after test start, resulting in a lack of usable data for the remainder of the test. Exterior Meter 4 was not utilized in Test 3 due to a pump malfunction prior to the start of the test.

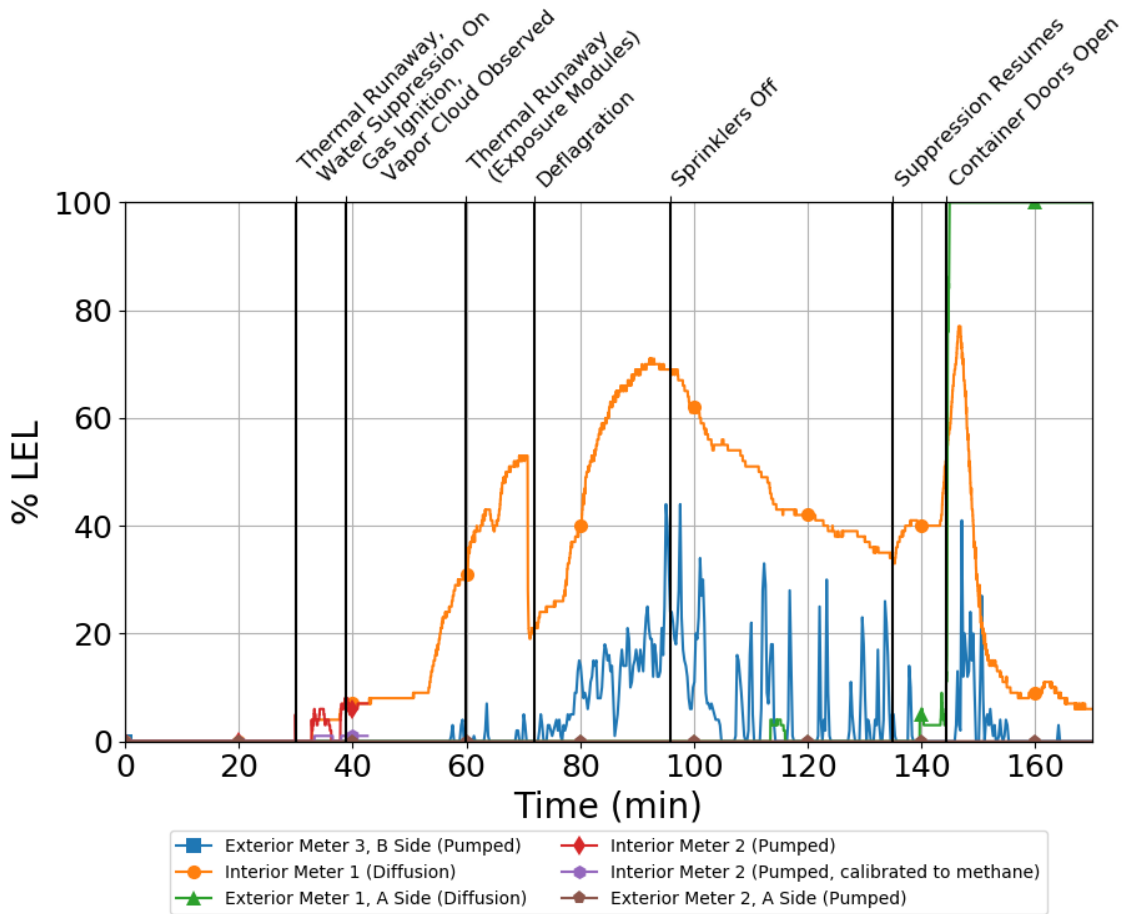
Figure 159 shows the flammable gas concentration measured by the meters inside and outside the container with respect to the LEL of their calibration gases. The two meters located within the container both indicated an increase in flammable gas concentrations after the smoke detectors activated and within two minutes of the initial thermal runaway event. This initial increase matched the trend in THC concentrations measured at the floor level.

Following an inflection point 53 minutes after test start, the flammable gas concentration measured by Interior Meter 1 began to increase at a faster rate and reached a peak value of 70% of the LEL of pentane at the time the deflagration was observed. A sharp drop in flammable gases was observed after the deflagration; flammable gases were consumed by the deflagration and also vented through the open deflagration vent. This was consistent with changes in gas concentration measured by gas measurement instrumentation.





# UL 9540A INSTALLATION LEVEL TESTS WITH OUTDOOR LITHIUM-ION ENERGY STORAGE SYSTEM MOCKUPS



**Figure 159 – Percentage of LEL measured by portable gas meters in Test 3.**

As thermal runaway continued to propagate after the deflagration, the flammable gas concentration measured in the container increased to an absolute peak of 71% of the LEL of pentane. This peak was observed with the shutoff of the suppression system. The flammable gas concentrations measured by Interior Meter 1 then decreased steadily to below 41% LEL at the time the container doors were opened. THC concentration measurements determined by FID were terminated prior to this point so direct hydrocarbon data comparison was not possible. The downward trend in flammable gas concentration measurements on the interior of the container did not mirror the increase in other gas concentrations (CO, CO<sub>2</sub>, H<sub>2</sub>) measured by gas measurement instrumentation in the period after suppression was shut down. A final peak was observed as the container doors were opened, in which the flammable gas concentration measurement momentarily increased to a value of 71% of the LEL of pentane. The final peak may have been caused by the mixing of air into the container, which could have increased oxygen available for the catalytic bead sensor to properly operate [35].

Elevated flammable gas concentration measurements outside the container were recorded by Exterior Meter 3, on the B-side. The flammable gas concentration measured



## UL 9540A INSTALLATION LEVEL TESTS WITH OUTDOOR LITHIUM-ION ENERGY STORAGE SYSTEM MOCKUPS

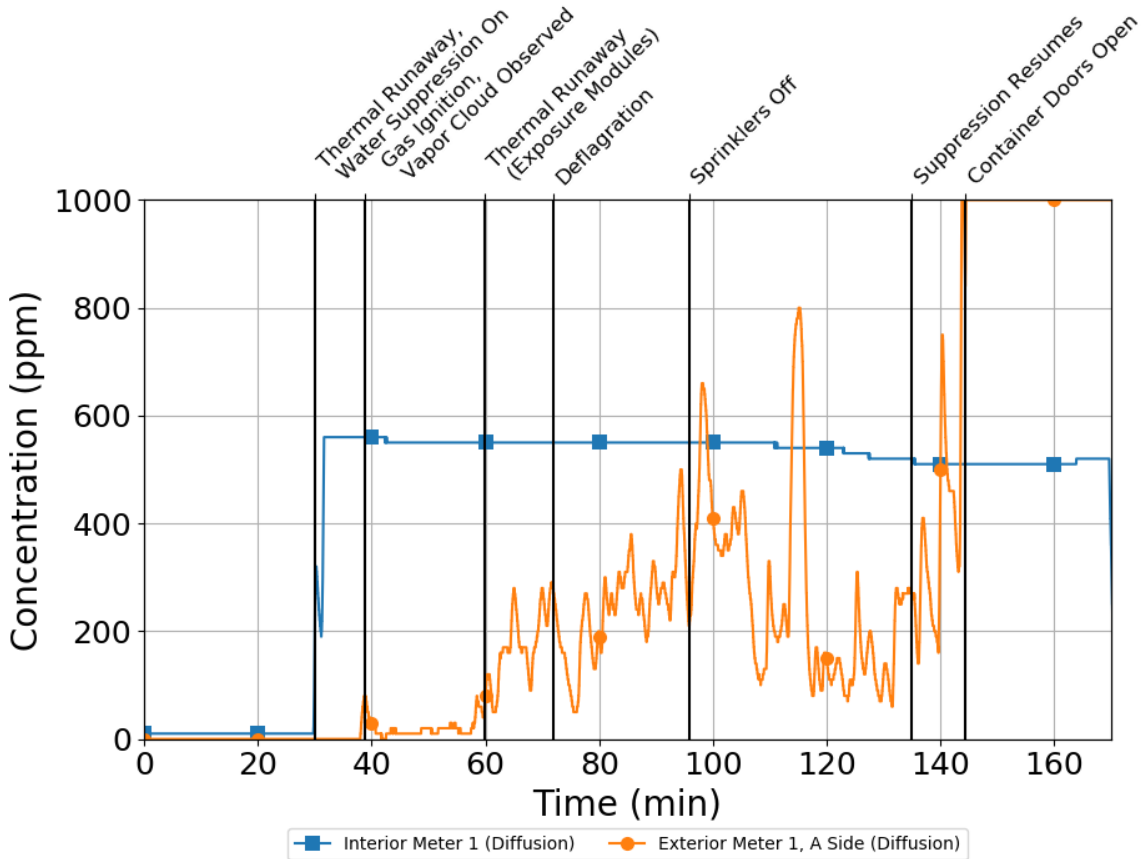
at this location first began to increase after the deflagration event, in parallel with the increase of CO and H<sub>2</sub> in the container. As observed in Test 2, The operation of the B-side deflagration vent created a leakage point for battery gases within the container to vent to the exterior and resulted in a sustained period of elevated flammable gas concentration measured by the B-side meter. Peaks as high as 40% of the LEL were recorded in the period after the sprinklers were shut down.

The peak flammable gas concentration measurements of the other exterior meters were considerably lower than Exterior Meter 3. Exterior Meter 1 registered a peak of 4% and Exterior Meter 2 recorded negligible values for the duration of the test. After the container doors were opened, the flammable gas concentrations measured by Exterior Meters 1 and 3 peaked in a similar manner to Interior Meter 1. While the peak measured by Exterior Meter 3 was only 40% of the LEL of pentane, the flammable gas concentration measured by Exterior Meter 1 exceeded 99% of the LEL of pentane, the upper measurement threshold.

Hydrogen gas was measured by the diffusion meters inside the container and on the A-side exterior. Figure 160 shows the H<sub>2</sub> measured by the interior diffusion meter first indicated an increase at the same time the flammable gas concentration at that location began to increase. The concentration rose to a value of approximately 560 ppm within one minute of the initial thermal runaway event and plateaued at that level for the duration of the test. This was not consistent with the hydrogen gas concentrations measured by the gas measurement instrumentation, which did not begin to increase until approximately 53 minutes after test start. It is possible that this inconsistency was a result of cross-sensitivity with other gases, a sensor error due to repeated thermal insult to Interior Meter 1, or a limitation of the 0.4 v% measurement threshold of the other hydrogen measurement equipment.



## UL 9540A INSTALLATION LEVEL TESTS WITH OUTDOOR LITHIUM-ION ENERGY STORAGE SYSTEM MOCKUPS



**Figure 160 – Hydrogen gas (H<sub>2</sub>) concentrations measured by portable gas meters in Test 3.**

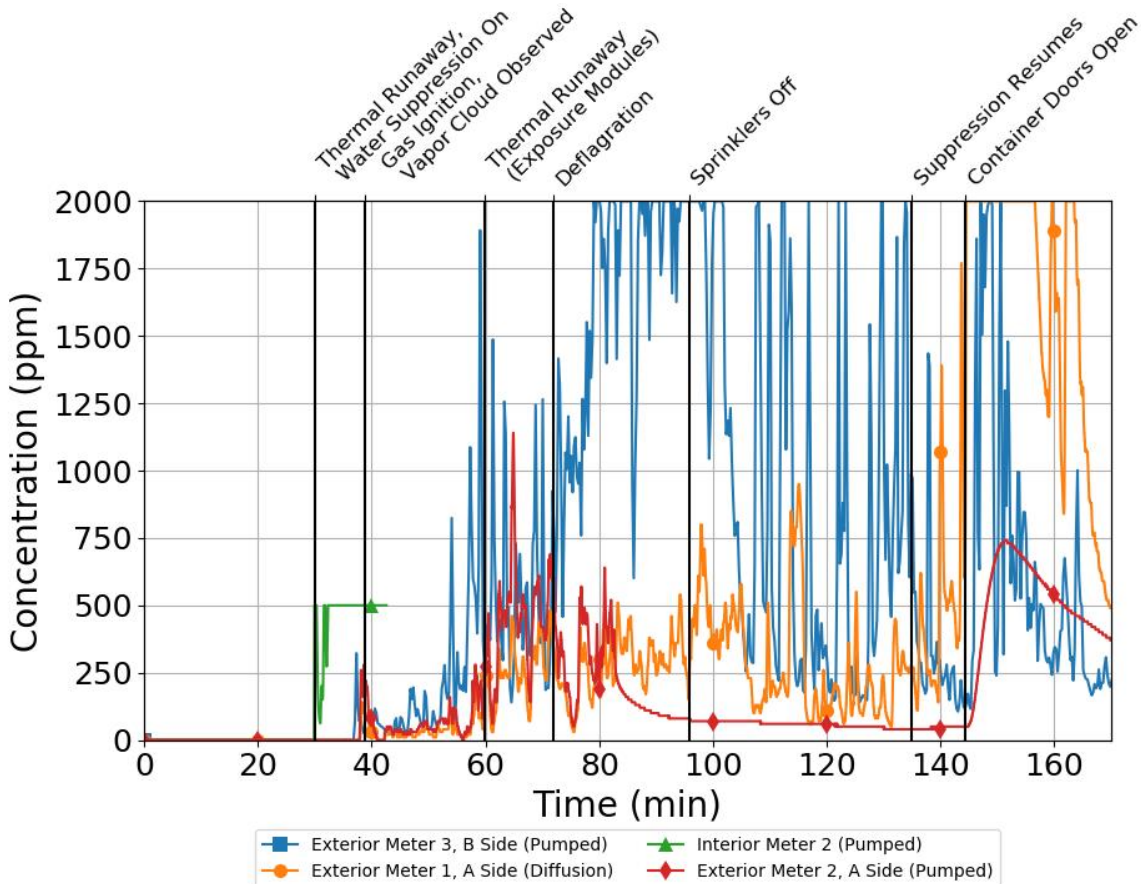
Exterior Meter 1 first indicated an increase in hydrogen measurements within 10 minutes of the initial thermal runaway event and continued to increase to a local peak before the deflagration event. After the deflagration, exterior hydrogen concentrations fluctuated with the size of the vapor cloud. The timing of the increase in exterior H<sub>2</sub> concentrations was consistent with both the formation of a visible vapor cloud and the time at which gas measurement instrumentation indicated H<sub>2</sub> and CO concentrations within the container began to increase.

After opening the door, the H<sub>2</sub> concentration measured by Exterior Meter 1 increased immediately to 1,000 ppm, the upper measurement threshold of the meter. This increase was consistent with the increase in flammable gas concentrations measured by this meter and Exterior Meter 3, on the B-side of the container.

Toxic gas concentrations within the container began to increase at the same time flammable gas concentrations began to increase. CO concentrations measured by Interior Meter 2 first increased within one minute of thermal runaway at the same time the smoke detectors activated, as shown in Figure 161. The increase in CO concentrations was consistent with the data recorded by the gas measurement instrumentation. Interior

## UL 9540A INSTALLATION LEVEL TESTS WITH OUTDOOR LITHIUM-ION ENERGY STORAGE SYSTEM MOCKUPS

Meter 1 and Interior Meter 2 did not collect CO data after 42 minutes due to a sensor error and pump error, respectively.



**Figure 161 – Carbon monoxide (CO) concentration measured by portable gas meters in Test 3.**

CO concentrations outside the container began to increase 37 minutes after test start with the formation of a visible vapor cloud. The CO concentrations at each of the exterior meter locations increased as additional modules began to undergo thermal runaway, approximately 50 minutes after test start. The magnitude of the measurements and the duration of this peak period varied among the three exterior meters. The highest CO concentrations were measured by Exterior Meter 3, located on the B-side of the container, which recorded peak CO concentrations at the upper threshold of the meter (2,000 ppm). The higher concentrations measured by this meter could be attributed to the operation of the adjacent deflagration panel, which created additional leakage area for battery gases to vent from the container. Steady CO concentrations of 1,750–2,000 ppm were measured by the B-side meter from approximately 80 minutes after test start until the suppression system was shut down. After waterflow was discontinued, CO concentrations at this location fluctuated between 100 ppm and peaks of 2,000 ppm, which aligned with fluctuations of the vapor cloud.



## UL 9540A INSTALLATION LEVEL TESTS WITH OUTDOOR LITHIUM-ION ENERGY STORAGE SYSTEM MOCKUPS

Exterior Meter 1 exhibited similar behavior to Exterior Meter 3. Exterior Meter 1 indicated CO concentrations between 250 and 500 ppm from 70 to 110 minutes after test start. This quasi-steady period was observed at the same time as gas measurement instrumentation reported increasing CO concentrations in the container. Exterior Meter 2 indicated peak CO concentrations of a similar magnitude, but the duration of the peak period from 70–90 minutes after test start was shorter than Exterior Meter 1.

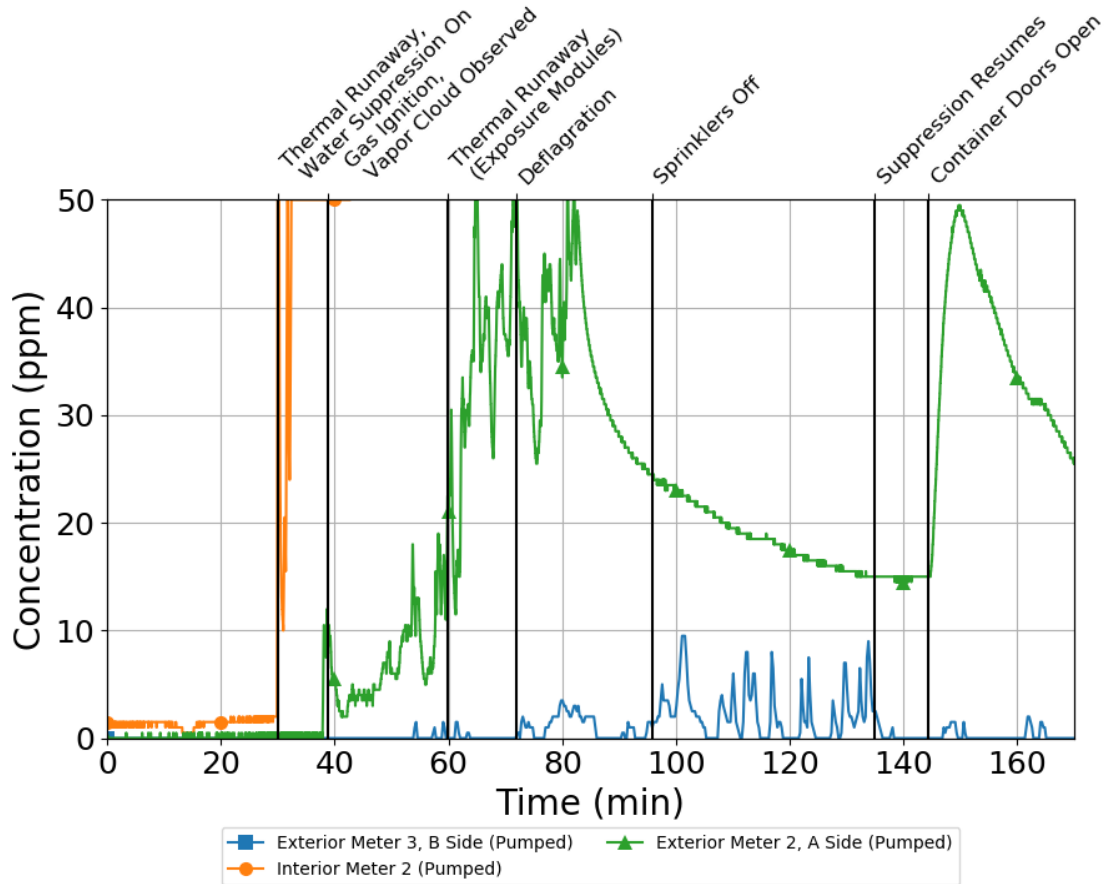
After the container door was opened (2:23:20 after test start), each of the three exterior meters measured a significant peak in CO concentration as vapors exhausted from the container. The magnitude of these peak concentrations exceeded 2,000 ppm at Exterior Meters 1 and 3. These peak values exceeded the threshold for IDLH conditions for CO (1,200 ppm). Exterior Meter 2 reported a maximum of 750 ppm after the doors were opened.

HCN concentrations inside and outside the container followed a similar trend to CO concentrations, as shown in Figure 162. HCN concentration measured by Interior Meter 2 began to increase and exceeded the upper threshold of the meter within one minute of the initial thermal runaway.

Two periods of elevated HCN measurements were recorded by Exterior Meter 2. The first period followed the deflagration, and the second occurred during test termination procedures after the doors had been opened. Exterior Meter 3 exhibited lower HCN values than Exterior Meter 2, with the highest values observed during the period without waterflow after the sprinklers were shut off.



## UL 9540A INSTALLATION LEVEL TESTS WITH OUTDOOR LITHIUM-ION ENERGY STORAGE SYSTEM MOCKUPS



**Figure 162 – Hydrogen cyanide (HCN) concentration measured by portable gas meters in Test 3.**

Other quantities measured by the meters included H<sub>2</sub>S, O<sub>2</sub>, and VOCs, shown in Figure 163, Figure 164, and Figure 165, respectively.

Figure 163 shows the H<sub>2</sub>S concentration measured by Interior Meter 2 began to increase within one minute of the initial thermal runaway event like the other gas concentrations measured at this location. Exterior Meter 2 (A-side) measured higher concentrations of H<sub>2</sub>S than Exterior Meter 3 (B-side). Overall, both meters registered elevated H<sub>2</sub>S concentrations in the period following the initial deflagration event. H<sub>2</sub>S concentrations measured in Test 3 remained below 20 ppm for all meters before the doors were opened. For less than five minutes following the opening of the container doors, H<sub>2</sub>S concentration measured by Exterior Meter 1 (A-side) exceeded 100 ppm, the upper threshold of the meter.



UL 9540A INSTALLATION LEVEL TESTS WITH OUTDOOR LITHIUM-ION ENERGY STORAGE SYSTEM MOCKUPS

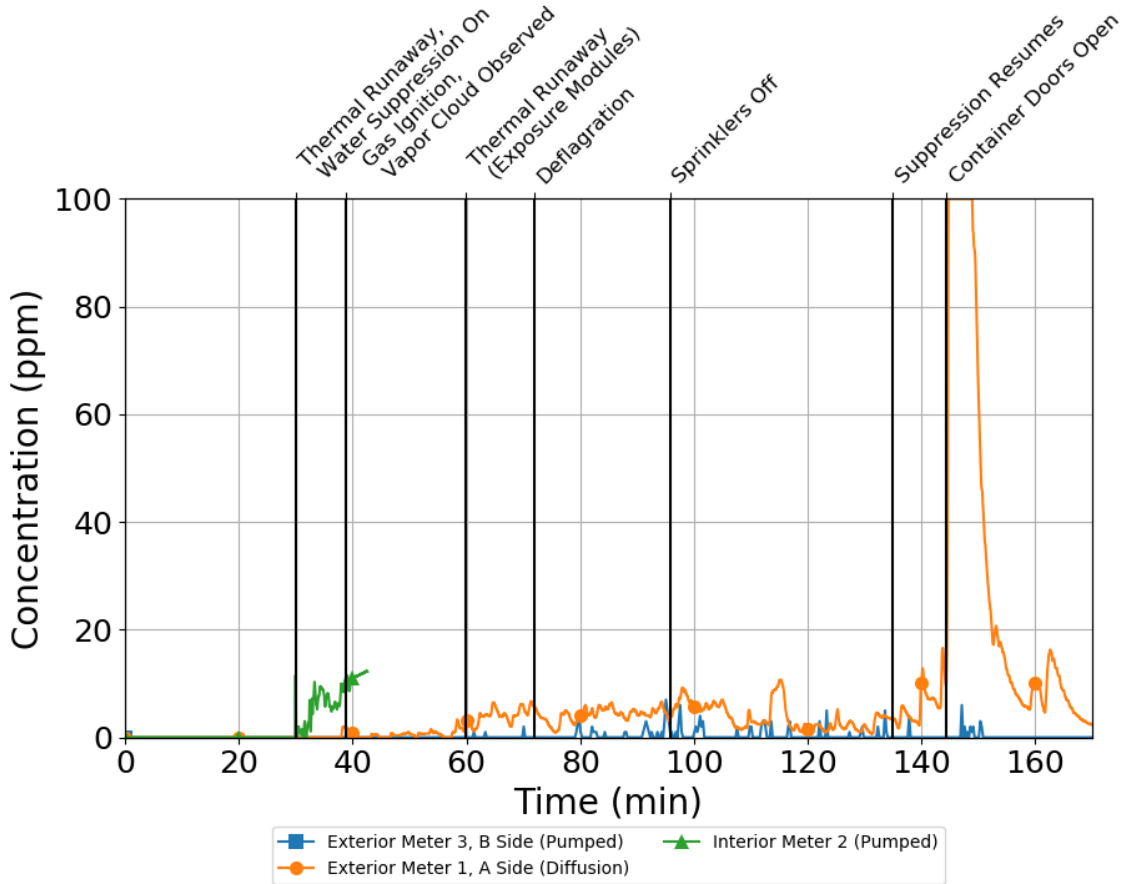


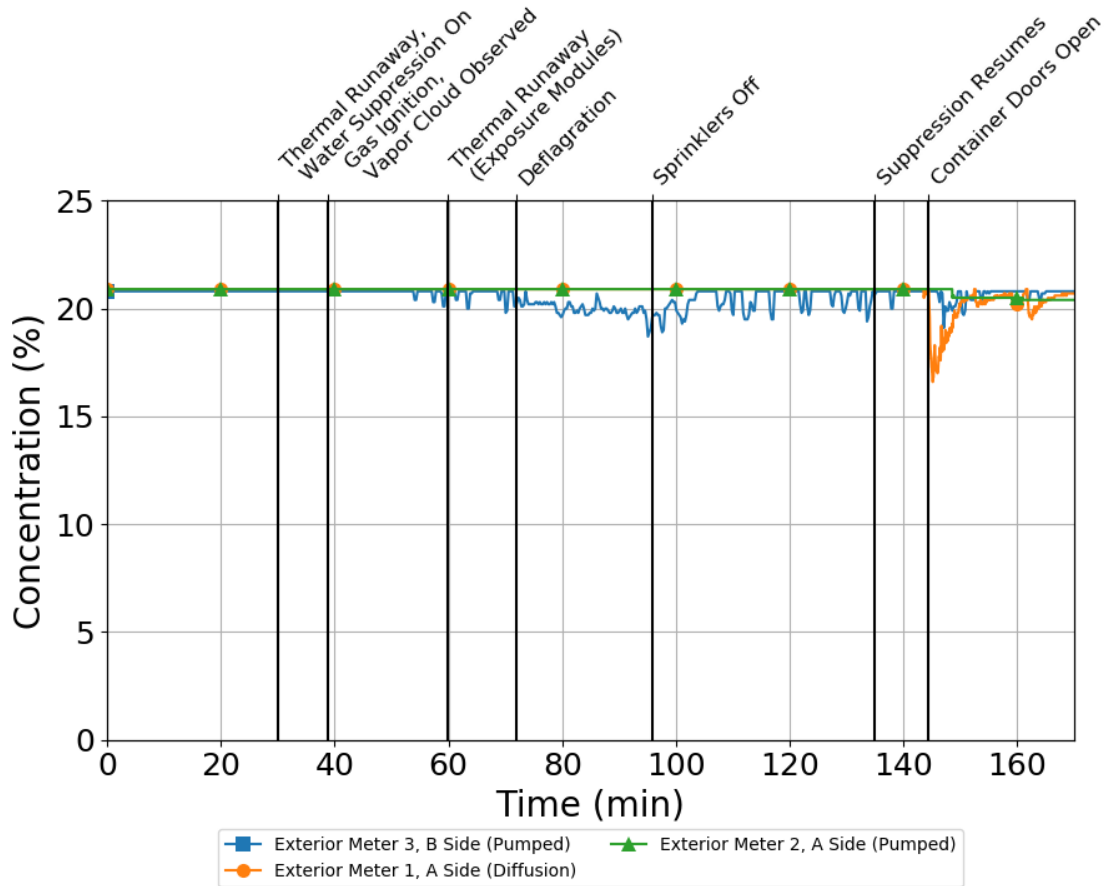
Figure 163 – Hydrogen sulfide (H<sub>2</sub>S) concentrations measured by portable gas meters in Test 3.

Figure 164 shows the oxygen concentrations measured by the exterior meters over the course of Test 3. The two A-side meters did not measure any decrease in oxygen concentration prior to the container doors opening at 2:24:26. After the doors were opened, both meters recorded a decrease in oxygen concentrations less than 5 v% as accumulated gases vented through the open doorway. This decrease is consistent with the increase in flammable gas concentrations, CO, and HCN measured at these locations.

The Exterior Meter 3 (B-side) measured decreases in oxygen concentration less than 1 v% starting after the initial deflagration event. The decreases observed at this meter were consistent with the increases in other gas concentrations measured by Exterior Meter 3 as a result of the nearby opened deflagration panel that allowed greater leakage at that location.



# UL 9540A INSTALLATION LEVEL TESTS WITH OUTDOOR LITHIUM-ION ENERGY STORAGE SYSTEM MOCKUPS



**Figure 164 – Oxygen (O<sub>2</sub>) concentrations measured by portable gas meters in Test 3.**

VOC concentration was only measured by the pumped meter on the A-side, as shown in Figure 165. The meter first measured an increase approximately 37 minutes after test start as thermal runaway propagated through the Initiating Module. A more rapid increase occurred after thermal runaway propagated to additional modules. VOC concentrations peaked in the period between thermal runaway propagation to additional modules and the failure of the sensor approximately 80 minutes after test start. The peak period aligned with visible vapor cloud formation outside the container.



# UL 9540A INSTALLATION LEVEL TESTS WITH OUTDOOR LITHIUM-ION ENERGY STORAGE SYSTEM MOCKUPS

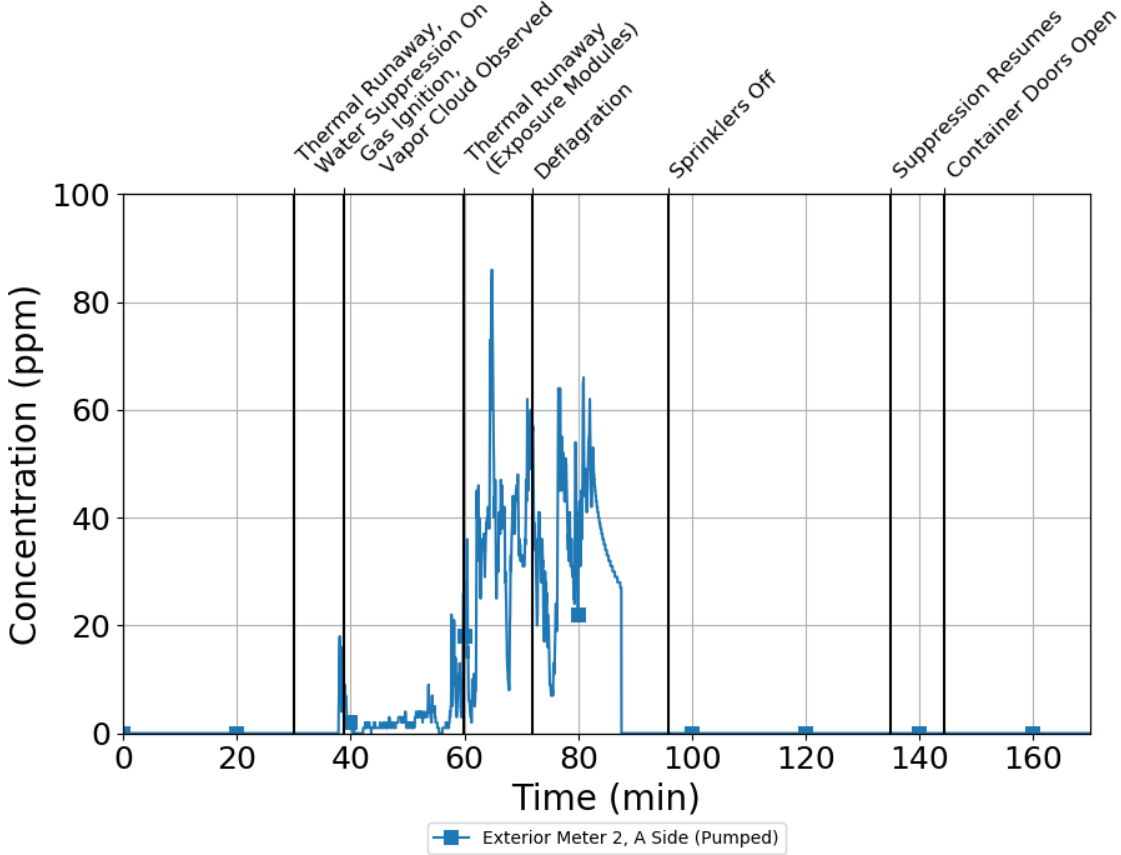


Figure 165 – Volatile organic compound (VOC) concentrations measured by portable gas meter on A-side of container in Test 3.



## 5 Discussion of Results

The test series results are discussed with a focus on fire protection to elicit the effectiveness of fire detection and mitigation methods and fire service size-up and tactical considerations.

### 5.1 Detection

All tests were instrumented with two smoke detectors, three catalytic bead combustible gas detectors, and one electrochemical carbon monoxide detector. Test 1 and Test 2 were instrumented with one electrochemical hydrogen detector.

In Test 1, the carbon monoxide, combustible gas, and hydrogen detectors responded within 27 seconds of the initial thermal runaway event. At this time, the combustible gas detector at the floor location was saturated at its full-scale output. This indicated a potentially combustible environment existed prior to the partial volume deflagration. The combustible gas detectors located at the mid-wall and ceiling heights did not indicate a potentially combustible environment, and the hydrogen detector measured less than 0.5 v% hydrogen prior to the partial volume deflagration. Both smoke detectors alarmed 47 seconds after the initial thermal runaway event, 16 seconds after the partial volume deflagration and after sustained flaming of battery gases and the plastic module enclosures.

In Test 2, the carbon monoxide and combustible gas detectors responded within 30 seconds of the initial thermal runaway event. The smoke detectors both alarmed 55 seconds after the initial thermal runaway event without ignition of the battery gases or plastic module materials. There was no measurement response from the combustible gas detectors when Novec 1230 was introduced, which suggests catalytic bead sensor technology is not cross-sensitive to Novec 1230. However, catalytic bead measurement integrity was likely compromised over time, because the sensor manufacturer identifies halogen compounds as sensor poisons [36].

Two events in Test 2 indicated the measurement integrity of the catalytic bead sensors was likely compromised. In the first event, ignition and low-velocity flame spread was observed in a transparent upper layer, above an opaque layer of gases and Novec 1230 vapor. The flaming event occurred 28 minutes after the Novec discharge. Prior to the flaming event, the catalytic bead sensors had been saturated above their measurement capacity at the mid-wall and ceiling heights. At the time of the flaming event, combustible gas measurements from both catalytic bead sensors indicated 10% of the LEL. In the second event, a deflagration occurred. Prior to the deflagration, combustible gas concentrations reported by the middle and ceiling level catalytic bead sensors were increasing, but still less than 50% of the LEL. This sensor behavior corroborated the hypothesis that the catalytic bead sensors had been poisoned (i.e., permanently damaged) by exposure to halocarbons. Halocarbons are poisons for catalytic bead sensors, as identified by the sensor manufacturer [36]. However, at the floor level, the catalytic bead sensor was saturated beyond its measurement capacity throughout both



## UL 9540A INSTALLATION LEVEL TESTS WITH OUTDOOR LITHIUM-ION ENERGY STORAGE SYSTEM MOCKUPS

the ignition of gases in the upper layer, and the deflagration that occurred later. It is unclear whether sustained exposure to halocarbons could cause the sensors to continue outputting an elevated apparent hydrocarbon measurement.

The hydrogen detector in Test 2 may have been compromised by Novec 1230 exposure or thermal stress. The hydrogen detector in Test 2 did not respond until after the deflagration, despite measurement of hydrogen as high as 3 v% by the palladium-nickel hydrogen sensor prior to the deflagration.

In Test 3, the carbon monoxide detector and combustible gas detectors all responded within 29 seconds of the initial thermal runaway event. Both smoke detectors alarmed within one minute of the initial thermal runaway event. All three combustible gas detectors reported a potentially flammable environment exceeding 50% LEL for 10 minutes prior to the deflagration.

### 5.2 Thermal Runaway Propagation

Cascading propagation of thermal runaway through the Initiating Unit demonstrated the potential risk of fire and deflagration hazards in an ESS installation. Neither the Novec 1230 system nor the water suppression system as used in the installation level tests prevented module-to-module propagation of thermal runaway in the Initiating Unit. Propagation to Target Units showed unit-to-unit thermal runaway propagation. These cascading events led to a subsequent increase in deflagration hazards.

Flaming across the front faces of the battery modules at the beginning of Test 1 contributed to the propagation of thermal runaway. However, thermal runaway propagated within the Initiating and Left Target modules independent of thermal contributions due to fire. Flaming ceased seven minutes after ignition because of low oxygen levels in the ISO container. Thermal runaway propagation was driven by heat transfer from modules generating thermal energy during thermal runaway to adjacent modules with intact cells. Thermal runaway propagated from the Initiating Module to a module above it 14 minutes after the Initiating Cell thermal runaway. Thermal runaway propagation continued upward through all modules in the Initiating Unit and Left Target Unit at a rate of two to 10 minutes between modules. Downward propagation occurred slower at a rate of one hour between modules. Five modules of the Front Target Unit, separated from the Initiating Unit by a 35 in aisle, exceeded the cell vent temperature during Test 1, though no modules of the Front Target Unit experienced thermal runaway.

The discharge of Novec 1230 in Test 2 cooled the container as the agent changed phase from liquid to vapor, but the phase change and ~8.5 v% Novec 1230 concentration did not remove sufficient heat from the cells to prevent propagation of thermal runaway. 3M states Novec 1230 total flooding applications are not intended to interrupt cascading thermal runaway processes [37]. Bench-scale experiments conducted by Said and Stoliarov have demonstrated that 8.5 v% Novec 1230 concentrations with crossflow conditions were effective in reducing the rate of propagation but did not completely stop propagation. In their experiments, 15.2 v% stopped propagation in 67% of tests. Therefore, an 8.5 v% Novec 1230 should not be anticipated to provide protection against



## UL 9540A INSTALLATION LEVEL TESTS WITH OUTDOOR LITHIUM-ION ENERGY STORAGE SYSTEM MOCKUPS

propagation of thermal runaway within ESS systems. Compared to Test 1, the initial thermal runaway propagation from the Initiating Module to modules above took an additional 32 minutes. Once thermal runaway propagation began, thermal runaway propagated upward through all modules in the Initiating Unit and Left Target Unit at one to 12 minutes between modules, which was similar to Test 1. Downward propagation of thermal runaway also occurred in both units.

Test 1 and Test 2 exhibited the same extent of thermal runaway propagation through all modules of the Initiating Unit and Left Target Unit. In both Test 1 and Test 2, some modules of the Front Target Unit exceeded the cell vent temperature prior to test termination, but the modules did not experience thermal runaway.

Water application in Test 3 moderated but did not eliminate thermal runaway propagation behavior. Water application was more effective in preventing thermal runaway propagation from the Initiating Unit to the Target Units than for providing control of thermal runaway within the Initiating Unit.

Target Unit temperatures resulting from exposure to thermal runaway in the Initiating Unit were lower in Test 3 than in Test 1. The cell vent temperature was not exceeded in the Target Units during the first period of waterflow in Test 3, which demonstrated the potential for water application to prevent cascading thermal runaway to adjacent ESS units. When waterflow was discontinued, temperatures in the Initiating Unit and Target Units increased. Two more modules of the Initiating Unit and one module of the Left Target Unit experienced thermal runaway before waterflow was restarted. During the second period of waterflow, one module of the Initiating Unit underwent thermal runaway. In total, seven out of nine modules of the Initiating Unit and one out of nine modules in the Left Target Unit experienced thermal runaway. The Front Target Unit remained beneath the cell vent temperature for the duration of Test 3.

In the Initiating Unit, propagation from the Initiating Module to the next module upwards occurred in 13 minutes, similar to Test 1. Three modules in the Initiating Unit experienced thermal runaway during the first period of waterflow. Water-based suppression did not significantly affect the rate temperatures decreased inside modules after thermal runaway as compared with Test 1. The ceiling-mounted nozzle array was not effective in delivering water into the tightly packed, sealed modules enclosures further confined within the unit enclosure. Thus, it was demonstrated that a traditional, ceiling-based water spray suppression system is likely to be challenged in delivering cooling, suppressing water to the heat sources driving thermal runaway propagation.

Test 3 showed that early activation of a water suppression system may assist in protecting ESS units from thermal exposure generated by an adjacent unit experiencing thermal runaway(s). Continuous operation of the water suppression system would likely have prevented propagation of thermal runaway from the Initiating Unit to the Left Target Unit for this ESS configuration.

The primary mechanism of thermal runaway propagation in this ESS installation was thermal exposure from cells and modules that have already experienced thermal





## UL 9540A INSTALLATION LEVEL TESTS WITH OUTDOOR LITHIUM-ION ENERGY STORAGE SYSTEM MOCKUPS

runaway. In all three tests, successive thermal runaways generated sustained high temperatures over 500 °C within the modules of the Initiating Unit. High temperatures within the modules created sufficient thermal exposure to propagate thermal runaway through the Initiating Unit without additional thermal exposure from flaming materials, as demonstrated by thermal runaway propagation in the Initiating Unit in all three tests.

Both ESS enclosure geometry and spacing influenced the thermal exposure to the Target Units. There was no barrier to impede heat transfer and zero clearance between the Left Target Unit and the Initiating Unit, whereas the Front Target Unit was separated by the width of the aisle (35 in). In all three tests, the temperature measurements in the modules of the Front Target Unit were lower than the Left Target Unit, and the modules of the Front Target Unit did not experience thermal runaway.

As observed in this test series, upward propagation of thermal runaway in a unit occurred faster than downward propagation due to natural convection heat transfer. In an ESS installation, a thermal runaway event that starts in a module near the bottom of a unit may result in more rapid or more extensive propagation of thermal runaway than an event that starts near the top of a unit.

### 5.3 Thermal Exposure

In all three tests, propagating thermal runaways generated sustained high temperatures over 500 °C within the modules of the Initiating Unit. High temperatures within the modules created thermal exposure to adjacent combustible construction. For combustible construction, a UL 9540A performance criterion for temperature is that instrumented wall surfaces shall not exceed 97 °C (175 °F) above ambient temperature.

Flaming at the beginning of Test 1 caused a rapid rise in gas temperatures. Flaming ceased when there was insufficient oxygen available in the container. Additionally, heat transfer was unmitigated from the hot Initiating Unit to closely spaced combustible construction. All temperature measurement locations on the wall behind the Initiating Unit and the wall on the right side of the Initiating Unit exceeded the combustible construction performance criteria for over two hours.

In Test 2, there was a delay between the thermal runaway in the Initiating Module and noncompliant temperature measurements due to the delay in thermal runaway propagation. Once the deflagration occurred and thermal runaway propagation began, temperatures on both walls were noncompliant for over an hour and reached the same magnitudes as Test 1.

In Test 3, the measurement locations on the upper portion of both walls exceeded temperature performance criteria during an initial flaming period. When water suppression was activated, surface temperatures on both walls were reduced to below 60 °C. When waterflow was discontinued, temperatures on both walls steadily increased due to the residual heat in the Initiating Unit. The wall sections located behind and adjacent to the modules that had experienced thermal runaway exceeded the temperature performance criteria while waterflow was discontinued. When waterflow was resumed, temperatures



## UL 9540A INSTALLATION LEVEL TESTS WITH OUTDOOR LITHIUM-ION ENERGY STORAGE SYSTEM MOCKUPS

on both walls decreased below the performance threshold within seconds. The temperatures on both instrumented walls were compliant during periods of waterflow in Test 3. Early activation of a water suppression system and sustained application are likely a viable approach for preventing temperature rise nearing that of ignition for combustible wall materials.

The module vent positions and direction towards the front and rear of the ESS unit strongly influenced the severity of the thermal exposure to the walls. During Test 1, Test 2, and the periods without waterflow in Test 3, temperatures measured on the rear wall were higher than corresponding locations on the side wall. Heat flux measurements on the rear wall were at least two times higher than the side wall.

In both Test 1 and Test 2, the oriented strand board underneath the gypsum board and adjacent to the Initiating Unit was charred through its full depth, which emphasized the extent of potential thermal exposure to combustible materials.

Hot gases were generated from each module undergoing thermal runaway. Due to obscuration in the ISO container from gases and smoke generated, flaming was not visually observed inside the container. It is likely flaming was limited by a number of factors such as underventilation (i.e., reduced oxygen concentration), gas concentrations exceeding the upper flammability limit, and the suppression agent. In Test 1, the oxygen concentration was less than 10 v% from 47 minutes to 160 minutes, well below the limiting oxygen concentration for methane. In Test 2, Novec 1230 likely precluded burning from the time of discharge until the Novec 1230 leaked from the container and flammable gases ignited 28 minutes later. Flaming was precluded again due to gas buildup from thermal runaways between 75 minutes and 157 minutes, when the oxygen concentration was consistently less than 11 v%. Continued propagation of thermal runaway events generated enough heat even without flaming to drive peak gas temperatures to 200 °C near the ceiling and approximately 50 °C at the floor level in Test 1 and Test 2. The vertical temperature profile of the container was representative of a single zone. Elevated gas temperatures in a confined space represented a significant hazard of potentially exponential propagation of thermal runaways; cells that had not yet undergone thermal runaway may be immersed in a gaseous environment at or above the temperature necessary to cause thermal runaway.

In Test 3, compartment temperatures increased rapidly following the ignition of battery gases and surrounding materials eight minutes after the initial thermal runaway. Temperature measurements were as high as 320 °C near the ceiling. The sprinkler link activated within 45 seconds of ignition, and the water spray suppressed the flames within five seconds of waterflow reaching the container. Container temperatures returned to initial ambient levels at this time. In contrast to Test 1 and Test 2, gas temperatures measured in Test 3 remained at initial ambient temperature levels during both periods of waterflow with short duration spikes above 100 °C when additional modules began thermal runaway. While waterflow was discontinued, container gas temperatures increased steadily but did not exceed 100 °C. Though water-based suppression did not eliminate thermal exposure to modules directly adjacent to the Initiating Unit, water spray



## UL 9540A INSTALLATION LEVEL TESTS WITH OUTDOOR LITHIUM-ION ENERGY STORAGE SYSTEM MOCKUPS

reduced compartment temperatures so that ESS modules elsewhere in the installation would not be subjected to thermal exposure from the Initiating Unit.

### 5.4 Gas and Deflagration Hazards

Deflagrations were observed in all three tests, but an engineered system of deflagration pressure relief vents prevented the rupture of the container. The Novec 1230 system or water suppression system as implemented in this investigation did not prevent the accumulation of flammable gases or subsequent deflagration.

In Test 1, a partial volume deflagration happened 31 seconds after the first cell thermal runaway. The battery gas volume released at this time was limited to what was generated from one cell. The deflagration resulted in the unlatching and opening of both container doors.

In Test 2, a deflagration occurred 43 minutes after Novec 1230 discharge and caused the operation of two deflagration vents. The deflagration in Test 2 occurred with the gases generated from one module in thermal runaway.

In Test 3, a deflagration occurred while the water suppression system was flowing and opened one deflagration vent. The deflagration in Test 3 coincided with thermal runaway beginning in the fourth module of the Initiating Unit.

Potential ignition sources in these tests included hot surfaces or sparks ejected from thermal runaway, or DC-powered wall mounted gas detectors not intended for explosive atmospheres. After the deflagrations occurred in all three tests, thermal runaway propagation continued, and gases accumulated inside the container again. Based on gas component concentration measurements, the gases accumulated to within the flammable range and ultimately exceeded the upper flammability limit (40 v% as determined by cell level gas testing).

Flaming was initiated by manual ventilation in Test 2 when the container door was opened during test termination procedures, and the accumulated gases ignited and led to flashover. Flaming was observed at a leakage point where air was able to mix with the thermal runaway gases, the floor level cable conduit penetration on the C-side of the container, during both Test 1 and Test 2. This condition was not compliant to the requirements of the 4<sup>th</sup> Edition of UL 9540A, because it represented a failure of fire containment and a hazard of fire spreading beyond the container. In practice, it may be possible to account for this flaming with appropriate siting of the ESS installation. This observation also demonstrated the potential for the development of fire, explosion, and toxicity hazards in adjacent volumes connected by conduits and penetrations. Flaming was not observed at the cable conduit penetration during Test 3.

In addition to the flammability and explosibility hazard of gas accumulation, the accumulation of battery gases created a toxicity hazard. Carbon monoxide and carbon dioxide were measured as high as 10 v% to 15 v% in Test 1 and Test 2, and as high as 8 v% in Test 3. Oxygen concentration was measured as low as 7 v% in Test 1 and Test



## UL 9540A INSTALLATION LEVEL TESTS WITH OUTDOOR LITHIUM-ION ENERGY STORAGE SYSTEM MOCKUPS

2, and as low as 10 v% in Test 3. Reduced propagation of thermal runaway while the suppression system was operating resulted in lower battery gas concentrations in Test 3 compared with Tests 1 and 2.

### 5.5 Fire Service Size-Up Indicators of a Thermal Runaway Event

Incidents involving ESS equipment in thermal runaway will likely present differently to responding firefighters than structure fires and require different interventions to mitigate the incident safely and effectively. Although potential fire service interventions are outside the scope of this project, the results of these experiments provided examples of visual cues that may indicate a thermal runaway is taking place.

A visible vapor cloud formed on the exterior of the container in all three tests. The vapor cloud formed when gases and vapors were emitted from cell thermal runaways without burning. The gas/vapor mixture accumulated within the container and leaked from seams around the doors and equipment penetrations. This cloud primarily hovered close to the ground, but more buoyant gases were also observed. Although this cloud could be seen visually outside the ISO container, it was not discernable in thermal imaging views. In Tests 1 and 3, the cloud was first observed approximately 38 minutes after test start. In Test 2, the release of Novec 1230 resulted in a delay in propagation of thermal runaway to exposure modules, which delayed the formation of the visible vapor cloud until approximately 57 minutes after test start. In each case, the vapor cloud began to form immediately after a substantial exhaust of gas from the container, and it was maintained during the period in which peak gas concentrations were recorded inside of the container. Although the phenomenon was present for the duration of this peak period, the size of the cloud fluctuated, increasing as additional modules entered thermal runaway and decreasing as gases in the lab dissipated.

The formation of a vapor cloud was accompanied by an increase in toxic gas concentrations at exterior portable gas meters. These meters were elevated 1 ft above the ground to simulate an entry team obtaining measurements within the cloud itself. The measurements taken by these meters were characterized by high concentrations of CO and HCN. The exterior meters closest to the container (3 ft and closer) measured peak CO and HCN concentrations during the period in which peak toxic gas concentrations within the container were measured. The peak exterior toxic gas concentrations exceeded the upper measurement limit of the meters (2,000 ppm and 50 ppm for CO and HCN, respectively). Additionally, meters located closer to the container (3 ft or less) measured elevated concentrations of flammable gases, although the magnitude of these measurements was less than the LEL of the gas to which they were calibrated. The size of the vapor cloud outside the container fluctuated proportionally with the magnitude of the toxic and flammable gas measurements captured by exterior portable gas meters.

The exterior thermal imaging cameras showed the construction of the container walls had a substantial impact on the heat transfer through the container, and subsequently the ability of thermal imaging cameras to detect changes in the thermal environment within the container. Insulated wall construction tended to limit thermal changes to hot spots—



## UL 9540A INSTALLATION LEVEL TESTS WITH OUTDOOR LITHIUM-ION ENERGY STORAGE SYSTEM MOCKUPS

local changes in temperature that did not appear until later in the test timeline. Uninsulated wall sections, on the other hand, tended to heat uniformly, quickly responding to changes in the interior temperature, providing indication of an abnormal condition on the interior.

Fire service thermal imaging cameras were able to discern hot gases exhausting from the container following thermal runaway. These gases were distinct from the Novec 1230 discharge in that they are hotter than ambient (bright colored), while Novec 1230 appeared cooler than ambient (dark colored). The information from thermal imagers is limited, but it can help identify conditions indicative of abnormally operating or failing equipment. Thermal runaways occurred sporadically over the course of the tests and the Novec 1230 discharge occurred for less than 10 seconds, but when these events occurred, the thermal imaging cameras were useful in identifying the abnormal conditions.

Although these cues may be a sign to firefighters that a thermal runaway event is underway, it is important to recognize that their absence does not mean a flammable or toxic atmosphere within the container does not exist. For example, prior to the deflagration in Test 2, the uninsulated side of the container showed signs of heating, while the insulated side of the container showed little evidence of elevated temperatures within the container. In this case, the insulated construction of the container may mask elevated thermal conditions on the inside of the container, but firefighters would likely be able to observe the presence of a visible vapor cloud accompanied by elevated measurements of toxic gases on the exterior of the container. These results demonstrate a clear need for responding firefighters to have access to data from instrumentation installed within an ESS, particularly gas measurement instrumentation, through a monitoring panel. Additionally, communication must be enabled between responding firefighters and personnel responsible for management of the ESS, who can aid in complete evaluation of system data to develop a more clear picture of system status and potential hazards.

In this set of experiments, deflagration events were generally preceded by the formation of a visible vapor cloud, elevated CO measurements by the exterior portable gas meters, and evidence of heating of uninsulated wall sections in exterior TIC views. These experiments did not examine the length of time these visual cues persisted, and whether an explosive environment was possible after visual indicators of thermal runaway had subsided. Such a scenario would be similar to the conditions reported by firefighters at an incident involving ESS equipment in thermal runaway that was investigated by UL FSRI [38]. Additionally, the formation of the visible vapor cloud as a hazard indicator may be affected by tighter or more leaky ESS construction and environmental factors such as wind.

Visual cues evident to arriving firefighters may vary depending on the building construction, suppression system, and individual circumstances of the incident (e.g., wind velocity and direction, terrain, etc). However, a comprehensive size up including both visual and technological means can indicate the presence of abnormalities to responding firefighters. It is important that firefighters familiarize with the construction of ESSs in their response area, consider all available size-up factors and understand the potential for





## UL 9540A INSTALLATION LEVEL TESTS WITH OUTDOOR LITHIUM-ION ENERGY STORAGE SYSTEM MOCKUPS

thermal runaway propagation to occur sporadically when making judgements as to potential conditions inside the container.

### 5.6 Test Termination

Termination procedures were developed in advance of the tests to provide safe and well-coordinated management of the fire, explosion, and toxicity hazards presented by the test setup. Test termination procedures were utilized in each test when temperature measurements were decreasing across all modules and thermal runaway activity appeared to subside. Though test termination procedures reflect laboratory safety practice and were not a feature of the ESS design, they demonstrated several considerations for ESS incident response.

A first consideration is re-ignition. In the context of ESS testing, re-ignition is defined by additional thermal runaway behavior that occurs after test termination procedures. Whereas test termination procedures in a laboratory are similar in some operations to a fire department response to an ESS installation, re-ignition after first responders complete an incident response presents a potentially unexpected challenge to what may be perceived as final extinguishment. A fire considered extinguished may re-ignite and continue to produce hazards that were previously thought to be remedied. Following a fire department response, the occurrence of re-ignition during the decommissioning process poses a hazard to personnel and facilities involved. Re-ignitions may occur in a laboratory setting, but final extinguishment in a laboratory is immediately followed by stranded energy and hazardous materials abatement, and all ESS test materials have been disposed of responsibly. Re-ignition was observed during Test 2 and Test 3.

A second consideration is the potential response of an ESS installation/container to changes in ventilation. The environment inside the container was near or above the upper flammability limit at the end of each test. Introduction of air into this environment could result in flaming or a deflagration. In Test 2, gases accumulated in the container ignited shortly after opening one door, and a flashover condition quickly developed. Under similar conditions, a change in ventilation associated with opening a door to an ESS in Surprise, Ariz., led to the explosion of the ESS [38]. After the flashover occurred in Test 2, two more modules in the Initiating Unit experienced thermal runaway. One module of the Left Target Unit underwent thermal runaway during the period of manual fire extinguishment after the flashover. A second and final module of the Left Target Unit went into thermal runaway after the doors were closed and the carbon dioxide system was discharged. At this point, thermal runaway was observed in all modules of the Initiating Unit and Left Target Unit, but it is likely the flashover condition could have greatly exacerbated thermal runaways in a larger ESS installation.

It is essential to account for waterflow duration during installation siting and incident size up, based on the thermal runaway propagation behavior observed in Test 3. Waterflow was discontinued in Test 3, 25 minutes after the last observed thermal runaway, one hour and 36 minutes into the test. Module-to-module propagation of thermal runaway resumed in the Initiating Unit eight minutes after waterflow was discontinued. No further thermal





## UL 9540A INSTALLATION LEVEL TESTS WITH OUTDOOR LITHIUM-ION ENERGY STORAGE SYSTEM MOCKUPS

runaways occurred after the final termination of waterflow and the test at three hours and 44 minutes of test time. The accumulation of water inside the test container emphasizes the critical importance of adequate drainage, lest flooding effects exacerbate the hazards and damage during fire protection system operation.

In Test 1, the container door was opened after discharging a carbon dioxide system inside the container to reduce the explosion hazard. There was no deflagration or ignition of gases when the door was opened. In Test 2, the container door was opened without discharging the carbon dioxide system. Upon opening the door of the container, the accumulated gases in the container ignited and resulted in flashover conditions within 21 seconds. The flashover conditions occurred for approximately 30 seconds, at which point accumulated flammable gases were consumed and flaming was limited to the remaining solid combustible materials. In Test 3, no flaming of the potentially flammable gas mixture occurred while the container was ventilated with the water suppression system active.



## 6 Summary of Findings

### **A. Commonly available combustible gas and hydrogen detectors were effective for indicating that a thermal runaway event had occurred but were not reliable for an ongoing assessment of hazard conditions.**

The primary function of detection equipment is to identify that a fire and/or thermal runaway event is developing and notify occupants, site managers, or incident responders. A beneficial secondary function of detection equipment could be to provide ongoing assessment of the hazard.

Based on the outcomes of the test series, commonly available combustible gas and hydrogen detectors are effective for indicating a thermal runaway event has occurred; this is an important piece of information for incident managers and first responders seeking size-up information to distinguish between room and contents fires and cascading thermal runaway events.

However, for ongoing assessment, commonly available gas detectors may not be a reliable indicator of the magnitude of hazard or the presence of a combustible environment. Gas detector performance is challenged by the harsh operating environment of a cascading thermal runaway event. The harsh environment includes heat, high quantities of particulate, reduced oxygen concentration, high concentrations of battery gases, and possibly water or other suppression agents. Battery gases are a mixture of carbon monoxide, carbon dioxide, hydrogen, various hydrocarbons, electrolytes, and other components that may be liberated from electrolyte decomposition, such as hydrogen fluoride. In addition to releasing gases and vapors, this test experience demonstrated that battery decomposition from thermal runaway generates an unusually high yield of soot compared with diffusion flaming of combustible materials.

All gas detectors are challenged by thermal stress on circuitry, as well as particulate clogging pumps or depositing on sensing element surfaces. Catalytic bead combustible gas detectors are further challenged by the composition of the gas mixture. Catalytic bead combustible gas detectors are calibrated for simple mixtures of a single hydrocarbon in air and are not designed to measure hydrocarbon mixtures [35]. Halocarbons, including Novec 1230, may poison the sensor based on exposure duration. Additionally, catalytic bead sensors require 10% oxygen for the catalytic reaction to take place for accurate measurement [39]. Oxygen concentration was measured as low as 7 v% in Test 1 and Test 2, and as low as 10 v% in Test 3.

Electrochemical sensor measurements may be impacted by cross sensitivity or sensor poisoning. The electrochemical hydrogen detector demonstrated cross sensitivity to carbon monoxide and vulnerability to damage from Novec 1230 exposure and thermal stress.

In addition to detector damage, some detector measurement ranges may be saturated and, therefore, cannot report an accurate representation of the current magnitude of

## UL 9540A INSTALLATION LEVEL TESTS WITH OUTDOOR LITHIUM-ION ENERGY STORAGE SYSTEM MOCKUPS

hazard. For example, the electrochemical carbon monoxide detector was saturated at 250 ppm, while the conditions inside the container often exceeded 100,000 ppm as gases accumulated.

### **B. Both module and unit enclosure geometry and spacing influenced the thermal exposure to the Target Units and combustible construction materials.**

The module vent positions and direction toward the front and rear of the ESS unit strongly influenced the severity of the thermal exposure to the walls. Throughout the test series, temperatures measured on the rear wall were higher than corresponding locations on the side wall.

There was no barrier to impede heat transfer and zero clearance between the Left Target Unit and the Initiating Unit, whereas the Front Target Unit was separated by the width of the aisle (35 in). In all three tests, the temperature measurements in the modules of the Front Target Unit were lower than the Left Target Unit, and the modules of the Front Target Unit did not experience thermal runaway. UL 9540A testing may be required if ESS enclosure geometry or spacing are altered from a design with established fire safety performance.

As observed in this test series, upward propagation of thermal runaway in a unit occurs faster than downward propagation due to natural convection heat transfer. In an ESS, a thermal runaway that starts in a module near the bottom of a unit may result in more rapid or more extensive propagation of thermal runaway than a runaway that starts near the top of a unit.

### **C. When simulating a total flooding system approach, the Novec 1230 system design used did not deliver sufficient cooling to prevent propagation of thermal runaway or to prevent thermal exposure to combustible construction materials.**

The discharge of Novec 1230 in Test 2 cooled the container as the agent changed phase from liquid to vapor, but the phase change and ~8.5 v% Novec 1230 concentration did not remove sufficient heat from the cells to prevent propagation of thermal runaway. 3M states that Novec 1230 total flooding applications are not intended to interrupt cascading thermal runaway processes [37]. Bench-scale wind tunnel experiments conducted by Said and Stoliarov have demonstrated that 8.5 v% Novec 1230 concentrations with crossflow conditions were effective in reducing the rate of propagation but did not completely stop propagation. In their experiments, 15.2 v% stopped propagation in 67% of tests [40]. In addition, Novec 1230 did not prevent heat transfer from the Initiating Unit to the combustible wall materials.

Typical durations of protection for clean agent systems designed in accordance with NFPA 2001 are 10 minutes [9]. The duration of thermal runaway activity in an ESS depends on how quickly propagation progresses and installation size, but could potentially be on the order of tens of hours. The difference in event time scale contributes to the limited effectiveness of Novec 1230 flooding approaches to mitigate thermal hazards in an ESS thermal runaway event.



## UL 9540A INSTALLATION LEVEL TESTS WITH OUTDOOR LITHIUM-ION ENERGY STORAGE SYSTEM MOCKUPS

A sufficiently high Novec 1230 concentration could prevent the ignition of battery gases as they vent from cells and enable the accumulation of unburned flammable gas. These tests did not demonstrate that this phenomena increased the potential likelihood or severity of an explosion hazard. Compared with Test 1, a 30-second delay between thermal runaway and battery gas ignition resulted in a partial volume deflagration. Compared with Test 3, battery gas ignited nine minutes after battery gas venting and a deflagration did not occur, as could have been expected. Later in Test 3, flaming self-extinguished after diminishing the oxygen available for combustion, and a deflagration ultimately did occur 42 minutes after the initial thermal runaway. Test 1 and Test 3 results demonstrate that the development of a deflagration hazard by accumulation and ignition of venting battery gases can occur with or without the involvement of Novec 1230.

**D. The ceiling-based water spray suppression system prevented unit-to-unit propagation and cooled combustible construction materials adjacent to a single unit experiencing propagating thermal runaway. However, it had limited effectiveness to prevent module-to-module thermal runaway propagation within a single unit.**

Overall, it was demonstrated in Test 3 that early activation of a water suppression system could be a viable approach for protecting ESS units and combustible construction materials from thermal exposure generated by an adjacent unit experiencing thermal runaway(s). Continuous operation of the water suppression system would likely have prevented propagation of thermal runaway from the Initiating Unit to the Left Target Unit for this ESS configuration.

The primary mechanism of thermal runaway propagation in this ESS installation was thermal exposure from cells and modules that had already experienced thermal runaway. In all three tests, successive thermal runaways generated sustained high temperatures over 500 °C within the modules of the Initiating Unit. High temperatures within the modules created sufficient thermal exposure to propagate thermal runaway through the Initiating Unit without additional thermal exposure from flaming materials, as demonstrated by thermal runaway propagation in the Initiating Unit in all three tests.

The ceiling-mounted nozzle water spray system was not effective in delivering water into the tightly packed, sealed modules enclosures further confined **within the unit enclosure**. It was demonstrated by temperature measurements that a traditional, ceiling-based water spray suppression system is challenged to deliver cooling, suppressing water to the heat sources driving thermal runaway propagation. Similar ceiling sprinkler-based suppression results have been documented by FM Global [41].

Large scale fire testing using UL 9540A is recommended for determining the effectiveness of a particular fire protection design, including water spray system configuration and ESS equipment spacing, for protecting against propagating thermal runaways and ignition and damage to nearby combustible materials.



## UL 9540A INSTALLATION LEVEL TESTS WITH OUTDOOR LITHIUM-ION ENERGY STORAGE SYSTEM MOCKUPS

### **E. The temperature increase of the gas environment in the ISO container can potentially increase the rate of thermal runaway propagation exponentially.**

In all three tests, propagating thermal runaways generated hot gases and sustained temperatures over 500 °C within the modules of the Initiating Unit. Accumulation of the thermal runaway off-gassing represented a significant hazard of potentially exponential increase in the propagation rate of thermal runaways; cells that had not yet undergone thermal runaway could be immersed in a gaseous environment at or above the temperature necessary to cause further thermal runaway. Flaming may exacerbate this scenario by increasing the temperature of the confined volume more quickly, but this process can occur without flaming.

Water spray was successful in maintaining compartment temperatures near ambient levels, which provided protection for thermal exposure throughout the installation.

### **F. The generation and accumulation of battery gases created an explosion hazard and was mitigated with an engineered deflagration protection system.**

Deflagrations were observed in all three tests, but an engineered system of deflagration pressure relief vents prevented the rupture of the container. The deflagrations all occurred at test times separated by tens of minutes to hours with little to no external indication of a potential explosion hazard. Further, the gas environment required special engineering to enable measurement for this test series, demonstrating that predicting the time of deflagration occurrence is not currently feasible in the field and difficult even with reliable gas concentration data.

Neither design of Novec 1230 system or water suppression system prevented the accumulation of flammable gases or subsequent deflagration. Potential ignition sources in these tests included hot surfaces or sparks ejected from thermal runaway, or DC-powered wall-mounted gas detectors not intended for explosive atmospheres. An actual ESS installation will likely present considerably more ignition sources [38].

The battery gas concentrations in a confined volume will increase with sporadic thermal runaway events and decrease with air and gas exchange through enclosure leakage or manual ventilation by first responders. A mixture that is above the upper flammability limit will present an explosion hazard with either a gradual exchange of off-gases with air through leakage points or a rapid influx of air by manual ventilation approaches. As flammable gas and vapor concentrations increase and decrease, the mixture may alternate between being above the upper flammability limit and within the flammability limits. Whenever gases are within the flammability limits, they present an explosion hazard. Flammability limits depend on temperature, oxygen concentration, and the concentrations of N<sub>2</sub> and CO<sub>2</sub>. Given the limitations of other gas detection equipment used in this test series it could be advantageous to consider the limiting oxygen concentrations for battery gas components against paramagnetic sensor measurement of oxygen concentration, as a means of providing a more reliable ongoing hazard assessment for an ESS experiencing a thermal runaway propagation incident.



## UL 9540A INSTALLATION LEVEL TESTS WITH OUTDOOR LITHIUM-ION ENERGY STORAGE SYSTEM MOCKUPS

Consideration must be given to explosion hazards of secondary volumes connected to an ESS. In this series of tests, flammable gases were observed exhausting in burning and unburned states from a floor-level instrumentation wire penetration. This condition demonstrated the potential for transmission of flammable gases via conduit, piping, or other penetrations. During incident size-up in the Surprise, Ariz., ESS explosion, a gas/vapor mixture was observed issuing from a distribution box and transformer connected by conduit to the ESS [38]. This demonstrates a clear need for conduit/penetration sealants in ESS installations.

### **G. Propagating thermal runaway events generate more severe flammability and toxicity hazards than typical room and content fires.**

In all three tests, battery gas concentrations were measured above their upper flammability limit (40 v%) and oxygen was measured as low as 7 v% to 10 v%. Carbon monoxide was measured 50 to 100 times greater than the IDLH concentration, 1,200 ppm [26]. Carbon monoxide was measured in yields two to three times higher than have been measured in under-ventilated compartment fires involving common combustibles such as plastics or polyurethane foam (e.g., as contained in upholstered furniture) [42, 43]. Carbon dioxide was measured two to four times higher than the IDLH, 40,000 ppm [26]. Independent of the toxic and asphyxiant gases present, the oxygen concentration was low enough to cause significant mental and physical impairment [44].



## 7 Fire Service Tactical Considerations

### A. Thermal imaging cameras do not enable evaluation of the number or location of ESS units in thermal runaway.

Thermal imaging cameras (TICs) were not shown to enable evaluating the location or number of ESS units in thermal runaway. The results of the three experiments showed that wall construction can have a substantial impact on the ability of a TIC to assess thermal conditions within the container. Surface temperature differences between the interior and exterior wall surface were measured for both insulated and uninsulated construction over the course of the experiment. In some cases, this temperature difference was several hundred degrees Celsius across the insulated wall sections of the container.

The exterior TICs showed that uninsulated wall sections tended to cool or heat uniformly, responding quickly to changes in the interior thermal environment. In contrast, the exterior thermal imaging views of the insulated wall sections did not immediately reflect changes in interior surface temperature. Insulated wall sections did not show obvious signs of heating until later in the experiment, and often showed no signs of cooling at all. Insulated construction tended to show heating as hot spots rather than uniform temperature increases.

In the absence of pre-plans, the construction details of an ESS may not be immediately obvious upon arrival. If TICs indicate heating, firefighters should consider that elevated temperature conditions may induce thermal runaways. If thermal runaways have already been occurring, it is unlikely TICs can be used to determine the exact location or number of ESS units involved.

If TICs do not indicate heating, firefighters should not assume the thermal runaways have not occurred. For example, in Test 2, immediately prior to gas ignition, battery gas was not venting from the container and there was no indication of an elevated thermal environment from exterior TIC views. Despite the lack of visual indicators, the concentration of clean agent had dissipated to the point where flaming was possible within the container. Thermal runaway continued to propagate as the test continued. Thus, the lack of indicators of thermal runaway should not immediately be taken as proof that thermal runaway is not underway.

Furthermore, the exact location and extent of thermal runaway is not the most important size up consideration. The environment inside the container should be considered hazardous if any evidence of thermal runaway is observed until appropriate resources arrive on scene to conclusively prove otherwise. Deflagration events were observed as soon as 30 seconds after thermal runaway. Thus, if the TIC does not indicate heating, but other visual cues (e.g., vapor clouds, gases venting from container) suggest thermal runaway is occurring, firefighters should assume the interior environment presents explosion and toxicity hazards and treat it as such.

## UL 9540A INSTALLATION LEVEL TESTS WITH OUTDOOR LITHIUM-ION ENERGY STORAGE SYSTEM MOCKUPS

### **B. Thermal imaging cameras enable a limited ability to determine whether a suppression system has operated or is operating.**

The ability of TICs to indicate whether suppression systems were active depended on the type of suppression system and the wall construction.

TIC views enabled visual indications of water suppression system operation, particularly with uninsulated wall sections of the container. Cooling resulting from suppression water flow was apparent in the TIC views of the uninsulated side of the container shortly after activation. This cooling was accompanied by water drainage from the container. The cooling effect of suppression water did not mask thermal runaway and flaming events within the container; heating was observed at several points during the period in which the water suppression system was operating during Test 3. After water flow was shut off, surface and interior temperatures within the container began to increase. Although this temperature increase was not immediately evident in the exterior TICs, the temperature increase became visible within six minutes.

Exterior thermal imaging views in Test 2 indicated cooling in the period immediately following Novec 1230 discharge in the uninsulated wall surfaces of the container. After agent discharge, the exterior TICs showed that uninsulated wall sections were cooler than ambient. Cooler than ambient exterior surface temperatures were visible early in the test and ended after flaming began in the container (27 minutes after agent discharge). After the exterior surface temperatures returned to ambient temperatures or above, there were no visible differences between the Novec 1230 (Test 2) and no suppression (Test 1) tests.

It is important to put the timeline of cooling due to Novec 1230 release into the context of a typical fire department response time. NFPA 1710 requires that a compliant fire department have a response time objective of eight minutes from the initial answering of the alarm [45]. The design hold time of Novec 1230 required by NFPA 2001 is 10 minutes, which is short compared to fire department response times, particularly in rural areas. (The clean agent hold time estimated for the Surprise, Ariz., ESS was 5.4–7.6 minutes [38].) By the time firefighters arrive, the agent may have begun to dissipate or may have already dissipated, leaving little evidence that a clean agent suppression system had activated. Because of this, firefighters should attempt to supplement their own size-up with information that may be available from alarm panels. Activated CO detectors, LEL detectors (as used in these tests), or water flow alarms may all be evidence of an abnormality within the container.

Although cooling could be observed in the uninsulated wall sections, there was little change observed as a result of sprinkler suppression in the insulated wall sections. Firefighters should rely on other visual cues, such as water discharge from the container or alarm activation to determine whether sprinkler activation had occurred in containers with insulated construction. It is more likely that cooling may be observed around ancillary features of the container, such as deflagration panels.



## UL 9540A INSTALLATION LEVEL TESTS WITH OUTDOOR LITHIUM-ION ENERGY STORAGE SYSTEM MOCKUPS

### **C. Thermal imaging cameras are not a viable tool for determining the nature of visible vapors (e.g., battery gas, steam, Novec 1230, etc.).**

TIC views can distinguish battery gases venting from the container at points of leakage. Gases were characterized as a bright (hot) thermal signature. Although these gases could be observed at the points they vented from the container, the vapor cloud that formed along the ground could not be distinguished in the exterior IR views. It is likely the lack of visibility of the vapor cloud in IR views was because the vapors that composed this cloud had cooled and diluted while accumulating.

Novec 1230 discharge from the container appeared different than the exhaust of battery gases in the thermal imaging camera. As opposed to the brightly colored (hot) battery gases, the Novec 1230 appeared darker than ambient (cold) in the thermal imaging views. Although the Novec 1230 could be distinguished in thermal imaging views, discharge occurred for less than 10 seconds, and visibility of the Novec 1230 vapors was limited to approximately 20 seconds in duration. After the Novec 1230 dissipated and flaming was observed in the container, the exterior thermal imaging views of the exhaust from the container were comparable to the test with no suppression system. Thus, if first responders arrive after Novec 1230 discharge in an incident, there likely would not be an obvious indication from thermal imaging views that clean agent discharge had taken place.

Following activation of the sprinkler system in Test 3, a combination of steam and products of thermal runaway could be observed exhausting from the container through leakage points. Although this discharge was visible to the naked eye, it was not discernable in the exterior thermal imaging views. It is likely these vapors were cooler and less optically dense than battery gases, making them more difficult for TICs to distinguish. Practically, the difference between steam and battery gas may be difficult to discern in the field. Thus, while exterior thermal imaging views were able to identify small differences between battery gases, Novec 1230, and steam discharge, TICs are not practical for distinguishing between different types of exhaust within a container.

### **D. First responders should consider the practicality of continuous monitoring of the interior and exterior gas environment.**

Portable gas meters located inside of the container in these experiments experienced sensor failures because of the interior conditions. Soot accumulation resulted in pump failure of one of the interior meters shortly after the onset of thermal runaway in all three tests. In the diffusion style meter, faults occurred in the electrochemical sensors because of thermal insult after the first test. Additionally, to insert a portable gas meter inside of the container, firefighters would have to make an opening into the container. This action is not advisable because the interior environment may contain sufficient flammable gases to lead to a deflagration, particularly if other evidence of thermal runaway is observed [38].

Further, the magnitude of carbon monoxide and hydrogen gas concentrations measured by gas measurement instrumentation within the container was often several orders of



## UL 9540A INSTALLATION LEVEL TESTS WITH OUTDOOR LITHIUM-ION ENERGY STORAGE SYSTEM MOCKUPS

magnitude higher than the upper measurement limit of the portable gas meters. For this reason, interior gas measurements made with portable gas meters may be of limited utility in an ESS incident. Instead, firefighters may be able to obtain information from built-in monitoring systems. Although built-in information systems may fail relatively early in the thermal runaway event, they may provide enough information to determine that a thermal runaway event has taken place, and that the interior environment is hazardous.

While portable gas meter measurements taken inside of the container tended to quickly saturate at the upper measurement threshold of the meter, portable gas measurements taken on the exterior of the container trended with gas concentrations measured on the interior of the container by gas measurement instrumentation. Many of these gas meters have remote monitoring capabilities, eliminating the need to have entry teams present in the hot zone. If responding firefighters have meters with remote monitoring capabilities, they should consider using them to monitor how exterior gas concentrations are changing as a function of time.

This test series demonstrates a clear need for responding firefighters to have access to data from instrumentation installed within an ESS, particularly gas measurement instrumentation, available through a monitoring panel. Additionally, communication must be enabled between responding firefighters and personnel responsible for management of the ESS, who can aid in complete evaluation of system data to develop a more clear picture of system status and potential hazards.

### **E. Gas meters and visual observations should be utilized for defining the hot zone or exclusion zone at ESS incidents.**

The Environmental Protection Agency defines an exclusion zone (i.e. a hot zone) at hazardous materials incidents as “The area, located on the site, where contamination is either known or expected to occur and where the greatest potential for exposure exists” [46]. In the context of ESS incidents, the primary hazardous substances of concern when defining the hot zone are the flammable and toxic gases that exhaust from the container.

Limited measurements were taken by fire service portable gas meters at various locations on the exterior of the container to characterize the response of these meters to products venting from the container. In general, the meters located close to the container (1 ft from the B-side and 3 ft from the A-side) measured high concentrations of CO and HCN, and sustained measurements of flammable gas greater than ambient. Note that to obtain these measurements, firefighters performing reconnaissance would have to physically sample within the vapor cloud, placing themselves close to the container, a dangerous position if a deflagration were to occur. At the tests’ more distant measurement location, flammable gas concentrations were not measured, but elevated CO concentrations were observed throughout the period when gas concentrations were at their highest within the container.

Reconnaissance using portable gas meters will be necessary to define the hot zone at ESS incidents. While the highest concentrations of flammable and toxic gases were measured in the visible vapor cloud, elevated CO concentrations were measured in the



## UL 9540A INSTALLATION LEVEL TESTS WITH OUTDOOR LITHIUM-ION ENERGY STORAGE SYSTEM MOCKUPS

absence of the vapor cloud. Wind speed and direction, terrain, and the presence of exposures are factors outside the scope of these tests that may affect the definition of the hot zone. Because of the aforementioned risks associated with flash fires, firefighters should consider focusing their efforts outside of the vapor cloud and consider projectile and blast wave hazards for ESS installations without deflagration pressure relief vents.

### **F. Full structural PPE (Level D ensemble) with full SCBA should be donned before performing size-up or operating within the hot zone.**

The results of these tests showed that hazardous concentrations of carbon monoxide (CO) and hydrogen cyanide (HCN) were measured by exterior portable gas meters. Meters located less than 3 ft away from the container measured peak CO concentrations greater than the upper measurement threshold of the meters (2,000 ppm) and exceeding IDLH concentrations. Meters located farther away from the container (10 ft) recorded peak CO concentrations less than the IDLH concentration, but still above 400 ppm. High concentrations of toxic gases emphasize the need for breathing protection in the form of SCBA while operating in or near the hot zone.

Because of the potential for accumulation of flammable gases in a vapor cloud outside an ESS container, Level D protection (structural turnout gear) should be utilized in addition to SCBA. If accumulated above the LFL, a vapor cloud could ignite and produce a short-term, high-flux thermal hazard without significant overpressure (e.g., a flash fire) [47, 48, 49]. Generally, the burning zone of a flash fire is defined as the area that contains 0.5 [48] to 1.0 [49] times the LEL of the gas mixture. Features external to the container, such as adjacent containers, buildings, terrain, or wind, may impact vapor accumulation. Unless the area surrounding the ESS is highly confined or congested, vapor cloud explosions are unlikely to occur [49].

Gases that have accumulated to higher concentrations inside the container likely present a deflagration hazard. If the container is not engineered with deflagration venting panels, there is a significantly more serious explosion hazard. It is essential that size up identify whether deflagration panels are part of an ESS design. The position and release direction of the deflagration panels must be considered. It is recommended that explosion hazards are assumed to exist while conducting size up if deflagration panels are not observed from a distance. Both the pressure of blast waves and projectiles should be considered as explosion hazards.

### **G. Portable gas meters have limited effectiveness to evaluate the potential for explosive atmosphere within the ESS container.**

Future work is needed to further characterize the connection between portable gas meter readings and the potential for an explosive environment within the container. In this set of tests, deflagrations were observed as early as 30 seconds after the start of thermal runaway, prior to any of the interior or exterior portable gas meters indicating an increase in flammable gas concentrations and prior to the development of a visible vapor cloud. The deflagration events in Tests 2 and 3 occurred after a vapor cloud had started to form on the exterior of the container, and exterior portable gas meters measured flammable





## UL 9540A INSTALLATION LEVEL TESTS WITH OUTDOOR LITHIUM-ION ENERGY STORAGE SYSTEM MOCKUPS

gas concentrations higher than zero. It is important to note, however, that the magnitude of these measurement was significantly less than the lower explosive limit of the gas to which the meters were calibrated. Thus, any measurement of flammable gases outside of the container may indicate a higher concentration of flammable gas inside of the container. Additionally, to get to the locations where these measurements were taken, the entry team would have to get quite close to the container, potentially exposing them to blast wave and projectile hazards. Because deflagration activity was observed prior to the development of a visible vapor cloud, it is recommended that firefighters approach the container as a potential explosion hazard until explosion safety design information can be reviewed, or until it is possible to determine the conditions inside the container.

### **H. Fire service portable gas meters have limitations in a battery gas environment.**

In this series of experiments, portable gas meters were used to assess the response of fire service gas monitoring equipment to battery gases at several locations inside and outside of the structure. These meters indicated elevated concentrations of flammable gases. Although the portable gas meter measurements of these flammable gases generally trended with the hydrocarbon and hydrogen gas measurements within the container, it is important to note that the meters were calibrated to a single gas, rather than to the mix of gases present within the vapor cloud or the atmosphere inside of the container. The sensors selected for these tests were calibrated to either the LEL of pentane or methane. Although these calibrations are well-suited for more routine incidents such as natural gas leaks, they may present shortcomings when attempting to measure the mix of toxic and flammable gases in the vapor cloud at an ESS incident. Firefighters should recognize this limitation of their meters when looking at trends in gas concentration (e.g., are the flammable gas values increasing or decreasing, is the meter detecting any flammable gas at all, etc.).

Additionally, each of the meters used in these experiments has cross-sensitivities that are documented by their manufacturer and described in Section 2.2.3. Since fire service portable gas meters were not co-located with scientific gas measurement instruments, making a direct evaluation of the cross-sensitivity of these meters outside the scope of these experiments. Further work is needed to assess how the manufacturer-listed cross sensitivities of these meters might affect their ability to accurately characterize battery gas.

### **I. Ventilation of an ESS installation may result in a deflagration or rapid transition to flashover.**

The results of all three tests emphasized the need to treat manual ventilation of an ESS installation with caution. Flammable gas accumulation hazards can exist whether there is visible evidence of thermal runaways or no clear indication of thermal runaways. Ignition of accumulated gases and rapid transition to flashover or deflagrations should be anticipated when changes in ventilation, whether manual or by other means, are made. Ventilation may be initiated by manual intervention or fan-driven systems. Where suppression systems are available, including inerting systems or fire department water connections, these systems may enable safer ventilation of an ESS.





## 8 References

- [1] Underwriters Laboratories Inc., "ANSI/CAN/UL 9540A Standard for Test Method for Evaluating Thermal Runaway Fire Propagation in Battery Energy Storage Systems," Underwriters Laboratories Inc., Northbrook, IL, 2019.
- [2] National Fire Protection Association, "NFPA 855: Standard for the Installation of Stationary Energy Storage Systems," National Fire Protection Association, Quincy, MA, 2019.
- [3] International Code Council, Inc., "International Fire Code," International Code Council, Inc., Country Club Hills, IL, 2017.
- [4] International Code Council, Inc., "International Residential Code," International Code Council, Inc., Country Club Hills, IL, 2017.
- [5] City of New York, "3 RCNY 608-1: Outdoor Stationary Storage Battery Systems.," City of New York, New York, NY, 2019.
- [6] National Fire Protection Association, "NFPA 68: Standard on Explosion Protection by Deflagration Venting, 2018 Edition," National Fire Protection Association, Quincy, Massachusetts, 2017.
- [7] Occupational Safety and Health Administration, "29 C.F.R. 1910.120 - Hazardous waste operations and emergency response".
- [8] J. Ingram, "Lithium-Ion Batteries: A Potential Fire Hazard," *Power Magazine*, May 2013.
- [9] National Fire Protection Association, "NFPA 2001: Standard on Clean Agent Fire Extinguishing Systems, 2018 Edition," National Fire Protection Association, Quincy, Massachusetts, 2017.
- [10] Fire Suppression Systems Association, "Guide to Estimating Enclosure Pressure and Pressure Relief Vent Area for Applications Using Clean Agent Fire Extinguishing Systems, 3rd edition," Fire Suppression Systems Association, Baltimore, MD, 2014.
- [11] National Fire Protection Association, "NFPA 13: Standard for the Installation of Sprinkler Systems, 2019 Edition," National Fire Protection Association, Quincy, MA, 2018.

## UL 9540A INSTALLATION LEVEL TESTS WITH OUTDOOR LITHIUM-ION ENERGY STORAGE SYSTEM MOCKUPS

- [12] National Fire Protection Association, "NFPA 15: Standard for Water Spray Fixed Systems for Fire Protection," National Fire Protection Association, Quincy, MA, 2016.
- [13] Figaro Engineering Inc., "Operating principle -Electrochemical-type gas sensor," Figaro Engineering Inc., 2018. [Online]. Available: <https://www.figaro.co.jp/en/technicalinfo/principle/electrochemical-type.html>. [Accessed 5 February 2020].
- [14] RAE Systems, "RAE Systems Technical Note TN-114: Sensor Specifications and Cross-Sensitivities," RAE Systems, 2018.
- [15] MSA, "ID 0802-91-MC / ALTAIR® 5X Multigas Detector," MSA, Cranberry Township, PA, 2011.
- [16] Industrial Scientific, "Ventis Pro Series Product Manual, Edition 9," Industrial Scientific, Pittsburgh, PA, 2017.
- [17] "Sensor Technology - Delphian Corporation," Delphian Corporation, 2020. [Online]. Available: <https://delphian.com/sensor-tech.htm>. [Accessed 29 January 2020].
- [18] Industrial Scientific Corporation, "What You Need to Know about Sensor Poisons and Inhibitors," Industrial Scientific Corporation, 5 February 2021. [Online]. Available: <https://www.indsci.com/en/the-monitor-blog/where-sensor-poisons-lurk/>. [Accessed 5 February 2021].
- [19] RAE Systems by Honeywell, "Application Note AP-219: Using Pids For 10% Of Lel Decisions," RAE Systems by Honeywell, 2010.
- [20] RAE Systems by Honeywell, "Technical Note TN-106: A Guideline for PID Instrument Response," RAE Systems by Honeywell, 2018.
- [21] RAE Systems by Honeywell, "Technical Note TN-169: Theory and Operation of NDIR Sensors," RAE Systems by Honeywell, 2002.
- [22] A. Dey, "Semiconductor metal oxide gas sensors: A review," *Materials Science & Engineering B*, no. 229, pp. 206-217, 2018.
- [23] National Fire Protection Association, "NFPA 80A: Recommended Practice for Protection of Buildings from Exterior Fire Exposures, 2017 Edition," National Fire Protection Association, Quincy, MA, 2016.
- [24] Fike Corporation, *Data Sheet: CV-S AND CV-S-HV EXPLOSION VENTS*, Blue Springs, MO: Fike Corporation, 2018.

## UL 9540A INSTALLATION LEVEL TESTS WITH OUTDOOR LITHIUM-ION ENERGY STORAGE SYSTEM MOCKUPS

- [25] ASTM International, "Standard Test Method for Concentration Limits of Flammability of Chemicals (Vapors and Gases)," ASTM International, West Conshohocken, PA, 2015.
- [26] H. R. Ludwig, S. G. Cairelli and J. J. Whalen, "Documentation for Immediately Dangerous To Life or Health Concentrations (IDLHs)," U.S. Department of Health and Human Services, Cincinnati, Ohio, 1994.
- [27] Society of Fire Protection Engineers, "Thermal Decomposition of Polymeric Materials," in *SFPE Handbook of Fire Protection Engineering, 5th Edition*, New York, Springer, 2016, p. 217.
- [28] P. Ribière, S. Grugeon, M. Morcrette, S. Boyanov, S. Laruelle and G. Marlair, "Investigation on the fire-induced hazards of Li-ion battery cells by fire calorimetry," *Energy & Environmental Science*, vol. 5, p. 5271, 2012.
- [29] F. Larsson, P. Andersson, P. Blomqvist and B. Mellander, "Toxic fluoride gas emissions from lithium-ion battery fires," *Scientific Reports*, vol. 7, pp. 1-13, 2017.
- [30] D. Sturk, L. Rosell, P. Blomqvist and A. Ahlberg Tidblad, "Analysis of Li-Ion Battery Gases Vented in an Inert Atmosphere Thermal Test Chamber," *Batteries*, vol. 5, no. 61, 2019.
- [31] O. Willstrand, R. Bisschop, P. Blomqvist, A. Temple and J. Anderson, "Toxic Gases from Fire in Electric Vehicles," RISE Research Institutes of Sweden, Borås, 2020.
- [32] W. D. Walton, P. H. Thomas and Y. Ohmiya, "Estimating Temperatures in Compartment Fires," in *SFPE Handbook of Fire Protection Engineering, 5th Edition* ed., vol. Volume 1, M. J. Hurley, Ed., New York, Springer, 2016, pp. 996-1023.
- [33] National Fire Protection Association, *NFPA 69: Standard on Explosion Prevention Systems*, Quincy, MA: National Fire Protection Association, 2019.
- [34] H. R. Ludwig, S. G. Cairelli and J. J. Whalen, "Documentation for Immediately Dangerous to Life or Health Concentrations (IDLHs)," U.S. Department of Health and Human Services, Cincinnati, 1994.
- [35] J. Chou, *Hazardous Gas Monitors: A Practical Guide to Selection, Operation and Applications*, McGraw-Hill and SciTech Publishing, 1999.
- [36] Aerionics, Inc., "Macurco™ GD-12 Combustible Gas Detector, Controller and Transducer User Instructions," Aerionics, Inc., Sioux Falls, SD, 2018.

## UL 9540A INSTALLATION LEVEL TESTS WITH OUTDOOR LITHIUM-ION ENERGY STORAGE SYSTEM MOCKUPS

- [37] 3M Company, "Technical Data - 3M™ Novec™ 1230 Fire Protection Fluid," 3M Company, St. Paul, MN, 2020.
- [38] M. B. McKinnon, S. DeCrane and S. Kerber, "Four Firefighters Injured In Lithium-Ion Battery Energy Storage System Explosion - Arizona," UL Firefighter Safety Research Institute, Columbia, MD, 2020.
- [39] Y. Wang, "Why Do You Need 10% Vol Oxygen to Operate a Catalytic Bead LEL Sensor?," *Occupational Health & Safety*, 1 August 2018. [Online]. Available: <https://ohsonline.com/Articles/2018/08/01/Why-Do-You-Need-Vol-Oxygen.aspx?Page=4>. [Accessed 21 2 2021].
- [40] A. O. Said and S. I. Stoliarov, "Analysis of effectiveness of suppression of lithium ion battery fires with a clean agent," *Fire Safety Journal*, vol. 121, 2021.
- [41] B. Ditch and D. Zeng, "Development of Sprinkler Protection Guidance for Lithium Ion Based Energy Storage Systems," FM Global, Norwood, MA, 2019.
- [42] A. Lock, M. Bundy, E. Johnsson, K. Opert, A. Hamins, C. Hwang and K. Y. Lee, "Chemical Species and Temperature Mapping in Full Scale Underventilated Compartment Fires," Interscience Communications Ltd, Hampshire, UK, 2010.
- [43] D. T. Gottuk, R. J. Roby, M. J. Peatross and C. L. Beyler, "Carbon Monoxide Production in Compartment Fires," *Journal of Fire Protection Engineering*, vol. 4, no. 4, pp. 133-150, 1992.
- [44] American Society of Safety Engineers, "ANSI/ASSE Z88.2 – 2015: Practices for Respiratory Protection," American National Standards Institute, Inc., Park Ridge, Illinois, 2015.
- [45] National Fire Protection Association, "NFPA 1710: Organization and Deployment of Fire Suppression Operations, Emergency Medical Operations, and Special Operations to the Public by Career Fire Departments," National Fire Protection Association, Quincy, MA, 2019.
- [46] Occupational Safety and Health Administration, "DIRECTIVE NUMBER: CPL 02-02-071," U.S. Department of Labor, Washington, DC, 2015.
- [47] Center for Chemical Process Safety, Guidelines for Vapor Cloud Explosion, Pressure Vessel Burst, BLEVE and Flash Fire Hazards, Hoboken, NJ: American Institute of Chemical Engineers, Inc., 2010.



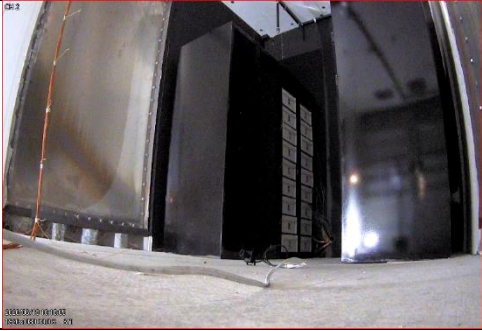
## UL 9540A INSTALLATION LEVEL TESTS WITH OUTDOOR LITHIUM-ION ENERGY STORAGE SYSTEM MOCKUPS

- [48] Center for Chemical Process Safety, Guidelines for Consequence Analysis of Chemical Releases, New York, New York: American Institute of Chemical Engineers, 1999.
- [49] D. P. Nolan, Handbook of Fire and Explosion Protection Engineering Principles for Oil, Gas, Chemical and Related Facilities, Cambridge, MA: Gulf Professional Publishing, 2019.
- [50] R. Zevotek, Stakes, K and W. J, "Impact of Fire Attack Utilizing Interior and Exterior Streams on Occupant Survival: Full Scale Experiments," Underwriters Laboratories, Northbrook, IL, 2017.
- [51] D. T. Gottuk, R. J. Roby, M. J. Peatross and C. L. Beyler, "Carbon Monoxide Production in Compartment Fires," *Journal of Fire Protection Engineering*, vol. 4, no. 4, pp. 133-150, 1992.
- [52] A. Lock, M. Bundy, E. Johnsson, K. Opert, A. Hamins, C. Hwang and K. Y. Lee, "Chemical Species and Temperature Mapping in Full Scale Underventilated Compartment Fires," in *12th International Conference on Fire Science and Engineering*, Nottingham, 2010.
- [53] National Fire Protection Association, *NFPA 2001: Standard on Clean Agent Fire Extinguishing Systems*, Quincy, MA: National Fire Protection Association, 2018.






## Appendix A: Detailed Visual Timeline of Test 1 Events

Table 20 – Timeline of major events for Test 1.

Time (HH:MM:SS)	Time After TR	Event	Visualization
00:00:00	-	Test start, heating begins at 6 °C/min.	
00:23:43	-	Venting observed in Initiating Cell.	
00:26:22	-	Thermal runaway observed in Initiating Cell (InitUnitMod3).	






**UL 9540A INSTALLATION LEVEL TESTS WITH OUTDOOR LITHIUM-ION ENERGY STORAGE SYSTEM MOCKUPS**

Time (HH:MM:SS)	Time After TR	Event	Visualization
00:26:37	00:00:15	Smoke observed outside of Initiating Module.	
00:26:42	00:00:20	First response from wall-mounted combustible gas detector at floor and alarm from CO detector. <sup>16</sup>	
00:26:44	00:00:22	>25% LEL measured by wall-mounted combustible gas detector at floor (13 second duration including seven second saturated at >50% LEL).	





<sup>16</sup>Carbon monoxide detector not configured for scaling signal output. Concentration cannot be determined but alarm condition from detector determined from video review.

**UL 9540A INSTALLATION LEVEL TESTS WITH OUTDOOR LITHIUM-ION ENERGY STORAGE SYSTEM MOCKUPS**

Time (HH:MM:SS)	Time After TR	Event	Visualization
00:26:48	00:00:26	First response from wall-mounted hydrogen detector and combustible gas detector at middle location. First signs of smoke external to container.	 <p>The visualization consists of two camera views. The top view shows smoke rising from a large, dark container. The bottom view shows a test area with a digital display showing 0:26:48 and TEST, with smoke visible in the background.</p>
00:26:49	00:00:27	First response from wall-mounted combustible gas detector at ceiling level.	 <p>The visualization shows a camera view from a higher angle, showing smoke rising from a container and spreading across the ceiling area.</p>
00:26:53	00:00:31	Gas accumulation in front of ESS units.	 <p>The visualization shows a camera view from a low angle, showing gas accumulation in front of ESS units.</p>







**UL 9540A INSTALLATION LEVEL TESTS WITH OUTDOOR LITHIUM-ION ENERGY STORAGE SYSTEM MOCKUPS**

Time (HH:MM:SS)	Time After TR	Event	Visualization
00:26:53	00:00:31	Ignition of gases.	
00:26:53	00:00:31	Partial volume deflagration opens doors.	
00:27:08	00:00:46	Smoke detector (Near) in alarm.	
00:27:09	00:00:47	Smoke detector (far) also in alarm.	







**UL 9540A INSTALLATION LEVEL TESTS WITH OUTDOOR LITHIUM-ION ENERGY STORAGE SYSTEM MOCKUPS**

Time (HH:MM:SS)	Time After TR	Event	Visualization
00:33:53	00:07:31	Flaming increases around Initiating Unit.	
00:33:57	00:07:35	Container doors closed, latched, and locked (Doors open for seven minutes, four seconds).	
00:34:22	00:08:00	Flaming increases around Initiating Unit.	
00:35:22	00:09:00	Flaming subsides around Initiating Unit.	









**UL 9540A INSTALLATION LEVEL TESTS WITH OUTDOOR LITHIUM-ION ENERGY STORAGE SYSTEM MOCKUPS**

Time (HH:MM:SS)	Time After TR	Event	Visualization
00:37:34	00:11:12	>25% LEL measured by wall-mounted hydrogen detector (sustained).	
00:38:16	00:11:54	Smoke and gas continuously observed leaking from several locations around the container.	
00:40:26	00:14:04	Thermal runaway propagation begins in Initiating Unit (InitUnitMod5).	
00:46:44	00:20:22	>25% LEL measured by wall-mounted combustible gas detector at ceiling (sustained).	





**UL 9540A INSTALLATION LEVEL TESTS WITH OUTDOOR LITHIUM-ION ENERGY STORAGE SYSTEM MOCKUPS**

Time (HH:MM:SS)	Time After TR	Event	Visualization
00:46:50	00:20:28	Wall-mounted hydrogen detector saturated at 4%.	
00:46:57	00:20:35	Thermal runaway propagation begins in Left Target Unit (LeftUnitMod4).	
00:48:32	00:22:10	>25% LEL measured by wall-mounted combustible gas detector at floor (sustained).	
00:48:54	00:22:32	>25% LEL measured by wall-mounted combustible gas detector at middle location (sustained).	









**UL 9540A INSTALLATION LEVEL TESTS WITH OUTDOOR LITHIUM-ION ENERGY STORAGE SYSTEM MOCKUPS**

Time (HH:MM:SS)	Time After TR	Event	Visualization
00:49:04	00:22:42	Thermal runaway propagation to InitUnitMod4.	
00:50:52	00:24:30	Wall-mounted combustible gas detector at floor saturated at >50% LEL (sustained).	
00:55:47	00:29:25	Thermal runaway propagation to LeftUnitMod5.	
00:57:26	00:31:04	Thermal runaway propagation to LeftUnitMod3.	







**UL 9540A INSTALLATION LEVEL TESTS WITH OUTDOOR LITHIUM-ION ENERGY STORAGE SYSTEM MOCKUPS**





Time (HH:MM:SS)	Time After TR	Event	Visualization
00:58:41	00:32:19	Thermal runaway propagation to LeftUnitMod6.	
01:00:55	00:34:33	Thermal runaway propagation to InitUnitMod6.	
01:04:26	00:38:04	Thermal runaway propagation to LeftUnitMod7.	
01:13:37	00:47:15	Thermal runaway propagation to InitUnitMod7.	



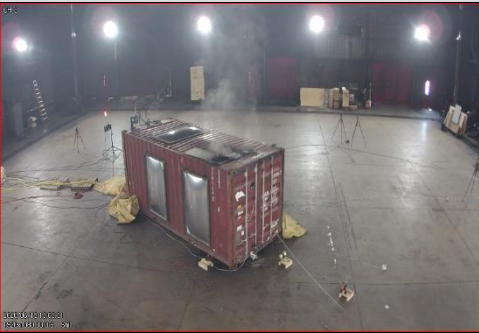



**UL 9540A INSTALLATION LEVEL TESTS WITH OUTDOOR LITHIUM-ION ENERGY STORAGE SYSTEM MOCKUPS**

Time (HH:MM:SS)	Time After TR	Event	Visualization
01:13:40	00:47:18	Intermittent flaming observed from cable conduit in container.	
01:15:10	00:48:48	Thermal runaway propagation to LeftUnitMod8.	
01:22:57	00:56:35	Thermal runaway propagation to InitUnitMod8.	
01:25:48	00:59:26	Thermal runaway propagation to InitUnitMod9.	

**UL 9540A INSTALLATION LEVEL TESTS WITH OUTDOOR LITHIUM-ION ENERGY STORAGE SYSTEM MOCKUPS**

Time (HH:MM:SS)	Time After TR	Event	Visualization
01:28:46	01:02:24	Thermal runaway propagation to LeftUnitMod9.	
01:31:28	01:05:06	Intermittent flaming observed from instrumentation cable conduit in container.	
01:54:53	01:28:31	Thermal runaway propagation to InitUnitMod2.	
02:08:06	01:41:44	Thermal runaway propagation to LeftUnitMod2.	




**UL 9540A INSTALLATION LEVEL TESTS WITH OUTDOOR LITHIUM-ION ENERGY STORAGE SYSTEM MOCKUPS**

Time (HH:MM:SS)	Time After TR	Event	Visualization
03:13:48	02:47:26	Thermal runaway propagation to LeftUnitMod1.	
03:14:04	02:47:42	Thermal runaway propagation to InitUnitMod1.	
03:21:51	02:55:29	Carbon dioxide system discharge.	
03:28:13	03:01:51	Container door opened remotely.	





**UL 9540A INSTALLATION LEVEL TESTS WITH OUTDOOR LITHIUM-ION ENERGY STORAGE SYSTEM MOCKUPS**





Time (HH:MM:SS)	Time After TR	Event	Visualization
03:29:03	03:02:41	Reignition of ESS materials inside container (doors open for 50 seconds).	
03:29:26	03:03:04	Fire growth inside opened container.	
03:56:40	03:30:18	Overhaul begins, flaming observed, stranded energy mitigation.	




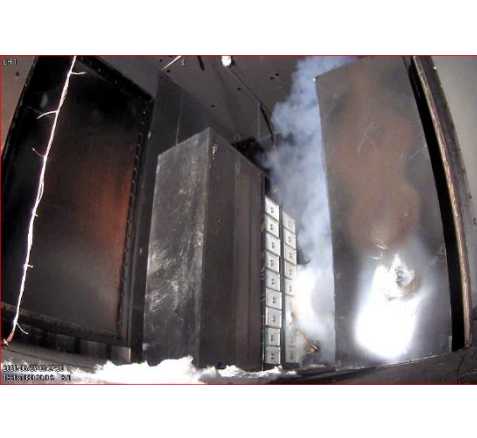




## Appendix B: Detailed Visual Timeline of Test 2 Events



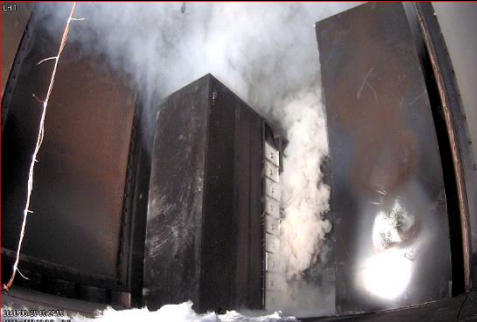

Table 21 – Timeline of major events for Test 2.

Time (HH:MM:SS)	Time After TR	Event	Visualization
00:00:00	-	Test start, heating begins at 6 °C/min.	
00:22:30	-	Venting observed in Initiating Cell.	
00:28:09	-	Thermal runaway observed in Initiating Cell (InitUnitMod3).	
00:28:10	00:00:01	Smoke observed outside of Initiating Module.	





**UL 9540A INSTALLATION LEVEL TESTS WITH OUTDOOR LITHIUM-ION ENERGY STORAGE SYSTEM MOCKUPS**

Time (HH:MM:SS)	Time After TR	Event	Visualization
00:28:30	00:00:21	First response from wall-mounted combustible gas detector at floor.	
00:28:32	00:00:23	>25% LEL measured by wall-mounted combustible gas detector at floor (15 second duration including nine seconds saturated at >50% LEL). First response from wall-mounted CO detector.	
00:28:34	00:00:25	Wall-mounted CO detector saturated at 250 ppm.	
00:28:37	00:00:28	First response from wall-mounted LEL detect at middle location.	

**UL 9540A INSTALLATION LEVEL TESTS WITH OUTDOOR LITHIUM-ION ENERGY STORAGE SYSTEM MOCKUPS**





Time (HH:MM:SS)	Time After TR	Event	Visualization
00:28:39	00:00:30	First response from wall-mounted combustible gas detector at ceiling.	
00:28:57	00:00:48	>25% LEL measured by wall-mounted combustible gas detector at middle location (10 second duration).	
00:28:58	00:00:49	>25% LEL measured by wall-mounted combustible gas detector at ceiling (13 second duration).	
00:29:02	00:00:53	First smoke detector in alarm (near).	

**UL 9540A INSTALLATION LEVEL TESTS WITH OUTDOOR LITHIUM-ION ENERGY STORAGE SYSTEM MOCKUPS**





Time (HH:MM:SS)	Time After TR	Event	Visualization
00:29:04	00:00:55	Second smoke detector in alarm (far).	 <p>A wide-angle, fisheye camera shot showing a large plume of white smoke rising from a central area between two tall, dark, rectangular mockups. The smoke is dense and fills the upper portion of the frame. The scene is dimly lit, with some light reflecting off the smoke particles.</p>
00:29:07	00:00:58	Novec 1230 discharge to 8 v%.	 <p>A wide-angle, fisheye camera shot showing a large plume of white smoke rising from a central area between two tall, dark, rectangular mockups. The smoke is dense and fills the upper portion of the frame. The scene is dimly lit, with some light reflecting off the smoke particles.</p>
00:36:40	00:08:31	>25% LEL measured by wall-mounted combustible gas detector at middle location (sustained).	 <p>A close-up, slightly blurred image of a wall-mounted combustible gas detector. The detector is a small, rectangular device with a circular lens or sensor area. The background is a plain, light-colored wall.</p>
00:36:51	00:08:42	>25% LEL measured by wall-mounted combustible gas detector located at ceiling (sustained).	 <p>A close-up, slightly blurred image of a wall-mounted combustible gas detector. The detector is a small, rectangular device with a circular lens or sensor area. The background is a plain, light-colored wall.</p>



**UL 9540A INSTALLATION LEVEL TESTS WITH OUTDOOR LITHIUM-ION ENERGY STORAGE SYSTEM MOCKUPS**





<b>Time (HH:MM:SS)</b>	<b>Time After TR</b>	<b>Event</b>	<b>Visualization</b>
00:36:53	00:08:44	Wall-mounted combustible gas detector at ceiling and middle locations saturated at >50% LEL.	
00:41:28	00:13:19	Visible stratification initially observed in gas layer.	
00:43:44	00:15:35	>25% LEL measured by wall-mounted combustible gas detector at floor (sustained).	
00:44:00	00:15:51	Visible stratification of the gas layer continues.	

**UL 9540A INSTALLATION LEVEL TESTS WITH OUTDOOR LITHIUM-ION ENERGY STORAGE SYSTEM MOCKUPS**





Time (HH:MM:SS)	Time After TR	Event	Visualization
00:52:39	00:24:30	Wall-mounted combustible gas detector located at floor saturated at >50% LEL (sustained).	
00:55:00	00:26:51	Visible stratification of the gas layer continues.	
00:56:41	00:28:32	Ignition of accumulated gases above opaque layer; flaming observed.	
00:56:44	00:28:35	Flaming observed above opaque gas layer.	







**UL 9540A INSTALLATION LEVEL TESTS WITH OUTDOOR LITHIUM-ION ENERGY STORAGE SYSTEM MOCKUPS**

Time (HH:MM:SS)	Time After TR	Event	Visualization
01:12:48	00:44:39	Deflagration observed; roof and side vent open; flaming outside container.	
01:14:35	00:46:26	Thermal runaway propagation to additional modules in Initiating Unit (InitUnitMod4).	
01:18:09	00:50:00	First response from wall-mounted hydrogen detector.	
01:20:58	00:52:49	>25% LEL measured by wall-mounted hydrogen detector (sustained).	

**UL 9540A INSTALLATION LEVEL TESTS WITH OUTDOOR LITHIUM-ION ENERGY STORAGE SYSTEM MOCKUPS**





Time (HH:MM:SS)	Time After TR	Event	Visualization
01:21:01	00:52:52	Wall-mounted hydrogen detector saturated at >4% hydrogen.	
01:29:09	01:01:00	Thermal runaway propagation into Left Target Unit (LeftUnitMod5).	
01:29:20	01:01:11	Smoke plume emitted from structure. Smoke plume varied between large plume and slow leak as thermal runaway propagation continued.	
01:34:29	01:06:20	Thermal runaway propagation to InitUnitMod5.	

**UL 9540A INSTALLATION LEVEL TESTS WITH OUTDOOR LITHIUM-ION ENERGY STORAGE SYSTEM MOCKUPS**

Time (HH:MM:SS)	Time After TR	Event	Visualization
01:34:40	01:06:31	Thermal runaway propagation to LeftUnitMod4.	
01:47:06	01:18:57	Thermal runaway propagation to InitUnitMod6.	
01:47:29	01:19:20	Thermal runaway propagation to LeftUnitMod6.	
01:57:36	01:29:27	Thermal runaway propagation to InitUnitMod7.	







**UL 9540A INSTALLATION LEVEL TESTS WITH OUTDOOR LITHIUM-ION ENERGY STORAGE SYSTEM MOCKUPS**

Time (HH:MM:SS)	Time After TR	Event	Visualization
01:57:43	01:29:34	Thermal runaway propagation to LeftUnitMod3.	
02:00:01	01:31:52	Thermal runaway propagation to LeftUnitMod7.	
02:05:42	01:37:33	Thermal runaway propagation to InitUnitMod8.	
02:13:18	01:45:09	Thermal runaway propagation to InitUnitMod9.	









**UL 9540A INSTALLATION LEVEL TESTS WITH OUTDOOR LITHIUM-ION ENERGY STORAGE SYSTEM MOCKUPS**

Time (HH:MM:SS)	Time After TR	Event	Visualization
02:16:30	01:48:21	Thermal runaway propagation to LeftUnitMod8.	
02:17:32	01:49:23	Flaming observed through cable conduit in container.	
02:22:05	01:53:56	Thermal runaway propagation to LeftUnitMod9.	
02:37:36	02:09:27	Container door opened remotely.	







**UL 9540A INSTALLATION LEVEL TESTS WITH OUTDOOR LITHIUM-ION ENERGY STORAGE SYSTEM MOCKUPS**

Time (HH:MM:SS)	Time After TR	Event	Visualization
02:37:57	02:09:48	Flashover inside container; flaming from open door.	
02:38:28	02:10:19	Flaming begins to subside inside container.	
02:40:29	02:12:20	Thermal runaway propagation to InitUnitMod1.	
02:41:01	02:12:52	Thermal runaway propagation to InitUnitMod2.	







**UL 9540A INSTALLATION LEVEL TESTS WITH OUTDOOR LITHIUM-ION ENERGY STORAGE SYSTEM MOCKUPS**

Time (HH:MM:SS)	Time After TR	Event	Visualization
02:44:56 – 03:03:56	02:16:47-02:35:47	Intermittent hose stream application, re-ignition, flaming, and thermal runaway propagation.	
02:51:09	02:23:00	Thermal runaway propagation to LeftUnitMod2.	
03:05:41	02:37:32	Doors closed.	
03:07:01	02:38:52	Carbon dioxide system discharge.	


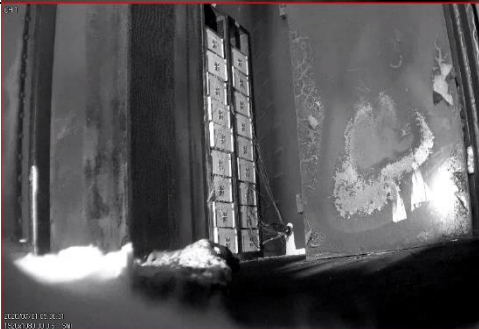


**UL 9540A INSTALLATION LEVEL TESTS WITH OUTDOOR LITHIUM-ION ENERGY STORAGE SYSTEM MOCKUPS**

Time (HH:MM:SS)	Time After TR	Event	Visualization
03:34:45	03:06:36	Thermal runaway propagation to LeftUnitMod1.	
05:07:20	04:39:11	Doors opened again; overhaul begins, no further flaming or thermal runaway activity observed, stranded energy mitigation.	







## Appendix C: Detailed Visual Timeline of Test 3 Events

Table 22 - Timeline of major events for Test 3.





Time (HH:MM:SS)	Time After TR	Event	Visualization
00:00:00	-	Test start, heating begins at 6 °C/min.	
00:21:37	-	Venting observed in Initiating Cell.	
00:29:53	00:00:00	Thermal runaway observed in Initiating Cell (InitUnitMod3).	
00:29:54	00:00:01	First signs of smoke external to Initiating Module.	

**UL 9540A INSTALLATION LEVEL TESTS WITH OUTDOOR LITHIUM-ION ENERGY STORAGE SYSTEM MOCKUPS**


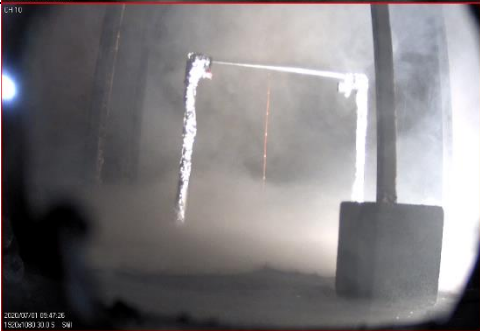


Time (HH:MM:SS)	Time After TR	Event	Visualization
00:29:57	00:00:04	First response from wall-mounted combustible gas detector at floor.	
00:30:03	00:00:10	First response from wall-mounted CO detector.	
00:30:09	00:00:16	Wall-mounted CO detector saturated at >250 ppm.	
00:30:16	00:00:23	>25% LEL measured from the wall-mounted combustible gas detector at floor (42 second duration including 15 seconds saturated at >50% LEL).	



**UL 9540A INSTALLATION LEVEL TESTS WITH OUTDOOR LITHIUM-ION ENERGY STORAGE SYSTEM MOCKUPS**

Time (HH:MM:SS)	Time After TR	Event	Visualization
00:30:20	00:00:27	First response from wall-mounted combustible gas detector in the middle location.	 <p>00:30:20 00:00:27 1500:00:00:27 0413</p>
00:30:22	00:00:29	First response from wall-mounted combustible gas detector located at ceiling.	 <p>00:30:22 00:00:29 1500:00:00:29 0413</p>
00:30:34	00:00:41	>25% LEL measured from the wall-mounted combustible gas detector in the middle location (3 second duration).	 <p>00:30:34 00:00:41 1500:00:00:41 0413</p>
00:30:43	00:00:50	First smoke detector activation (near).	 <p>00:30:43 00:00:50 1500:00:00:50 0413</p>

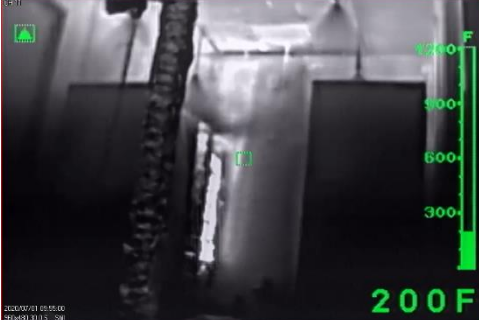



**UL 9540A INSTALLATION LEVEL TESTS WITH OUTDOOR LITHIUM-ION ENERGY STORAGE SYSTEM MOCKUPS**

Time (HH:MM:SS)	Time After TR	Event	Visualization
00:30:53	00:01:00	Second smoke detector activation (far).	 <p><small>CCTV07/01 05:30:47 1500/000 0015 50</small></p>
00:32:31	00:02:38	>25% LEL measured from the wall-mounted combustible gas detector at floor (9 second duration).	 <p><small>CCTV07/01 05:32:26 1500/000 0015 50</small></p>
00:38:42	00:08:49	Ignition leading to sustained flaming.	 <p><small>CCTV07/01 05:38:36 1500/000 0015 50</small></p>
00:39:27	00:09:34	Standard response, 165 °F sprinkler link activation.	 <p><small>CCTV07/01 05:39:21 1500/000 0015 50</small></p>













# UL 9540A INSTALLATION LEVEL TESTS WITH OUTDOOR LITHIUM-ION ENERGY STORAGE SYSTEM MOCKUPS

Time (HH:MM:SS)	Time After TR	Event	Visualization
00:40:06	00:10:13	Water suppression system flowing 0.5 gpm/ft <sup>2</sup> .	
00:43:18	00:13:25	Thermal runaway propagation to modules in Initiating Unit (InitUnitMod4).	
00:47:02	00:17:09	Thermal runaway propagation to InitUnitMod5.	
01:11:55	00:42:02	Thermal runaway propagation to InitUnitMod6.	





**UL 9540A INSTALLATION LEVEL TESTS WITH OUTDOOR LITHIUM-ION ENERGY STORAGE SYSTEM MOCKUPS**

Time (HH:MM:SS)	Time After TR	Event	Visualization
00:54:27	00:24:34	>25% LEL measured from wall-mounted combustible gas detector located at ceiling and middle (sustained).	
00:55:04	00:25:11	>25% LEL measured from the wall-mounted combustible gas detector at floor (sustained).	
00:58:36	00:28:43	Wall-mounted LEL meter at middle location saturated at >50% LEL.	
00:58:46	00:28:53	Wall-mounted LEL meter at ceiling saturated at >50% LEL.	

**UL 9540A INSTALLATION LEVEL TESTS WITH OUTDOOR LITHIUM-ION ENERGY STORAGE SYSTEM MOCKUPS**

Time (HH:MM:SS)	Time After TR	Event	Visualization
00:58:52	00:28:59	Wall-mounted LEL meter at floor saturated at >50% LEL.	
01:11:55	00:42:02	Deflagration; vent operation, flaming, continued thermal runaway activity.	
01:35:48	01:05:55	Waterflow discontinued.	
01:42:58	01:13:05	Thermal runaway propagation continues through Initiating Unit (InitUnitMod7).	




**UL 9540A INSTALLATION LEVEL TESTS WITH OUTDOOR LITHIUM-ION ENERGY STORAGE SYSTEM MOCKUPS**

Time (HH:MM:SS)	Time After TR	Event	Visualization
02:03:49	01:33:56	Thermal runaway propagation to InitUnitMod8.	
02:15:06	01:42:13	Thermal runaway propagation to Left Target Unit (LeftUnitMod8).	
02:16:16	01:46:23	Waterflow continued at 0.5 gpm/ft <sup>2</sup> .	
02:19:47	01:49:54	Thermal runaway propagation continues through Initiating Unit (InitUnitMod9).	





# UL 9540A INSTALLATION LEVEL TESTS WITH OUTDOOR LITHIUM-ION ENERGY STORAGE SYSTEM MOCKUPS

Time (HH:MM:SS)	Time After TR	Event	Visualization
02:24:23	01:54:30	Door opened; waterflow continues at 0.5 gpm/ft <sup>2</sup> ; thermal runaway propagation continues.	
02:29:03	01:59:10	Venting container; pooling vapor cloud.	
02:39:22	02:09:29	Thermal runaway activity continues.	
03:14:20	02:44:27	Overhaul begins; end of test data collection.	